

The Expression Topography and Function of “Sensory Neuron Membrane Proteins” in Insect Olfactory Systems

Dissertation

zur Erlangung des
Doktorgrades der Naturwissenschaften (Dr. rer. nat.)

Der

Naturwissenschaftlichen Fakultät I – Biowissenschaften

der Martin-Luther-Universität
Halle-Wittenberg

vorgelegt

von Frau Sina Cassau

Gutachter:

Prof. Jürgen Krieger

Prof. Monika Stengl

PD Dr. Dieter Wicher

Tag der Verteidigung:

17.06.2024

Table of Contents

Abbreviations	3
Summary	5
Chapter 1. Introduction	6
1.1 Relevance of olfaction for insects	6
1.2 The olfactory system of insects.....	9
1.2.1 General odor recognition	9
1.2.2 Antennal morphology	11
1.3 Olfactory sensilla on the antenna	12
1.3.1 Morphological and functional classes of sensilla	12
1.3.2 Cellular repertoire and fine structure of sensilla	14
1.4 Molecular elements of odor detection	17
1.4.1 Olfactory receptors	17
1.4.2 Olfactory binding proteins and odorant degrading enzymes	19
1.5 Sensory neuron membrane proteins	22
1.5.1 Expression topography of SNMPs in the antenna.....	23
1.5.2 Function of SNMPs in insect olfaction.....	26
1.6 Aims of the thesis	29
Chapter 2. Manuscript 1	30
Chapter 3. Manuscript 2	55
Chapter 4. Manuscript 3	65
Chapter 5. Discussion	80
5.1 Expression topography of SNMPs in locusts	80
5.1.1 SNMP1 expression and function in olfactory sensory neurons	80
5.1.2 SNMP1 and SNMP2 expression in non-neuronal support cells	83
5.2 The roles of SNMP2 and support cells in sensillum lymph clearance	86
References	94

Acknowledgments	107
Curriculum vitae	109
List of Publications.....	113
Appendix.....	114

Abbreviations

4VA	4-vanylanisole
AF488	Alexa Fluor 488
AF647	Alexa Fluor 647
AP	Alkaline phosphatase
BODIPY	Boron-dipyrromethene
BODIPY C4C9	BODIPY conjugated within a 16 carbon fatty acid chain
BODIPY FL C16	BODIPY conjugated at the omega end of a 16 carbon fatty acid
bp	Base pairs
CD36	Cluster of Differentiation 36
cVA	11- <i>cis</i> -vaccenyl acetate
Cy3	Cyanine 3
DAPI	4',6-Diamidino-2-phenylindole
Den	Dendrites
dH₂O	Deionized water
Dig	Digoxigenin
DMSO	Dimethyl sulfoxide
dNTP	Deoxynucleoside-triphosphate
ectoSNMP	Ectodomains of SNMP proteins
FA	Fatty acid
FIHC	Fluorescence immunohistochemistry
FISH	Fluorescence <i>in situ</i> hybridization
GPCR	G-protein coupled receptor
GR	Gustatory receptor
HEK293	Human embryonic kidney cells 293
IHC	Immunohistochemistry
IR	Ionotropic receptor
kDa	Kilo Dalton
LSM	Laser scanning microscope
MIP	Maximum intensity projection
Mv	Microvilli
OBP	Olfactory binding protein
ODE	Odorant degrading enzyme
OR	Odorant receptor
ORco	Odorant receptor co-receptor
OSN	Olfactory sensory neuron
PAGE	Polyacrylamide gel electrophoresis

PAN	Phenylacetonitrile
PBP	Pheromone binding protein
PBS	Phosphate buffered saline
PCR	Polymerase chain reaction
PDE	Pheromone degrading enzyme
PFA	Paraformaldehyde
PR	Pheromone receptor
PVDF	Polyvinylidene difluoride
s.b.	Basiconic sensillum
s.c.	Coeloconic sensillum
s.t.	Trichoid sensillum
SC	Support cell
SDS	Sodium dodecyl sulfate
SEM	Scanning electron microscope
SNMP	Sensory neuron membrane protein
SNMP1	Sensory neuron membrane protein 1
SNMP2	Sensory neuron membrane protein 2
SSO	Sulfo-N-succinimidyl oleate
SSR	Single sensillum recording
TBS	Tris buffered saline
TEM	Transmission electron microscope
TMD	Transmembrane domain
TREx	Tetracycline repressor expression system [used in HEK293 cells]
TREx/S2	SNMP2-expressing TREx cells
WB	Western Blot
WM-FIHC	Whole mount fluorescence immunohistochemistry
WM-FISH	Whole mount fluorescence <i>in situ</i> hybridization
Z11:16Ald	Z11-Hexadecenal
Z9:14Ald	Z9-Tetradecenal
$\Delta F/F_0$	Relative change of fluorescent intensity over time

Summary

Insects are capable of navigating through a complex chemical world with the use of their highly sophisticated olfactory system. Odorants are detected via sensilla found on the antennae, which are filled with a sensillum lymph and house olfactory sensory neurons (OSNs) and support cells. Both the OSNs and the support cells express the proteins required for the efficient detection of odorants, including the sensory neuron membrane protein types SNMP1 and SNMP2, which are members of the CD36 protein family. While SNMP1 in moths and *Drosophila* is localized in dendrites of OSNs and was found crucial for the detection of pheromones in holometabolous insects, SNMP2 appears to be exclusively expressed in the non-neuronal support cells, however, its specific function in olfactory processes is unclear. Before this background, this thesis aimed to elucidate the detailed expression topography and subcellular localization of the two SNMP proteins within the antenna and to characterize the function of support cell-expressed SNMP2. Using custom-made antibodies in immunohistochemistry experiments, the sensillum-specific expression patterns of SNMP1 and SNMP2 were analyzed on the adult antennae of the hemimetabolous desert locust *Schistocerca gregaria*. SNMP1 was detected in the somata and dendrites of all OSNs of trichoid sensilla and in subsets of OSNs innervating the basiconic sensilla as well as in the support cells of these sensillum types, suggesting a dual role for SNMP1. In contrast, the SNMP2 protein was confined to support cells of the basiconic and coeloconic sensilla. In accordance with a dual function of SNMP1 in OSNs and support cells and a sole function of SNMP2 in support cells, immunogold labelling visualized SNMP1 in subsets of OSN dendrites and both SNMP1 and SNMP2 in the microvilli of basiconic support cells. To assess whether the adult *S. gregaria* SNMP expression pattern is established early and retained throughout development, the expression topography of SNMP1 and SNMP2 was analyzed in the 1st, 3rd and 5th instar nymphs. Similar to adults, SNMP1 was detected in OSNs and support cells of the trichoid and basiconic sensilla, while SNMP2 was detected only in the support cells of the basiconic and coeloconic sensilla, demonstrating that the SNMP expression topography is already established in the first developmental stage and is conserved until adulthood. Finally, given the SNMP2 expression in the microvilli membranes of support cells and its membership to the CD36 family of lipid transporters, a proposed role of SNMP2 in sensillum lymph clearance processes were analyzed in the moths *Heliothis virescens* and *Bombyx mori*. In these species, their sex pheromone components are inactivated to long-chain fatty acids that need to be eliminated from the sensillum lymph to maintain the proper function of the olfactory unit. Using a fluorescent long-chain fatty acid analog, an increased uptake of the analog was observed in an SNMP2-expressing cell line, which could be abolished by the CD36 inhibitor SSO. Moreover, experiments with the fatty acid analog and the antennae of *H. virescens* and *B. mori* showed that SNMP2-expressing support cells can take up fatty acids from the sensillum lymph. Furthermore, a reduced support cell uptake was observed in *B. mori* antennae treated with SSO. Additionally, SSO pretreatment of *B. mori* antennae led to a significantly prolonged behavioral response upon sex pheromone exposure. This indicates impaired sensillum lymph clearance processes by blocking SNMP2. Altogether, these results suggest an important role for support cell expressed SNMP2 in the maintenance of the sensillum lymph, which is crucial for the proper response to odorants.

Chapter 1. Introduction

1.1 Relevance of olfaction for insects

Chemosensation is an ancient sensory modality, which enables animals the accurate and efficient evaluation of their complex chemical environment (Hansson and Stensmyr, 2011; Dahanukar et al., 2005). Most animals rely on the recognition of external chemical stimuli in order to survive and thrive in an inherently intricate world (Renou and Anton, 2020). Accordingly, insects have developed exceptionally sensitive and precise olfactory systems to detect a wide range of diverse airborne chemical compounds, or odorants that can vary in their molecular structures and chemical properties (de Bruyne and Baker, 2008). The proper recognition of odorants is often crucial for survival and reproduction, and they can stem from various sources including plant volatiles, conspecifics or other animals, which give information about potential food sources, hosts, oviposition sites, mating partners or even predators and lethal substances (Steele et al., 2023).

Many insects produce specific chemical cues for intraspecific communication classified as pheromones (Schneider, 1992; Karlson and Lüscher, 1959). Pheromones are defined as substances that are emitted from one individual to evoke assorted behavioral, physiological, or developmental responses in another individual of the same species (Regnier and Law, 1968; Stengl, 2010). The first pheromone characterized was Bombykol (10E,12Z-Hexadecadienol), the major component of the sex pheromone blend of the silk moth *Bombyx mori* (Butenandt et al., 1959), an important model organism in studying the pheromone communication system in insects (Sakurai et al., 2014). Such sex pheromones play important roles in reproductive behaviors and can give information about potential mating partners (Gomez-Diaz and Benton, 2013; Stengl, 2010). An integral part of this thesis focuses on sex pheromones in moths (Lepidoptera), where females typically release species-specific compounds in order to attract male mating partners over remarkably vast distances (Steinbrecht, 1996). For *B. mori* males, minute amounts of Bombykol are sufficient to elicit immediate searching behavior of the calling female. In addition to Bombykol, a minor component of the sex pheromone blend was also discovered, termed Bombykal (10E,12Z-Hexadecadienal), which appears to act as a behavioral antagonist in receiving males (Kaissling et al., 1978; Kasang et al., 1978).

Since the discovery of Bombykol, sex pheromones have been identified in numerous Lepidopteran species, which are often unsaturated long-chain aliphatic alcohols, aldehydes, and acetates derived from long-chain fatty acids and produced in the sex pheromone glands found in the caudal end of the abdomen in females (Koutroumpa and Jacquin-Joly, 2014). For instance, the tobacco budworm *Heliothis virescens* analyzed in the framework of this thesis, uses Z11-Hexadecenal (Z11:16Ald) and

Z9-Tetradecenal (Z9:14Ald), as the respective major and minor components of their sex pheromone blend (Almaas and Mustaparta, 1990; Baker et al., 2004; Roelofs et al., 1974). This well-studied phytophagous pest species is currently named *Chloridea virescens* (Pogue, 2013) but will be referred to as the former name for coherence with earlier work.

Generally, moth sex pheromones are complex mixtures of multiple components, often comprising a major and one or more minor components of defined ratios (Vickers et al., 1991). The correct ratio of individual compounds in the female sex pheromone blend is so vital for proper sexual communication that slight variations can lead to a complete loss of attraction in males (Vickers et al., 1991; Klun et al., 1979; Ramaswamy and Roush, 1986). The biological relevance of male attraction only by the right components and ratios is to limit hybridization, i.e. cross-species mating between sympatric species, that use overlapping constituents in their sex pheromone blends (Berg et al., 2014). For instance, in the two sympatric noctuid moth species *Helicoverpa armigera* and *Helicoverpa assulta*, the sex pheromone blends both contain Z11:16Ald and Z9-Hexadecenal, but in opposite ratios (Xu et al., 2016). That means one substance that is defined as the major component in one species is the minor component in the other species and vice versa.

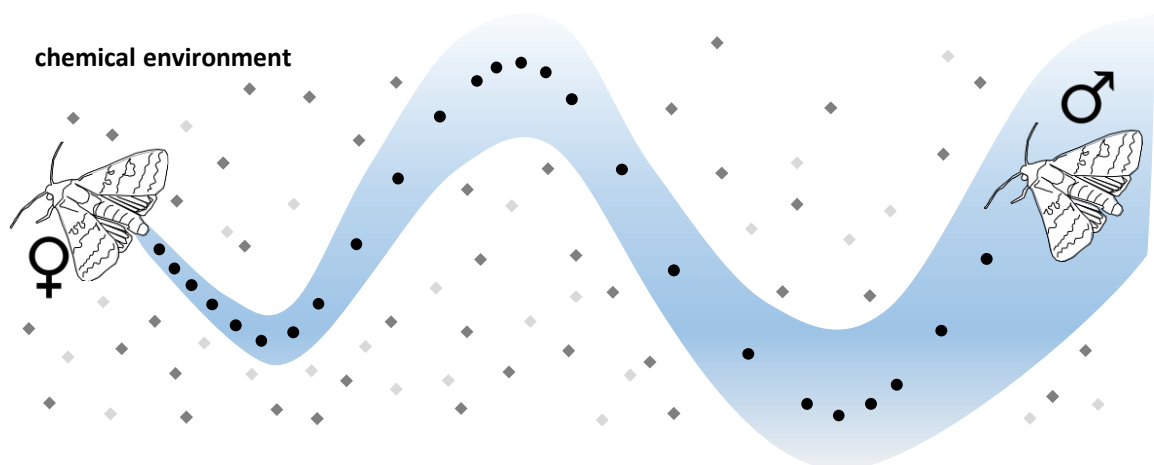


Fig. 1 Schematic depiction of a complex insect odor scape. Moth female-emitted pheromones are dispersed in a complex chemical environment that are detected by a receiving male individual despite the presence of background odors.

Pheromones play important roles in the communication and behavior of various other holometabolous insect orders, including species of Diptera, Hymenoptera and Coleoptera (Symonds and Elgar, 2008). For instance, in the well-studied fruit fly *Drosophila melanogaster* the males release the long-chain 11-*cis*-vaccenyl acetate (cVA), which initiates sexual receptivity in females while evoking a courtship-inhibition behavior in males (Benton, 2022; Ha and Smith, 2006;

Kurtovic et al., 2007; Brieger and Butterworth, 1970). Queens of the eusocial western honeybee *Apis mellifera* emanate the so-called queen mandibular pheromone, which induces the division of labor in the female worker bees and obstructs the development of their reproductive organs (Slessor et al., 2005; Slessor et al., 1988; Jarriault and Mercer, 2012). Certain species of bark beetles, such as *Ips pini*, rely on aggregation pheromones to coordinate the colonization of host trees to reach their phloem (Tittiger and Blomquist, 2017).

While detailed knowledge has accumulated on pheromones in holometabolous insects, comparatively little is known about the use and chemical identity of pheromones in hemimetabolous insects, like locusts (Orthoptera), which, in addition to moths, were analyzed in the framework of this thesis. In phase transitioning locusts, such as species of *Locusta* and *Schistocerca*, pheromones, along with mechanosensory and other chemosensory cues, are implicated in driving the shift from the solitary to the gregarious state and vice versa, however, the exact mechanisms involved in this process remain largely elusive (Uvarov, 1966; Nakano et al., 2022; Hassanali et al., 2005). Gregarious phase locusts differ from the solitary locusts as they have a propensity to aggregate into large destructive swarms made up of millions of individuals that travel together, thereby causing devastating losses to the landscape vegetation and agricultural crops (Nakano et al., 2022). Recent studies have provided evidence that pheromones are involved in swarm-formation processes and may trigger and control behaviors necessary for locust aggregation, survival and synchronization under crowded conditions. For instance, the migratory locust *Locusta migratoria* releases the substance 4-vinylanisole (4VA) that is detected by adults and younger nymph stages and is proposed to drive aggregation behavior (Guo et al., 2020). *L. migratoria* individuals also produce phenylacetonitrile (PAN), which triggers an aversive response in conspecifics (Chang et al., 2023). PAN is implicated to function as an anti-cannibalism signal, as PAN released by hoppers prohibits their consumption by conspecifics, thus ensuring their survival in large, swarming populations (Chang et al., 2023). PAN is also produced by the gregarious phase desert locust *Schistocerca gregaria* and was initially described as an aggregation pheromone (Torto et al., 1994; Torto et al., 1996). Yet, this was disputed in later studies showing that PAN in *S. gregaria*, similar to *L. migratoria*, is aversive to conspecifics (Seidelmann et al., 2000; Seidelmann and Ferenz, 2002). However, in *S. gregaria* PAN is only released by adult males under crowded conditions (Seidelmann et al., 2000), thus indicating male identity and moreover was described to function as a courtship-inhibition pheromone that repels rival males from their female mating partners (Seidelmann and Ferenz, 2002).

1.2 The olfactory system of insects

1.2.1 General odor recognition

The detection of odorants, independent of their behavioral significance, is established through the bipolar olfactory sensory neurons (OSNs) that transform chemical signals into a train of action potentials (Boeckh et al., 1965). OSNs are housed in hair-like cuticular protrusions called sensilla that are mainly located on the antenna (Sanes and Hildebrand, 1976a; Zacharuk, 1980). In addition, lower numbers of OSNs are located in other insect body appendages, including the palps and proboscis (Sanes and Hildebrand, 1976a). However, the antennae are considered the main olfactory organs in insects, as they contain the majority of OSNs and are vital for the detection of most behaviorally relevant odorants.

Despite the extreme diversity in the antennal morphology across the different insect orders and species, the overall anatomical organization of the peripheral olfactory system remains similar (Hansson and Stensmyr, 2011; Elgar et al., 2018), as shown in Figure 2. Different populations of OSNs are dispersed along the antenna and are housed in different types of olfactory sensilla. The OSNs project their axons into one of the two antennal nerves, which run along the entire span of the antenna (Sanes and Hildebrand, 1976b). Ultimately, the axons of the OSNs terminate in the first processing center for odor information, the antennal lobes, found laterally in the deutocerebrum of the insect brain (Vosshall et al., 2000; Ai and Kanzaki, 2004; Boeckh and Boeckh, 1979). The antennal lobes comprise of neuropil subunits called glomeruli, which are individually identifiable structures where antennal OSN axons terminate and form synapses with projection neurons, which wire the olfactory information to higher brain centers, the mushroom bodies and the lateral horn of the protocerebrum (Patel and Rangan, 2021). The overall organization and functions of the antennal lobe is conserved across the insect taxa (Hildebrand and Shepherd, 1997; Schachtner et al., 2005) and have been intensively studied in holometabolous insects, mostly in *D. melanogaster* and moths (Kvello et al., 2009; Couto et al., 2005). Maps have been established to determine which OSN populations innervate distinctive glomeruli, revealing that OSNs of the same responsiveness, i.e. populations of the same olfactory receptor identity, converge in the same glomerulus (Couto et al., 2005; Silbering et al., 2011; Grabe et al., 2015; Vosshall et al., 2000).

In moths, which have evolved to sensitively detect sex pheromone components, there is a sexual dimorphism in the antennal lobe organization, as male glomeruli can be distinguished into two groups: the macroglomerular complex and the ordinary glomeruli (Berg et al., 2014). The ordinary glomeruli, found in both males and females, are associated with the detection of general odorants

such as plant volatiles (Skiri et al., 2004). Whereas the male-specific macroglomerular complex is deemed as the first processing center for pheromone sensitive OSNs in moths such as *H. virescens* and *B. mori* (Berg et al., 1998; Sakurai et al., 2014).

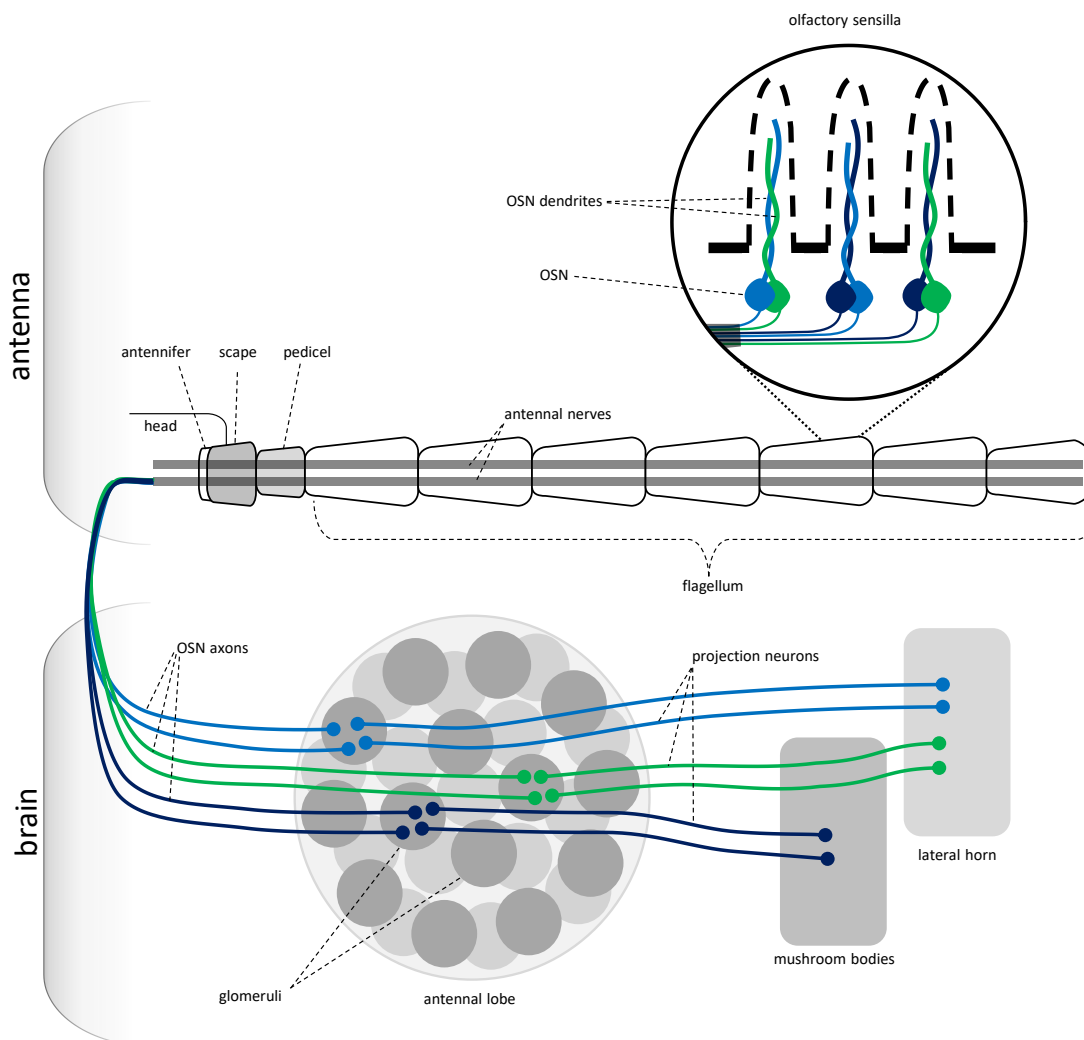


Figure 2. Schematic diagram of the organizational structure of the olfactory system in insects. The dendrites of the olfactory sensory neurons (OSNs) innervate the sensilla found along the antenna. The antenna is composed of the flagellum, which comprise numerous segments, the pedicel and the scape. It is attached to the insect head via the antennifer. The axons of the OSNs converge into the antennal nerves, which span the length of the antenna and lead to the antennal lobe in the insect brain. The axons project into the glomeruli situated in the antennal lobe. Axons from OSNs of the same population converge in a specific glomerulus distinct from glomeruli targeted by other OSNs. The OSN axons synapse with projection neurons, which lead to higher brain centers, the mushroom bodies and the lateral horn.

Noteworthy, in locusts such as *S. gregaria* and *L. migratoria*, a different, extremely complex innervation of the antennal lobe has been found. In these species, the axons of individual OSNs branch out in the antennal lobe and synapse in several small glomeruli, so-called microglomeruli of

which an extraordinarily large number (up to 1000) can be found (Anton and Hansson, 1996). The unique antennal lobe organization and innervation pattern of these hemimetabolous insects was described as a possible mechanism to accommodate for their successive growth and increase in OSN number after each molt, allowing for more flexibility during development (Bicker and Stern, 2020).

1.2.2 Antennal morphology

All insects possess a pair of bilateral antennae that protrude from their heads and generally consist of three main parts (Kaissling, 2014; Schneider, 1964), as depicted in Figure 2. The most proximal section is called the scape and is attached to the head via the antennifer (Schneider, 1964). The scape is conjoined by the pedicel segment that contains the Johnston's organ and muscles allowing for antennal movement. Finally, the pedicel is attached to the flagellum, which harbors the majority of the olfactory sensilla and can be composed of different numbers of segments or annuli (Schneider, 1964).

In some moths, like *H. virescens*, the around 80 annuli do not branch out and the sensilla are distributed on the main, filiform antennal stem (Jorgensen et al., 2007). Whereas in other lepidopteran species, such as the silk moths *B. mori* and *Antheraea polyphemus*, the flagellum does branch out, creating elaborate pectinate antennae (Keil and Steiner, 1990; Keil, 1992; Maida et al., 2005). These feathery antennae have an increased surface area supposed to help with the sensitive detection of volatile chemicals (Jaffar-Bandjee et al., 2020).

Generally, moth antennae are covered with numerous extremely long sensilla considered as evolutionary adaptations to sex pheromone reception (Hansson and Stensmyr, 2011; Kaissling, 2014). These long sensilla grant an increased surface area of the antenna creating a type of sieve to improve the capture of volatile molecules (Baker et al., 2022; Elgar et al., 2018; Su et al., 2019). In moths, the detection of sex pheromones is often associated with sexual dimorphism, i.e. the antennal structure differs between males and females. For instance, in noctuid moth species, males can have both long and short so-called trichoid sensilla, both of which are sensitive to female sex pheromone components (Baker et al., 2004), whereas the female antennae only possess the short trichoid sensillum type but they appear to have more sensilla overall (Berg et al., 2014). Such is the case for *H. virescens* males, where the antenna is covered by around 12000 sensilla while in females, this number goes up to about 17000 (Almaas and Mustaparta 1991). However, a clear sexual dimorphism is not always pronounced in moths. For example, in *B. mori*, the same sensillum types are present on the antenna of both sexes, although they tend to be slightly shorter in females (Maida et al., 2005).

The morphology of the adult moth antenna, composed of numerous segments and covered by thousands of sensilla, bears no resemblance to the rudimentary antenna of the larval stage. In *H. virescens*, it is composed of only three small segments carrying a total of just nine sensilla (Zielonka et al., 2016). Since moths are holometabolous insects, their antennae undergo drastic changes during metamorphosis, allowing for a complete restructuring of their overall anatomy and OSN innervation to accomplish the detection of odorants required in the adult stage.

The situation is completely different in hemimetabolous insects as from the first instar to the adult stage, their antennae do not undergo extreme changes throughout development. The most obvious morphological differences are observed in their overall size, as well as segment and sensilla number (Ochieng et al., 1998). In gregarious *S. gregaria*, the first instar nymph antennae possess 11 annuli, and are approximately 3 mm in total length (Ochieng et al., 1998). Their antennae grow successively with each molt, reaching a length of 14 mm in adults, which possess 24 antennal segments (Ochieng et al., 1998). During all stages, the locust antenna exhibits a filiform shape with no sexual dimorphism observed (Ochieng et al., 1998; Chapman and Greenwood, 1986). Despite minimal morphological differences between juvenile and adult locusts, it is so far unclear if the successive development of the locust antenna shows age specific differences on the cellular and molecular level.

1.3 Olfactory sensilla on the antenna

Insect olfaction begins when odorants enter the olfactory sensilla housing the dendrites of OSNs. A defining characteristic of olfactory sensilla is that they are covered by multiple pores in their cuticle, allowing airborne chemicals to permeate into the sensillum shaft from the outer environment (Steinbrecht, 1997; Keil, 1989; Steinbrecht, 1996) as opposed to gustatory sensilla, which are equipped with a single pore at the terminal end of the shaft. The number and distribution of the pores along olfactory sensilla have been well studied through scanning electron microscopy (SEM) conducted among others on Noctuid and Bombycid moth species, as well as on locusts, revealing the overall architecture and distribution of the olfactory sensilla along the antenna (Maida et al., 2005; Wang et al., 2023; Ochieng et al., 1998; Gohl and Krieger, 2006).

1.3.1 Morphological and functional classes of sensilla

Olfactory sensilla are morphologically diverse across insects and even on the antenna of a single species. Based on their outer morphology, sensilla can be categorized into different types (Steinbrecht, 1996). The most abundant olfactory sensilla types in insects are the slender trichoid

sensilla, the shorter and more compact basiconic sensilla, and the grooved coeloconic sensilla that are often situated in pits on the antennal surface. The number of OSNs which are housed in a sensillum varies depending on the sensillum type and insect species. Sensilla trichodea and sensilla coeloconica of moths and locusts are typically innervated by two to four OSNs (Keil, 2012; Keil, 1984; Ochieng et al., 1998). Similarly, the basiconic sensilla of moths are usually innervated by two to four OSNs (Shields and Hildebrand, 2001). Whereas in locusts, this sensillum type has been described to house 30 to 50 OSNs that exhibit massive dendritic arborization (Ochieng et al., 1998). The exceptional variability in structure and OSN number in the olfactory sensilla types in locusts is shown exemplarily in Figure 3. In addition to olfactory sensilla, the antenna of most insects also possess single-pore sensilla chaetica (not shown), which are involved in mechanosensory and gustatory sensory modalities and are usually innervated by three to four sensory neurons.

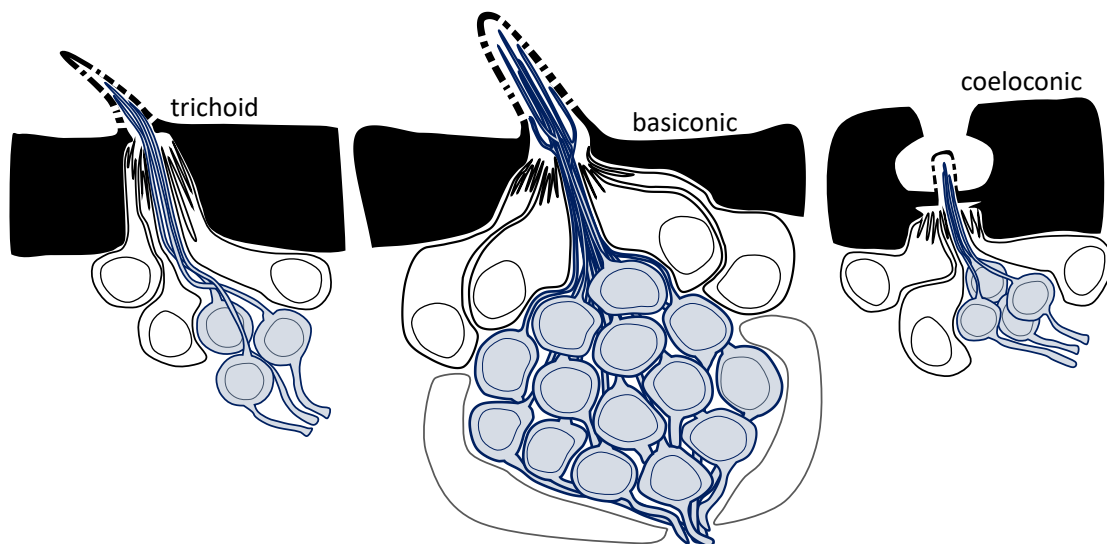


Figure 3. The different morphological classes of olfactory sensilla found on the antenna of *S. gregaria*. Left: the trichoid sensilla are elongated and exhibit a pointed tip. Middle: the basiconic sensilla are often wider and have a blunt end. Right: coeloconic sensilla are positioned in pits on the antennal surface. The different sensilla types can be innervated by numerous numbers of OSNs (blue), found beneath the base of the sensillum's shaft.

The morphologically different classes of sensilla can display defined response profiles to odorants of specific chemical structures or behavioral relevance (Steinbrecht, 1996; Schmidt and Benton, 2020). For instance, in moths and flies, the OSNs of coeloconic sensilla have been shown to primarily respond to acids, amines and ammonia (Yao et al., 2005; Pophof, 1997; Menuz et al., 2014), while those of basiconic sensilla are often associated with the detection of general odorants of various chemical classes, such as those emitted by food sources or host plant volatiles (Grabe and Sachse, 2018). Meanwhile, the OSNs of trichoid sensilla are often tuned to detecting long-chain fatty acid derived pheromones as well as host plant volatiles (Grabe and Sachse, 2018; Heinbockel and Kaisling, 1996; Stengl, 2010).

The behavioral relevance of sensillum-specific odor profiles is particularly reflected in male moths that have an established sex pheromone detection system. In this respect, a single antenna of *H. virescens* males possesses up to 12000 trichoid sensilla containing OSNs tuned to the sex pheromone components, Z11-16Ald and Z9-14Ald (Almaas and Mustaparta, 1991). Likewise, the antenna of male *B. mori* is covered with up to 17000 trichoid sensilla, most of which house a pair of OSNs sensitively detecting Bombykol and Bombykal (Steinbrecht, 1970; Kaissling et al., 1978). However, certain subpopulations of both male and female trichoid sensilla have also been shown to detect relevant plant volatiles (Boeckh et al., 1965).

In the locust *S. gregaria*, the antenna is most abundantly covered by basiconic sensilla (>2100) followed by coeloconic sensilla (>1200), while the least abundant olfactory sensillum type is the trichoid sensilla (>400) (Ochieng et al., 1998). In *S. gregaria*, some trichoid OSNs are indicated to respond to pheromone components (Ochieng and Hansson, 1999). While in *L. migratoria*, the OSNs of the basiconic sensillum responds to the pheromone components PAN and 4VA (Guo et al., 2020; Chang et al., 2023). This suggests that in locusts, both the trichoid and basiconic sensilla play integral roles in the detection of various behaviorally relevant pheromone signals.

1.3.2 Cellular repertoire and fine structure of sensilla

The olfactory sensillum is considered as an olfactory unit that consists of the sensillum shaft, the OSNs and the support cells (Zacharuk, 1980), which is depicted in a schematic diagram in Figure 4. The cell body of OSNs is located beneath the base of the sensillum, which tends to exhibit a compact spherical shape with a large nucleus in relation to the perinuclear cytoplasm (Zacharuk, 1980). Ciliary dendrites, which protrude out of the apex of the OSN somata into the sensillum lumen, which is filled with the so-called sensillum lymph, curl around each other like tendrils (Keil, 1984; Schmidt and Benton, 2020).

Ultrathin cross-sections of moth olfactory sensilla, analyzed through transmission electron microscopy (TEM) have revealed that olfactory dendrites have a microtubule framework with a classical axoneme arrangement that is quintessential for cilia (Keil, 2012). Although olfactory cilia have demonstrated a degree of mobility in openly prepared sensilla (Williams, 1988; Keil, 1993), they are considered primary cilia, which lack the central microtubule pair and are generally non-motile, which is typical for sensory cilia (Kaissling, 1996; Keil, 2012). Despite possessing the basic ciliary components, the transport of the molecular elements necessary for olfaction into the dendrites appear independent of the cilia-specific intraflagellar transport pathway (Jana et al., 2021). As these primary cilia are necessary for the recognition of olfactory stimuli and are the sites of ligand detection and transduction, for simplicity they will be referred to as dendrites in the

upcoming sections. Extending out of the other side of the OSN somata are the axons, which project towards the antennal lobe and ultimately synapse in glomeruli.

So-called support cells, also named auxiliary cells, envelop the OSNs at the base of the sensillum and directly border the sensillum lymph (Keil, 1989). Support cells seal off the entire olfactory unit, forming an independent compartment and upholding a microenvironment within each sensillum (Keil and Steinbrecht, 1983; Keil, 1987; Shanbhag et al., 2000). Morphologically, antennal support cells can exhibit varied shapes and sizes in insects. Each sensillum supposedly has three different types of support cells that have first been characterized in early TEM studies conducted with moths (Steinbrecht et al., 1989). The innermost support cell that completely ensheaths the OSNs is called the thecogen cell. In moths, this cell type is characterized by its small, irregularly shaped nucleus, thin cell body and less developed endoplasmatic reticulum (Steinbrecht and Gnatzy, 1984; Shields and Hildebrand, 2001). The thecogen cell is bordered by the trichogen cell, which in turn is adjoined by the tormogen cell. Both of the latter support cell types show great variability in their morphology even within the antenna of the same species (Shields and Hildebrand, 2001). They are generally characterized by their large, ellipsoidal form and their membrane invaginations on the apical side, forming microvilli that border the sensillum lumen (Steinbrecht and Gnatzy, 1984; Keil, 1989). Whether the innermost thecogen cell also forms microvilli structures is unclear, but all three support cell types have direct contact to the sensillum lymph.

Differentiating between the support cell types from one another can be difficult without the use of high resolution electron microscopy. Genetic tools to distinguish the support cell types are only available for *D. melanogaster*'s tormogen and thecogen cells, but not trichogen cells in adults. The tormogen cell can be identified by tagging the ASE5 promotor while the thecogen cell expresses the protein *nompA* (Barolo et al., 2000; Chung et al., 2001), corroborated in a recent study using the promotor driven expression of fluorescent proteins in the antenna of *D. melanogaster* (Prelic et al., 2022). However, such genetic markers have not been identified in other insect species such as in moths or locusts. Additionally, the number of different support cell types can vary across different species. While in moths experimental evidence points to each sensillum containing three support cells (Steinbrecht et al., 1989), a subset of sensilla in *D. melanogaster* have been shown to possess four support cells (Shanbhag et al., 2000) while in the locust *S. gregaria*, up to seven support cells have been counted in basiconic sensilla (Ochieng et al., 1998). For this reason, most studies simply refer to support cells as a uniformed group and refrain from naming the individual support cell types.

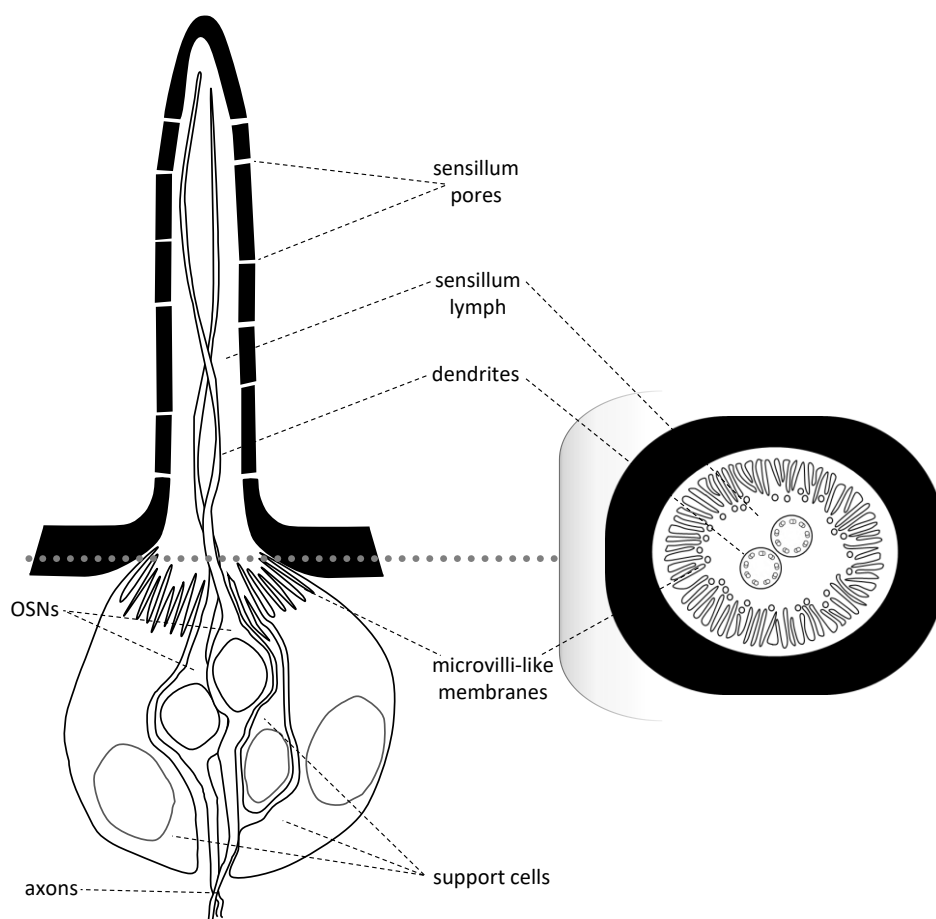


Figure 4. Schematic depiction of olfactory sensilla and their cellular repertoire. All olfactory sensilla possess multiple pores on their cuticle. They are filled with the fluid sensillum lymph and are innervated by the ciliated dendrites of the OSNs. At the base of the sensillum are the somata of the OSNs followed by their axon projections. The OSN somata are bordered by support cells, that have microvilli-like membranes facing the sensillum lumen. The left side depicts the longitudinal view of a sensillum while the right side shows a cross-section of the same sensillum at its base.

Aside from surrounding the OSNs and segregating the sensillum, multifunctional roles have been reported for the non-neuronal support cells, ranging from the biogenesis of the sensillum to the expression of proteins involved in odor detection (Klein, 1987; Kaissling, 2009; Schmidt and Benton, 2020). Early studies conducted on the antenna of *Manduca sexta* documented that support cells secrete chitin and proteinaceous components necessary for sensillar formation (Sanes and Hildebrand, 1976b; Keil, 1997). Moreover, experiments conducted on the *D. melanogaster* antenna showed that support cells play a part in the correct formation of sensillum pores, which are necessary for the proper entrance of odorants into the sensillum lumen (Ando et al., 2019). Additionally, support cells produce and determine the composition of the sensillum lymph and its ionic constituents (Thurm and Küppers, 1980), thereby being crucial for the regulation of the sensillum lymph homeostasis that is integral for the proper detection of odorants. In this context, it has been speculated that the support cells extract “waste products” such as inactivated odor

molecules from the sensillum lymph, which could otherwise interfere with the detection of newer, incoming odorants (Vogt and Riddiford, 1981; Pelletier et al., 2023). Generally, support cells appear to play a vital purpose in the maintenance of the sensillar unit as a whole, however, the extent of their functions remain largely elusive.

1.4 Molecular elements of odor detection

Odorant detection employs different molecular elements expressed by the OSNs and the support cells of olfactory sensilla. Members of different protein families are involved in the detection of odorants as well as the transport of odorant molecules across the sensillum lymph and the eventual signal termination, as depicted in Figure 5.

1.4.1 Olfactory receptors

The recognition of odorants by the OSNs is accomplished by olfactory receptors localized in their dendritic membranes. In insects, olfactory receptors encompass different protein families (Fleischer et al., 2018; Wicher and Miazzi, 2021). The majority of the olfactory receptors belong to the generally large family of odorant receptors (ORs) (Clyne et al., 1999; Gao and Chess, 1999; Vosshall et al., 1999; Fleischer et al., 2018) and the smaller family of ionotropic receptors (IRs) that are related to the ionotropic glutamate receptors (Yao et al., 2005; Benton et al., 2009). Additionally, certain gustatory receptors (GRs) are associated with olfactory detection processes, specifically in the recognition of CO₂ (Kwon et al., 2007). More recently, other receptor types have been implicated in odor detection, including ammonium transporters (Vulpe et al., 2021), as well as members of the pickpocket and transient receptor potential protein families (Joseph and Carlson, 2015; Kim et al., 2010).

The largest and best-characterized olfactory receptor family in insects is the divergent OR family, which comprise ORs that recognize a broad spectrum of odorants including terpenes, aromatics, alcohols, aldehydes, and acetates stemming from a wide range of sources (Fleischer et al., 2018; Ha and Smith, 2009). In insects, the OR repertoire varies across different insect species and orders (Brand et al., 2018), ranging from only 10 OR genes in head lice (Kirkness et al., 2010), to 60 in the fruit fly *D. melanogaster* (Robertson et al., 2003), to over 300 OR genes in ants (Zhou et al., 2012). The OR repertoire of noctuid moths ranges from 40 to 60 ORs (de Fouchier et al., 2017; Poivet et al., 2013) while in *B. mori* this extends to 71 candidate OR genes (Tanaka et al., 2009; Qiu et al., 2018). The locusts *L. migratoria* and *S. gregaria*, on the other hand were shown to express

considerably more OR genes with 142 and 119 ORs detected respectively in genomic and transcriptomic datasets (Pregitzer et al., 2017; Wang et al., 2015).

Similar to classical G-protein coupled receptors (GPCRs), ORs are characterized by their seven transmembrane domains (TMDs), however, they lack sequence similarity with the GPCRs of the vertebrate and nematode OR families (Fleischer et al., 2018). Moreover, insect ORs display an inverted membrane topology to GPCRs, with an intracellular N-terminus and an extracellular C-terminus (Lundin et al., 2007; Benton et al., 2006; Smart et al., 2008), suggesting an alternative signal transduction mechanism for insect ORs compared to G-protein dependent signaling.

Interestingly, in numerous insect orders including Lepidoptera, Orthoptera, and Diptera, a highly conserved member of the OR gene family was discovered, which is expressed in all OR-expressing OSN populations and was named as odorant receptor co-receptor (ORco) (Larsson et al., 2004; Vosshall and Hansson, 2011). ORco was shown to be necessary for the integration of the ligand-binding ORs (tuning ORs) into the dendrites of OSNs, as well as the proper detection of cognate odorants by the OSNs (Zufall and Domingos, 2018). ORco and a tuning odorant receptor (OR_x) heteromerize and together form a ligand-gated cation channel (Sato et al., 2008; Wicher et al., 2008), with the tuning OR_x serving as the determinant required for the detection of odorants. First structural cryo-electron microscopy investigations of homomeric OR and ORco complexes revealed they are composed of four symmetrical subunits, which together form a hydrophobic central channel pore capable of widening and becoming hydrophilic, enabling the entrance of hydrated cations into the OSN, supporting the notion of an OR-ORco ligand gated ion channel (Butterwick et al., 2018; Del Marmol et al., 2021).

Although many olfactory receptors have shown a high degree of promiscuity in their detection to multiple odorants, certain receptors were shown to be much more finely tuned to distinct ligands. This is especially the case for ORs tuned to pheromone molecules also termed as pheromone receptors (PRs) (Fleischer and Krieger, 2018). The first PRs identified and functionally characterized were of the moths *H. virescens* and *B. mori*, which are expressed in the pheromone sensitive OSNs of the trichoid sensilla (Krieger et al., 2004; Sakurai et al., 2004). The male-specific receptors BmorOR1 and BmorOR3 of *B. mori* were verified to mediate the detection of major (Bombykol) and minor (Bombykal) sex pheromone components (Krieger et al., 2005; Nakagawa et al., 2005). Likewise, in *H. virescens*, the receptors HR13 and HR6 mediate specific responses to the sex pheromone components Z11:16Ald and Z9:14Ald respectively (Gohl and Krieger, 2006; Grosse-Wilde et al., 2007). In Lepidopteran species, sequence based analyses revealed that sex pheromone receptors are highly conserved, forming a separate, highly related group within the OR family (Engsontia et al., 2014; Koenig et al., 2015; Steinwender et al., 2015).

Recently, members of the OR family in locusts have also been shown to respond to pheromone components, even though they are phylogenetically distinct from the moth PRs. In *L. migratoria* the receptor LmigOR70a, expressed in OSNs of basiconic sensilla, mediates the detection of PAN (Chang et al., 2023), while a second receptor type, LmigOR35, was identified as a receptor specific to 4VA (Guo et al., 2020). The narrow tuning of pheromone responsive ORs is also reflected in *D. melanogaster* where the male-released pheromone cVA is recognized by trichoid OSNs expressing DmelOR67d (Kurtovic et al., 2007).

Similar to the OR-expressing OSNs responsive to general odorants, ORco is also co-expressed with pheromone detecting PRs (Fleischer and Krieger, 2018). In *D. melanogaster*, the response of OR67d expressing OSNs to cVA is abolished in the absence of ORco (Jin et al., 2008). In the noctuid moth *Spodoptera frugiperda*, knock-out of ORco abolished the response of males to the main female sex pheromone components, with males being unable to successfully mate with females (Sun et al., 2023). However, in contrast to the notion of an OR/ORco mediated ionotropic pathway in general odor detection and in pheromone detection in *D. melanogaster*, studies conducted on the moth *M. sexta* have not found any evidence for ORco-dependent ionotropic pheromone transduction (Nolte et al., 2013; Nolte et al., 2016). Instead, it was proposed that ORco may act as a pacemaker channel that influences the kinetics of the pheromone response, putting forth the concept that pheromone evoked signal transduction processes may even rely on a metabotropic pathway in moths (Nolte et al., 2016). Noteworthy, in locusts, ORco is expressed in all OSNs of the basiconic sensilla (Yang et al., 2012), which house the OSNs expressing the pheromone receptors LmigOR70a and LmigOR35 (Chang et al., 2023; Guo et al., 2020). Indeed, in *L. migratoria*, targeted knock out of ORco resulted in severe impairments in the olfactory response to the pheromone PAN (Li et al., 2016). Although it is unclear what underlying role ORco plays in pheromone signal transduction processes in insects, it appears as a necessary element in the molecular machinery of pheromone responsive OSNs. In addition to ORco, verified PRs and other putative pheromone detecting ORs are co-expressed in OSNs with another protein called sensory neuron membrane protein 1 (SNMP1), required for a proper response to pheromones, which will be introduced in chapter 1.5.

1.4.2 Olfactory binding proteins and odorant degrading enzymes

In addition to the olfactory receptors located in OSN dendrites, sensillum lymph proteins expressed and secreted by support cells are necessary for the efficient and sensitive detection of odorants. Such proteins play a role in so-called perireceptor events by influencing the transient odorant-receptor interactions, either before or after odorant binding (Vogt et al., 2020). These are primarily members of the odorant binding protein (OBP) and the odorant degrading enzyme (ODE) families.

The OBPs are a well-studied and large family of globular proteins secreted into the aqueous sensillum lymph in strikingly high concentrations that possess lipophilic binding cavities (Steinbrecht, 1996; Steinbrecht et al., 1992; Klein, 1987; Galindo and Smith, 2001). OBPs were first discovered in moths but have since been found ubiquitously in other insects, including in flies and locusts, with each species expressing multiple OBP genes (Vogt and Riddiford, 1981; Brito et al., 2016; Jiang et al., 2018; Kim et al., 1998). They exhibit binding affinities to a broad spectrum of odorants and are proposed to help the solubilization and transport of the often hydrophobic odorant molecules from the sensillum pores towards the dendritic membrane (Vogt and Riddiford, 1981; Brito et al., 2016; Rihani et al., 2021; Leal, 2013). However, their significance in odor detection is being disputed since in some cases, loss of OBPs did not impact the sensitive detection to certain odors (Larter et al., 2016; Xiao et al., 2019), suggesting that the role of OBPs might depend on the chemical properties of the odorants.

Within the OBP family, a subset of members are attributed to pheromone detection and are called pheromone binding proteins (PBPs). PBPs were first discovered in the Lepidopteran species *A. polyphemus* (Vogt and Riddiford, 1981). High concentrations of PBPs were found in the sensillum lymph (Klein, 1987), and were deemed vital for the selective as well as sensitive detection of pheromones by their cognate PRs (Leal, 2013; Xu et al., 2005). An interplay of PBPs with distinct PRs has been proposed, as demonstrated for the moths *H. virescens* and *A. polyphemus* through functional experiments with cell lines expressing PRs that were stimulated with combinations of different PBP subtypes and pheromone components (Grosse-Wilde et al., 2006; Forstner et al., 2009). Similarly in *D. melanogaster*, OBP76a, also referred to as LUSH, is required to trigger the response of OR67d-expressing OSNs to the pheromone cVA, with the OSN's sensitivity considerably reduced in LUSH-deficient mutants (Xu et al., 2005; Laughlin et al., 2008; Stowers and Logan, 2008).

After the odorants trigger responses in OSNs, odorant molecules are supposed to be enzymatically inactivated by ODEs to prohibit a recurring reactivation of the receptors by the same ligands (Vogt et al., 1985; Chertemps et al., 2012). They thus play an integral part in rapid signal termination, which is crucial to sustain a proper olfactory response to repetitive stimuli (Vogt et al., 2020). ODEs comprise several classes of enzymes, such as aldehyde oxidases, aldehyde dehydrogenases, carboxylesterases, cytochrome P450s and various transferases, which are active towards specific functional groups of odorant molecules, such as alcohols, acetates, and aldehydes (Leal, 2013; Younus et al., 2014). In the antenna of *D. melanogaster*, 123 putative ODEs were described, with several members discovered per enzyme class (Younus et al., 2014). This is similar for the moth *B. mori*, where 127 antennal ODEs have been identified (Qiu et al., 2018). The high variety of ODEs expressed in the antenna are suggested to accommodate for a wide range of odorants and volatile

chemicals that may enter the sensillum lymph (Vogt et al., 2020). Yet surprisingly little is known about the functional mechanisms of this broad group of proteins in olfactory processes in insects.

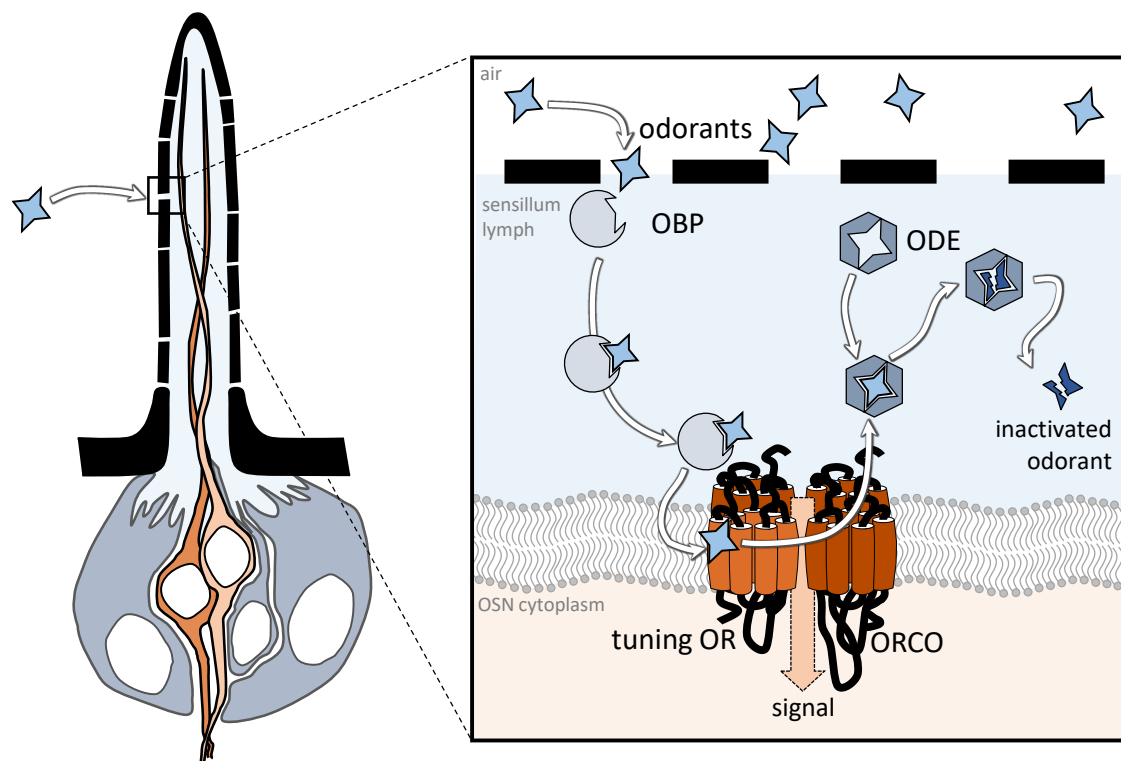


Figure 5. Model of sensillum processes in insect odorant detection. Odorants enter the sensillum through pores, where they are solubilized in the sensillum lymph by odorant binding proteins (OBPs) and then transported to the OSN dendrite membrane. They then bind to the tuning odorant receptor (OR) that is part of a heterotetrameric ligand gated ion channel complex together with the odorant receptor co-receptor (ORCO), initiating signal transduction. Afterwards, the odorant molecules are inactivated by odorant degrading enzymes (ODEs) to prohibit the prolonged or repeated binding to the tuning OR.

The best-characterized ODEs are those of moth pheromone-sensitive sensilla. Indeed, the first ODE identified was a male-specific esterase from the moth *A. polyphemus*, which is found in the sensillum lymph of the long trichoid sensilla (Vogt et al., 1985). Initial reports suggested that the sensillum esterase degrades the acetate component of the female's sex pheromone blend (Vogt et al., 1987; Vogt et al., 1988), which was later corroborated with kinetic studies of the purified enzyme revealing the rapid degradation rate of the added pheromone molecule (Ishida and Leal, 2005).

Studies were also conducted on the moth *B. mori*, where alcohol dehydrogenase was found to catalyze Bombykol to Bombykal, which is subsequently inactivated by an aldehyde oxidase to a long-chain fatty acid (E10,Z12-Hexadecanoic acid) (Pelletier et al., 2007; Kasang and Weiss, 1974; Rybczynski et al., 1990). In the *H. virescens* two ODEs were identified, aldehyde oxidase and aldehyde dehydrogenase, that inactivate the major (Z11:16Ald) and minor (Z9:14Ald) sex pheromone components to long-chain fatty acids of the same chain length (Tasayco and Prestwich,

1990). The altered moieties of the products assure that the compounds would no longer be able to activate the corresponding PRs. However, what remains unclear is how these inactivation products are ultimately removed from the sensillum lymph.

1.5 Sensory neuron membrane proteins

In addition to the molecular elements described earlier, another protein was uncovered in dendrites innervating the pheromone sensitive sensilla of the male moth *A. polyphemus*, which was somewhat arbitrarily called sensory neuron membrane protein or SNMP (Rogers et al., 1997; Vogt et al., 2020).

Soon after its discovery in *A. polyphemus*, studies conducted on the moth *M. sexta* have not only identified an SNMP ortholog, but revealed that there are two SNMP types in the antenna, SNMP1 and SNMP2 (Robertson et al., 1999). Later on, both types were identified in more Lepidopteran species, such as the moths *H. virescens* and *B. mori* (Rogers et al., 2001a). The availability of genomic and transcriptomic data from numerous species confirmed that SNMPs are ubiquitously expressed across the insect class, found in both holometabolous and hemimetabolous orders including Diptera, Hymenoptera, Coleoptera, Hemiptera and Orthoptera (Cassau and Krieger, 2021). More recently, a third SNMP type (SNMP3) was reported in the genome of several moth species, however in the case of *B. mori* and *H. armigera*, it does not appear expressed in the antenna but rather in the midgut, indicating a role outside of olfaction (Zhang et al., 2020; Xu et al., 2020).

Throughout the insect taxa, the antennal SNMP subtypes appear to be highly conserved, with SNMP1 orthologs of different species showing a higher sequence identity compared to SNMP2 of the same species, as they generally share a sequence similarity of 25-35% (Forstner et al., 2008; Zhang et al., 2020; Shan et al., 2020). For instance, HvirSNMP1 of the holometabolous moth *H. virescens* shares a higher sequence identity to SgreSNMP1 of the hemimetabolous locust *S. gregaria* than it does to HvirSNMP2 (Jiang et al., 2016).

Interestingly, expression of SNMP1 and SNMP2 subtypes have also been identified in organs beyond the antenna (Cassau and Krieger, 2021). Although SNMP1 is exclusively expressed in the antenna of most species (Zhang et al., 2020; Rogers et al., 1997; Leal et al., 2009; Jiang et al., 2016), it has been found in other chemosensory organs such as in the palps of *S. gregaria* and the moth *Spodoptera litura* (Lemke et al., 2020; Zhang et al., 2015b). In contrast, the SNMP2 type exhibits a much broader tissue distribution, found not only in organs associated with chemodetection, such as mouthparts and legs, but also in the abdomen, thorax and head (Zhang et al., 2015a; Xu et al., 2020; Liu et al., 2014; Jiang et al., 2016; Shan et al., 2020; Zhang et al., 2020). This suggests that

SNMP2 is involved with divergent functions, in addition to a proposed role in antennal olfactory processes.

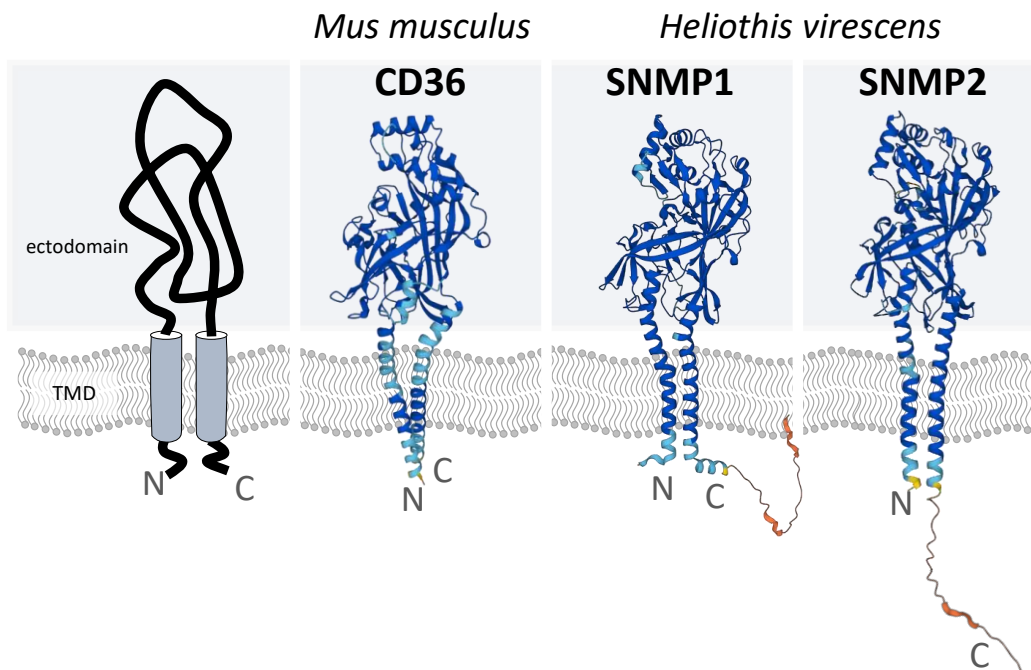


Figure 6. The membrane topology of CD36 proteins is conserved across the different homologs. CD36 proteins, such as *Mus musculus* CD36 and *H. virescens* SNMP1 and SNMP2 proteins possess two transmembrane domains (TMD) with intracellular N- and C-termini. They possess a large ectodomain with a hydrophobic internal tunnel-like structure. Predicted 3D structures were taken from the AlphaFold Protein Structure Database (EMBL-EBI). Blue colors indicate high model confidence, orange and yellow indicate low model confidence. AlphaFoldDB identification numbers: MmusCD36 = Q08857; HvirSNMP1 = Q9U1G3; HvirSNMP2 = B2RFN2.

Sequence based analyses have classified the SNMPs as insect-specific members of the large CD36 (cluster of differentiation 36) gene family, based on the eponymous CD36 protein first found in mammals (Rogers et al., 1997; Nichols and Vogt, 2008). Vertebrate CD36 proteins have exhibited diverse tissue distribution patterns and functional roles, including as receptors and transporters of various lipids and lipoproteins (Pepino et al., 2014; Silverstein and Febbraio, 2009). Typical for members of the CD36 family, SNMPs structurally form a protein with two relatively short transmembrane spanning domains and a large, ligand-interacting ectodomain (Jiang et al., 2016; Gomez-Diaz et al., 2016; Vogt et al., 2020), as shown in Figure 6.

1.5.1 Expression topography of SNMPs in the antenna

The analysis of the antennal expression topography and cellular localization of the SNMP types using *in situ* hybridization (ISH) and immunohistochemistry (IHC), as well as promoter driven expression of fluorescent proteins, has provided compelling evidence in support of their role in

olfaction (Rogers et al., 1997; Benton et al., 2007; Forstner et al., 2008; Blankenburg et al., 2019; Shan et al., 2020; Sun et al., 2019; Jiang et al., 2016; Rogers et al., 2001b).

The first identified SNMP type, ApolSNMP1 was immuno-localized in the dendrites of OSNs that extended into the sensillum shaft of male antennae (Rogers et al., 1997) and not long after, was also localized in the OSN dendrites of female antennae (Rogers et al., 2001b). Similar results were obtained through ISH and IHC experiments conducted with other lepidopteran species, localizing the respective SNMP1 orthologs in subsets of OSNs in *M. sexta*, *H. virescens*, and *Agrotis ipsilon* (Rogers et al., 2001a; Forstner et al., 2008; Gu et al., 2013). Moreover, the OSN expression of the SNMP1 subtype extends to other insect orders, namely the dipteran *D. melanogaster*, hymenopteran *Microplitis mediator*, and the orthopteran *S. gregaria* (Benton et al., 2007; Shan et al., 2020; Jiang et al., 2016). In fact, in all studied species, antennal SNMP1 appears exclusively expressed in neurons with the only exception observed in *D. melanogaster*, where SNMP1 was also detected in the support cells associated with SNMP1-positive OSNs (Benton et al., 2007).

Overall, SNMP1's presence in the OSNs provided the first indications that it may play an important role in primary odor detection processes. This is further supported by co-localization studies conducted on the antennae of *D. melanogaster*, *S. gregaria* and *H. virescens* with SNMP1 and ORco (used as a marker for OR-expressing OSNs), revealing that SNMP1 is found in a subset of OR-positive neurons (Benton et al., 2007; Jiang et al., 2016; Zielonka et al., 2018). In contrast, co-labelling studies with members of the IR receptor family depicted no co-expression with SNMP1 (Shan et al., 2020).

In moths, SNMP1 is specifically associated with the detection of pheromones due to its increased expression prior to adult eclosion (Rogers et al., 1997; Gu et al., 2013; Liu et al., 2013; Sun et al., 2019), coinciding with an increase in expression of putative PRs as well as its initial localization in pheromone sensitive sensilla of *A. polyphemus* (Gohl and Krieger, 2006; Rogers et al., 1997). Similar results were corroborated in the moth *H. virescens* through detailed fluorescence immunohistochemistry (FIHC) experiments, as SNMP1-positive OSNs were shown to innervate the pheromone detecting trichoid sensilla but not the basiconic sensilla (Blankenburg et al., 2019). These experiments also detailed the sexual dimorphism in the expression pattern of SNMP1 within the antenna, as males possess only a single SNMP1-positive OSN out of the total two to three OSNs per trichoid sensillum, while in females, all OSNs of a given sensillum are SNMP1-positive, indicating that males and females require SNMP1 in different capacities (Blankenburg et al., 2019). In light of its proposed role in pheromone detection, double FISH experiments revealed that all HR13- and HR6-expressing OSNs, which detect the cognate pheromone components Z11:16Ald and Z9:14Ald respectively, are co-expressed with HvirSNMP1 (Krieger et al., 2002; Pregitzer et al., 2014; Zielonka

et al., 2018). Coincidentally, even in the rudimentary larval antenna HvirSNMP1 was shown to be co-expressed with HR6-positive OSNs, and indeed, the larvae are capable of detecting the minor component Z9:14Ald (Zielonka et al., 2016). Its implied role in pheromone detection has also been suggested for *D. melanogaster*, where DmelSNMP1 is co-expressed in the OR67d-positive OSNs housed in trichoid sensilla that react to the pheromone component cVA (Benton et al., 2007; Kurtovic et al., 2007).

However, the proposed role of SNMP1 in locust pheromone detection does not appear to be as clear, since there are no co-labelling studies with confirmed pheromone sensitive ORs, such as LmigOR70a and LmigOR35 housed in basiconic sensilla (Chang et al., 2023; Guo et al., 2020). In fact, the antennal expression topography of SNMP1 has not been elucidated yet for *L. migratoria*. Instead, the expression pattern of SNMP1 was analyzed for the locust *S. gregaria* via fluorescence *in situ* hybridization (FISH) experiments, revealing that SgreSNMP1 transcripts are found in subsets of basiconic OSNs and likely all OSNs of trichoid sensilla (Jiang et al., 2016). Additionally, SgreSNMP1 was shown co-expressed with 33 out of a total of 83 tested ORs, underlining its importance for olfactory processes in the desert locust (Jiang et al., 2016).

Despite variability in the expression pattern across the different insect species, SNMP1 appears absent in coeloconic sensilla (Blankenburg et al., 2019; Jiang et al., 2016). This is in line with results showing that OSNs innervating the coeloconic sensilla express IRs, as opposed to ORs (Benton et al., 2009; Silbering et al., 2011).

In contrast to SNMP1, initial FISH analyses conducted on antennal sections of the moths *H. virescens* and *A. polyphemus* using SNMP2 riboprobes exhibited a specific support cell labelling pattern (Forstner et al., 2008). Additionally, a differential expression pattern emerged in co-labelling experiments visualizing both SNMP1 and SNMP2, supporting the novel non-neuronal expression of the SNMP2 type (Forstner et al., 2008). This expression pattern was substantiated in later experiments conducted in other insects, where SNMP2 appears exclusively expressed in antennal support cells of *A. ipsilon*, *M. mediator* and *S. gregaria* (Gu et al., 2013; Shan et al., 2020; Jiang et al., 2016). These findings contradict the nomenclature of the protein, as the SNMP2 type has not been detected in any sensory neurons in the antenna.

Another key difference of SNMP2 compared to SNMP1 is that SNMP2 appears to be expressed much broader along the antenna, having been visualized in most, if not all, support cells of various sensilla types with no sex-specific differences noted (Blankenburg et al., 2019; Shan et al., 2020; Gu et al., 2013). In fact, co-labelling studies visualizing SNMP2-positive cells alongside neurons have

demonstrated that multiple support cells underneath the sensilla express SNMP2, which appear to envelop the same OSN clusters (Blankenburg et al., 2019; Forstner et al., 2008; Sun et al., 2019).

So far, detailed analyses of the SNMP2 protein's localization are sparse, as FHC experiments have only been performed on the moths *A. ipsilon* and *H. virescens* (Gu et al., 2013; Blankenburg et al., 2019). In the former, immunogold labelling data showed the presence AipsSNMP2 in close proximity to the trichoid sensillum shaft (Gu et al., 2013). Alike for *H. virescens*, FHC experiments detected HvirSNMP2 in the apical most region of the support cells bordering the sensillum's lumen (Blankenburg et al., 2019). These regions of the support cells are distinguished by extensive microvilli-like membranes that are in direct contact with the sensillum lymph (Keil, 1989). Unfortunately, clear protein distribution of SNMP2 is missing in insects of other orders, thereby making it difficult to make general conclusions about SNMP2's function in insect olfaction.

However, the differential expression of SNMP1 and SNMP2 in OSNs and support cells, suggests a functional specialization of the SNMP types in the antenna. This raises the question, what roles may the neuronal and the non-neuronal SNMPs perform in insect olfactory sensilla?

1.5.2 Function of SNMPs in insect olfaction

The link between SNMP1 and pheromone detection has been envisioned early on with the discovery of ApolSNMP1 in pheromone-responsive sensilla followed by the co-localization of HvirSNMP1 and DmelSNMP1 with the respective pheromone receptors (Rogers et al., 1997; Benton et al., 2007; Pregitzer et al., 2014; Zielonka et al., 2018).

This has led to a model in which SNMP1 might operate as an additional co-receptor to the OR_x/ORco complex by passing signal molecules to the adjacent receptor (Vogt, 2003). In light of this view, split-ubiquitin yeast hybridization assays of moth BmorSNMP1 and HarmSNMP1 demonstrated protein interactions with the respective pheromone receptors BmorOR1 and HarmOR13 (Xu et al., 2020; Zhang et al., 2020). Additionally, *in vitro* and *in vivo* studies were conducted with *D. melanogaster*, where Förster resonance energy transfer assays using cell culture and fluorescent protein fragment complementation assays on the antenna revealed protein-protein interactions of DmelSNMP1 with ORs (German et al., 2013; Benton et al., 2007). Overall, these interaction studies indicate that SNMP1 orthologs are in close proximity to their respective co-expressed ORs, hinting at the formation of heteromeric SNMP1/OR_x/ORco complexes.

First functional studies of SNMP1 validated its relevance in pheromone detection in *D. melanogaster* SNMP1-knock outs, where single sensillum recordings (SSR) of DmelSNMP1-deficient mutants displayed significantly attenuated responses to cVA in OR67d-OSNs that was

restored in DmelSNMP1 neuronal rescues (Benton et al., 2007). Comparable results were obtained for SNMP1-null mutants of the noctuid moth *H. armigera*, where HarmSNMP1 was described as indispensable for the appropriate detection of the long-chain sex pheromone components Z11:16Ald and Z9:16Ald (Liu et al., 2020). Additionally, mating behavior observations of HarmSNMP1-null mutant males showed lowered attraction to calling females, which ultimately resulted in significantly decreased copulation (Liu et al., 2020). Furthermore, in RNA interference based experiments knocking down SNMP1 in *B. mori*, males were hindered in their ability to locate pheromone-releasing females (Zhang et al., 2020).

The importance for SNMP1 in facilitating the detection of fatty acid derived pheromones was investigated in calcium imaging experiments of cell lines heterologously expressing *H. virescens* HR13 alone or with HvirSNMP1 (Pregitzer et al., 2014). The presence of HvirSNMP1 increased the sensitivity of the cells to the main sex pheromone component by about 1000-fold (Pregitzer et al., 2014). Furthermore, analysis of the response kinetics of OR67d-OSNs in DmelSNMP1-deficient flies uncovered that SNMP1 was not only found to be required for a sensitive pheromone response but may also play an important role in the rapid activation and inactivation after the applied pheromone stimulus (Li et al., 2014).

Structure-activity based analysis revealed that SNMP1's ectodomain was deemed essential for its proper function, in contrast to the more dispensable intracellular and transmembrane domains (Gomez-Diaz et al., 2016). This was evident in SSR studies of various *D. melanogaster* mutants expressing DmelSNMP1 with single amino acid exchanges along the ectodomain, where a loss of pheromone-evoked responsiveness was observed in the trichoid sensilla (Gomez-Diaz et al., 2016). In fact, the ectodomain of mammalian CD36 protein was sufficient to show the wide range of ligand binding capability to the pheromone molecules cVA, Bombykol and Z11:16Ald, all long-chain aliphatic molecules, in surface plasmon resonance assays, thus also demonstrating that different members of the CD36 family can interact with similar molecules (Gomez-Diaz et al., 2016).

To further elucidate the role of the ectodomain for its function, homology based modelling of insect SNMPs to mammalian CD36 homolog LIMP-2 was performed (Gomez-Diaz et al., 2016). This revealed a putative tunnel spanning through SNMP1's ectodomain, with an internal diameter wide enough to allow the passage of pheromone molecules (Gomez-Diaz et al., 2016). Consequently, blocking the tunnel with amino-acid substitutions caused a diminished pheromone-evoked response in OSNs (Gomez-Diaz et al., 2016). This establishes a model in which neuronal SNMP1 allocates the extracellular hydrophobic pheromones via its tunnel-structure from PBPs to the ligand-binding site of the cognate pheromone receptors, as demonstrated for the moth *H. virescens* in Figure 7.

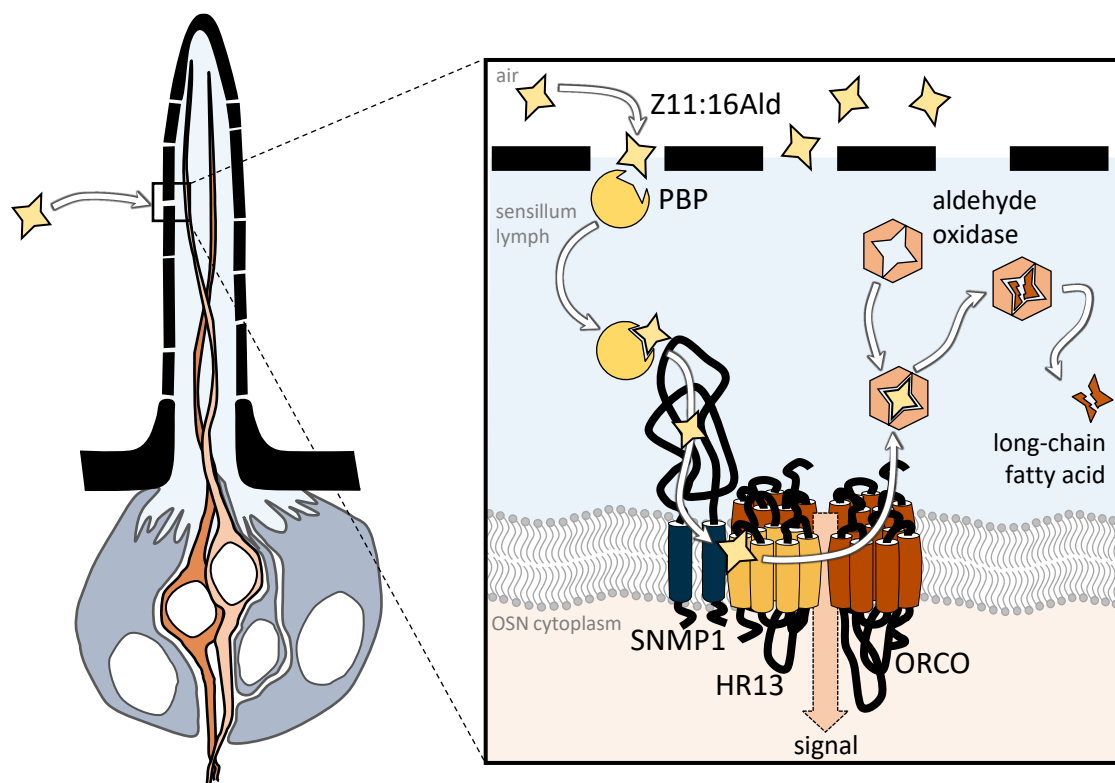


Figure 7. Proposed role of SNMP1 in pheromone detection as exemplified for the moth *H. virescens*. Pheromone molecules (Z11:16Ald) that enter the sensillum bind to pheromone binding proteins (PBPs) that transport the pheromone to the dendritic membrane of a pheromone-responsive OSN. Here, it first binds to the sensory neuron membrane protein 1 (SNMP1), which funnels the pheromone molecule to the adjacent pheromone receptor (HR13)/ORCO complex. After the receptor activation, the pheromone molecule is released from the receptor complex and is then inactivated by the pheromone degradation enzyme, aldehyde oxidase, which converts Z11:16Ald to a long-chain fatty acid of the same chain length.

In stark contrast to SNMP1, considerably much less is known about the support cell expressed SNMP2. A role in olfactory processes can be deduced by its antennal expression pattern and the protein's cellular localization, the latter of which is only known for moths (Rogers et al., 1997; Gu et al., 2013; Blankenburg et al., 2019). Considering that SNMP2 is expressed more broadly than SNMP1 and is not found in the OSNs, its contribution to olfaction may be more general compared to SNMP1's specific role in pheromone recognition. Therefore, based on SNMP2's localization in numerous support cells and its homology to CD36 proteins, which include transporters of various long chain lipids, an earlier study proposed that it may mediate the removal of lipophilic substances out of the sensillum lymph (Forstner et al., 2008). In fact, non-SNMP insect CD36 members have been noted to perform similar functions, such as *D. melanogaster* NinaD and Santa Maria that act as fatty acid transporters (Kiefer et al., 2002; Giovannucci and Stephenson, 1999; Wang et al., 2007). In support of this concept, SNMP2 is localized at the apex of the support cells, which directly border the sensillum lymph (Blankenburg et al., 2019). However, due to the overall lack of functional studies conducted on SNMP2, its relevance for olfaction remains to be determined.

1.6 Aims of the thesis

Currently, our knowledge on the role of SNMPs in the insect olfactory system is limited. In particular, there is lack of comprehensive studies investigating the cellular expression and addressing the specific function of the SNMP types. Therefore, this thesis aims to elucidate the topographic distribution and subcellular localization of SNMPs in the antenna and assess the functional relevance of support cell-expressed SNMP2 in the insect olfactory system. The upcoming three chapters consist of three published manuscripts that focus on specific aspects of SNMPs expression and olfactory function in different insect species and orders.

While there are studies on the cellular distribution of SNMP1 and SNMP2 proteins in holometabolous insects, little is known about their expression topography in the antenna of hemimetabolous species, such as locusts. Therefore, **Manuscript 1** focuses on investigating the sensillum-specific expression and subcellular localization of the SNMP1 and SNMP2 proteins along the antenna of the desert locust *S. gregaria*.

As hemimetabolous insects, the general antennal morphology of *S. gregaria* exhibits little changes throughout its development. However, it is unclear whether a sensilla- and cell-type-specific SNMP distribution pattern is established in the nymphal stages and whether a pattern established in the first nymph stage remains conserved throughout locust development. To address the question, **Manuscript 2** focuses on the topography of SNMP1 and SNMP2 expression in the antenna of different juvenile stages of the desert locusts.

In moths and flies, OSN-expressed SNMP1 has been demonstrated as a requirement for the efficient detection of pheromones. However, currently there are no studies regarding the role of support cell-expressed SNMP2 despite its broad expression in the antenna of moths such as *H. virescens*, a model organism which has been extensively studied in the context of pheromone detection. To gain first insights into SNMP2 function in support cells, **Manuscript 3** focuses on assessing the roles of both the SNMP2 protein as well as support cells in pheromone-responsive sensilla of the moths *H. virescens* and *B. mori* through functional and behavioral assays.

Chapter 2. Manuscript 1



Article

The Sensilla-Specific Expression and Subcellular Localization of SNMP1 and SNMP2 Reveal Novel Insights into Their Roles in the Antenna of the Desert Locust *Schistocerca gregaria*

Sina Cassau ^{1,*}, Doreen Sander ¹, Thomas Karcher ^{1,2}, Michael Laue ³, Gerd Hause ⁴, Heinz Breer ⁵ and Jürgen Krieger ^{1,*}

- ¹ Department of Animal Physiology, Institute of Biology / Zoology, Martin Luther University Halle-Wittenberg, 06120 Halle (Saale), Germany; doreen.sander@zoologie.uni-halle.de (D.S.); thomas.karcher@bmglabtech.com (T.K.)
 - ² BMG Labtech GmbH, 77799 Ortenberg, Germany
 - ³ Advanced Light and Electron Microscopy, Centre for Biological Threats and Special Pathogens 4 (ZBS 4), Robert Koch Institute, 13353 Berlin, Germany; lauem@rki.de
 - ⁴ Microscopy Unit, Biocenter, Martin Luther University Halle-Wittenberg, 06120 Halle (Saale), Germany; gerd.hause@biozentrum.uni-halle.de
 - ⁵ Institute of Physiology, University of Hohenheim, 70599 Stuttgart, Germany; h.breer@uni-hohenheim.de
- * Correspondence: sina.cassau@zoologie.uni-halle.de (S.C.); juergen.krieger@zoologie.uni-halle.de (J.K.)



Citation: Cassau, S.; Sander, D.; Karcher, T.; Laue, M.; Hause, G.; Breer, H.; Krieger, J. The Sensilla-Specific Expression and Subcellular Localization of SNMP1 and SNMP2 Reveal Novel Insights into Their Roles in the Antenna of the Desert Locust *Schistocerca gregaria*. *Insects* **2022**, *13*, 579. <https://doi.org/10.3390/insects13070579>

Academic Editor: Daniel Doucet

Received: 1 June 2022

Accepted: 22 June 2022

Published: 25 June 2022

Publisher's Note: MDPI stays neutral with regard to jurisdictional claims in published maps and institutional affiliations.



Copyright: © 2022 by the authors. Licensee MDPI, Basel, Switzerland. This article is an open access article distributed under the terms and conditions of the Creative Commons Attribution (CC BY) license (<https://creativecommons.org/licenses/by/4.0/>).

Simple Summary: The desert locust, *Schistocerca gregaria*, can form gigantic swarms of millions of individuals that devastate the vegetation of invaded landscapes. Locust food search, reproduction, and aggregation behaviors are triggered and controlled by complex olfactory signals. Insects detect odorants through different types of olfactory sensilla on the antenna that house olfactory sensory neurons and associated support cells, both of which express the proteins required for olfactory signaling. Among these proteins, two members of the CD36 lipid transporter/receptor family, named sensory neuron membrane proteins 1 and 2 (SNMP1 and SNMP2), are indicated to be of vital importance. Towards a better understanding of the role of the two SNMPs in the olfactory system of *S. gregaria*, we have analysed their antennal topography and subcellular localization using specific antibodies. The results indicate sensilla type- and cell type-specific distribution patterns of the SNMP proteins. SNMP1 was located in the receptive dendrites of subpopulations of olfactory sensory neurons as well as in the microvilli of associated support cells, suggesting a dual function of this protein, both in olfactory signal detection and in sensillum lymph maintenance, respectively. In contrast, SNMP2 was found solely in support cells and their microvilli membranes, suggesting a role limited to sensillum lymph recovery processes.

Abstract: Insect olfactory sensilla house olfactory sensory neurons (OSNs) and support cells (SCs). The olfactory sensory processes require, besides the odorant receptors (ORs), insect-specific members of the CD36 family, named sensory neuron membrane proteins (SNMPs). While SNMP1 is considered to act as a coreceptor in the OR-mediated detection of pheromones, SNMP2 was found to be expressed in SCs; however, its function is unknown. For the desert locust, *Schistocerca gregaria*, we previously visualized mRNA for SNMP1 in OSNs and SNMP2 mRNA in cells associated with OSN clusters. Towards an understanding of their functional implication, it is imperative to explore the cellular and the subcellular localization of the SNMP proteins. Therefore, we have generated polyclonal antibodies against SNMP1 and SNMP2 and used fluorescence immunohistochemistry (FIHC) to visualize the SNMP proteins. We found SNMP1 in the somata and respective dendrites of all OSNs in trichoid sensilla and in subsets of OSNs in basiconic sensilla. Notably, SNMP1 was also detected in SCs of these sensilla types. In contrast, SNMP2 protein was only visualized in SCs of basiconic and coeloconic sensilla, but not of trichoid sensilla. Exploring the subcellular localization by electron microscopy using anti-SNMP1-ab and anti-SNMP2-ab revealed an immunogold labelling of SC microvilli bordering the sensillum lymph. Together our findings suggest a dual role of SNMP1 in the antenna of *S. gregaria*, in some OSN subpopulations in odor detection as well as in functions of some SCs, whereas the role of SNMP2 is limited to the functions of support cells.

Keywords: olfaction; locust; sensilla; olfactory sensory neuron; support cell; odorant detection; sensory neuron membrane protein

1. Introduction

The desert locust, *Schistocerca gregaria*, is dreaded for its ability to form huge swarms of many millions of individuals that have devastating impacts on the vegetation and crops of invaded landscapes. In locusts, odorants originating from food sources and oviposition sites or released as pheromones from conspecifics are important olfactory cues that trigger various behaviors crucial for survival and reproduction [1–4]. Odorant detection in locusts is accomplished by olfactory sensory neurons (OSNs) located in thousands of olfactory units, called sensilla, found mainly on the antenna [5,6] and in low numbers on mouthparts, i.e., the labial and maxillary palps [7,8]. On the antenna, locusts comprise three morphologically different sensilla with basiconic sensilla housing up to 50 OSNs, trichoid sensilla having 3 OSNs, and coeloconic sensilla bearing 4 OSNs. In each case, the OSNs are associated with several glia-like support cells [6]. In insects, both OSNs and support cells (SCs) express the proteins acting in the primary processes of odorant detection. While OSNs comprise olfactory receptors in their dendritic membrane that belong to the families of insect odorant receptors (ORs) and ionotropic receptors (IRs) [9–12], SCs express odorant binding proteins (OBPs) supposed to mediate the transfer of odorants through the sensillum lymph towards olfactory receptors [13–15]. In addition, so-called sensory neuron membrane proteins (SNMPs) are of critical importance in insect olfactory signaling [16–18].

SNMPs form an insect-specific lineage within the CD36 family of lipid/lipoprotein receptors and transporters [16,19]. CD36 proteins are characterized by two transmembrane domains and a large extracellular domain that is critical for ligand interaction [20,21]. Mammalian CD36 proteins, as well as non-SNMP family members in insects, have vital functions in the transport and reception of lipophilic compounds, lipoprotein scavenging, innate immune signalling, and cell adhesion [19,22–24]. Worth mentioning, in mice, a role of CD36 was reported in oleic acid detection by OSNs [25,26] as well as in sensing fatty acids by taste cells [27].

Insect SNMPs form a diverse gene family with variable numbers of SNMPs across species and orders. For example, only two SNMPs are found in *Drosophila melanogaster* [19] and *Schistocerca gregaria* [28], whereas 16 SNMPs were identified in the dung beetle *Onthophagus taurus* [29]. Based on phylogenetic relationships, insect SNMPs have been classified into four main groups (SNMP1–4) [29,30], with members of the SNMP1 and SNMP2 groups present in each species analyzed to date [31]. Consequently, studies on the expression and function of SNMPs in the olfactory system have concentrated on these two subtypes. The SNMP1 type has been discovered as protein expressed in the dendrites of pheromone-sensitive OSNs of the moth *Antheraea polyphemus* [32] and found to be essential for a sensitive detection of lipophilic pheromones in *Drosophila melanogaster* [17,18] and heliothine moth species [33,34]. Additionally, a requirement for rapid activation and deactivation of pheromone-induced activity of OSNs has been reported [35]. Most recent data indicate binding of ligands to the large, tunnel-like ectodomain of SNMP1 [21] and colocalization in the dendritic membrane with the OR/odorant receptor–coreceptor (Orco) complex [30,36,37], supporting SNMP1 as further coreceptor possibly involved in the transfer of odorant molecules from OBPs to their cognate OR.

SNMP2s have been classified as a second SNMP type in moths, locusts, and other insect species reviewed in [31] and shares about 25–30% amino acid sequence identity to SNMP1. However, despite its name, sensory neuron membrane protein 2, SNMP2, exhibits a broad expression in support cells of olfactory sensilla [38,39], which are thought to control the composition of the sensillum lymph [40,41]. Given its expression in support cells and apparent evolutionary relationship to CD36 family proteins, SNMP2 has been suggested to function in clearing the sensillum lymph from lipophilic odorants or their degradation

products [39,42]. However, so far only two immunohistochemical studies in the moths *Heliothis virescens* [39] and *Agrotis ipsilon* [38] provide a hint for localization of the protein in the microvillar protrusions of support cells bordering the sensillum lymph.

In *Schistocerca gregaria*, the expression of SNMP1 and SNMP2 in the antenna has only been studied on the mRNA level. Using fluorescence in situ hybridization (FISH), SNMP1 transcripts were found in a subpopulation of the antennal OSNs, whereas SNMP2 expression was detected in cells surrounding OSN clusters, likely the support cells [28]. In addition, FISH experiments revealed co-expression of SNMP1 and certain members of the desert locust OR family in a subpopulation of OSNs located in basiconic sensilla and trichoid sensilla, but not in coeloconic sensilla [43]. Notably, SNMP1 was found co-expressed with 33 ORs of 83 ORs tested, suggesting that SNMP1 might function not only in the sensitive detection of pheromones but also of other important olfactory cues [44,45]. Together, the FISH experiments revealed a first picture of the expression of SNMP1 and SNMP2 on the mRNA level. However, with regard to the functions of SNMPs in the olfactory system of locusts, it is of critical importance to elucidate the cellular and subcellular localization of the SNMP proteins. Therefore, we set out to analyze the topography of SNMP subtypes in the antennae of *S. gregaria* on the protein level. Towards this goal, we have generated specific antibodies against the extracellular domains of the two proteins and used them in comprehensive fluorescent immunohistochemical approaches to explore the locust antenna. Furthermore, immunogold labelling experiments with transmission electron microscopy were performed to determine the subcellular localization of SNMP1 and SNMP2 in cells of olfactory sensilla.

2. Materials and Methods

2.1. Animal Rearing

Desert locusts, *Schistocerca gregaria*, and migratory locusts, *Locusta migratoria*, were reared under crowded (gregarious) conditions as described in Seidelmann et al. [46]. Briefly, 100 to 150 individuals were kept in metal cages (50 × 50 × 50 cm) with metal grids at the bottom and at two sides. The photoperiod was 12L: 12D. The temperature was 34 °C during the day and 27 °C at night. The insects were fed with fresh wheat seedlings and flaked oats.

2.2. Bacterial Expression of *S. gregaria* SNMP Ectodomains (SgreSNMPecto)

The large ectodomains of SgreSNMP1 and SgreSNMP2 were expressed as His-tagged proteins using the pASK-IBA37plus expression system. The extracellular domains of the SNMPs were predicted with the THMMH 2.0 program [47] and amplified from plasmids containing the full-length coding regions using the following oligonucleotide primers: SgreSNMP1: 5'-AAG GAA TTC AAG CTC ATC TCC AGC CAG ATA-3' and 5'-AAG CCC AAG CTT TTA GCC CTG CAT CCG GAA-3'; SgreSNMP2: 5'-AAG GAA TTC TTC CCC GCC ATT CTC ACC-3' and 5'-AAG AAG CTT TTA CAT CGA CGC CCG CGC-3'. The PCR products were first cloned into the pGEM-T Easy Plasmid (Promega, Madison, WI, USA), excised from the vector by digestion with EcoRI-HF and HindIII (New England Biolabs, Ipswich, MA, USA) and subsequently ligated into the corresponding sites of the pASK-IBA37plus expression vector (IBA Lifesciences GmbH, Göttingen, Germany). The resulting SNMP1ecto/pASK-IBA37plus and SNMP2ecto/pASK-IBA37plus expression vectors were transformed into the *E. coli* strain MG1655. For SNMPecto expression, single colonies of the respective bacteria were inoculated in 100 mL LB medium with 100 µg/mL ampicillin. Bacteria were grown at 200 rpm and 37 °C until an OD₆₀₀ between 0.6–0.7 was obtained. Then, expression was induced by adding 200 µg/L anhydrotetracycline. After incubation for 3 h, the bacteria were harvested by centrifugation at 5000 rpm for 15 min at 4 °C and resuspended in 6 mL of Tris-HCl buffer (50 mM Tris-HCl, 500 mM NaCl, 20 mM imidazole) supplemented with 1 mM phenylmethylsulfonyl fluoride (PMSF), 6 mM MgCl₂, 4M urea, and 0.2 mg/mL lysozyme.

Successful bacterial overexpression of SNMP1ecto and SNMP2ecto proteins was verified by analyzing aliquots of induced and non-induced bacterial lysates by SDS-PAGE of on 12% gels and comparing protein patterns after Coomassie blue staining. Predicted sizes (including the His-tag and some vector-encoded amino acids) were 50.57 kDa for SNMP1ecto and 50.64 kDa for SNMP2ecto proteins and were evaluated by comparison to a protein molecular weight ladder (Thermo Scientific, Waltham, MA, USA).

2.3. Antibody Production

Proteins of induced bacteria overexpressing SNMP1ecto and SNMP2ecto proteins, respectively, were separated on parallel lanes by 12% SDS-PAGE and visualized by Coomassie blue staining. Intensive protein bands corresponding to the predicted size of the recombinant SgreSNMP1 and SgreSNMP2 proteins were excised out of the gels using a scalpel and collected to give an estimated amount of about 1.5 mg protein each. The proteins in gel fragments were used by a custom service (Davids Biotechnologie GmbH, Regensburg, Germany) to generate polyclonal antibodies against the ectodomains of SgreSNMP1 and SgreSNMP2 in rabbits using standard procedures and immunization for 63 days. The resulting antibodies, named anti-SNMP1-ab and anti-SNMP2-ab in the following, were purified using an antigen-specific affinity matrix.

2.4. Western Blot Analysis

For SDS-PAGE and Western blot analysis, 5 µg of total protein from bacterial lysates of induced and non-induced bacteria were separated in 12% gels. Two gels were prepared in parallel and either stained with Coomassie blue, or electroblotted with a semi-dry apparatus onto a PVDF membrane soaked in transfer buffer (25 mM Tris, 192 mM glycine, 20% methanol) at 200 mA for 1 h. The blotted membranes were then incubated for 1 h in TBST (100 mM Tris, 150 mM NaCl, pH 7.5 supplemented with 0.05% Tween 20) with 7% milk powder, followed by treatment with the primary antibodies, either anti-SNMP1-ab (1:7000) or anti-SNMP2-ab (1:7000), diluted in TBST with 3.5% milk powder overnight at 4 °C. Subsequently, the membranes were washed 3 times for 10 min with TBST, then incubated with goat-anti-rabbit alkaline phosphatase (ref. number 31346, Thermo Scientific) diluted 1:10,000 in TBST with 3.5% milk powder for 1h. After washing 3 times for 10 min each with TBST and 2 times for 10 min in substrate buffer (100 mM Tris-HCl, 100 mM NaCl, 5 mM MgCl₂, pH 9.5), immune reactivity was detected by incubation in 0.0225% NBT (nitro blue tetrazolium) and 0.0175% BCIP (5-brom-4-chlor-3-indolyl phosphate) in substrate buffer.

2.5. Fluorescent Immunohistochemistry (FIHC)

Fluorescence immunohistochemistry (FIHC) was performed as previously described [39,48] with few modifications. Adult male and female *S. gregaria* and *L. migratoria* were removed from the stock cultures and cold anesthetized on ice. The antennae were carefully dissected and immediately embedded into Tissue-Tek O.C.T. freezing medium (Sakura Finetek, Alphen aan den Rijn, The Netherlands) at −20 °C. Cryosections (12 µM) of the samples were prepared with a Cryostar NX50 cryostat (Thermo Scientific) at −20 °C. Sections were thaw-mounted onto SuperFrost Plus slides (Thermo Scientific) and kept cold at −20 °C until encircling them using colourless ROTI[®]Liquid Barrier Marker (Carl Roth, Karlsruhe, Germany). Next, sections were fixed by incubation of the slides for 20 min at 4 °C with 4% paraformaldehyde dissolved in phosphate buffered saline (PBS, 145 mM/L NaCl, 1.4 mM/L KH₂PO₄, 8 mM/L Na₂HPO₄, pH 7.4). Afterwards, the sections were rinsed at room temperature consecutively in PBS two times for 5 min, in PBS with 0.01% Tween20 for 5 min, in 50 mM NH₄Cl in PBS for 5 min, and finally in PBS for 5 min. After incubating the samples in blocking solution (10% normal goat serum, 0.5% Triton-X100 in PBS) for 30 min at room temperature, the sections were incubated with the primary antibody diluted in blocking solution overnight at 4 °C in a humid box (anti-SNMP1-ab 1:500 on *S. gregaria* sections and 1:250 on *L. migratoria* sections; anti-SNMP2-ab 1:100). The slides were then

washed three times for 5 min with PBS and subsequently treated with goat-anti-rabbit AF488-conjugated secondary antibodies (1:1000) (Jackson ImmunoResearch, Ely, Great Britain), goat-anti-HRP Cy3 (1:400) (Jackson ImmunoResearch), and DAPI (1:500, Thermo Fisher Scientific) diluted in PBS, for 1 h at room temperature in a humid box. Finally, the slides were washed two times for 5 min in PBS, once for 5 min in H₂O, and then mounted in Mowiol solution.

2.6. Combined FIHC and Fluorescent In Situ Hybridization (FISH)

Orco and SNMP1 antisense riboprobes were generated as described previously [8]. Briefly, specific primers were used to amplify coding sequences of *SgreOrco* (5'-CACTGGATGCTCGAGTACAGCGGCG and 5'-CGAGCTCTCTTCAATGAGCCTGTIG). The resulting products were cloned into pGEM-T Easy Plasmids (Invitrogen), which were subsequently used to generate digoxigenin-labelled Orco- and SNMP1-specific antisense RNAs using the T7/Sp6 RNA transcription system (Roche Diagnostics, Mannheim, Germany) as recommended by the manufacturer.

For combined FIHC/FISH experiments, antennae from *S. gregaria* were prepared, embedded, and sectioned into 12 µm slices as described above. After sectioning, the samples were treated for 20 min at 4 °C with 4% paraformaldehyde dissolved in PBS, washed in PBS for 5 min, and then incubated in 0.2 M HCl for 10 min. After washing the samples two times for 2 min in PBS, the slides were transferred into pre-hybridization solution (5× SSC (0.75 M NaCl, 0.075 M sodium citrate, pH 7.0) and 50% formamide) for 10 min. Next, each slide was covered with 130 µL hybridization solution (50% formamide, 25% H₂O, 25% Microarray Hybridization Solution Version 2.0 (GE Healthcare, Freiburg, Germany)) containing either the ORCO or the SNMP1 antisense riboprobe. After placing a coverslip on top, slides were incubated in a humid box (50% formamide) at 60 °C overnight. The slides were then washed two times for 30 min each in 0.1× SSC at 60 °C. The sections were then washed with Tris-buffered saline (TBS; 100 mM Tris, 150 mM NaCl, pH 7.5) for 5 min at room temperature, which was followed by a blocking step in 1% blocking reagent (Roche Diagnostics, Mannheim, Germany) in TBS supplemented with 0.3% Triton X-100 for 30 min at RT. Afterwards, 130 µL of a mixture of anti-digoxigenin alkaline phosphatase-conjugated antibody (Roche Diagnostics) (1:500) and anti-SgreSNMP1-ab (1:200) diluted in 1% blocking reagent in TBS, 0.3% Triton X-100, were added on each slide. A coverslip was placed on top, and the slides were incubated at 4 °C overnight. The sections were then washed three times for 5 min in TBS supplemented with 0.05% Tween20 (TBST) and were transferred into 150 mM Tris-HCl solution (pH 8.3) for 5 min. For visualization of the digoxigenin-labelled probes, the Vector red alkaline phosphatase substrate kit (Vector Laboratories, Burlingame, CA, USA) was used according to the manufacturer. Briefly, 50 µL of each Vector red reagent (1,2, and 3) were diluted in 5 mL of 150 mM Tris-HCl (pH 8.3) to create the substrate solution that was applied to each section for 1h at room temperature. The sections were then washed three times for 5 min in TBST, followed by an incubation with goat-anti-rabbitAF488 1:1000 and DAPI (1:500) diluted in TBST for 1 h at room temperature. The sections were then washed two times for 5 min in H₂O, then mounted in Mowiol. In combined FIHC/FISH experiments where FIHC was used to visualize neurons, the goat-anti-HRP Alex Fluor 647-conjugated antibody (Jackson ImmunoResearch) (1:200) was used in place of anti-SNMP1-ab and goat-anti-rabbitAF488.

2.7. Analysis of Antennal Sections by Confocal Microscopy

Sections from FIHC and FISH experiments were analysed on confocal laser scanning microscopes (LSM 880 and LSM780, Carl Zeiss Microscopy, Jena, Germany). Confocal image stacks of the fluorescence and transmitted-light channels were taken and used to generate either pictures representing single optical planes or projections of optical planes applying the ZEN software (Carl Zeiss Microscopy, Jena, Germany). Pictures were not altered except for adjusting the brightness or contrast for a uniform tone within a single figure.

2.8. Sample Preparation for Electron Microscopy and Immunogold Labelling

The antenna of *S. gregaria* were removed from the head, dissected into 1–2 mm long segments and transferred into the indentations of an aluminum specimen carrier (3 mm wide and 100 µm deep), which was filled with 1-hexadecene. Subsequently, the specimen carrier was covered by another aluminum specimen carrier (3 mm wide, flat) and high-pressure frozen with HPF01 compact (Engineering Office M. Wohlwend, Sennwald, Switzerland). Samples were freeze-substituted in acetone containing 0.5% glutaraldehyde, 5% distilled water for 24 h at $-86\text{ }^{\circ}\text{C}$ in an automatic freeze substitution system (AFS, Leica Microsystems, Wetzlar Germany). After increasing the temperature to $-70\text{ }^{\circ}\text{C}$ ($1\text{ }^{\circ}\text{C}/\text{h}$), samples were incubated for 12 h at $-70\text{ }^{\circ}\text{C}$, and then the temperature was raised to $0\text{ }^{\circ}\text{C}$ ($5\text{ }^{\circ}\text{C}/\text{h}$). After further 4 h incubation at $0\text{ }^{\circ}\text{C}$, the samples were briefly washed with acetone at room temperature, followed by washing twice for 5 min each with ethanol at room temperature. Subsequently, the antennal fragments were infiltrated with hard-grade LR White (Science Services, Germany) mixed 1:1 with ethanol for 30 min, followed by an ascending concentration of 2:1 (LR White:ethanol) for 30 min at room temperature and overnight incubation in pure LR White at $5\text{--}8\text{ }^{\circ}\text{C}$. After the samples were incubated in fresh LR White for additional 5 h at room temperature, the antenna were embedded in pure LR White and polymerized at $60\text{ }^{\circ}\text{C}$. Ultrathin sections (70 nm) were generated using an ultramicrotome (Ultracut S, Leica Microsystems) and collected on formvar coated nickel grids subsequently treated with blocking solution (1% acetylated BSA in PBS) for 30 min at room temperature then incubated with the primary antibodies (anti-SNMP1-ab 1:100, anti-SNMP2-ab 1:100) diluted in blocking solution over night at $4\text{ }^{\circ}\text{C}$. Afterwards, the samples were then rinsed 4 times for 5 min with blocking solution at room temperature, followed by treatment of the secondary anti-rabbit-antibody conjugated with 10 nm gold granules (G7402, Sigma-Aldrich, St. Louis, MO, USA) diluted 1:100 in blocking solution for 90 min at room temperature. After washing the samples four times for 5 min with distilled water, the grids were left to air dry and were ready for assessment with the transmission electron microscope (EM900, Carl Zeiss Microscopy) operating at 80 kV. The images were recorded using a Variosped SSCCD camera SM-1k-120 (TRS, Moorenweis, Germany).

3. Results

3.1. Bacterial Expression of SNMP Ectodomains and Generation of Anti-SNMP Antibodies

In order to generate specific antibodies against *S. gregaria* SNMP1 and SNMP2, we have expressed the ectodomains of the respective proteins (Figure S1) in *E. coli* bacteria using an inducible expression system. The successful overexpression of the SNMP1ecto and SNMP2ecto proteins in induced bacteria was documented by SDS-polyacrylamide gel electrophoresis (PAGE) and Coomassie blue staining of total bacterial proteins from comparing induced (+) and not induced (–) samples (Figure 1A). Intense protein bands at the predicted molecular weight of the ectodomains of about 51 kDa were found only in the induced samples (Figure 1A). In a next step, the respective intense protein bands were excised from SDS-polyacrylamide gels and used to produce polyclonal antibodies against the SNMP1ecto and SNMP2ecto proteins in rabbits.

To assess the efficiency and specificity of the two newly created antibodies for SNMP1 and SNMP2, respectively, Western blot experiments with induced and uninduced samples from SNMP1ecto and SNMP2ecto bacteria were performed. The ectodomains of SNMP1 and SNMP2 share a sequence identity of approximately 34% (Figure S1) that is assumed to exclude a cross reaction of the corresponding antibodies. In accordance with this notion, anti-SNMP1-ab only detected an intense band of the correct size in the induced SNMP1ecto sample (Figure 1B), demonstrating the efficiency and specificity of the antibody for SNMP1. Similarly, anti-SNMP2-ab visualized a very strong band in the induced SNMP2ecto sample (Figure 1C). Faint bands were also visualized in the uninduced bacteria samples and the induced bacteria sample from SNMP1ecto. This is likely due to the detection of low amounts of native bacterial proteins that may have been present in the excised gel fragments used to generate the anti-SNMP2-ab. We also noticed that in the induced SNMP1ecto

sample, the thin band runs slightly lower than in the non-induced samples, possibly due to displacement of reactive bacterial proteins by the huge amount of SNMP1ecto proteins, which most importantly are not detected by anti-SNMP2-ab (asterisk, Figure 1C). Since the presence of reactive bacterial proteins is very unlikely in antennal preparations, the observed cross reaction can be assumed to not disturb experiments with antenna. Together, the results indicate successful generation of specific antibodies against the ectodomains of *S. gregaria* SNMP1 and SNMP2, respectively, that were subsequently used for fluorescence immunohistochemical (FIHC) analysis.

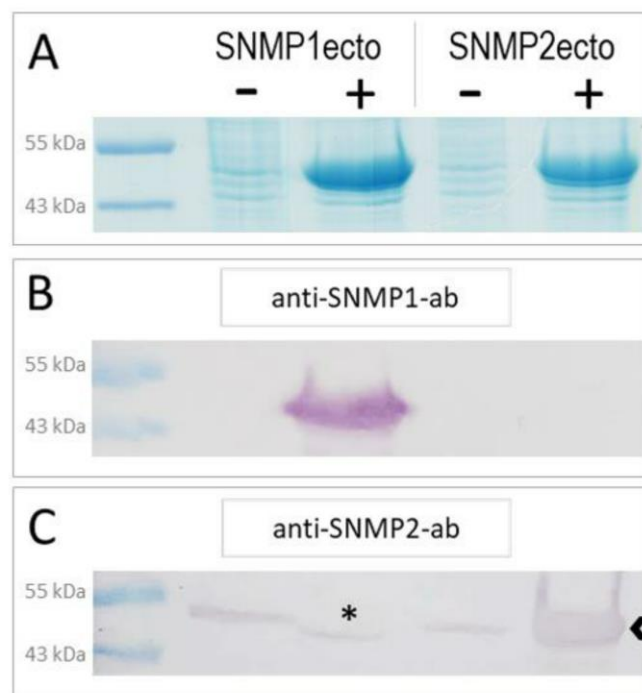


Figure 1. Heterologous expression of *S. gregaria* SNMP1 and SNMP2 ectodomains. (A) SDS-PAGE analysis of lysates from non-induced (–) and induced (+) SNMP1ecto and SNMP2ecto bacteria. In the induced samples, strong bands at the molecular weight predicted for the recombinant SNMP1ecto and SNMP2ecto proteins are visible at about 51 kDa indicating large amounts of expressed SNMP protein. (B) Western blot analysis of bacterial lysates as shown in (A) using the anti-SNMP1-ab showing intense labelling of a band only in induced SNMP1ecto bacteria. (C) Western blot analysis with the anti-SNMP2-ab showing labelling of a strong band in the induced SNMP2ecto bacteria (arrowhead). Weak labelling of bands in the other lanes indicate some cross reactivity of the antibody to endogenous bacterial proteins at about the molecular weight of SNMP2ecto, which results from using proteins from excised gel slices of induced bacteria for antibody generation. The asterisk denotes a possible displacement of a labelled band in the induced SNMP1ecto sample caused by the high amount of overexpressed protein.

3.2. Immunolocalization of SNMP1 Expression in the Antenna of *S. gregaria*

To investigate the identity and distribution of the SNMP-expressing cells along the antenna of *S. gregaria*, we first conducted immunohistochemical approaches on tissue sections through the antenna with the newly generated anti-SNMP1-antibody. On longitudinal sections, anti-SNMP1-positive cells were found quite abundant within antennal segments and distributed in the tissue directly underneath the cuticle (Figure 2A).

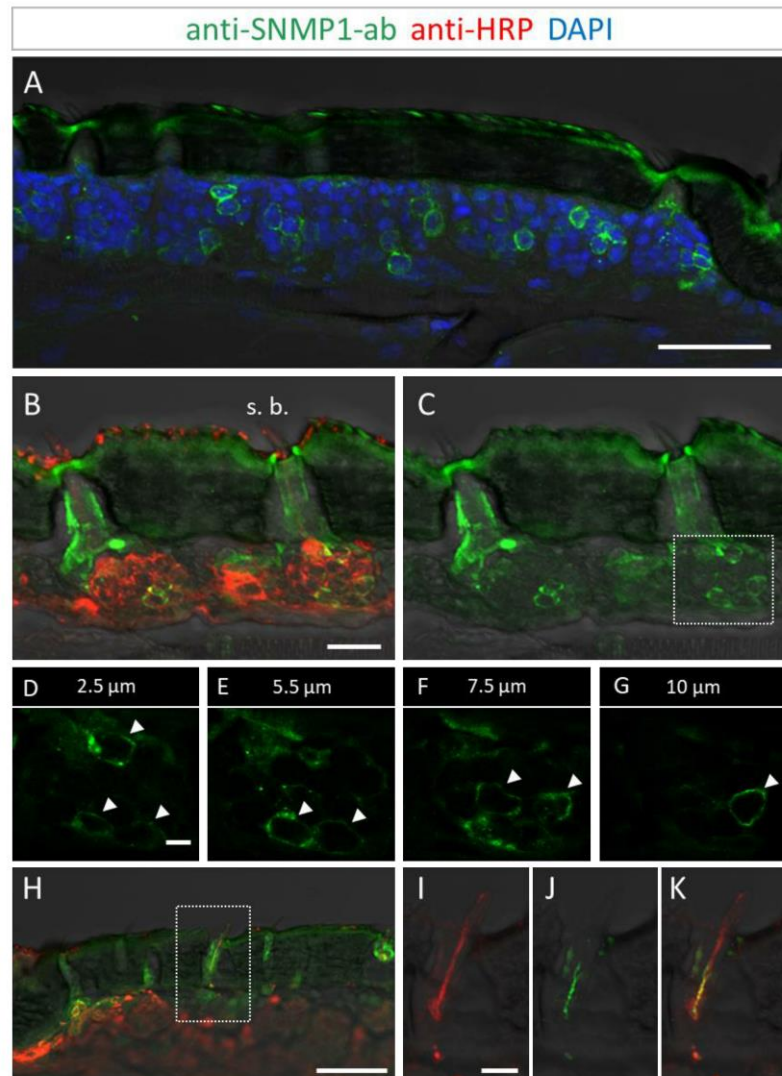


Figure 2. SNMP1 expression in a subset of OSNs in the antenna of *S. gregaria*. SNMP1-positive cells were visualized by FIHC in longitudinal sections using anti-SNMP1-ab (green). Neurons were identified by an anti-HRP-antibody (red) and nuclei were stained with DAPI (blue). (A) Distribution of multiple SNMP1 cells in an antennal segment. (B,C) Expression of SNMP1 (green channel) in a fraction of the OSNs (red channel) of basiconic sensilla (s. b.). (D–G) Higher magnifications of the OSN cluster boxed in (C) shown at different optical planes of a confocal z-stack; arrows denote SNMP1-positive neurons. (H–K) Localization of SNMP1 in OSN dendrites of a basiconic sensillum. (I–K) Higher magnifications of the area boxed in (H) showing the red (I, OSN) and green (J, SNMP1) channels separately or overlaid (K). The transmitted light channel was overlaid with fluorescent channels in (A–C,H–K). Scale bars: (A,H) = 50 μm ; (B) = 20 μm ; (D) and (I) = 5 μm .

Utilizing the anti-SNMP1 antibody in combination with an anti-HRP antibody for labelling of all neurons, we set out to simultaneously visualize the SNMP1-expressing cells and OSNs projecting to olfactory sensilla types. Comprehensive examinations of the

anti-SNMP1-ab and anti-HRP immune reactivity revealed SNMP1 expression in the somata of distinct OSNs underneath basiconic sensilla (Figure 2B,C). Closer inspection of OSN clusters innervating a basiconic sensillum showed that multiple OSNs are SNMP1-positive, encompassing a subpopulation of the entire cluster (Figure 2D–G). This SNMP1 protein expression pattern is in accordance with previous *in situ* hybridization results [28,43,45]. Moreover, the SNMP1 protein was also visible in the dendrites of OSNs protruding into the shaft of basiconic sensilla (Figure 2H–K). In order to show the association of SNMP1 protein with OR-expressing OSNs, we performed combined fluorescence *in situ* hybridization (FISH) and FIHC experiments. Using a riboprobe for the OR-coreceptor Orco and the anti-SNMP1 antibody, SNMP1 immune reactivity was located in a subset of Orco-positive cells of a basiconic sensillum (Figure S2), demonstrating the expression of SNMP1 in OR-expressing OSNs.

To further determine the topographic localization of SNMP1 protein, we next assessed the two other olfactory sensilla types on desert locust antenna. No anti-SNMP1-ab labelling of OSNs were found associated with coeloconic sensilla (Figure 3A,B). In contrast, intensive anti-SNMP1-ab immune reactivity was observed with cells underneath trichoid sensilla (Figure 3A). Closer inspection of the cells of trichoid sensilla indicated that unlike in the basiconic sensilla, in trichoid sensilla all innervating OSNs were positive for SNMP1 (Figure 3C,G, asterisks). However, the most intensive labelling was attributed to non-neuronal cells of trichoid sensilla that are closely associated with the OSNs and presumably represent support cells (Figure 3C–G). Analyzing different confocal planes of the tissue section exposed multiple support cells, which were positioned apical to a cluster of three OSNs that were anti-SNMP1-ab positive (Figure 3D,F, arrows). Analysis of another SNMP1-positive OSN cluster innervating a trichoid sensillum depicted up to three support cells that were labelled by anti-SNMP1-ab (Figure S3). In view of this finding, we reinspected basiconic sensilla. It was found that also here apical cells bordering OSN clusters, likely representing support cells of this sensillum type, were anti-SNMP1-ab-positive (Figure S4).

To further validate the observation that in *S. gregaria* SNMP1 is expressed in non-neuronal cells, we conducted experiments combining *in situ* hybridization and immunohistochemistry approaches using an antisense-SNMP1 riboprobe and the anti-HRP antibody to visualize neurons. As shown for a trichoid sensillum in Figure S5, we detected SNMP1 mRNA within the two depicted OSNs as well as in the adjacent non-neuronal support cells, corroborating the finding that the SNMP1 protein is present in both neuronal and non-neuronal cells in the antenna of *S. gregaria*.

To address the question of whether the expression of SNMP1 in OSNs and support cells is unique to the desert locust *S. gregaria* or also occurs in other locust species, FIHC experiments with anti-SNMP1-ab were performed on the section through the antenna of the migratory locust, *Locusta migratoria*. Since the SNMP1 ectodomains of the two locust species show about 90% sequence identity, cross-reaction of anti-SNMP1-ab with the SNMP1 of *Locusta migratoria* could be assumed.

The results of the FIHC experiments indicate that the localization of SNMP1 in *L. migratoria* antenna mirrored the antennal topography of SNMP1 in *S. gregaria*. Anti-SNMP1-ab labelling was observed in cells underneath trichoid sensilla (Figure 4A). When viewed in a higher magnification, it became apparent that not only are all three OSNs innervating the sensillum positive for SNMP1, but the most intensive labelling was detected in a neighboring support cell (Figure 4B–D).

Similar to *S. gregaria*, SNMP1 expression in *Locusta migratoria* was also found in distinct OSNs innervating basiconic sensilla (Figure 4E), whereas no signal was detected in coeloconic sensilla (Figure 4A,E). Like in *S. gregaria*, only a subset of OSNs in basiconic sensilla appeared to be SNMP1-positive. Furthermore, the anti-SNMP1-ab visualized dendrites protruding from SNMP1-positive OSN towards the sensillum shaft (Figure 4G). Taken together, these results indicate the distinctive expression pattern of SNMP1 in locust antennae, with SNMP1 found not only in OSNs but also in support cells.

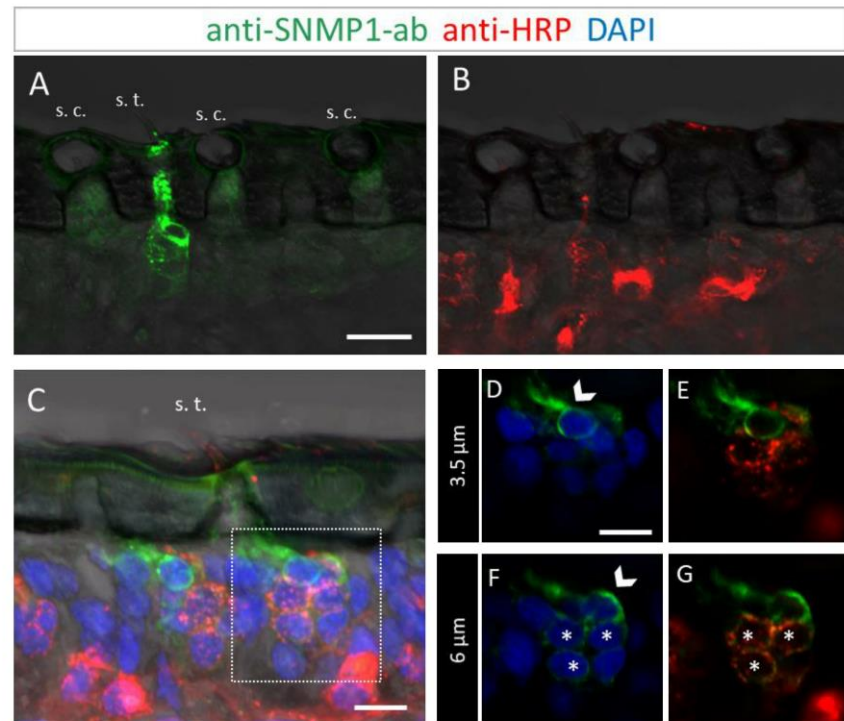


Figure 3. SNMP1 is localized in OSNs of trichoid sensilla (s. t.) but not of coeloconic sensilla (s. c.) in *S. gregaria*. In FIHC experiments with antennal sections, SNMP1-expressing cells (green) were visualized by anti-SNMP1-ab and neurons (red) by the anti-HRP-antibody. DAPI was used to stain nuclei (blue). (A,B) show anti-SNMP1-ab labelling of cells in trichoid, but not of coeloconic sensilla (A) and OSNs innervating the two sensilla types visualized in the red fluorescent channel (B). (A,C) trichoid sensillum from another treated section. (D–G) show a higher magnification of the area boxed in C showing the cell at the base in different optical planes and channels. (D,E) A non-neuronal, SNMP1-positive support cell is visible above an OSN cluster on a higher optical plane. (F,G) A second non-neuronal SNMP1-positive support cell as well as three OSNs are visualized in a deeper optical plane. Arrows indicate the SNMP1-positive support cells, asterisks the SNMP1-positive OSNs. The transmitted light channel was overlaid with the fluorescent channels in (A–C). Scale bars: (A) = 20 μm , (C,D) = 10 μm .

3.3. Immunolocalization of SNMP2 Expression in the Antenna of *S. gregaria*

In order to analyze the cellular expression pattern of the SNMP2 protein in *S. gregaria* antennae and to compare it to SNMP1, we next conducted FIHC experiments using anti-SNMP2-ab and anti-HRP antibodies. As exemplarily demonstrated on the longitudinal section shown in Figure 5A, large numbers of anti-SNMP2-ab-positive cells were visible across different antennal segments below the cuticle. In addition, the anti-HRP antibody visualized numerous clusters of neuronal cells (OSNs) that were not labeled by the anti-SNMP2 antibody.

This was more clearly seen upon closer inspection of basiconic sensilla at higher magnification (Figure 5B,C). While no anti-SNMP2-ab immunoreactivity was detected within any of the OSN somata, large cells situated beneath the sensillum shaft were found positive for SNMP2 (Figure 5B). These observations suggest that support cells are directly associated with the entire cluster of OSNs, seemingly enveloping the base of bundled dendrites projecting into the sensillum (Figure 5C). Attempts to assess the localization of

SNMP2 protein in trichoid sensilla using the anti-SgreSNMP2 antibody showed no clear results. Occasionally, very weak labeling of non-neuronal cells hardly above background staining was observed. In contrast, intensive immunolabelling by the anti-SgreSNMP2-ab was obtained for cells directly beneath coeloconic sensilla (Figure 6). Anti-HRP counter staining for neurons confirmed that, similar to basiconic sensilla (Figure 5), the anti-SNMP2-ab-positive cells of coeloconic sensilla are non-neuronal cells (Figure 6B,C), most likely the support cells associated with the OSNs. Attempts to label SNMP2-expressing cells in the antenna of the closely related species *L. migratoria* with the anti-SNMP2-ab did not lead to conclusive results.

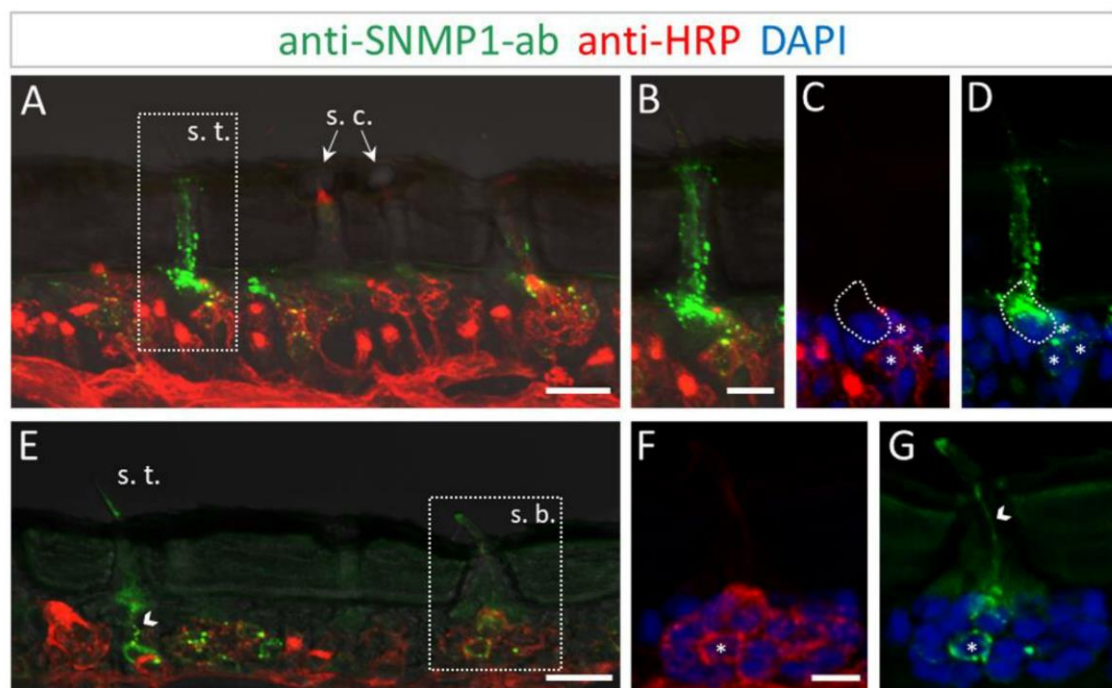


Figure 4. SNMP1 distribution in the antenna of *L. migratoria*. SNMP1-positive cells and neurons were visualized by FIHC on the longitudinal section using anti-SNMP1-ab (green) and anti-HRP-antibody (red), respectively. Nuclei were stained with DAPI (blue). (A) Shows that SNMP1 is localized in cells associated with the trichoid sensillum (s. t.). No labelling was found associated coeloconic sensilla (s. c.). (B–D) Displays the trichoid sensillum boxed in (A) in a higher magnification. (B) Green and red channels, (C) red and blue channels, and (D) green and blue channels. (E). Visualization of SNMP1-positive OSNs in trichoid and basiconic sensilla (s. b.). (F,G) Higher magnification of the basiconic sensillum boxed in (E) with (F) showing neuronal and (G) anti-SNMP1-ab labelling combined with nuclei staining. The asterisks denote SNMP1-positive neurons while the arrow heads indicate SNMP1-labelling of the dendrites. The encircled area indicates SNMP1 expression in a non-neuronal support cell. The transmitted light channel was overlaid with the fluorescent channels in (A,B,E). Scale bars: (A,E) = 20 μ m; (B,F) = 10 μ m.

3.4. Subcellular Localization of SNMP1 and SNMP2 within Sensilla

In order to evaluate the subcellular localization of SNMPs, we analyzed their expression topography on ultrathin sections on the antenna of *S. gregaria* by transmission electron microscopy (TEM). In the immunogold labelling experiments, we obtained clear results for both SNMP types and the abundant basiconic sensilla, whereas our attempts to clarify

their subcellular localization in trichoid and coeloconic sensilla were not successful and would require further investigations.

Assessment of a longitudinal section through a basiconic sensillum treated with the anti-SNMP1 antibody showed multiple dendritic structures in the sensillum shaft in accordance with multiple OSNs housed in this sensillum type that comprise branched dendrites (Figure 7A). At higher magnification, it became apparent that the membranes of some of the dendritic structures were intensively immunogold labelled (Figure 7B, arrows; Figure S7B), whereas others showed no or only little labelling (Figure 7B, asterisk). Corresponding control experiments omitting the primary SNMP antibodies showed no labelling demonstrating no unspecific binding of the secondary antibody to structures within a sensillum (Figure S6). Together, the results show that SNMP1 is located only in a subset of the dendritic structures within a basiconic sensillum. This finding is in line with the expression of SNMP1 in only a subset of the OSNs in basiconic sensilla (Figure 2).

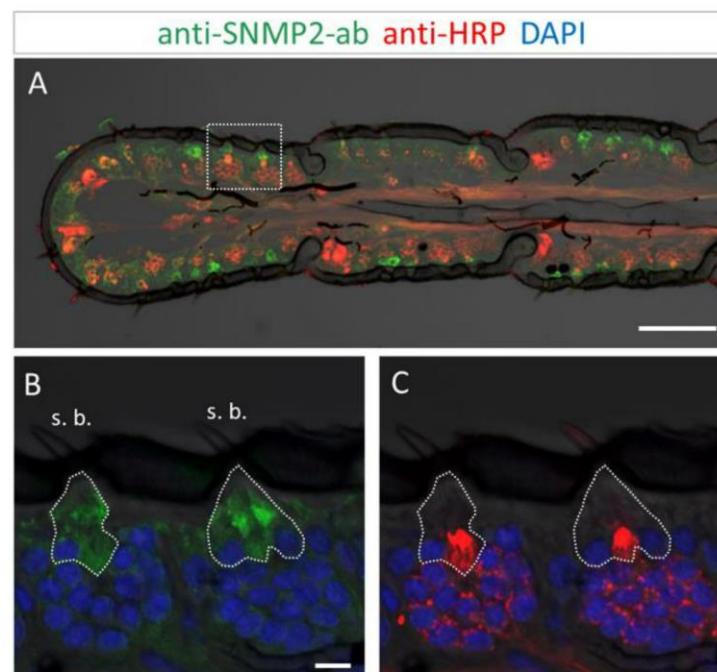


Figure 5. SNMP2 expression in cells of the *S. gregaria* antenna. SNMP2-positive cells were visualized by FIHC in the longitudinal section using anti-SNMP2-ab (green). Neurons were visualized by anti-HRP-antibody (red) and nuclei by staining with DAPI (blue). (A) Topography of SNMP2-expressing cells in multiple antennal segments. (B,C) Displays the area boxed in (A) in a higher magnification and different channel. (B) Shows the green and blue channels, demonstrating the expression of SNMP2 in support cells (encircled) underneath basiconic sensilla (s. b.). (C) Shows the red and blue channels, displaying the clusters of OSNs housed in the basiconic sensilla. Neuronal labelling within the encircled area corresponds to the dendrites of OSNs passing by support cells on the way to the hair shaft. In all images, the fluorescent channels were overlaid with the transmitted light channel. Scale bars: (A) = 100 μ M; (B) = 10 μ M.

Our FIHC results on the light microscope level have indicated expression of SNMP1 also by support cells of basiconic sensilla (Figure S4). In accordance with this finding, we analysed the base of the basiconic sensilla (Figures 7C and S7C) and found anti-SNMP1 immunogold labelling associated with microvilli bordering the sensillum lymph. These

membraneous microvilli structures form the apical region of the support cells that are situated directly beneath the sensillum lumen. These findings further substantiate the expression of SNMP1 in support cells and localize the protein in non-neuronal microvilli protruding towards the sensillum's base.

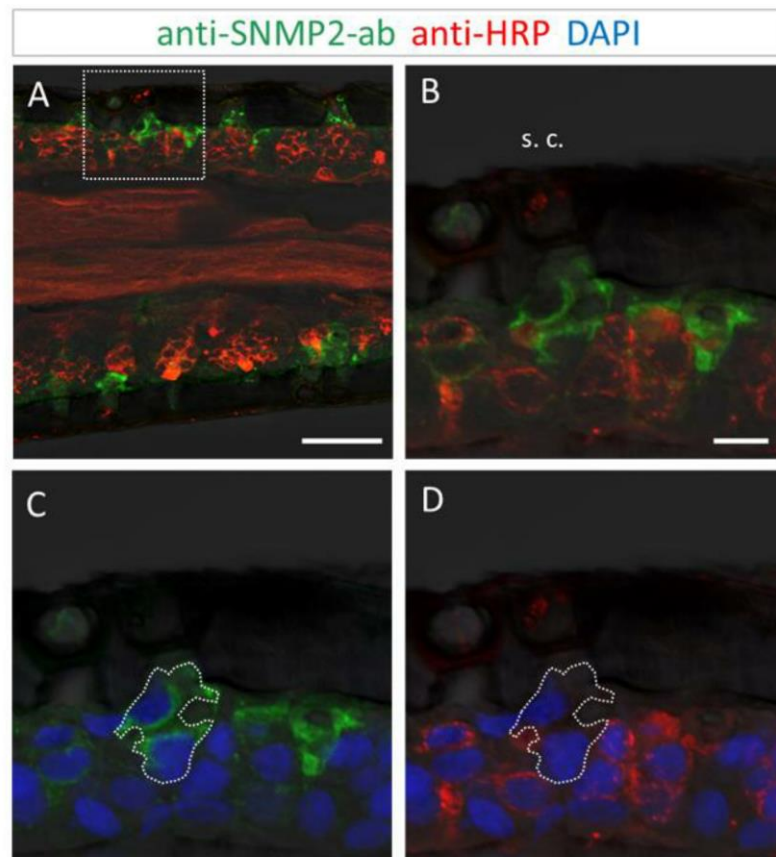


Figure 6. SNMP2 is expressed in non-neuronal cells of coeloconic sensilla in the antenna of *S. gregaria*. Longitudinal sections were assessed by FIHC using anti-SNMP2-ab to identify SNMP2-expressing cells (green) and anti-HRP to visualize OSNs (red); sections were stained with DAPI to visualize nuclei (blue). (A–D) Localization of SNMP2 in multiple non-neuronal cells. (B–D) Show the boxed area in (A) in a higher magnification. (B) Red and green fluorescent channels, (C) green and blue channels, and (D) red and blue channels. The encircled area denotes SNMP2-positive labelling of support cells under a coeloconic sensillum (s. c.). In all images the fluorescent channels were overlaid with the transmitted light channel. Scale bars: (A) = 50 μ M; (B) = 10 μ M.

Next, we examined the subcellular localization of SNMP2 in basiconic sensilla. Figure 8 shows the result of an ultrathin section consecutive to that shown in Figure 7. Intensive anti-SNMP2-ab immunogold labelling was found associated with microvilli structures originating from support cells at the base of the sensillum shaft (Figure 8A–C); no labelling of dendritic structures within the sensillum lumen was observed. To assess the anti-SNMP2-ab labelling of the microvilli in relation to the sensillum's lumen, a cross-section through the base of a basiconic sensillum innervated by dendrites of multiple OSNs was inspected in more detail (Figure 8D,E). Again, inspection of the dendritic bundle in the center of the

sensillum at a higher magnification showed only single gold grains, which most probably represent background labelling (Figure 8H). In contrast, vast anti-SNMP2-ab immunogold labelling was found associated with microvilli structures of support cells that completely surround the internal sensillum lumen (Figure 8E). Analyzing the microvilli structures at a higher magnification demonstrates that the SNMP2 protein is localized at the direct interface between the support cell and the lymph space (Figure 8F,G). Taken together, these results clearly indicate that SNMP2 protein is solely present in non-neuronal support cells and localized in the microvilli that protrude directly into the sensillum lymph filling the sensillum shaft.

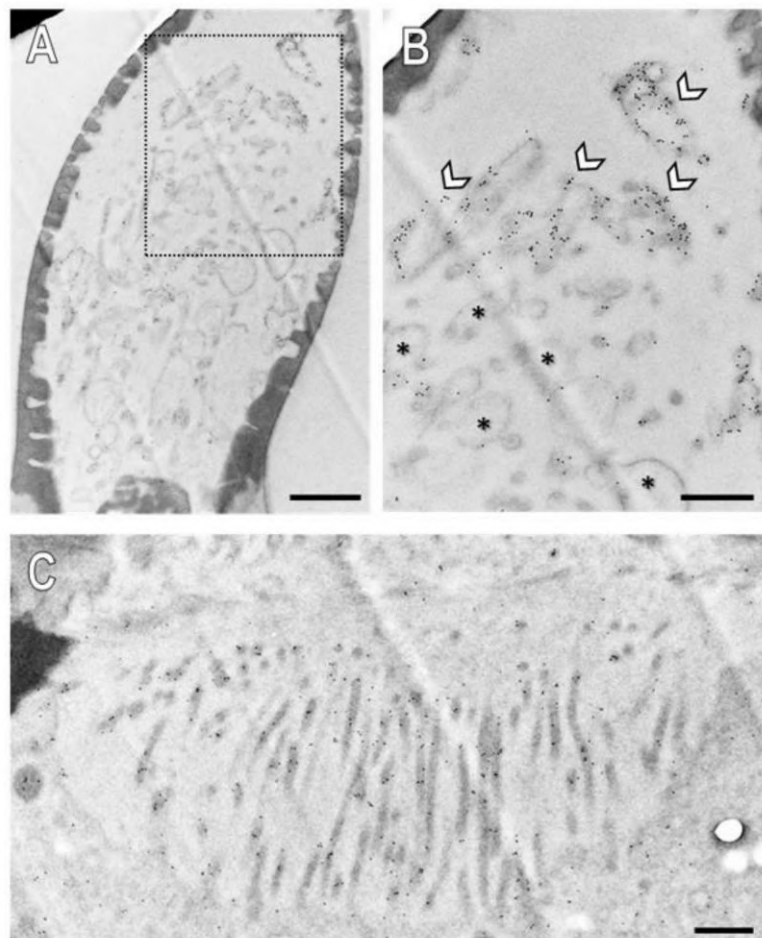


Figure 7. Subcellular localization of SNMP1 within a basiconic sensillum of the *S. gregaria*. Ultrathin sections were assessed by transmission electron microscopy after treatment with anti-SNMP1-ab and a secondary anti-rabbit antibody coupled with colloidal gold. (A) Shaft of a basiconic sensillum with multiple dendritic structures in the lumen. (B) Higher magnified image of the area boxed in (A). Intense immunogold labelling is observed associated with the membranes of a subset of dendritic structures (arrows). The asterisks denote dendritic structures with little to no immunogold labelling. (C) Microvilli structures of support cells at the base of the sensillum. Significant immunogold labelling was found associated with the microvilli including their membranes. Scale bars: (A) = 1 μ m; (B,C) = 500 nm.

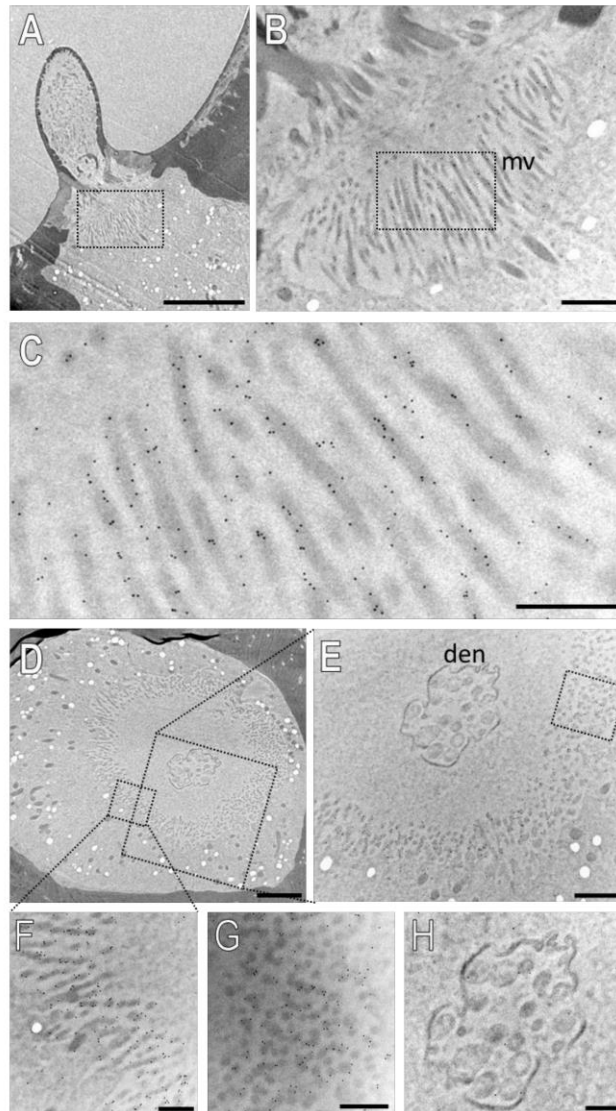


Figure 8. SNMP2 is localized in microvilli of support cells of basiconic sensilla. Ultrathin sections were treated with anti-SNMP2-ab in immunogold labelling experiments and assessed by transmission electron microscopy. (A) Longitudinal section through a basiconic sensillum. (B) Higher magnification of the region boxed in (A), showing microvilli structures (mv) at the base of the sensillum. (C) Higher magnified image of the region boxed in (B), displaying clear anti-SNMP2-ab immune reactivity associated with microvilli. (D) Cross section through the base of another basiconic sensillum. (E) Higher magnified image of the large box depicted in (D). A higher magnification of the smaller box in (D) is shown in (F), indicating strong immunogold labelling of microvilli structures. (G) is a higher magnification of the microvilli boxed in (E), depicting SNMP2-labelling associated with transversely cut microvilli. (H) is a higher magnification of the dendrites (den) shown in (D,E), indicating only low levels of background signal. Scale bars: (A) = 5 μm ; (B,E) = 1 μm ; (D) = 2 μm ; (C,F–H) = 500 nm.

4. Discussion

In this study, we examined the topography and subcellular localization of SNMP1- and SNMP2-protein in the antennae of the desert locust *S. gregaria* using specific antibodies targeting the ectodomains of the respective proteins.

Performing FIHC-experiments using the anti-SNMP1 antibody resulted in visualization of SNMP1 protein in populations of Orco-positive OSNs including their dendrites, which project into trichoid and basiconic sensilla. These results confirm our previous findings visualizing cells with mRNA for SNMP1 by in situ hybridization experiments [28,45] but reveal the cellular and subcellular localization of the SNMP1 protein. Immunolabeling for SNMP1 was not detected in OSNs of coeloconic sensilla, which in *S. gregaria* express IRs [49]. Similarly, a co-expression of SNMP1 with ORs but not with IRs in OSNs has been reported for *D. melanogaster* [17] and *Microplitis mediator* [50]. Together, these results further substantiate the notion that SNMP1 expression is confined to OR-expressing OSNs, which appears to be a conserved pattern across different species.

Using anti-SNMP1-ab, we found all OSNs innervating a trichoid sensillum to be SNMP1-positive, while in basiconic sensilla only a subset of OSNs express SNMP1. The same result was obtained for the related species, *L. migratoria*, demonstrating a conserved distribution pattern of SNMP1-expressing OSNs across olfactory sensilla of locusts. Hence, the data indicate that basiconic and trichoid sensilla of locusts not only differ in their morphology, but also in the molecular equipment of their OSNs, suggesting that all OSNs of trichoid sensilla employ SNMP1 in odor detection. An expression of SNMP1 in all OSNs of trichoid sensilla has also been reported for *D. melanogaster* [17] and females of the moth *Heliothis virescens*. In contrast, in males of *H. virescens*, only one of the 2–3 OSNs housed in the trichoid sensilla were found SNMP1-positive [39,51], demonstrating that SNMP1 expression is not generally associated with the OSNs of trichoid sensilla.

Various studies on fly [17,18,35] and moth species [33,34] have shown that SNMP1-positive OSNs of trichoid sensilla are associated with the sensitive detection of pheromones, suggesting that OSNs in locust trichoid sensilla may also serve in pheromone detection. In accordance with this notion, previous single sensillum recordings from *S. gregaria* trichoid sensilla revealed OSNs that are tuned to a possible sex pheromone component [52]. However, although all OSNs in trichoid sensilla of *L. migratoria* express SNMP1, distinct OSNs of trichoid sensilla express the receptor type OR3 that is activated by various non-pheromonal odorants [53]. Hence, expression of SNMP1 in trichoid OSNs may not necessarily be linked to pheromone detection.

In both assessed locust species, we found that only a subset of the antennal OSNs innervating basiconic sensilla were SNMP1-positive indicative for SNMP1-dependent and SNMP1-independent mechanisms of signal processing in basiconic OSNs. This notion is in accordance with our recent finding that from the 80 OR types expressed in basiconic OSNs of *S. gregaria*, only 30 OR types are co-expressed with SNMP1 [43,45].

Single sensillum recordings from locust basiconic sensilla, which house up to 50 OSNs, revealed sensilla responses to a variety of general odorants (plant volatiles), odorant mixtures representing adult and nymphal body odors, as well as to verified pheromones [2,52]. Due to the large number of neurons, an assignment of odor responses to a distinct OSN is unfortunately not possible, but the results indicate that the ensemble of OSNs in basiconic sensilla allows a contribution in the detection of specific pheromones as well as general odorants. Given the rather broad expression of SNMP1 in populations of basiconic OSNs expressing many different OR types, it is therefore conceivable that in locusts the neuronal SNMP1 is not an obligate co-receptor required for a sensitive response of OSNs to pheromones. Instead it may also act in a sensitive detection of behaviorally important non-pheromonal odorants originating from various biological sources, such as preferred food plants or oviposition sites [1,4] as indicated for *D. melanogaster* SNMP1 that was found essential for sensitive pheromone detection [17,18], but was also shown to be required for the proper response of OR83c-expressing OSNs to the plant-derived odorant farnesol [54].

Notably, SNMP1 was also present in non-neuronal SCs of trichoid and basiconic sensilla from *S. gregaria* as well as *L. migratoria*. Expression of SNMP1 in SCs was not noticed in previous *in situ* hybridization experiments possibly due to a missing neuronal counter stain [28]. In trichoid sensilla, we detected up to three SNMP1-positive SCs adjacent to three SNMP1-positive OSNs. This SNMP1 expression pattern resembles the situation in *D. melanogaster*, where the SNMP1-positive OSNs of trichoid sensilla are associated with several SNMP1-expressing SCs [17]. Together, the current data suggest that SNMP1 plays a distinct role in OSNs and SCs in the olfactory system of locusts and flies. In contrast, in moths, SNMP1-expression in trichoid sensilla was found to be restricted to OSNs, whereas SNMP2 was exclusively expressed in SCs [39,55,56], suggesting some functional specialization of moth SNMP1.

In comparison to SNMP1, the SNMP2 protein was solely detected in SCs. Strong labelling was obtained for SCs in basiconic and coeloconic sensilla, the two most abundant sensillum types on the antenna of *S. gregaria*. Despite considerable efforts, we could not visualize unambiguous SNMP2 immune reactivity in SCs of the trichoid sensilla. Whether this was due to very low levels of SNMP2 protein or due to the absence of the SNMP2 protein in trichoid SCs remains elusive. In this context, it is interesting to note that SNMP1 is clearly expressed in SCs of trichoid sensilla. It is therefore tempting to speculate that in SCs of trichoid sensilla, SNMP1 has replaced SNMP2 and may fulfill a function similar to SNMP2 in SCs of other sensilla types.

In accordance with the notion that the two SNMP types fulfil similar functions in SCs, the immunogold-labelling experiments demonstrate a similar subcellular localization for *S. gregaria* SNMP1 and SNMP2. Both proteins were located to the membranous microvilli of SCs directly bordering the lymph-filled sensillum lumen; these microvilli are considered as a site of high transmembrane transport and exchange activity [41]. Consistently, FIHC experiments have indicated that in the antenna of the moth *Heliothis virescens*, SNMP2 was located in the most apical region of the SCs [39], suggesting conserved roles of SNMPS in SC across insect orders and a function at the interface to the sensillum lymph. While the specific role of non-neuronal SNMPS awaits further investigation, based on the function of other CD36 family members it is conceivable that SNMP2 may operate as transporter involved in the maintenance of the sensillum lymph. Mammalian CD36 proteins and insect members of the CD36 family outside of olfaction, such as NinaD and Santa Maria are vital for the capture and uptake of lipophilic molecules including fatty acids into cells [57–60]. Accordingly, SNMPS in the microvilli membrane of SCs may play an integral role in capturing lipophilic molecules (odorant, pheromones, or their degradation products) emerging in the sensillum lymph during olfactory processes and the subsequent translocation of the “waste product”, either by themselves or in cooperation with other transport proteins, into the SC for further disposal.

In view of a putative function in the lymph clearance, it is interesting to note that SNMP1 is expressed in SCs associated with OSNs that express SNMP1. Thus, SNMP1 in SCs of trichoid and basiconic sensilla may be involved in the clearance of “waste products” resulting from odorants that are detected by OSNs, which use SNMP1 as a co-receptor. Correspondingly, SNMP2 may function in SCs of basiconic and coeloconic sensilla in order to eliminate “waste products” arising from SNMP1-independent odorant detection processes.

In conclusion, we have demonstrated that SNMP1-protein is present in populations of OSNs and in non-neuronal supporting cells of olfactory sensilla on the locust antenna.

An assessment of the subcellular localization revealed SNMP1 protein was present in the dendritic membrane of OSNs as well as in the microvilli of the SCs. In contrast, SNMP2 protein was exclusively located in the microvilli of the SCs. Thus, in olfactory sensory neurons, SNMP1 may function as coreceptor involved in signal recognition, whereas in non-neuronal cells both SNMP subtypes may be involved in the maintenance of the sensillum lymph and, due to its homology to CD36 proteins might be involved in the uptake of lipophilic “waste products”.

Supplementary Materials: The following file contains the supplementary Figures S1–S7 and can be downloaded at: <https://www.mdpi.com/article/10.3390/insects13070579/s1>; Figure S1: Alignment of the amino acid sequences of *S. gregaria* SNMP 1 and SNMP 2.; Figure S2: SNMP 1 is expressed in a subset of Orco positive OSNs in basiconic sensilla.; Figure S3: FISH experiment showing that SNMP 1 is expressed in OSNs and the associated support cells of a trichoid sensillum; Figure S4: SNMP 1 is expressed in distinct OSNs and support cells of a basiconic sensillum in *S. gregaria*; Figure S5: SNMP 1 is expressed in support cells and OSNs of a *S. gregaria* trichoid sensillum; Figure S6: Assessment of secondary antibody binding to ultrathin sections of the *S. gregaria* antenna; Figure S7: Localization of SNMP 1 within dendrites of OSNs and microvilli structures of support cells in a basiconic sensillum of *S. gregaria*.

Author Contributions: Conceptualization, S.C. and J.K.; methodology, S.C., G.H., M.L. and T.K.; investigation, S.C. and D.S.; analysis of data, S.C., J.K., G.H., D.S. and H.B.; resources, H.B. and T.K.; Visualization/data presentation, S.C.; writing S.C. and J.K.; review and editing, S.C., J.K., H.B., G.H., M.L. and D.S. All authors have read and agreed to the published version of the manuscript.

Funding: This research was funded by a grant to J.K. from the Deutsche Forschungsgemeinschaft. Grant number KR1786/5-1.

Institutional Review Board Statement: Not applicable.

Informed Consent Statement: Not applicable.

Data Availability Statement: Data is contained within the article or supplementary material.

Acknowledgments: Simone Fraas is acknowledged for excellent technical assistance. We thank Martin Schattat for giving access to the LSM780.

Conflicts of Interest: The authors declare no conflict of interest. The funders had no role in the design of the study; in the collection, analyses, or interpretation of data; in the writing of the manuscript, or in the decision to publish the results.

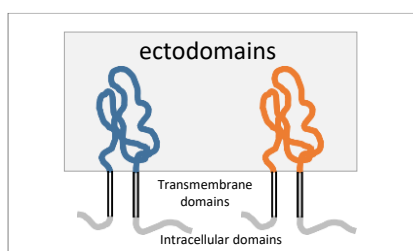
References

- Hassanali, A.; Njagi, P.G.; Bashir, M.O. Chemical Ecology of Locusts and Related Acridids. *Annu. Rev. Entomol.* **2005**, *50*, 223–245. [[CrossRef](#)] [[PubMed](#)]
- Guo, X.; Yu, Q.; Chen, D.; Wei, J.; Yang, P.; Yu, J.; Wang, X.; Kang, L. 4-Vinylanisole is an aggregation pheromone in locusts. *Nature* **2020**, *584*, 1–5. [[CrossRef](#)] [[PubMed](#)]
- Chen, D.; Hou, L.; Wei, J.; Guo, S.; Cui, W.; Yang, P.; Kang, L.; Wang, X. Aggregation pheromone 4-vinylanisole promotes the synchrony of sexual maturation in female locusts. *eLife* **2022**, *11*. [[CrossRef](#)] [[PubMed](#)]
- Nakano, M.; Morgan-Richards, M.; Treweek, S.A.; Clavijo-McCormick, A. Chemical Ecology and Olfaction in Short-Horned Grasshoppers (Orthoptera: Acrididae). *J. Chem. Ecol.* **2022**, *48*, 1–20. [[CrossRef](#)] [[PubMed](#)]
- Greenwood, M.; Chapman, R.F. Differences in numbers of sensilla on the antennae of solitary and gregarious *Locusta migratoria* L. (Orthoptera: Acrididae). *Int. J. Morphol. Embryol.* **1984**, *13*, 295–301. [[CrossRef](#)]
- Ochieng, S.A.; Hallberg, E.; Hansson, B.S. Fine structure and distribution of antennal sensilla of the desert locust, *Schistocerca gregaria* (Orthoptera: Acrididae). *Cell. Tissue Res.* **1998**, *291*, 525–536. [[CrossRef](#)]
- Blaney, W.M.; Chapman, R.F.; Cook, A.G. The structure of the terminal sensilla on the maxillary palps of *Locusta migratoria* (L.), and changes associated with moulting. *Z. Zellforsch. Mikrosk. Anat.* **1971**, *121*, 48–68. [[CrossRef](#)]
- Lemke, R.-S.; Pregitzer, P.; Eichhorn, A.-S.; Breer, H.; Krieger, J.; Fleischer, J. SNMP1 and odorant receptors are co-expressed in olfactory neurons of the labial and maxillary palps from the desert locust *Schistocerca gregaria* (Orthoptera: Acrididae). *Cell Tissue Res.* **2020**, *379*, 275–289. [[CrossRef](#)]
- Rytz, R.; Croset, V.; Benton, R. Ionotropic Receptors (IRs): Chemosensory ionotropic glutamate receptors in Drosophila and beyond. *Insect Biochem. Mol. Biol.* **2013**, *43*, 888–897. [[CrossRef](#)]
- Montagné, N.; de Fouchier, A.; Newcomb, R.D.; Jacquín-Joly, E. Advances in the Identification and Characterization of Olfactory Receptors in Insects. *Prog. Mol. Biol. Transl. Sci.* **2015**, *130*, 55–80. [[CrossRef](#)]
- Fleischer, J.; Pregitzer, P.; Breer, H.; Krieger, J. Access to the odor world: Olfactory receptors and their role for signal transduction in insects. *Cell. Mol. Life Sci.* **2017**, *75*, 485–508. [[CrossRef](#)] [[PubMed](#)]
- Wicher, D.; Miazzi, F. Functional properties of insect olfactory receptors: Ionotropic receptors and odorant receptors. *Cell Tissue Res.* **2021**, *383*, 7–19. [[CrossRef](#)] [[PubMed](#)]
- Leal, W.S. Odorant Reception in Insects: Roles of Receptors, Binding Proteins, and Degrading Enzymes. *Annu. Rev. Entomol.* **2013**, *58*, 373–391. [[CrossRef](#)]

14. Pelosi, P.; Iovinella, I.; Zhu, J.; Wang, G.; Dani, F.R. Beyond chemoreception: Diverse tasks of soluble olfactory proteins in insects. *Biol. Rev.* **2017**, *93*, 184–200. [\[CrossRef\]](#)
15. Rihani, K.; Ferveur, J.-F.; Briand, L. The 40-Year Mystery of Insect Odorant-Binding Proteins. *Biomolecules* **2021**, *11*, 509. [\[CrossRef\]](#)
16. Rogers, M.E.; Krieger, J.; Vogt, R.G. Antennal SNMPs (sensory neuron membrane proteins) of lepidoptera define a unique family of invertebrate CD36-like proteins. *J. Neurobiol.* **2001**, *49*, 47–61. [\[CrossRef\]](#)
17. Benton, R.; Vannice, K.S.; Vosshall, L.B. An essential role for a CD36-related receptor in pheromone detection in *Drosophila*. *Nature* **2007**, *450*, 289–293. [\[CrossRef\]](#) [\[PubMed\]](#)
18. Jin, X.; Ha, T.S.; Smith, D.P. SNMP is a signaling component required for pheromone sensitivity in *Drosophila*. *Proc. Natl. Acad. Sci. USA* **2008**, *105*, 10996–11001. [\[CrossRef\]](#) [\[PubMed\]](#)
19. Nichols, Z.; Vogt, R.G. The SNMP/CD36 gene family in Diptera, Hymenoptera and Coleoptera: *Drosophila melanogaster*, *D. pseudoobscura*, *Anopheles gambiae*, *Aedes aegypti*, *Apis mellifera*, and *Tribolium castaneum*. *Insect Biochem. Mol. Biol.* **2008**, *38*, 398–415. [\[CrossRef\]](#)
20. Pepino, M.Y.; Kuda, O.; Samovski, D.; Abumrad, N.A. Structure-Function of CD36 and Importance of Fatty Acid Signal Transduction in Fat Metabolism. *Annu. Rev. Nutr.* **2014**, *34*, 281–303. [\[CrossRef\]](#)
21. Gomez-Diaz, C.; Bargeton, B.; Abuin, L.; Bukar, N.; Reina, J.H.; Bartoi, T.; Graf, M.; Ong, H.; Ulbrich, M.H.; Masson, J.-F.; et al. A CD36 ectodomain mediates insect pheromone detection via a putative tunnelling mechanism. *Nat. Commun.* **2016**, *7*, 11866. [\[CrossRef\]](#) [\[PubMed\]](#)
22. Silverstein, R.L.; Febbraio, M. CD36, a Scavenger Receptor Involved in Immunity, Metabolism, Angiogenesis, and Behavior. *Sci. Signal.* **2009**, *2*, 1–8. [\[CrossRef\]](#) [\[PubMed\]](#)
23. Martin, C.; Chevrot, M.; Poirier, H.; Passilly-Degrace, P.; Niot, I.; Besnard, P. CD36 as a lipid sensor. *Physiol. Behav.* **2011**, *105*, 36–42. [\[CrossRef\]](#) [\[PubMed\]](#)
24. Chen, Y.; Zhang, J.; Cui, W.; Silverstein, R.L. CD36, a signaling receptor and fatty acid transporter that regulates immune cell metabolism and fate. *J. Exp. Med.* **2022**, *219*, e20211314. [\[CrossRef\]](#) [\[PubMed\]](#)
25. Ozdener, M.H.; Subramaniam, S.; Sundaresan, S.; Sery, O.; Hashimoto, T.; Asakawa, Y.; Besnard, P.; Abumrad, N.A.; Khan, N.A. CD36- and GPR120-Mediated Ca²⁺ Signaling in Human Taste Bud Cells Mediates Differential Responses to Fatty Acids and Is Altered in Obese Mice. *Gastroenterology* **2014**, *146*, 995–1005.e5. [\[CrossRef\]](#) [\[PubMed\]](#)
26. Oberland, S.; Ackelst, T.; Gaab, S.; Pelz, T.; Spehr, J.; Spehr, M.; Neuhaus, E.M. CD36 is involved in oleic acid detection by the murine olfactory system. *Front. Cell. Neurosci.* **2015**, *9*, 366. [\[CrossRef\]](#) [\[PubMed\]](#)
27. Gaillard, D.; Laugerette, F.; Darcel, N.; El-Yassimi, A.; Passilly-Degrace, P.; Hichami, A.; Khan, N.A.; Montmayeur, J.; Besnard, P. The gustatory pathway is involved in CD36-mediated orosensory perception of long-chain fatty acids in the mouse. *FASEB J.* **2007**, *22*, 1458–1468. [\[CrossRef\]](#) [\[PubMed\]](#)
28. Jiang, X.; Pregitzer, P.; Grosse-Wilde, E.; Breer, H.; Krieger, J. Identification and Characterization of Two “Sensory Neuron Membrane Proteins” (SNMPs) of the Desert Locust, *Schistocerca gregaria* (Orthoptera: Acrididae). *J. Insect Sci.* **2016**, *16*, 33. [\[CrossRef\]](#)
29. Zhao, Y.-J.; Li, G.-C.; Zhu, J.-Y.; Liu, N.-Y. Genome-based analysis reveals a novel SNMP group of the Coleoptera and chemosensory receptors in *Rhaphuma horsfieldi*. *Genomics* **2021**, *112*, 2713–2728. [\[CrossRef\]](#)
30. Zhang, H.-J.; Xu, W.; Chen, Q.-M.; Sun, L.-N.; Anderson, A.; Xia, Q.-Y.; Papanicolaou, A. A phylogenomics approach to characterizing sensory neuron membrane proteins (SNMPs) in Lepidoptera. *Insect Biochem. Mol. Biol.* **2020**, *118*, 103313. [\[CrossRef\]](#)
31. Cassau, S.; Krieger, J. The role of SNMPs in insect olfaction. *Cell Tissue Res.* **2010**, *383*, 21–33. [\[CrossRef\]](#) [\[PubMed\]](#)
32. Rogers, M.E.; Sun, M.; Lerner, M.R.; Vogt, R.G. Snmp-1, a Novel Membrane Protein of Olfactory Neurons of the Silk Moth *Antheraea polyphemus* with Homology to the CD36 Family of Membrane Proteins. *J. Biol. Chem.* **1997**, *272*, 14792–14799. [\[CrossRef\]](#) [\[PubMed\]](#)
33. Pregitzer, P.; Greschista, M.; Breer, H.; Krieger, J. The sensory neuron membrane protein SNMP1 contributes to the sensitivity of a pheromone detection system. *Insect Mol. Biol.* **2014**, *23*, 733–742. [\[CrossRef\]](#) [\[PubMed\]](#)
34. Liu, S.; Chang, H.; Liu, W.; Cui, W.; Liu, Y.; Wang, Y.; Ren, B.; Wang, G. Essential role for SNMP1 in detection of sex pheromones in *Helicoverpa armigera*. *Insect Biochem. Mol. Biol.* **2020**, *127*, 103485. [\[CrossRef\]](#) [\[PubMed\]](#)
35. Li, Z.; Ni, J.D.; Huang, J.; Montell, C. Requirement for *Drosophila* SNMP1 for Rapid Activation and Termination of Pheromone-Induced Activity. *PLoS Genet.* **2014**, *10*, e1004600. [\[CrossRef\]](#)
36. German, P.F.; van der Poel, S.; Carraher, C.; Kralicek, A.V.; Newcomb, R.D. Insights into subunit interactions within the insect olfactory receptor complex using FRET. *Insect Biochem. Mol. Biol.* **2013**, *43*, 138–145. [\[CrossRef\]](#)
37. Xu, W.; Zhang, H.; Liao, Y.; Papanicolaou, A. Characterization of sensory neuron membrane proteins (SNMPs) in cotton bollworm *Helicoverpa armigera* (Lepidoptera: Noctuidae). *Insect Sci.* **2020**, *28*, 769–779. [\[CrossRef\]](#)
38. Gu, S.-H.; Yang, R.-N.; Guo, M.-B.; Wang, G.-R.; Wu, K.-M.; Guo, Y.-Y.; Zhou, J.-J.; Zhang, Y.-J. Molecular identification and differential expression of sensory neuron membrane proteins in the antennae of the black cutworm moth *Agrotis ipsilon*. *J. Insect Physiol.* **2013**, *59*, 430–443. [\[CrossRef\]](#)
39. Blankenburg, S.; Cassau, S.; Krieger, J. The expression patterns of SNMP1 and SNMP2 underline distinct functions of two CD36-related proteins in the olfactory system of the tobacco budworm *Heliothis virescens*. *Cell Tissue Res.* **2019**, *378*, 485–497. [\[CrossRef\]](#)

40. Thurm, U.; Küppers, J. Epithelial physiology of insect sensilla. In *Insect Biology in the Future*; Locke, M., Smith, D.S., Eds.; Academic Press: New York, NY, USA, 1980; pp. 735–763.
41. Steinbrecht, R.A.; Gnatzy, W. Pheromone receptors in *Bombyx mori* and *Antheraea pernyi*. I. Reconstruction of the cellular organization of the *Sensilla trichodea*. *Cell Tissue Res.* **1984**, *235*, 25–34. [[CrossRef](#)]
42. Forstner, M.; Gohl, T.; Gondesens, I.; Raming, K.; Breer, H.; Krieger, J. Differential Expression of SNMP-1 and SNMP-2 Proteins in Pheromone-Sensitive Hairs of Moths. *Chem. Senses* **2008**, *33*, 291–299. [[CrossRef](#)] [[PubMed](#)]
43. Jiang, X.; Breer, H.; Pregitzer, P. Sensilla-Specific Expression of Odorant Receptors in the Desert Locust *Schistocerca gregaria*. *Front. Physiol.* **2019**, *10*, 1052. [[CrossRef](#)] [[PubMed](#)]
44. Pregitzer, P.; Jiang, X.; Grosse-Wilde, E.; Breer, H.; Krieger, J.; Fleischer, J. In Search for Pheromone Receptors: Certain Members of the Odorant Receptor Family in the Desert Locust *Schistocerca gregaria* (Orthoptera: Acrididae) Are Co-expressed with SNMP. *Int. J. Biol. Sci.* **2017**, *13*, 911–922. [[CrossRef](#)] [[PubMed](#)]
45. Pregitzer, P.; Jiang, X.; Lemke, R.-S.; Krieger, J.; Fleischer, J.; Breer, H. A Subset of Odorant Receptors from the Desert Locust *Schistocerca gregaria* Is Co-Expressed with the Sensory Neuron Membrane Protein 1. *Insects* **2019**, *10*, 350. [[CrossRef](#)]
46. Seidelmann, K.; Lubner, K.; Ferenz, H.-J. Analysis of Release and Role of Benzyl Cyanide in Male Desert Locusts, *Schistocerca gregaria*. *J. Chem. Ecol.* **2000**, *26*, 1897–1910. [[CrossRef](#)]
47. Krogh, A.; Larsson, B.; von Heijne, G.; Sonnhammer, E.L. Predicting transmembrane protein topology with a hidden Markov model: Application to complete genomes. *J. Mol. Biol.* **2001**, *305*, 567–580. [[CrossRef](#)] [[PubMed](#)]
48. Gohl, T.; Krieger, J. Immunolocalization of a candidate pheromone receptor in the antenna of the male moth, *Heliothis virescens*. *Invertebr. Neurosci.* **2006**, *6*, 13–21. [[CrossRef](#)] [[PubMed](#)]
49. Guo, M.; Krieger, J.; Große-Wilde, E.; Mißbach, C.; Zhang, L.; Breer, H. Variant Ionotropic Receptors Are Expressed in Olfactory Sensory Neurons of Coeloconic Sensilla on the Antenna of the Desert Locust (*Schistocerca gregaria*). *Int. J. Biol. Sci.* **2014**, *10*, 1–14. [[CrossRef](#)]
50. Shan, S.; Wang, S.; Song, X.; Khashaveh, A.; Lu, Z.; Dhiloo, K.H.; Li, R.; Gao, X.; Zhang, Y. Molecular characterization and expression of sensory neuron membrane proteins in the parasitoid *Microplitis mediator* (Hymenoptera: Braconidae). *Insect Sci.* **2019**, *27*, 425–439. [[CrossRef](#)]
51. Zielonka, M.; Breer, H.; Krieger, J. Molecular elements of pheromone detection in the female moth, *Heliothis virescens*. *Insect Sci.* **2016**, *25*, 389–400. [[CrossRef](#)]
52. Ochieng', S.A.; Hansson, B.S. Responses of olfactory receptor neurones to behaviourally important odours in gregarious and solitary desert locust, *Schistocerca gregaria*. *Physiol. Entomol.* **1999**, *24*, 28–36. [[CrossRef](#)]
53. You, Y.; Smith, D.P.; Lv, M.; Zhang, L. A broadly tuned odorant receptor in neurons of trichoid sensilla in locust, *Locusta migratoria*. *Insect Biochem. Mol. Biol.* **2016**, *79*, 66–72. [[CrossRef](#)] [[PubMed](#)]
54. Ronderos, D.; Lin, C.-C.; Potter, C.; Smith, D.P. Farnesol-Detecting Olfactory Neurons in *Drosophila*. *J. Neurosci.* **2014**, *34*, 3959–3968. [[CrossRef](#)] [[PubMed](#)]
55. Zhang, J.; Liu, Y.; Walker, W.B.; Dong, S.-L.; Wang, G.-R. Identification and localization of two sensory neuron membrane proteins from *Spodoptera litura* (Lepidoptera: Noctuidae). *Insect Sci.* **2014**, *22*, 399–408. [[CrossRef](#)]
56. Sun, L.; Wang, Q.; Zhang, Y.; Yan, Y.; Guo, H.; Xiao, Q.; Zhang, Y. Expression patterns and colocalization of two sensory neuron membrane proteins in *Ectropis obliqua* Prout, a geometrid moth pest that uses Type-II sex pheromones. *Insect Mol. Biol.* **2018**, *28*, 342–354. [[CrossRef](#)]
57. Giovannucci, D.R.; Stephenson, R.S. Identification and distribution of dietary precursors of the *Drosophila* visual pigment chromophore: Analysis of carotenoids in wild type and *ninaD* mutants by HPLC. *Vis. Res.* **1999**, *39*, 219–229. [[CrossRef](#)]
58. Kiefer, C.; Sumser, E.; Wernet, M.F.; von Lintig, J. A class B scavenger receptor mediates the cellular uptake of carotenoids in *Drosophila*. *Proc. Natl. Acad. Sci. USA* **2002**, *99*, 10581–10586. [[CrossRef](#)]
59. Wang, T.; Jiao, Y.; Montell, C. Dissection of the pathway required for generation of vitamin A and for *Drosophila* phototransduction. *J. Cell Biol.* **2007**, *177*, 305–316. [[CrossRef](#)]
60. Yang, J.; O'Tousa, J.E. Cellular sites of *Drosophila* NinaB and NinaD activity in vitamin A metabolism. *Mol. Cell. Neurosci.* **2007**, *35*, 49–56. [[CrossRef](#)]

Supplementary Data for Manuscript 1



SgreSNMP1	1	-----MQLPVGLAAGGGVFFMAVVAGWYGMP	KLISSQIASGLA	39		
SgreSNMP2	1	MLSARVCGCGRRLWWGLAA-GAALLAVALVLRWAA	FPAILLTAKIKQAVQ	49		
SgreSNMP1	40	LKKGSDIRQMWSNFS	SDPIDFRVYVNLNLTNPEAVHRGEKPIVQEIGPYFYE	89		
SgreSNMP2	50	LHDGSPAMERFVQLPQPLLYKVVYLFNVTNPDEVE	QGAQKPVLLQQVGPYVYE	99		
SgreSNMP1	90	EYKQKVKLRDHKEDD	TVSYNNKITWLFNQGKSAPGLTGDELVTLPHPLLL	139		
SgreSNMP2	100	EWRRRRDV-TRMANGSLDYRLETTYHFS	PERS-PGLSEDEFTYLNVMV	147		
SgreSNMP1	140	GLLLTLERDKPGMLALVNKAIPPLFRKPESIFVTAPVRN	FLFDGI-VINC	188		
SgreSNMP2	148	GIVVQVSEDYSSLLSMVEPVLSELVPGGAQLFQ	RASARQLLWSGVPTVDC	197		
SgreSNMP1	189	TVTDFSAKALCTGLKKE---	AKELKREGDNFFSFFGHKNGTVDAGRRLV	235		
SgreSNMP2	198	RGNSAVATLACGALPSLLPATVQQTEPGVYV	SFFGFKNGT-SKQWWRV	246		
SgreSNMP1	236	KRGIQNIDDLGRVVAFN	GEPEKMSAW--RGDPCNDRGTDSTIFPPFRDPK	283		
SgreSNMP2	247	DSGVEDVRTLGSVISYD	NSRRLKVVSPNSPCNEIRGTDSTLFPFITPN	296		
SgreSNMP1	284	EPIVAFGPDCLCSL	GANWERKAEYMGVPGNRYTAELPDMKGNPEHHCYCP	333		
SgreSNMP2	297	DTIYIFAHDICRSM	HAERYEQDVSGVHGLRFVAGSLLRRGGPNACTCP	346		
SgreSNMP1	334	TEQTCLEKGTLDL	SPCAGAPVIATLPHFYLASETYLQTVSGLQPTKENHE	383		
SgreSNMP2	347	-DGRCLATGAI	SVRECFRAPIAVSFPHFYQASPEYLQYAEGLSPNKELHE	395		
SgreSNMP1	384	LFMVFESTTGSP	MEARKRLQFNMF LHKINKIDLLANVPYALMPLIWVEEG	433		
SgreSNMP2	396	TFVVIEPETGT	PLVGAKRLQFNMKAVRVSQVPALRNVS	DGLFPLLWVEEG	445	
SgreSNMP1	434	LALEEKYVSTLR	MLFRMQ	IMSGVKWTLMAVGMGMAGAGGYLHFKRRKEL	483	
SgreSNMP2	446	VELEEKQLSQ	VRALYVARASM	GGVAWAVLAVGV---AALLFCAVRLAKA	491	
SgreSNMP1	484	VVGPAEPKVVAGH	DTTGHP	IRLESSHSRY-----	513	
SgreSNMP2	492	RVAERNRSL	SLEKGV	TAGGKLSVPTLGAAYPESATKRPSPPAAAPA	AASTA	541
SgreSNMP1	514	-----	513			
SgreSNMP2	542	PAAPVDATHF	551			

Figure S1. Alignment of the amino acid sequences of *S. gregaria* SNMP1 and SNMP2. Pairwise sequence alignment were conducted with EMBOS Needle. Light grey underlined sequences represent intracellular regions of the proteins while black underlined areas denote predicted transmembrane domains. The region indicated by the grey background show the extracellular domains of the proteins used to generate antibodies. The ectodomains of SNMP1 (blue) and SNMP2 (orange) have a sequence identity of 33.7%.

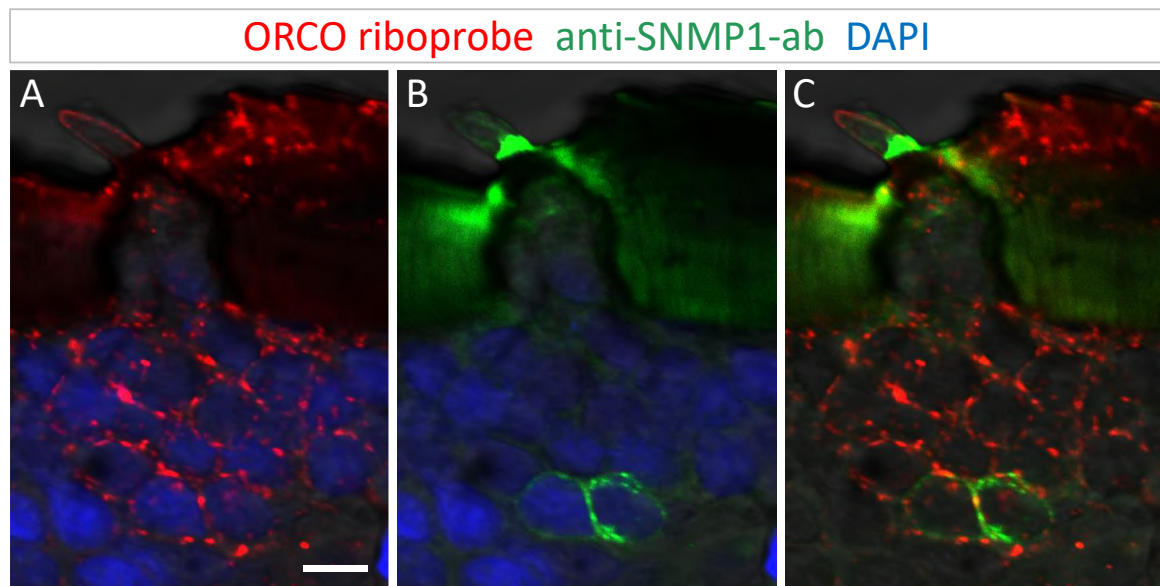


Figure S2. SNMP1 is expressed in a subset of Orco-positive OSNs in basiconic sensilla. In combined FISH/FIHC, Orco-positive cells were visualized using an antisense-Orco riboprobe (red), whereas SNMP1-positive cells were detected using anti-SNMP1-ab (green). Nuclei were stained with DAPI (blue). **A** red and blue channel. **B** green and blue channel. **C** merged depiction of the green and red channel. In all images, the fluorescent channels were overlaid with the transmitted light channel. Scale bar = 10 μ m.

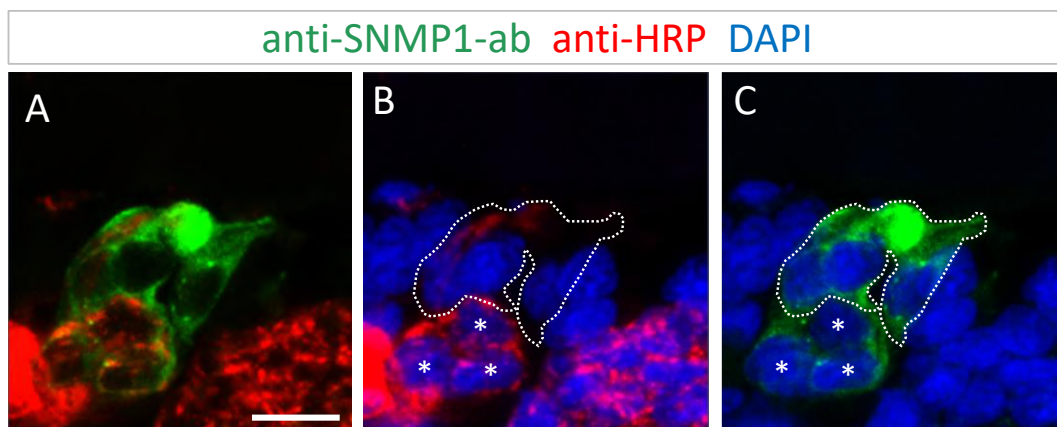


Figure S3. FIHC experiment showing that SNMP1 is expressed in OSNs and the associated support cells of a trichoid sensillum. The anti-SNMP1-ab labelling is shown in green. Neurons are labelled with anti-HRP and shown in red while the nuclei are stained with DAPI shown in blue. **A** green and red channel. **B** red and blue channel. **C** green and blue channel. The encircled area denotes the SNMP1 positive support cells and the asterisks show the SNMP1-positive OSNs. Scale bar = 10 μ m.

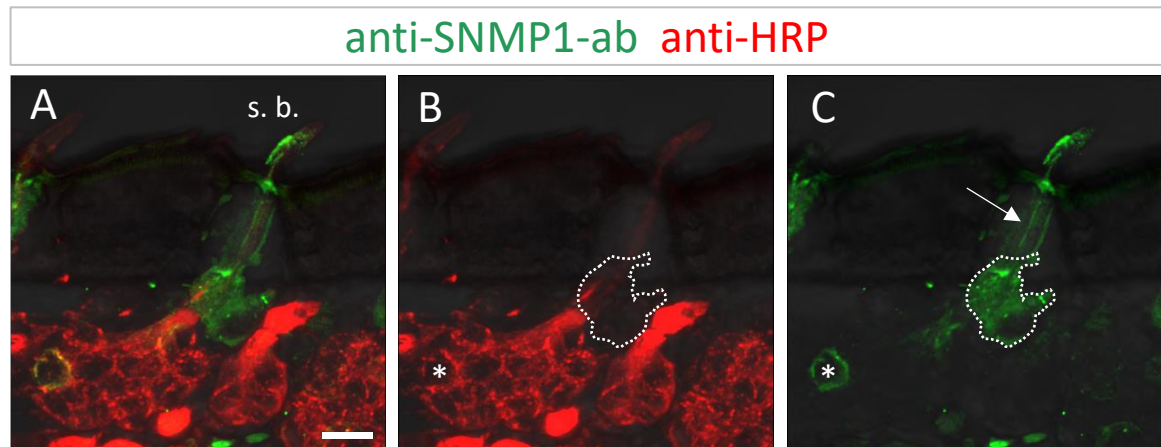


Figure S4. SNMP1 is expressed in distinct OSNs and support cells of a basiconic sensillum in *S. gregaria*. **A-C** FIHC experiment, showing anti-SNMP1-ab immunoreactive cells in the green (**A, C**) and OSNs labelled with anti-HRP in the red (**A, B**) fluorescence channels; the transmitted light channel was overlaid to better display the basiconic sensillum (s. b.). The region encircled denotes the SNMP1-positive support cells; the asterisk marks a SNMP1-expressing OSN within a basiconic OSN cluster. The arrow indicates dendritic labelling by anti-SNMP1-ab. Scale bar = 10 μ m.

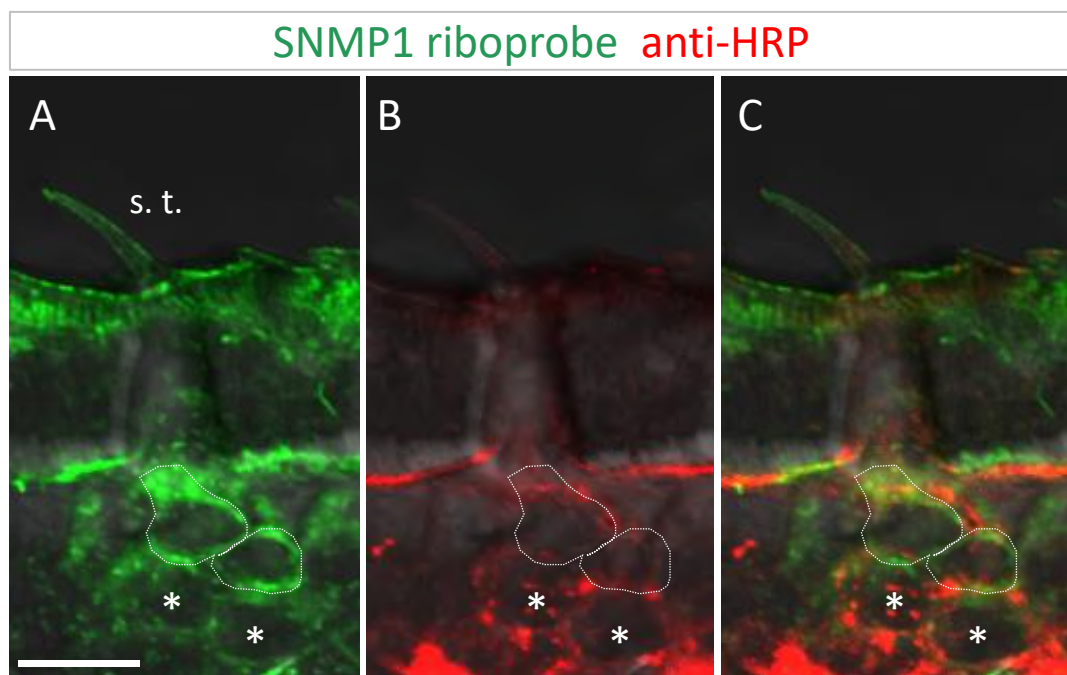


Figure S5. SNMP1 is expressed in support cells and OSNs of a *S. gregaria* trichoid sensillum. The SNMP1-positive cells were visualized by Combined FISH and FIHC using an specific antisense-SNMP1 riboprobe and anti-HRP for labelling of OSN. **A** Cells comprising SNMP1 transcripts visualized in the green fluorescent channel. **B** Labelling of OSNs (red fluorescent channel). **C** merged image of the red and green channels. The encircled areas cells indicated the location of non-neuronal SNMP1-positive support cells while the asterisks show SNMP1-positive OSNs. In all images, the fluorescent channels were overlaid with the transmitted light channels. Scale bar = 10 μ m.

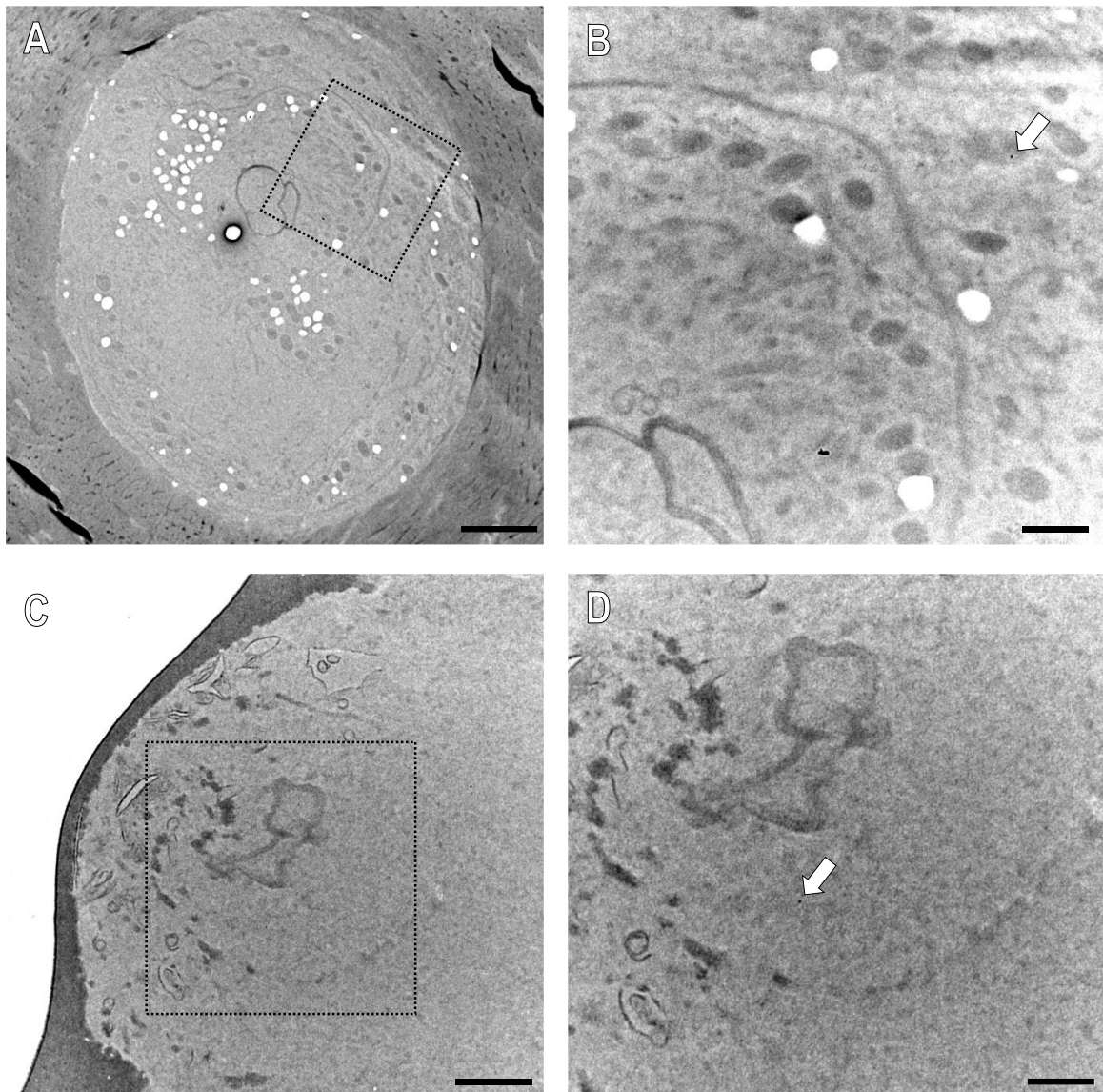


Figure S6. Assessment of secondary antibody binding to ultrathin sections of the *S. gregaria* antenna. Immunogold labelling experiments were conducted omitting the primary antibody, but applying the secondary antibody coupled with colloidal gold. **A** and **C** Overviews of cross section through different sensilla. **B** and **D** show the region boxed in **A** and **C**, respectively, at higher magnifications. Arrows denote single gold grains indicating negligible background labelling of the secondary antibody. Scale bars: A = 2 μm ; C = 1 μm ; B and D = 500 nm.

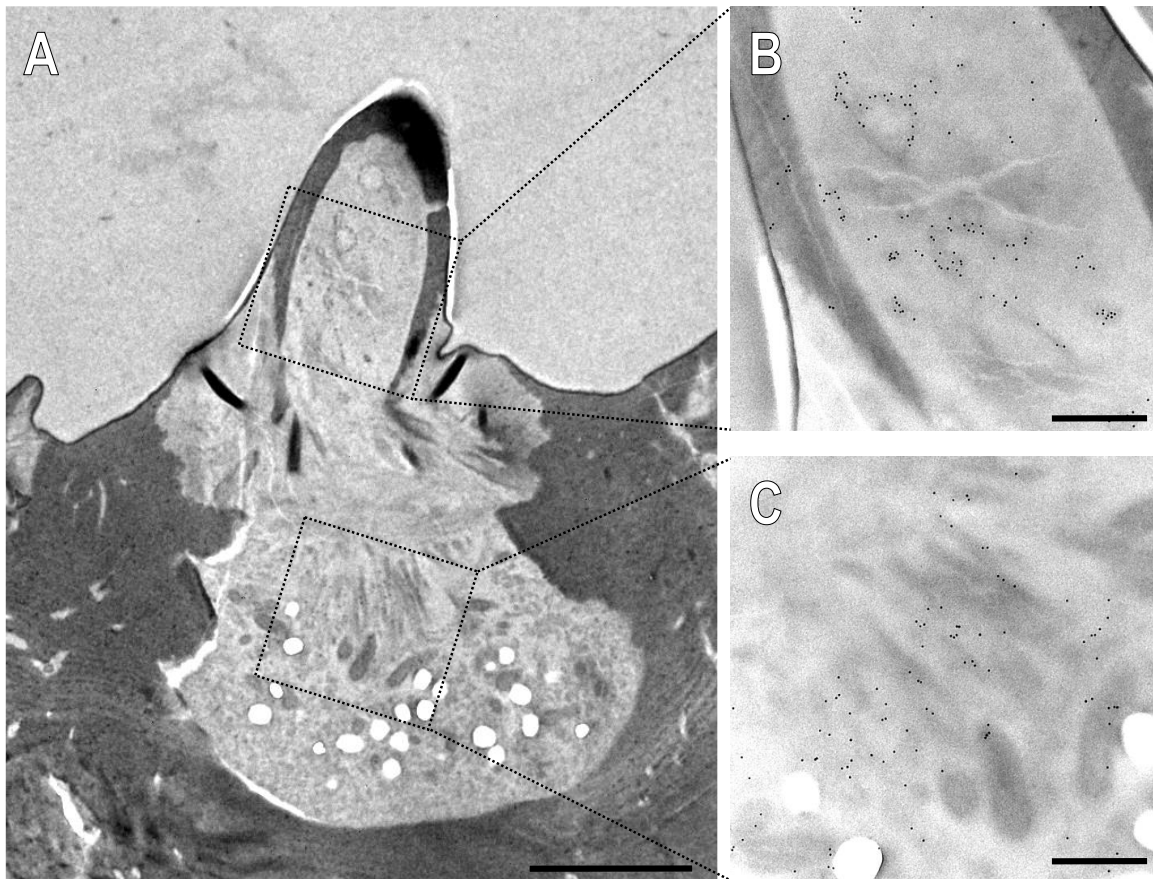


Fig. S7 Localization of SNMP1 within dendrites of OSNs and microvilli structures of support cells in a basiconic sensillum of *S. gregaria*. Ultrathin sections of antenna were used in immunogold-labelling experiments with anti-SNMP1-ab and assessed by transmission electron microscopy. **A** Overview image showing a basiconic sensillum. **B** Higher magnification of the sensillum shaft. Strong anti-SNMP1-ab immunoreactivity is associated with membranes of dendritic structures within the sensillum shaft. **C** Higher magnification of an area at the base of the sensillum demonstrating anti-SNMP1-ab labeling associated with microvilli structures of support cells. Scale bars: A = 2 μm ; B and C = 500 nm.

Chapter 3. Manuscript 2

Current Research in Insect Science 3 (2023) 100053



Contents lists available at ScienceDirect

Current Research in Insect Science

journal homepage: www.elsevier.com/locate/cris

The specific expression patterns of sensory neuron membrane proteins are retained throughout the development of the desert locust *Schistocerca gregaria*

Sina Cassau^a, Angelina Degen^a, Stephanie Krüger^{b,c}, Jürgen Krieger^{a,*}^a Martin Luther University Halle-Wittenberg, Institute of Biology/Zoology, Department of Animal Physiology, 06120 Halle (Saale), Germany^b Martin Luther University Halle-Wittenberg, Institute of Biology/Zoology, Department of Developmental Biology, 06120 Halle (Saale), Germany^c Martin Luther University Halle-Wittenberg, Biocenter, Microscopy Unit, 06120 Halle (Saale), Germany

ARTICLE INFO

Keywords:

Olfaction
 Locust development
 Olfactory sensory neuron
 Support cell
 Sensory neuron membrane proteins

ABSTRACT

The desert locust *Schistocerca gregaria* detects odorants through olfactory sensory neurons (OSNs) that are surrounded by non-neuronal support cells (SCs). OSNs and SCs are housed in cuticle structures, named sensilla found abundantly on the antenna in all developmental stages of the hemimetabolic insect. In insects, multiple proteins expressed by OSNs and SCs are indicated to play a pivotal role in the detection of odorants. This includes insect-specific members of the CD36 family of lipid receptors and transporters called sensory neuron membrane proteins (SNMPs). While the distribution pattern of the SNMP1 and SNMP2 subtypes in OSNs and SCs across different sensilla types has been elucidated for the adult *S. gregaria* antenna, their localization in cells and sensilla of different developmental stages is unclear. Here, we determined the SNMP1 and SNMP2 expression topography on the antenna of the first, third and fifth instar nymphs. Through FIHC experiments we found that in all developmental stages SNMP1 is expressed in OSNs and SCs of the trichoid and basiconic sensilla while SNMP2 is restricted to the SCs of the basiconic and coeloconic sensilla thus resembling the adult arrangement. Our results demonstrate that both SNMP types have defined cell- and sensilla-specific distribution patterns established already in the first instar nymphs and retained into the adult stage. This conserved expression topography underlines the importance of SNMP1 and SNMP2 in olfactory processes throughout the development of the desert locust.

Introduction

The ability to sensitively and precisely detect behaviorally relevant olfactory cues originating from conspecifics, food sources, or oviposition sites is of vital importance during all stages of insect life. This also applies to the hemimetabolic desert locust *Schistocerca gregaria* that can detect a plethora of relevant odorants including pheromones in all developmental stages (Ochieng and Hansson, 1999; Byers, 1991; Torto et al., 1996; Hassanali et al., 2005; Nakano et al., 2022; Njagi and Torto, 1996). Odor detection in the desert locust is accomplished via specialized olfactory sensory neurons (OSNs), mainly located on the antennae and palps (Greenwood and Chapman, 1984; Blaney, 1977; Lemke et al., 2020) where groups of OSNs are housed in a multitude of tiny hair-like structures called sensilla (Ochieng et al., 1998).

Olfactory sensilla comprise a perforated cuticle allowing for the entrance of odor molecules. Following sensillum entry, odor molecules are supposed to be transferred by odorant binding proteins (OBPs) in the sensillum lymph (Leal, 2013; Rihani et al., 2021) towards specific ol-

factory receptors in the membrane of the receptive dendrites of OSNs, that in insects mainly belong to the families of odorant receptors (ORs) and ionotropic receptors (IRs) (Fleischer et al., 2018; Wicher and Mazzi, 2021). At the base of the olfactory sensilla, OSNs are closely associated with non-neuronal support cells (SCs), which regulate the composition of the sensillum lymph and secrete OBPs into the fluid (Thurm and Küppers, 1980; Rihani et al., 2021). Thus, both the OSNs and the SCs of a sensillum express the proteins acting in the primary process of odor detection. In addition to OBPs and olfactory receptors, studies mainly in moths, flies and locusts (Rogers et al., 1997; Benton et al., 2007; Jiang et al., 2016; Cassau et al., 2022; Blankenburg et al., 2019) have demonstrated that certain OSNs and SCs also express subtypes of so-called sensory neuron membrane proteins (SNMPs) representing another group of proteins critical in the primary process of odor detection (Cassau and Krieger, 2021).

SNMPs are insect-specific members of the CD36 protein family (Rogers et al., 2001; Nichols and Vogt, 2008). Members of the CD36 protein family serve versatile functions including the reception and trans-

* Corresponding author.

E-mail address: juergen.krieger@zoologie.uni-halle.de (J. Krieger).<https://doi.org/10.1016/j.cris.2023.100053>

Received 6 October 2022; Received in revised form 10 February 2023; Accepted 17 February 2023

2666-5158/© 2023 The Authors. Published by Elsevier B.V. This is an open access article under the CC BY-NC-ND license

<http://creativecommons.org/licenses/by-nc-nd/4.0/>

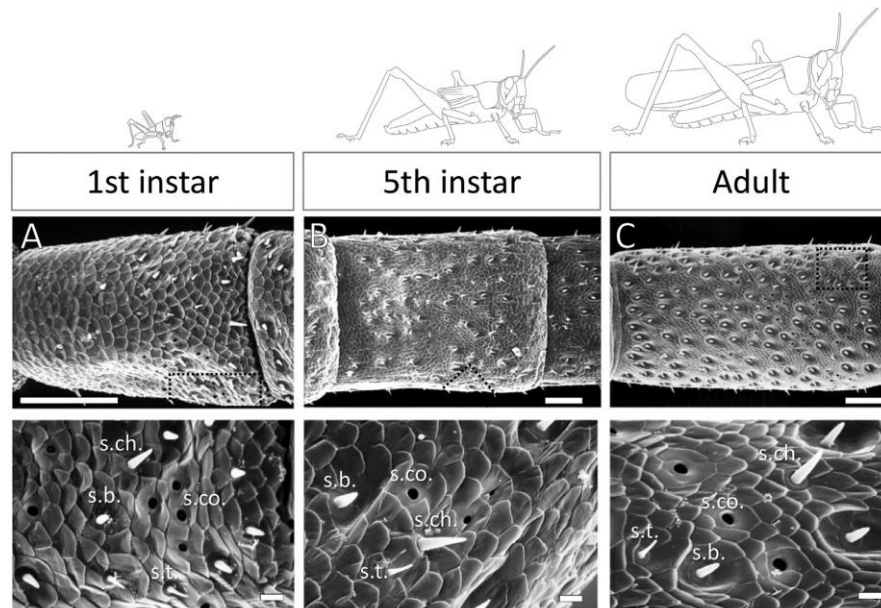


Fig. 1. Morphological classes of sensilla found on the antenna of *S. gregaria* in different developmental stages. The SEM images depict the middle antennal segments corresponding to: **A** first instar, segment 6, **B** fifth instar, segment 11 and **C** adult, segment 12. The lower row of images shows higher magnified areas of the regions boxed in the upper row. s.b. – sensillum basiconicum; s.ch. – sensillum chaeticum; s.co. – sensillum coeloconicum; s.t. – sensillum trichodeum. Scale bars: upper row = 100 μ m; lower row = 10 μ m.

port of lipids, lipophilic compounds and lipoproteins (Chen et al., 2022; Silverstein and Febbraio, 2009) and are distinguished by two trans-membrane domains and a large ligand-interacting ectodomain (Gomez-Diaz et al., 2016; Pepino et al., 2014). Variable numbers of SNMPs have been identified across insect species and orders, forming a diverse SNMP gene family divided into four groups (SNMP1-SNMP4) based on phylogenetic relationships (Zhang et al., 2020; Zhao et al., 2020). Studies on the expression, localization and function of SNMPs in the olfactory system have concentrated on SNMP1 and SNMP2 subtypes found in all insect species studied so far (Cassau and Krieger, 2021). In *Drosophila melanogaster* (Benton et al., 2007; Jin et al., 2008; Gomez-Diaz et al., 2016) and heliothine moth species (Pregitzer et al., 2014; Liu et al., 2020), the SNMP1 subtype was found essential for the sensitive detection of lipophilic pheromone compounds by OSNs. Data from *Drosophila* suggest a function of SNMP1 as a co-receptor that might mediate a transfer of pheromones or other odorants from OBPs to cognate ORs via its tunnel-like ectodomain (Gomez-Diaz et al., 2016). Furthermore, a rapid activation and deactivation of pheromone-induced activity of OSNs was found to depend on SNMP1 (Li et al., 2014). While functional studies on the SNMP2-type are missing, the current data demonstrate broad expression in antennal SCs (Gu et al., 2013; Blankenburg et al., 2019; Jiang et al., 2016) and a localization in their microvilli membrane bordering the sensillum lymph (Cassau et al., 2022). Based on these findings and its homology to the CD36 protein family of lipid receptors and transporters, a role of SNMP2 in clearing the sensillum lymph from lipophilic odorants or their degradation products has been suggested (Cassau and Krieger, 2021; Forstner et al., 2008; Blankenburg et al., 2019).

Recently, we elucidated the expression topography of the SNMP1 and SNMP2 protein in the antenna of adult *S. gregaria* in the gregarious phase (Cassau et al., 2022). Using fluorescence immunohistochemistry (FIHC) and immunogold labelling experiments we revealed a detailed picture of their expression and localization across the OSNs and SCs of

the three morphologically distinct olfactory sensilla types (Fig. 1). These are: broad and blunt sensilla basiconica, which house up to 30-50 OSNs, thin and sharp sensilla trichodea, bearing two to three OSNs, and sensilla coeloconica that are engulfed in pits in the antennal surface with three to four OSNs (Ochieng et al., 1998). Notably, sensilla chaetica are found as a fourth type of sensillum that are characterized by single pore openings at their tips and are supposed to serve gustatory and mechanosensory functions (Ochieng et al., 1998). In the adult desert locust, we found SNMP1 localized in a subset of OSNs innervating basiconic sensilla and in all OSNs innervating trichoid sensilla. Additionally, SNMP1 immune reactivity was detected in some SCs adjacent to the respective SNMP1-positive OSN clusters. In contrast, SNMP2 was localized solely in non-neuronal SCs of basiconic and coeloconic sensilla. Together our data suggest a role of SNMP2 limited to the functions of SCs, whereas SNMP1 seems to fulfill a dual function in the antenna of adult *S. gregaria*, i.e. in odor detection in OSN subpopulations as well as a function in certain SCs (Cassau et al., 2022).

Schistocerca gregaria is a hemimetabolic insect that develops through 5 nymphal stages into adulthood (Steedman, 1990). In contrast to the detailed picture revealed on the topography of SNMP1 and SNMP2 expression in adult desert locust antenna, the expression of the two SNMPs over the course of its development is unknown. So far, their developmental expression has been analyzed only by PCR on the transcript level demonstrating the presence of mRNA for SNMP1 and SNMP2 in the five nymphal instars of *S. gregaria* (Jiang et al., 2016). The *S. gregaria* antenna undergoes a successive development; with each moult, the locust antenna increase in length (from 3 mm in the 1st instar to 14 mm in the adults) as well as total number of segments (12 annuli in the 1st instar to 24 annuli in adults) (Ochieng et al., 1998; Chapman, 2002). This goes along with a massive increase in the total number of the olfactory sensilla types and consequently the overall number of OSNs on the antenna (Ochieng et al., 1998). Moreover, adult and juvenile stages

of locusts differ in their responsiveness to behaviorally relevant odors (Obeng-Ofori et al., 1994; Torto et al., 1994), as well as in the expression levels of ORs, IRs and OBPs in the olfactory appendages during development (Li et al., 2018; Wang et al., 2015; Xu et al., 2013). This implies differences in the expression of olfactory proteins across OSNs, SCs and sensilla between juvenile and adult locusts. Given this scenario, in this study we aimed at elucidating the SNMP1 and SNMP2 protein expression in different juvenile stages of *S. gregaria* in order to scrutinize whether the cell-type and sensilla-specific expression pattern of SNMPs observed in adult antenna is different in nymphal instars or alternatively already exists in the first nymphal stage and is retained during locust development. Towards this goal, we used SNMP-specific antibodies in immunohistochemical approaches to analyze the expression topography of the two SNMP types in cells of basiconic, trichoid and coeloconic sensilla on the antenna of first, third and fifth instar nymphs and compared it to adults.

Materials and methods

Animal rearing

Desert locusts, *Schistocerca gregaria*, were reared under crowded (gregarious) conditions as previously described (Seidelmann et al., 2000; Cassau et al., 2022). Briefly, 100 to 150 individuals were kept in metal cages (50 × 50 × 50 cm) with metal grids at the bottom and at two sides. The photoperiod was 12L: 12D. The temperature was 34°C during the day and 27°C at night. The insects were fed with fresh wheat seedlings and flaked oats. The females were given cups of sand for oviposition, which were afterwards transferred to an empty cage for the development of the locusts. First, third and fifth instars were classified based on the number of eye stripes, as the number of stripes corresponds to their instar stage (Uvarov, 1966).

Scanning electron microscopy (SEM)

Antennae from cold anesthetized adults, fifth and first instar nymphs were carefully removed from the head and fixed for 15 min in a modified Carnoy's solution (ethanol, chloroform, acetic acid in a ratio of 3:1:1). For each stage one individual was examined. The samples were then dehydrated in a graded ethanol series of 60%, 70%, 80%, 90%, and 100% for at least 15 min in each solution, followed by 5 min in hexamethyldisilazane. The samples were placed onto a filter paper and left to dry overnight. Afterwards, they were mounted onto aluminum specimen stubs with double-sided adhesive pads. The following day, the samples were sputter-coated with gold for 200 s at 20 mA using a Balzers SCD 004 sputter coater (BAL-TEC, Balzers, Liechtenstein). The samples were examined with a Hitachi SEM S-2400 scanning electron microscope (Hitachi, Tokyo, Japan) at 12–18 kV and images were captured on ILFORD FP 4 black-and-white film (Harman Technology, Moberley, UK). Contrast, brightness and tonal values of the images were adjusted to create uniformed figures.

Fluorescent immunohistochemistry (FIHC)

Fluorescence immunohistochemistry (FIHC) with the anti-SNMP-antibodies was performed as previously described (Cassau et al., 2022). For each stage we analysed at least 4 individuals. Third and fifth instars of *S. gregaria* were removed from the stock cultures and cold anesthetized on ice. The antennae were carefully dissected and immediately embedded into Tissue-Tek O.C.T. freezing medium (Sakura Finetek, Alphen aan den Rijn, the Netherlands) at -20°C. Cryosections (12 µm) of the samples were prepared with a Cryostar NX50 cryostat (Thermo Scientific) at -20°C. Sections were thaw-mounted onto SuperFrost Plus slides (Thermo Scientific) and kept cold at -20°C until encircling them using colourless ROTI@Liquid Barrier Marker (Carl Roth, Karlsruhe, Germany). Next, sections were fixed by incubation of the slides for 20 min

at 4°C with 4% paraformaldehyde (PFA) dissolved in phosphate buffered saline (PBS, 145 mM/L NaCl, 1.4 mM/L KH₂PO₄, 8 mM/L Na₂HPO₄, pH 7.4). Afterwards, the sections were rinsed at room temperature consecutively in PBS two times for 5 min, in PBS with 0.01% Tween20 for 5 min, in 50 mM NH₄Cl in PBS for 5 min and finally in PBS for 5 min. After incubating the samples in blocking solution (10% normal goat serum, 0.5% Triton-X100 in PBS) for 30 min at room temperature, the sections were incubated with the primary antibodies. The antibodies were diluted in blocking solution and added onto the sections, which were then incubated over night at 4°C in a humid box (rabbit-anti-SgreSNMP1-ab 1:500; rabbit-anti-SgreSNMP2-ab 1:100). The slides were then washed three times for 5 min with PBS and subsequently treated with goat-anti-rabbit AF488-conjugated secondary antibodies (1:1000) (Jackson ImmunoResearch, Ely, Great Britain), goat-anti-HRP Cy3 (1:400) (Jackson ImmunoResearch), and DAPI (1:500, Thermo Fisher Scientific) diluted in PBS, for 1 h at room temperature in a humid box. Finally, the slides were washed two times for 5 min in PBS, once for 5 min in dH₂O and then mounted in mowiol solution.

Whole mount immunohistochemistry

Preparation of histological sections from the first instar locust antenna for FIHC experiments were not suitable. We therefore attempted whole mount (WM) FIHC to obtain meaningful results. Finally, we found this method applicable for first instar antenna, which, due to their small size and relatively thin cuticle, allow for analysis of WM-preparation with the LSM.

For WM-FIHC experiments with first instar nymphs the same solutions were used as described for FIHC on sections. For this stage we investigated at least six individuals for SNMP1 and SNMP2, respectively. All incubation steps were conducted on an overhead shaker and in 0.3 ml reaction tubes. Antenna were carefully excised from the head and portioned into 2 mm sections then immediately transferred into 4% PFA in PBS with 0.5% Triton-x100 over night at 4°C. Afterwards, the samples were washed three times for 10 min with PBS followed by 10 min in 50 mM NH₄Cl in PBS and an overnight treatment in blocking solution at 4°C. The antennal fragments were then treated with the primary antibodies diluted in blocking solution (rabbit-anti-SgreSNMP1 1:200; rabbit-anti-SgreSNMP2 1:100) and incubated for 48h at 4°C. After washing the samples three times for 10 min with blocking solution, they were treated with goat-anti-rabbit AF488 (1:1000), goat-anti-HRP Cy3 (1:200) and DAPI (1:250) diluted in blocking solution for two days at 4°C. The antennal samples were then washed three times for 10 min with PBS and finally rinsed with dH₂O for at least 5 min and ultimately mounted with mowiol solution on microscope slides covered with cover slips.

Confocal microscopy

Sections from FIHC experiments and samples from the whole mount FIHC were analyzed on a confocal laser scanning microscope (LSM 880, Carl Zeiss Microscopy, Jena, Germany). Confocal image stacks of the fluorescence and transmitted-light channels were taken and used to generate either pictures representing single optical planes or projections of optical planes applying the ZEN software (Carl Zeiss Microscopy). Pictures were not altered except for adjusting the brightness or contrast for a uniform tone within a single figure.

Results

Sensilla types on the developing antenna

In order to confirm the conservation of the outer olfactory sensilla morphology during development, we first had a look if there are any obvious differences in the structures of the antennal sensilla types i.e. sensilla basiconica, s. trichodea, s. coeloconica and s. chaetica between

different developmental stages. Figure 1 shows sensilla on the approximate middle segments of a locust antenna from the first instar (segment 6), fifth instar (segment 11) and an adult (segment 12). In accordance with an earlier study (Ochieng et al., 1998), significant differences in the density of sensilla among these developmental stages of *S. gregaria* are immediately evident, with a dramatic increase in sensilla number from the first instar nymph to the adults. Yet, closer inspection of each individual sensillum type revealed no obvious differences between the olfactory sensilla of different developmental stages. Similar to adults, the sensilla basiconica of the first and fifth instars have wide shafts without a socket at their base and protrude out of flattened depressions in the cuticular surface. In all stages analyzed, the trichoid sensilla also appear similar; they are slightly arched and more slender compared to the basiconic sensilla. No obvious morphological changes during the development were also indicated for the coeloconic sensilla that are found in pits of the cuticular surface (Fig. 1C and Fig. S1). Higher magnification of a coeloconic sensillum reveals longitudinal ridges among the sensillum's shaft present in the first and adult stage (Fig. S1). Finally, the largest and massive gustatory/mechanosensory sensilla chaetica arise from basal sockets and look morphologically similar in the developmental stages analyzed (Fig. 1). Overall, although we examined only one individual per stage, the antennal sensilla types do not exhibit any notable morphological differences in locusts of different ages.

SNMP1 and SNMP2 expression in the antenna of the developing locust

In order to compare the distribution patterns of SNMP1 and SNMP2 proteins in the antenna of different juvenile stages and adults of the desert locust, we conducted comprehensive FIHC experiments. Towards this goal, we employed specific antibodies to discern the SNMP1 and SNMP2 expression topography together with an anti-HRP antibody and DAPI, that label neurons and nuclei, respectively.

First, we analyzed the fifth instar nymph, since their antennal morphology mostly resembles that of the adult locust. A representative result for the anti-SNMP1 immuno-labelling pattern obtained with an antennal section of the fifth nymphal stage is shown in Fig. 2A depicting several anti-SNMP1-ab immuno-labelled cells distributed across the section. Higher magnification of the boxed area in Fig. 2A shows two SNMP1-positive cells localized within a cluster of neuronal cells (Fig. 2B and C).

Next, we set out to determine the expression of SNMP1 in cells of the three different olfactory sensilla types of the fifth instar antenna (Fig. 2, D-I). In accordance with the finding that basiconic sensilla house about 30-50 OSNs (Ochieng et al., 1998), evaluation of this sensillum type revealed labeling of clusters of neurons with the anti-HRP antibody (Fig. 2D and E). The simultaneous visualization of neurons (anti-HRP) and SNMP1-positive cells (anti-SNMP1-ab) demonstrated that SNMP1 is expressed in a subpopulation of basiconic OSNs (Fig. 2, D-F, asterisks). In addition, anti-SNMP1-immune reactivity was also detected above the OSN cluster, labelling a large non-neuronal SC (Fig. 2, D-F, encircled area). For trichoid sensilla we found strong SNMP1 immunolabelling of multiple cells underneath the sensillum base (Fig. 2G and H). Merging the signals obtained with anti-SNMP1-ab and anti-HRP demonstrate expression of SNMP1 in an OSN (asterisk) that projects into the sensillum (Fig. 2G). The anti-SNMP1-ab clearly visualizes three more cells, which are non-neuronal and are situated between the SNMP1-positive OSN and the trichoid sensillum's base (encircled region Fig. 2, G-I). Thus, these FIHC results suggest that the trichoid sensilla of the fifth instar possess SNMP1-positive OSNs and multiple SNMP1-positive support cells. In contrast to basiconic and trichoid sensilla, inspection of the third olfactory sensillum type, i.e. coeloconic sensilla, did not reveal any SNMP1-positive cells.

Having established the SNMP1 distribution pattern in the fifth instar, we next set out to determine the expression topography of SNMP2 in this developmental stage (Fig. 3). Utilizing the anti-SgreSNMP2-ab we localized the SNMP2 protein in cells underneath basiconic and coe-

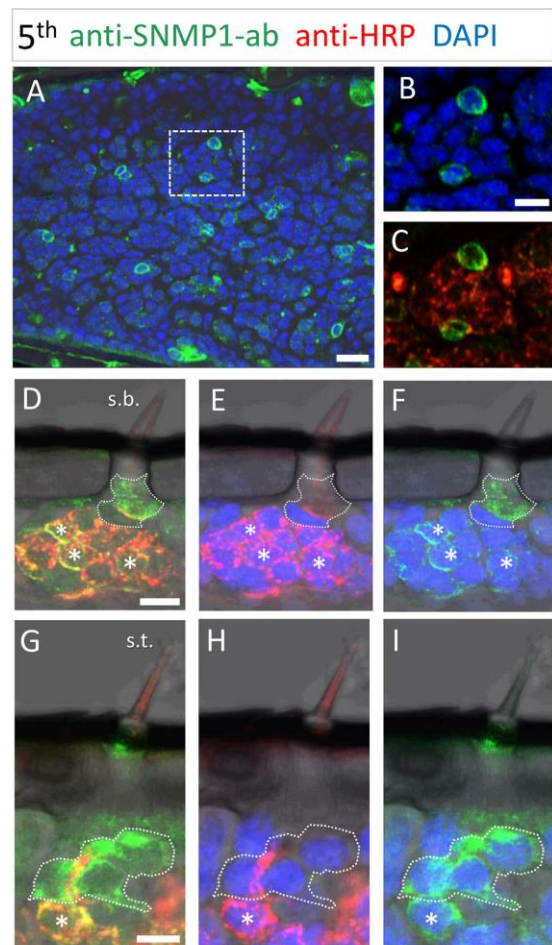


Fig. 2. SNMP1 expression in the antenna of the fifth instar of *Schistocerca gregaria*. SNMP1-positive cells were visualized by FIHC in longitudinal sections using anti-SgreSNMP1-ab (green). Neurons were identified by an anti-HRP-antibody (red) and nuclei were stained with DAPI (blue). A distribution of multiple SNMP1 cells in an antennal segment. **B, C** Higher magnification of the area boxed in (A) showing expression of SNMP1 (green) in a fraction of the OSNs (red), while C, D, G represent overlays of the red and green channels. **E and F**, overlays of the red and blue channels. The transmitted light channel was overlaid with the fluorescent channels in A and D-I. Asterisks (*) denote SNMP1-positive OSNs. Encircled areas denote SNMP1-positive support cells. s.b. - sensillum basiconicum; s.t. - sensillum trichodeum. Scale bars: A = 20 µm; B, D, G = 10 µm.

loconic sensilla (Fig. 3A). The magnified image of the basiconic sensillum from Fig. 3A depicts a large SNMP2-positive cell underneath the sensillum's base (Fig. 3, B-D). Through simultaneous visualization of the neurons by anti-HRP, it is evident that SNMP2 is not located in the OSNs of basiconic sensilla but most likely expressed in associated non-neuronal SCs (Fig. 3C and D, encircled). Similarly, for coeloconic sensilla we found strong anti-SNMP2-ab immune reactivity with non-neuronal cells just underneath the cuticle (Fig. 3 E-F). These SNMP2

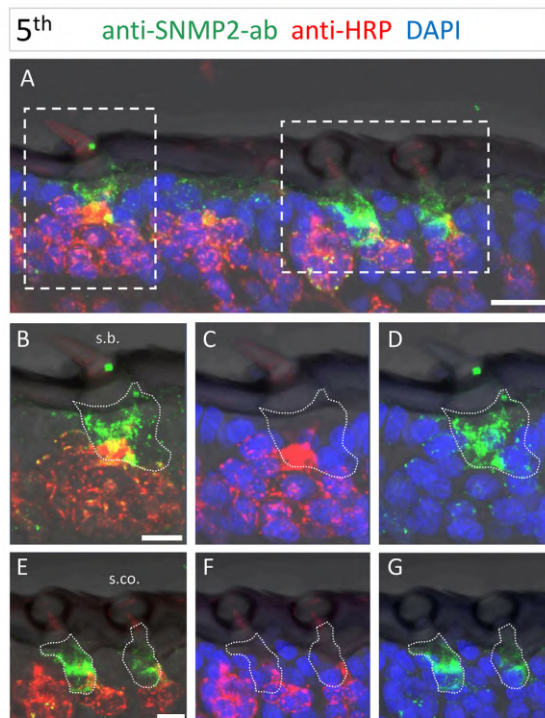


Fig. 3. Sensilla-specific distribution of SNMP2 in the 5th instar's antenna. SNMP2-positive cells were visualized by FIHC in the longitudinal section using anti-SgreSNMP2-ab (green). Neurons were visualized by an anti-HRP-antibody (red) and nuclei by staining with DAPI (blue). In all images the fluorescence channels were overlaid with the transmitted light channel. **A** Topography of SNMP2-expressing cells underneath sensilla shown in all fluorescence channels. **B-D** displays the area with the basiconic sensillum (s.b.) boxed in (A). Accordingly, **E-G** shows two sensilla coeloconica (s.co.) boxed in the right area in (A). **B** and **C**, overlays of the green and red fluorescence channels. **C** and **F**, red and blue channels. **D** and **G**, green and blue channels. The encircled areas denote SNMP2 positive support cells. Scale bars: **A** = 20 μ m; **B** and **E** = 10 μ m.

positive cells directly border a cluster of 3-4 OSNs that innervate the coeloconic sensilla (Fig. 3F and G, encircled). Along the antennal tissue, the anti-SgreSNMP2-ab did not generate any specific signals in neuronal cells.

Taken together, the analysis of the fifth instar antenna revealed that SNMP2 is expressed in OSNs of basiconic as well as trichoid sensilla and in addition in some SCs cells of these sensillum types. In contrast, SNMP2 was restricted to SCs of basiconic and coeloconic sensilla. Overall, these expression patterns match the SNMP1 and SNMP2 distribution patterns we previously obtained for the adult antenna (Cassau et al., 2022).

Approaching the SNMP1 and SNMP2 expression topography in the third instar nymph of desert locusts led to results similar to fifth instar nymphs. As demonstrated by Fig. S2, we found SNMP1 expression in a subset of OSNs of basiconic sensilla and in SCs of this sensillum type. In addition, all three OSNs of the trichoid sensillum were SNMP1-positive (Fig. S2, asterisks) as well as several adjacent non-neuronal SCs (Fig. S2, encircled area). In the antenna of the third instar nymph, anti-SNMP2-ab generated immune reactivity exclusively in non-neuronal cells of basiconic and coeloconic sensilla, suggesting that also in this developmental stage, the SNMP2 protein is restricted to SCs (Fig. S3).

Having revealed conserved antennal expression patterns for SNMP1 and SNMP2 in third and fifth instar nymphs, we set out to examine the antenna of the freshly hatched first instar nymphs. Because FIHC on sections was challenging and did not reveal clear results, we established whole mount FIHC (WM-FIHC) for the antenna of the first instar. In this developmental stage, the sensilla are most abundant in the distal half of the antenna (Fig. S4) covering both the ventral as well as the dorsal sides of the segments. With this background, we used segments one to six (Fig. S4, A and B) in our analyses of the SNMP expression topography.

A representative result of a WM-FIHC using anti-HRP and anti-SNMP1-ab on the antenna of first instar nymph is depicted in Fig. 4. Using the anti-HRP, we were able to visualize numerous antennal neurons (OSNs) organized in clusters in the whole mount preparation (Fig. 4A). In comparison, the SNMP1 antibody labeled a lower number of cells across an antennal segment (Fig. 4B). In the overlay of the anti-SNMP1 (green) and neuronal (red) labeling (Fig. 4C), it is immediately clear that SNMP1 is expressed in a subpopulation of OSNs also in this developmental stage. Closer inspection of a basiconic sensillum reveals that it is innervated by a large number of OSNs (Fig. 4D), comparable to basiconic sensilla of third and fifth instar nymphs (Fig. S2, Fig. 2). Of these OSNs, only some are SNMP1-positive (Fig. 4D and E, asterisks). Furthermore, similar to the later developmental stages, anti-SNMP1 immune reactivity was detected above the OSNs beneath the base of the sensillum's shaft, suggesting that SNMP1 is also expressed in the non-neuronal support cells in the first instar (Fig. 4D, encircled area). Upon inspection of the labeling of cells in first instar trichoid sensilla we found numerous SNMP1-positive cells (Fig. 4E and F), three of which were OSNs innervating the sensillum as indicated by positive anti-HRP labeling (Fig. 4G and H, asterisks). Moreover, SNMP1 immune reactivity was localized to three non-neuronal cells that are most likely SCs associated with the adjacent OSN cluster (Fig. 4G and H, encircled area). Similar to the other nymphal stages studied, no SNMP1 immune reactivity was detected in cells underneath coeloconic sensilla.

As with SNMP1, we assessed the SNMP2 distribution in the first instar's antenna utilizing anti-SgreSNMP2-ab in WM-FIHC experiments (Fig. 5). As shown by the representative image of an antennal segment, we found strong labelling of several cells indicative for SNMP2 expression (Fig. 5A). Through simultaneous anti-HRP labelling, we could show that SNMP2 that is not expressed in neurons i.e. OSNs but in the closely associated non-neuronal SCs (Fig. 5B). To define the topographic localization of SNMP2 in the antenna further, we assessed basiconic sensilla and detected SNMP2-positive cells in up to two cells above the cluster of OSNs, which project into the sensillum's shaft (Fig. 5, C-E, encircled). Similarly, SNMP2 immune reactivity was discovered beneath the non-neuronal SCs of coeloconic sensilla (Fig. 5, F-H, encircled areas). These SNMP2-positive cells are closely associated with the bordering OSNs, apparently enveloping the sensory neurons. Overall, the results obtained by analyzing the developing antenna strongly suggest that the specific expression topography of both SNMP1 and SNMP2 is already predetermined in the first instar nymph and subsequently retained throughout all stages of development towards the adult stage.

Discussion

In this study, we assessed the cell type- and sensilla-specific distribution pattern of the SNMP1 and SNMP2 proteins in the antennae of different developmental stages of the hemimetabolic desert locust *S. gregaria*. Initially, we inspected the outer morphology of the sensilla on the antenna of adults and the first and fifth juvenile stage. In agreement and extension of previous studies in *S. gregaria* (Ochieng et al., 1998) we identified four types of sensilla in each developmental stage i.e. the olfactory basiconic, trichoid and coeloconic sensilla and the presumed gustatory/mechanosensory sensilla chaetica, which all showed no obvious morphological differences along the development. Four basic sensillum types displaying similar morphologies were also reported for nymphal stages and adults of the related locust species *Schisto-*

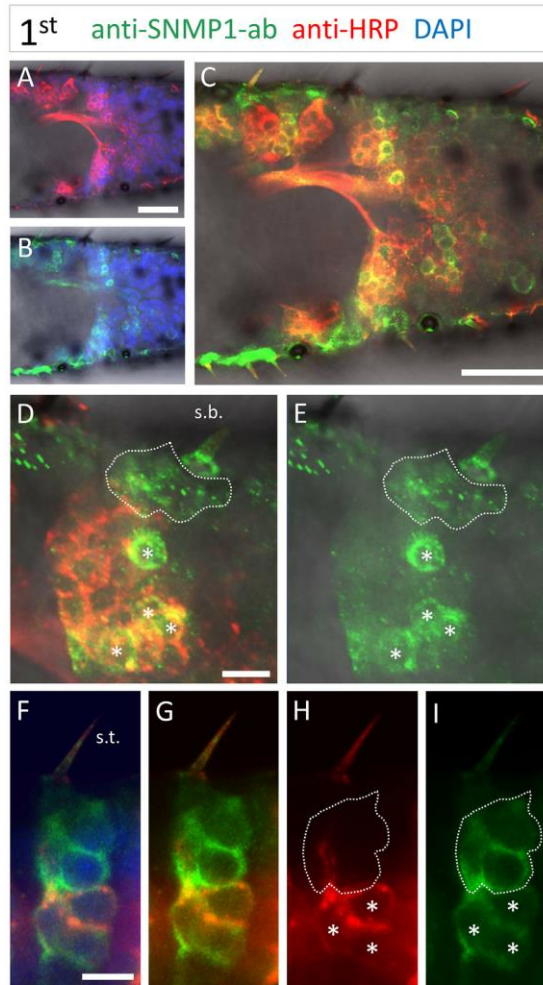


Fig. 4. SNMP1 expression in cells and sensilla of the antenna of first instar *S. gregaria*. Antennal segments were treated in whole-mount FIHC experiments using anti-SNMP1-ab (green), anti-HRP to visualize neurons (red) and DAPI to visualize nuclei (blue). **A-C** depiction of multiple OSN clusters and SNMP1-positive cells within an antennal segment, shown by different fluorescence channel combinations. **D-E** displays SNMP1-expression in subsets of OSNs and a support cell underneath a basiconic sensillum (s.b.). **F-I** multiple SNMP1-positive OSNs and support cells in a trichoid sensillum. **A**, red and blue fluorescence channels. **B**, green and blue channels. **C, D, G** red and green channels. **E** and **I**, green channel. **F**, green, blue and red channels. **H**, red channel. In **A-E**, the fluorescence channels are overlaid with the transmitted light channel. Asterisks (*) indicate SNMP1-positive OSNs. Encircled regions indicate SNMP1-positive support cells. Scale bars: **A** and **C** = 50 μm ; **D** and **F** = 10 μm .

cerca americana (Chapman, 2002) and *Locusta migratoria* (Chapman and Greenwood, 1986) indicating a similar sensillum type equipment of the antenna in different locust species and their successive development stages.

Our FIHC analyses of the SNMP1 protein expression in the antenna of first, third and fifth nymphal instars revealed similar distribution patterns. We found the protein in all OSNs of trichoid and a subpop-

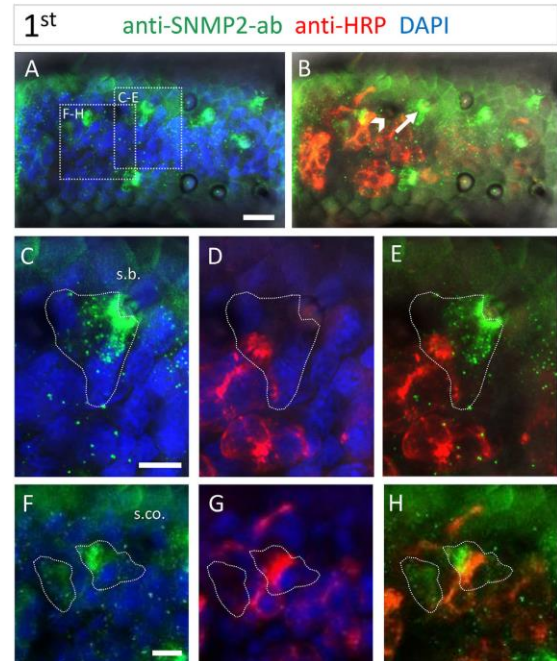


Fig. 5. Expression topography of SNMP2 in the antenna of the first instar of *S. gregaria*. The anti-SNMP2-ab was used in whole-mount FIHC experiments with antennal segments utilized to visualize SNMP2-positive cells (green). Anti-HRP and DAPI were used to visualize neurons (red) and nuclei (blue) respectively. **A-B** display the SNMP2-positive cells alone (**A**) or in combination with labelled neurons (**B**) indicating the non-neuronal expression of SNMP2 across the antennal segment. **C-E** higher magnified images of the right box in figure (**A**) illustrating SNMP2 expression in support cells underneath a basiconic sensillum (s.b.). **F-H** shows higher magnification of the left box in (**A**), depicting SNMP2-positive support cells associated with a coeloconic sensillum (s.co.). **A, C, F**, overlay of the green and blue fluorescence channels. **B, E, H**, green and red channels. **D** and **G**, red and blue channels. Encircled regions indicate SNMP1 positive support cells. In **B** the arrowhead denotes position of the coeloconic sensillum while the arrow indicates the position of the basiconic sensillum. Scale bars: **A** = 20 μm ; **C** and **F** = 10 μm .

ulation of OSNs in basiconic sensilla, but not in OSNs of coeloconic or chaetic sensilla. In addition, in all stages tested, SNMP1 was detected in non-neuronal SCs of trichoid and basiconic sensilla. The anti-SNMP1-ab labelling of SCs was most prominent for trichoid sensilla, enabling the detection of three SCs of this sensillum type in the first, third and fifth instar nymphs. Overall, the determined expression pattern of SNMP1 across cells and sensilla of antenna from nymphal instars perfectly matches the SNMP1 topography that we determined recently for the antenna of adult desert locusts (Cassau et al., 2022). This suggests similar functions of SNMP1 in the olfactory system of adults and in the different developmental stages of *S. gregaria*.

While currently no functional data exist for the role of SNMP1 in locusts, studies performed in the adult stage of the holometabolous fly *Drosophila melanogaster* and some moth species demonstrated a requirement of SNMP1 for a sensitive detection of pheromones and distinct plant odorants by OSNs of trichoid sensilla (Benton et al., 2007; Liu et al., 2020; Ronderos et al., 2014). Additionally, results from *Drosophila* suggest that SNMP1 may act as a co-receptor mediating the transfer of pheromone molecules from OBPs to neighboring ORs in the membrane of OSNs (Gomez-Diaz et al., 2016).

Given the proposed co-receptor function of SNMP1 in trichoid OSNs of the fly and of moths and its presence in adults and the larval stages of these holometabolous insects (Zielonka et al., 2016; Forstner et al., 2008; Herboso et al., 2011), it is conceivable that in the hemimetabolous desert locust SNMP1 may also serve in pheromone detection by trichoid OSNs and through certain OSNs of basiconic sensilla in adults and juvenile stages. This notion would fit with our yet limited knowledge of pheromone-detecting OSNs in locusts. In *S. gregaria*, single sensillum recordings from antenna revealed trichoid and basiconic OSNs are responsive to the putative pheromone (E,Z)-2,6-nonadienal and the pheromone phenylacetoneitril (PAN), respectively (Ochieng and Hansson, 1999; Seidelmann and Ferenz, 2002). Moreover, in the migratory locust *Locusta migratoria* the aggregation pheromones 4-vinylanisol is detected by distinct OR35-expressing OSNs of basiconic sensilla in all developmental stages (Guo et al., 2020). However, given the finding that in *S. gregaria* adults (Pregitzer et al., 2017; Pregitzer et al., 2019) and nymphal instars (this study) SNMP1 shows a rather wide expression in OSNs and, moreover, SNMP1 was found co-expressed with at least 33 of the 119 ORs in adults (Pregitzer et al., 2019), it is unlikely that its function is limited to a role in pheromone detection. Instead, it may possibly have versatile roles in the reception of other behaviorally relevant odorants, such as olfactory cues indicating appropriate food sources for both nymphs and adults. Noteworthy, in adults (Cassau et al., 2022) and all juvenile stages studied we found SNMP1 in only a subset of the OSNs of basiconic sensilla, corroborating the presence of SNMP1-dependent and SNMP1-independent odorant detection pathways in all developmental stages of the locust.

Similar to *Drosophila* (Benton et al., 2007), we also found SNMP1 expressed in non-neuronal cells of olfactory sensilla indicating a dual role of this SNMP-type in OSNs and SCs. In contrast, the FIHC results obtained for SNMP2 with the antenna of the first, third and fifth instars revealed anti-SNMP2 labelling only of non-neuronal SCs located underneath basiconic and coeloconic sensilla. This SNMP2 expression pattern resembles the situation in adult locusts (Cassau et al., 2022) and demonstrates that also for this SNMP-type a cell-type- and sensilla-specific expression pattern is retained during development.

The function of SNMP1 and SNMP2 in the support cells of olfactory sensilla is presently unclear. As members of the CD36 family of lipid transporters/receptors, SNMPS in SCs are generally discussed as membrane proteins involved in the removal of lipophilic “waste products” from the sensillum lymph, such as odorants following receptor activation or their degradation products (Cassau and Krieger, 2021). In this context, CD36 proteins have been reported to act as membrane transporters of lipophilic compounds including fatty acids (Giovannucci and Stephenson, 1999; Kiefer et al., 2002; Wang et al., 2007; Yang and O'Tousa, 2007). Alternatively, it is possible that SNMPS facilitates the uptake of lipophilic compounds by a caveolae-dependent endocytotic pathway, as recently demonstrated for the CD36-mediated uptake of fatty acids into adipocytes (Hao et al., 2020).

In support of this concept, we recently localized both SNMP1 and SNMP2 in the apical microvilli membranes of SCs bordering the sensillum lymph of basiconic sensilla through immunogold labelling experiments (Cassau et al., 2022). Notably, SNMP1-expressing SCs, are found exclusively in sensillum types that also house SNMP1-expressing OSNs (trichoid, basiconic). Thus, it is tempting to speculate that SNMP1-expressing SCs may be involved in the clearance of compounds detected via SNMP1-expressing OSNs, whereas SNMP2 serves the removal of waste resulting from non-SNMP1-mediated odor detection. While SCs of trichoid sensilla only expresses SNMP1, we found both SNMP1 and SNMP2 in SCs underneath basiconic sensilla. However, our FIHC experiments with nymphal stages and adults (Cassau et al., 2022) did not allow us to unequivocally clarify the expression of the two SNMP-types in separate cells or a possible co-expression in some SCs.

In conclusion, we have revealed cell type- and sensillum type-specific expression patterns for SNMP1 and SNMP2 that are already established in the first instar and are retained to the adult stage. This conservation

underlines the important roles of the two SNMP types in olfactory processes throughout development. Thereby, SNMP1 is indicated to have a function in a subpopulation of OSNs and in support cells, whereas SNMP2 serve a function only in support cells.

Data availability statement

Data are shown in the main manuscript or in the Supplementary Material. In addition, data from independent FIHC experiments conducted on different individuals of the 1st, 3rd and 5th nymphal stages of *S. gregaria* have been compiled in an “Additional Data File”.

Author Contributions

Sina Cassau: Conceptualization, Investigation, Methodology, Analysis and Interpretation of data, Visualization, Writing – original draft; Angelina Degen: Investigation, Methodology, Analysis of data; Stephanie Krüger: Investigation, Methodology; Jürgen Krieger: Conceptualization, analysis and interpretation of data, Writing – review & editing.

Declaration of competing interest

The authors declare that they have no known competing financial interests or personal relationships that could have appeared to influence the work reported in this paper.

Data availability

Data will be made available on request.

Acknowledgments

Doreen Sander is acknowledged for excellent technical assistance.

Funding

This research was funded by a grant to J.K. from the Deutsche Forschungsgemeinschaft. Grant number KR1786/5-1.

Supplementary materials

Supplementary material associated with this article can be found, in the online version, at doi:10.1016/j.cris.2023.100053.

References

- Benton, R., Vannice, K.S., Vosshall, L.B., 2007. An essential role for a CD36-related receptor in pheromone detection in *Drosophila*. *Nature* 450, 289–293.
- Blaney, W.M., 1977. The ultrastructure of an olfactory sensillum on the maxillary palps of *Locusta migratoria* (L.). *Cell Tissue Res.* 184, 397–409.
- Blankenburg, S., Cassau, S., Krieger, J., 2019. The expression patterns of SNMP1 and SNMP2 underline distinct functions of two CD36-related proteins in the olfactory system of the tobacco budworm *Heliothis virescens*. *Cell Tissue Res.* 378, 485–497.
- Byers, J.A., 1991. Pheromones and chemical ecology of locusts. *Biol. Rev.* 66, 347–378.
- Cassau, S., Krieger, J., 2021. The role of SNMPS in insect olfaction. *Cell Tissue Res.* 383, 21–33.
- Cassau, S., Sander, D., Karcher, T., Laue, M., Hause, G., Breer, H., Krieger, J., 2022. The sensilla-specific expression and subcellular localization of SNMP1 and SNMP2 reveal novel insights into their roles in the antenna of the desert locust *Schistocerca gregaria*. *Insects* 13.
- Chapman, R.F., 2002. Development of phenotypic differences in sensillum populations on the antennae of a grasshopper, *Schistocerca americana*. *J. Morphol.* 254, 186–194.
- Chapman, R.F., Greenwood, M., 1986. Changes in distribution and abundance of antennal sensilla during growth of *Locusta migratoria* L. (Orthoptera: Acrididae). *Int. J. Morphol. and Embryol.* 15, 83–96.
- Chen, Y., Zhang, J., Cui, W., Silverstein, R.L., 2022. CD36, a signaling receptor and fatty acid transporter that regulates immune cell metabolism and fate. *J. Exp. Med.* 219.
- Fleischer, J., Pregitzer, P., Breer, H., Krieger, J., 2018. Access to the odor world: olfactory receptors and their role for signal transduction in insects. *Cell. Mol. Life Sci.* 75, 485–508.
- Forstner, M., Gohl, T., Gondesen, I., Raming, K., Breer, H., Krieger, J., 2008. Differential expression of SNMP-1 and SNMP-2 proteins in pheromone-sensitive hairs of moths. *Chem. Senses* 33, 291–299.

- Giovannucci, D.R., Stephenson, R.S., 1999. Identification and distribution of dietary precursors of the *Drosophila* visual pigment chromophore: analysis of carotenoids in wild type and ninaD mutants by HPLC. *Vision Research* 39, 219–229.
- Gomez-Diaz, C., Bargeton, B., Abuin, L., Bukar, N., Reina, J.H., Bartoi, T., Graf, M., Ong, H., Ulbrich, M.H., Masson, J.F., Benton, R., 2016. A CD36 ectodomain mediates insect pheromone detection via a putative tunnelling mechanism. *Nat. Commun.* 7, 11866.
- Greenwood, M., Chapman, R.F., 1984. Differences in numbers of sensilla on the antennae of solitary and gregarious *Locusta migratoria* L. (Orthoptera: Acrididae). *Int. J. Morphol. and Embryol.* 13, 295–301.
- Gu, S.H., Yang, R.N., Guo, M.B., Wang, G.R., Wu, K.M., Guo, Y.Y., Zhou, J.J., Zhang, Y.J., 2013. Molecular identification and differential expression of sensory neuron membrane proteins in the antennae of the black cutworm moth *Agrotis ipsilon*. *J. Insect Physiol.* 59, 430–443.
- Guo, X., Yu, Q., Chen, D., Wei, J., Yang, P., Yu, J., Wang, X., Kang, L., 2020. 4-Vinylanisole is an aggregation pheromone in locusts. *Nature* 584, 584–588.
- Hao, J.W., Wang, J., Guo, H., Zhao, Y.Y., Sun, H.H., Li, Y.F., Lai, X.Y., Zhao, N., Wang, X., Xie, C., Hong, L., Huang, X., Wang, H.R., Li, C.B., Liang, B., Chen, S., Zhao, T.J., 2020. CD36 facilitates fatty acid uptake by dynamic palmitoylation-regulated endocytosis. *Nat. Commun.* 11, 4765.
- Hassanali, A., Njagi, P.G., Bashir, M.O., 2005. Chemical ecology of locusts and related acridids. *Annu. Rev. Entomol.* 50, 223–245.
- Herboso, L., Talamillo, A., Perez, C., Barrio, R., 2011. Expression of the scavenger receptor class B type I (SR-BI) family in *Drosophila melanogaster*. *Int. J. Dev. Biol.* 55, 603–611.
- Jiang, X., Pregitzer, P., Grosse-Wilde, E., Breer, H., Krieger, J., 2016. Identification and characterization of two 'Sensory Neuron Membrane Proteins' (SNMPs) of the desert locust, *Schistocerca gregaria* (Orthoptera: Acrididae). *J. Insect Sci.* 16, 33.
- Jin, X., Ha, T.S., Smith, D.P., 2008. SNMP is a signaling component required for pheromone sensitivity in *Drosophila*. *Proc. Natl. Acad. Sci. U.S.A.* 105, 10996–11001.
- Kiefer, C., Sumser, E., Wernet, M.F., Von Lintig, J., 2002. A class B scavenger receptor mediates the cellular uptake of carotenoids in *Drosophila*. *Proc. Natl. Acad. Sci. U.S.A.* 99, 10581–10586.
- Leal, W.S., 2013. Odorant reception in insects: roles of receptors, binding proteins, and degrading enzymes. *Annu. Rev. Entomol.* 58, 373–391.
- Lemke, R.S., Pregitzer, P., Eichhorn, A.S., Breer, H., Krieger, J., Fleischer, J., 2020. SNMP1 and odorant receptors are co-expressed in olfactory neurons of the labial and maxillary palps from the desert locust *Schistocerca gregaria* (Orthoptera: Acrididae). *Cell Tissue Res.* 379, 275–289.
- Li, H., Wang, P., Zhang, L., Xu, X., Cao, Z., Zhang, L., 2018. Expressions of olfactory proteins in locust olfactory organs and a palp odorant receptor involved in plant aldehydes detection. *Front. Physiol.* 9, 663.
- Li, Z., Ni, J.D., Huang, J., Montell, C., 2014. Requirement for *Drosophila* SNMP1 for rapid activation and termination of pheromone-induced activity. *PLoS Genet.* 10, e1004600.
- Liu, S., Chang, H., Liu, W., Cui, W., Liu, Y., Wang, Y., Ren, B., Wang, G., 2020. Essential role for SNMP1 in detection of sex pheromones in *Helicoverpa armigera*. *Insect. Biochem. Mol. Biol.* 127, 103485.
- Nakano, M., Morgan-Richards, M., Trewick, S.A., Clavijo-Mcormick, A., 2022. Chemical ecology and olfaction in short-horned grasshoppers (Orthoptera: Acrididae). *J. Chem. Ecol.* 48, 121–140.
- Nichols, Z., Vogt, R.G., 2008. The SNMP/CD36 gene family in Diptera, Hymenoptera and Coleoptera: *Drosophila melanogaster*, *D. pseudoobscura*, *Anopheles gambiae*, *Aedes aegypti*, *Apis mellifera*, and *Tribolium castaneum*. *Insect Biochem. Mol. Biol.* 38, 398–415.
- Njagi, P.G.N., Torto, B., 1996. Responses of nymphs of desert locust, *Schistocerca gregaria* to volatiles of plants used as rearing diet. *Chemoeology* 7, 172–178.
- Obeng-Ofori, D., Torto, B., Njagi, P.G., Hassanali, A., Amiani, H., 1994. Fecal volatiles as part of the aggregation pheromone complex of the desert locust, *Schistocerca gregaria* (Forsk.) (Orthoptera: Acrididae). *J. Chem. Ecol.* 20, 2077–2087.
- Ochieng, S.A., Hallberg, E., Hansson, B.S., 1998. Fine structure and distribution of antennal sensilla of the desert locust, *Schistocerca gregaria* (Orthoptera: Acrididae). *Cell Tissue Res.* 291, 525–536.
- Ochieng, S.A., Hansson, B.S., 1999. Responses of olfactory receptor neurones to behaviourally important odours in gregarious and solitary desert locust, *Schistocerca gregaria*. *Physiol. Entomol.* 24, 28–36.
- Pepino, M.Y., Kuda, O., Samovski, D., Abumrad, N.A., 2014. Structure-function of CD36 and importance of fatty acid signal transduction in fat metabolism. *Annu. Rev. Nutr.* 34, 281–303.
- Pregitzer, P., Greschista, M., Breer, H., Krieger, J., 2014. The sensory neuron membrane protein SNMP1 contributes to the sensitivity of a pheromone detection system. *Insect Mol. Biol.* 23, 733–742.
- Pregitzer, P., Jiang, X., Grosse-Wilde, E., Breer, H., Krieger, J., Fleischer, J., 2017. In search for pheromone receptors: certain members of the odorant receptor family in the desert locust *Schistocerca gregaria* (Orthoptera: Acrididae) are co-expressed with SNMP1. *Int. J. Biol. Sci.* 13, 911–922.
- Pregitzer, P., Jiang, X., Lemke, R.S., Krieger, J., Fleischer, J., Breer, H., 2019. A subset of odorant receptors from the desert locust *Schistocerca gregaria* is co-expressed with the sensory neuron membrane protein 1. *Insects* 10, 350.
- Rihani, K., Ferveur, J.F., Briand, L., 2021. The 40-year mystery of insect odorant-binding proteins. *Biomolecules* 11.
- Rogers, M.E., Krieger, J., Vogt, R.G., 2001. Antennal SNMPs (sensory neuron membrane proteins) of Lepidoptera define a unique family of invertebrate CD36-like proteins. *J. Neurobiol.* 49, 47–61.
- Rogers, M.E., Sun, M., Lerner, M.R., Vogt, R.G., 1997. Snmp-1, a novel membrane protein of olfactory neurons of the silk moth *Antheraea polyphemus* with homology to the CD36 family of membrane proteins. *J. Biol. Chem.* 272, 14792–14799.
- Ronderos, D.S., Lin, C.C., Potter, C.J., Smith, D.P., 2014. Farnesol-detecting olfactory neurons in *Drosophila*. *J. Neurosci.* 34, 3959–3968.
- Seidelmann, K., Ferenz, H.J., 2002. Courtship inhibition pheromone in desert locusts, *Schistocerca gregaria*. *J. Insect Physiol.* 48, 991–996.
- Seidelmann, K., Lüber, K., Ferenz, H.J., 2000. Analysis of release and role of benzyl cyanide in male desert locusts, *Schistocerca gregaria*. *J. Chem. Ecol.* 26, 1897–1910.
- Silverstein, R.L., Febbraio, M., 2009. CD36, a scavenger receptor involved in immunity, metabolism, angiogenesis, and behavior. *Sci. Signal* 2, 1–8.
- Steedman, A., 1990. *Locust Handbook*. Overseas Development Natural Resource Institute, Chatham.
- Thurm, U., Küppers, J., 1980. Epithelial physiology of insect sensilla. In: Locke, M., Smith, D.S. (Eds.), *Insect biology in the future*. Academic Press, New York, pp. 735–763.
- Torto, B., Njagi, P.G.N., Hassanali, A., Amiani, H., 1996. Aggregation pheromone system of nymphal gregarious desert locust, *Schistocerca gregaria* (Forsk.). *J. Chem. Ecol.* 22, 2273–2281.
- Torto, B., Obeng-Ofori, D., Njagi, P.G., Hassanali, A., Amiani, H., 1994. Aggregation pheromone system of adult gregarious desert locust *Schistocerca gregaria* (Forsk.). *J. Chem. Ecol.* 20, 1749–1762.
- Uvarov, B.P., 1966. *Grasshoppers and Locusts: A Handbook of General Acridology*. Cambridge University Press.
- Wang, T., Jiao, Y., Montell, C., 2007. Dissection of the pathway required for generation of vitamin A and for *Drosophila* phototransduction. *J. Cell Biol.* 177, 305–316.
- Wang, Z., Yang, P., Chen, D., Jiang, F., Li, Y., Wang, X., Kang, L., 2015. Identification and functional analysis of olfactory receptor family reveal unusual characteristics of the olfactory system in the migratory locust. *Cell. Mol. Life Sci.* 72, 4429–4443.
- Wicher, D., Miazzi, F., 2021. Functional properties of insect olfactory receptors: ionotropic receptors and odorant receptors. *Cell Tissue Res.* 383, 7–19.
- Xu, H., Guo, M., Yang, Y., You, Y., Zhang, L., 2013. Differential expression of two novel odorant receptors in the locust (*Locusta migratoria*). *BMC Neurosci.* 14, 50.
- Yang, J., O'tousa, J.E., 2007. Cellular sites of *Drosophila* NinaB and NinaD activity in vitamin A metabolism. *Mol. Cell. Neurosci.* 35, 49–56.
- Zhang, H.J., Xu, W., Chen, Q.M., Sun, L.N., Anderson, A., Xia, Q.Y., Papanicolaou, A., 2020. A phylogenomics approach to characterizing sensory neuron membrane proteins (SNMPs) in Lepidoptera. *Insect. Biochem. Mol. Biol.* 118, 103313.
- Zhao, Y.J., Li, G.C., Zhu, J.Y., Liu, N.Y., 2020. Genome-based analysis reveals a novel SNMP group of the Coleoptera and chemosensory receptors in *Rhaphuma horsfieldi*. *Genomics* 112, 2713–2728.
- Zielonka, M., Gehrke, P., Badeke, E., Sachse, S., Breer, H., Krieger, J., 2016. Larval sensilla of the moth *Heliothis virescens* respond to sex pheromone components. *Insect Mol. Biol.* 25, 666–678.

Supplementary Data for Manuscript 2

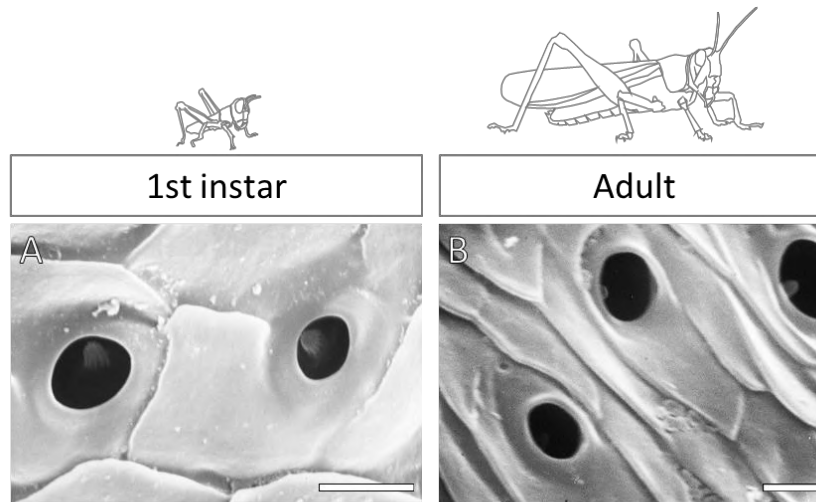


Figure S1. SEM images of coeloconic sensilla found on the antenna of juvenile and adult stages of *S. gregaria*. A – first instar nymph. B – adult. Scale bars = 5 μ m.

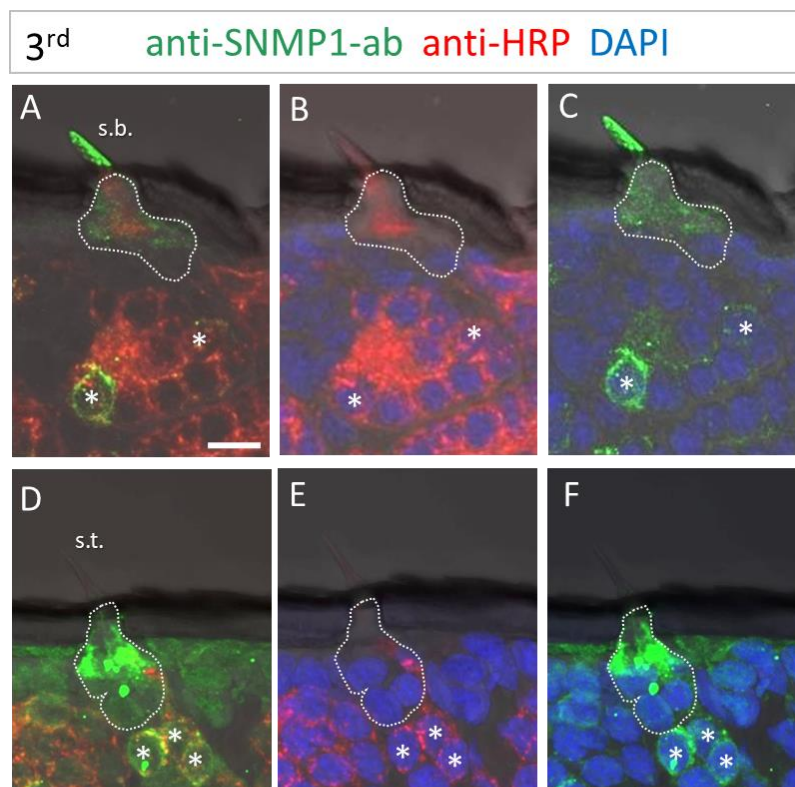


Figure S2. SNMP1 expression in the antenna of *S. gregaria*'s third instar stage. Longitudinal sections were assessed by FIHC using anti-SgreSNMP1-ab (green) and anti-HRP (red); sections were counter stained with DAPI (blue). **A-C** Localization of OSNs and SNMP1-positive cells underneath a basiconic sensillum (s.b.), depicted in different fluorescent channels. **D-F** show the neurons and the SNMP1-positive cells of a trichoid sensillum (s.t.) in different fluorescence channels. The encircled area denotes SNMP1-positive labelling of support cells. Asterisks (*) signify SNMP1-positive OSNs. A and D, overlay of the red and green fluorescence channels. B and E, overlay of the red and blue channels. C and F, overlay of the green and blue channels. In all images the fluorescent channels were overlaid with the transmitted light channel. Scale bars = 10 μ m

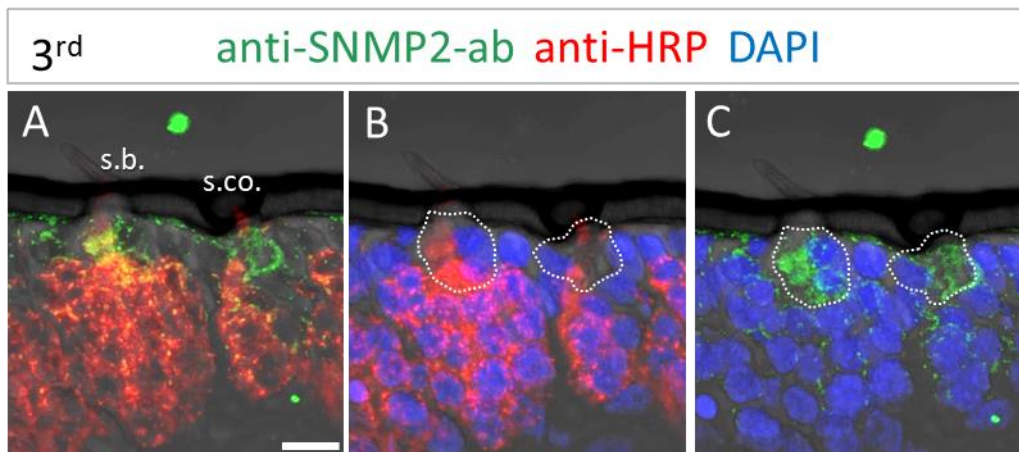


Figure S3. SNMP2 expression in the antenna of a third instar stage of *S. gregaria*. Sections were assessed for SNMP-positive cells by FIHC using anti-SgreSNMP2-ab (green) along with anti-HRP (OSNs, red) and DAPI (nuclei, blue). SNMP2 was detected in the support cells (denoted by encircled areas) underneath the basiconic sensillum (s.b.) and the coeloconic sensillum (s.co.). **A** overlay of the red and green fluorescence channels. **B** red and blue channels. **C** green and blue channels. All images were overlaid with the transmitted light channel. Scale bar = 10 μ m.

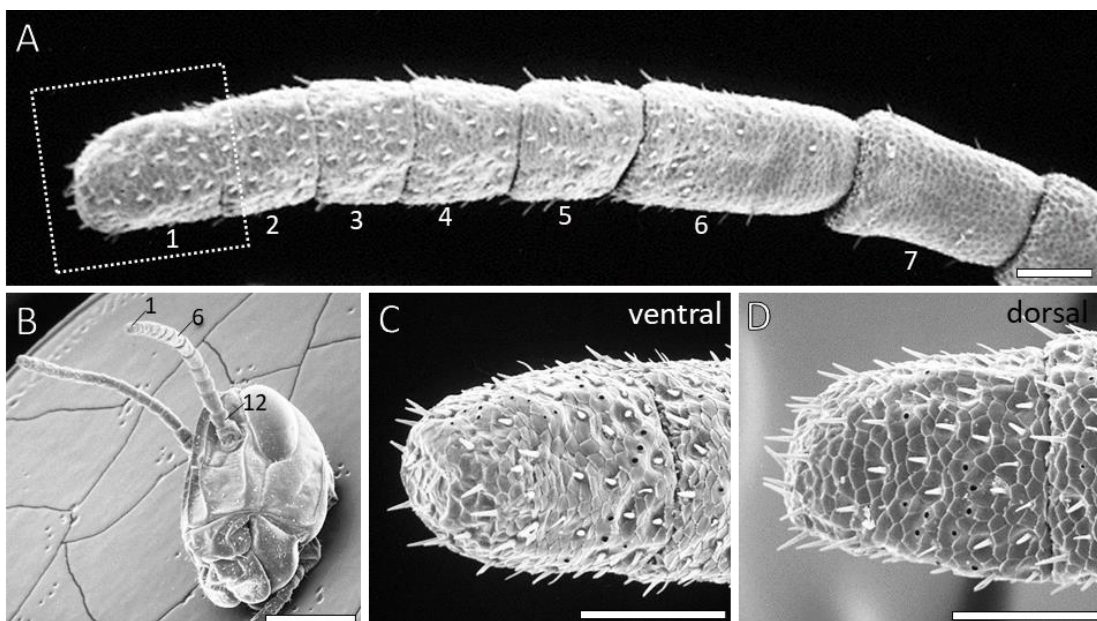


Figure S4. Sensilla on the antenna of first instar nymphs of *S. gregaria*. **A** Segments 1-7 of a first instar antenna depicting the distribution of the sensilla along the most distal segments. **B** head with antenna of a first instar nymph illustrating the numbering of the 12 antennal segments. **C** shows the ventral side of the most distal segment boxed in (A). **D** shows the dorsal side of the distal segment boxed in (A). Scale bars: A, C, D = 100 μ m, B = 1 mm.

Chapter 4. Manuscript 3

Insect Biochemistry and Molecular Biology 164 (2024) 104046



Contents lists available at ScienceDirect

Insect Biochemistry and Molecular Biology

journal homepage: www.elsevier.com/locate/ibmb

Evidence for a role of SNMP2 and antennal support cells in sensillum lymph clearance processes of moth pheromone-responsive sensilla

Sina Cassau, Jürgen Krieger*

Martin Luther University Halle-Wittenberg, Institute of Biology/Zoology, Department of Animal Physiology, 06120 Halle (Saale), Germany

ARTICLE INFO

Keywords:

Olfaction
Moth
Sensory neuron membrane protein support cell
Long-chain fatty acids
Sensillum lymph

ABSTRACT

In insect antenna, following the activation of olfactory sensory neurons, odorant molecules are inactivated by enzymes in the sensillum lymph. How the inactivation products are cleared from the sensillum lymph is presently unknown. Here we studied the role of support cells (SCs) and the so-called sensory neuron membrane protein 2 (SNMP2), a member of the CD36 family of lipid transporters abundantly expressed in SCs, in sensillum lymph clearance processes in the moths *Heliothis virescens* and *Bombyx mori*. In these species, the sex pheromone components are inactivated to long-chain fatty acids. To approach a role of SNMP2 in the removal of such inactivation products, we analyzed the uptake of a fluorescent long-chain fatty acid analog into a newly generated HvirSNMP2-expressing cell line. We found an increased uptake of the analog into SNMP2-cells compared to control cells, which could be blocked by the CD36 protein inhibitor, SSO. Furthermore, analyses of sensilla from antenna treated with the fatty acid analog indicated that SNMP2-expressing SCs are able to take up fatty acids from the sensillum lymph. In addition, sensilla from SSO-pretreated antenna of *B. mori* showed reduced removal of the fluorescent analog from the sensillum lymph. Finally, we revealed that SSO pretreatment of male silkmoth antenna significantly prolonged the duration of the female pheromone-induced wing-fluttering behavior, possibly as a result of impaired lymph clearance processes. Together our findings in *H. virescens* and *B. mori* support a pivotal role of olfactory SCs in sensillum lymph maintenance processes and suggest an integral role of SNMP2 in the removal of lipophilic “waste products” such as fatty acids resulting from sex pheromone inactivation.

1. Introduction

The precise and sensitive detection of female-released sex pheromones by conspecific males is critical for the initiation of reproductive behaviors and mate finding in moths (Zhang et al., 2015; Stengl, 2010; Carde and Willis, 2008). Sex pheromones, like other volatile odorants, are detected by specialized olfactory sensory neurons (OSNs) on the antenna that extend their dendrites into hair-like cuticular protrusions, named sensilla (Zacharuk, 1985). The dendritic membranes of pheromone-sensitive OSNs contain narrowly tuned pheromone receptors (PRs) that transduce the chemical signal into an electrical response (Fleischer and Krieger, 2018; Stengl, 2010). Pheromone molecules enter the sensillum lumen through multiple cuticle pores (Keil, 1982, 1989; Steinbrecht, 1997). The lumen is filled with aqueous sensillum lymph that contains pheromone binding proteins supposed to transfer pheromone molecules through the lymph to their respective PRs. The protein and ionic composition of the sensillum lymph is

maintained and regulated by so-called support cells (Leal, 2013; Thurm and Küppers, 1980; Schmidt and Benton, 2020), which border the sensillum lymph and moreover surround the OSNs at the bases of a sensillum, thus completing the olfactory unit (Sanes and Hildebrand, 1976; Steinbrecht and Gnatzy, 1984; Keil, 1989).

While the function of OSNs in the reception and discrimination of pheromones has thoroughly been investigated (Fleischer and Krieger, 2018; Zhang et al., 2015; Yew and Chung, 2017; Benton, 2022; Renou, 2014; Van der Goes van Naters, 2014), the specific role of the support cells in peripheral olfactory processes is largely unclear. A possible function of support cells has been suggested in governing sensillum lymph clearance processes by expressing proteins necessary for the elimination of “waste products” e. g. inactivated pheromone and odorant molecules (Vogt and Riddiford, 1981; Pelletier et al., 2023). In moths, such “waste products” are produced by different kinds of odorant degrading enzymes (ODEs) expressed in the antenna (Leal, 2013; Vogt et al., 2020), including aldehyde oxidases and dehydrogenases, which

* Corresponding author.

E-mail addresses: sina.cassau@zoologie.uni-halle.de (S. Cassau), juergen.krieger@zoologie.uni-halle.de (J. Krieger).<https://doi.org/10.1016/j.ibmb.2023.104046>

Received 15 September 2023; Received in revised form 10 November 2023; Accepted 28 November 2023

Available online 2 December 2023

0965-1748/© 2023 The Authors. Published by Elsevier Ltd. This is an open access article under the CC BY license (<http://creativecommons.org/licenses/by/4.0/>).

rapidly inactivate pheromones and thus prevent repeated stimulation of OSNs by the same molecule (Ishida and Leal, 2005; Vogt and Riddiford, 1981). For instance, in the major and minor sex pheromone components of the noctuid moth *Heliothis virescens*, Z11-Hexadecenal and Z9-Tetradecenal, the aldehyde moieties are transformed by ODEs into a carboxyl group resulting in the respective long-chain fatty acids of the same chain lengths (Tasayco and Prestwich, 1990). Similarly, in the silkmoth *Bombyx mori* ODEs transform the sex pheromone components, bombykol and bombykal in the sensillum lymph, to the long-chain fatty acid, E10, Z12-Hexadecadienoic acid (Fig. S1) (Pelletier et al., 2007; Rybczynski et al., 1990; Kasang and Weiss, 1974).

We previously identified a protein expressed in support cells potentially being involved in sensillum lymph clearance processes in moths, the so-called sensory neuron membrane protein type 2 (SNMP2) (Forstner et al., 2008; Cassau and Krieger, 2021; Blankenburg et al., 2019). SNMPs form an insect-specific clade of the large CD36 family of proteins (Robertson et al., 1999; Vogt et al., 2009; Nichols and Vogt, 2008) characterized by two transmembrane domains and a large extracellular region. Members of the CD36 family are described to act as lipid/lipoprotein receptors and transporters with CD36 itself facilitating the uptake of extracellular long-chain fatty acids (Pepino et al., 2014; Chen et al., 2022). While in moths as well as in flies the SNMP1 type is expressed in OSNs and implicated as a co-receptor for the sensitive and rapid detection of sex pheromones by PRs (Pregitzer et al., 2014; Benton et al., 2007; Jin et al., 2008), the SNMP2 type in moths is selectively expressed in support cells and its function is unexplored (Forstner et al., 2008; Blankenburg et al., 2019; Cassau and Krieger, 2021). By means of immunohistochemistry on antennal sections of *H. virescens*, we have localized HvirSNMP2 to the apical side of the support cells in olfactory sensilla adjacent to the sensillum lymph (Blankenburg et al., 2019). Due to its localization at the support cell/sensillum lymph interface and its membership to the CD36 protein receptor/transporter family, we hypothesize that SNMP2 in moths could potentially be involved in the removal of the lipophilic fatty acid pheromone inactivation products from the sensillum lymph. Therefore, in this study we aimed to assess the ability of the *H. virescens* SNMP2 protein to mediate the cellular uptake of long-chain fatty acids. Towards this goal, we generated a stable modified HEK293 cell line expressing HvirSNMP2 and tested SNMP2's ability to facilitate the uptake of a fluorescent long-chain fatty acid analog. Moreover, we analyzed if support cells in the antenna of *H. virescens* and another moth species, *B. mori*, are able to take up the fluorescent fatty acid analog from the sensillum lymph. Finally, we examined the consequences of an SNMP2-inhibitor on the cellular uptake of fatty acids into support cells as well as the impact on the behavioral responses of male *B. mori* to female released sex pheromones. Overall, our data suggest a role of support cells and SNMP2 in sensillum lymph clearance processes that are of crucial importance for maintaining the functionality of pheromone-responsive sensilla in moths.

2. Materials and methods

2.1. Animals

Pupae of the tobacco budworm *Heliothis virescens* were kindly provided by Bayer CropScience AG, Monheim, Germany. Pupae of the silkmoth *Bombyx mori* were purchased from Laboratorio die Sericoltura, Centro die Ricerca Agricoltura e Ambiente (Padova, Italy). All animals were allowed to develop into adults and were used in experiments 0- to 4-days after eclosion.

2.2. Expression of HvirSNMP2 in Flp-In T-Rex293 cells

For the generation of a stable cell line allowing tetracycline-induced expression of HvirSNMP2 the components of the Flp-In-System (Thermo Fisher Scientific, Waltham, MA, USA) and a modified HEK 293 cell line (Flp-In T-Rex293/G_α15) were used. Following protocols successfully

applied previously (Grosse-Wilde et al., 2006; Pregitzer et al., 2014), the coding region of HvirSNMP2 (Acc. No. AM905328) were first PCR-amplified from vector containing the HvirSNMP2 cDNA (Forstner et al., 2008) using specific primers (HvirSNMP2: 5'- A TTT GCG GCC GCG ATG TTG GGC AAA CAC TCG AA-3' and 5'- CCG GTC GAC CCA TCA ATT TCC TTT ATT AAC CTG -3') and integrated into the pcDNA5/FRT/TO expression vector (Thermo Fisher Scientific). Subsequently Flp-In T-Rex293/G_α15 cells were transfected with the HvirSNMP2/pcDNA5/FRT/TO construct using Lipofectamine™ 2000 Transfection Reagent (Thermo Fisher Scientific) according to the supplier's instructions. Briefly, 2 x 10⁵ cells were seeded into single wells of a sterile 24-well cell culture plate (Greiner Bio-One, Frickenhausen, Germany) and transfected 24h later with 500 ng expression vector construct and 1 μL Lipofectamine 2000 reagent. 48h post transfection, cells were selected for SNMP2 genome integration using media supplemented with 100 mg/L hygromycin finally revealing the T-Rex293/G_α15/SNMP2 cell line, named TReX/S2 cells in the following. TReX/S2 cells and control cells (T-Rex293/G_α15/SNMP2), named TReX cells in the following, were cultured in T75 flasks (Sarstedt, Nümbrecht, Germany) using Dulbecco's Modified Eagle Medium (DMEM, Thermo Fisher Scientific) with 10% fetal bovine serum (Thermo Fisher Scientific) and supplemented with either 10 mg/L blasticidin, 200 mg/L geneticin in regular alternation. In the case of TReX/S2 cells, 100 mg/L hygromycin were regularly included. The heterologous expression of HvirSNMP2 in the TReX/S2 cells was induced by the addition of 5 μg/ml tetracycline to the cell culture medium.

2.3. RNA extraction and reverse transcription PCR

Total RNA was extracted from 90 to 95% confluent cells in T75 flasks pretreated with 5 μg/ml tetracycline 24h prior to using TRIzol reagent (Thermo Fisher Scientific) according to manufacturer protocol. Briefly, cells were suspended in 1 ml Trizol reagent, transferred into a 1.5 ml reaction tube and incubated for 5 min at room temperature. After adding 200 μL chloroform the samples were gently inverted for 30 s, followed by incubation for 2 min at room temperature and centrifugation for 15 min (12000 g at 4 °C). The clear upper aqueous layers were transferred to a fresh reaction tube, mixed with 500 μL isopropanol and kept overnight at -20 °C. After centrifugation for 30 min (12000 g, 4 °C), the supernatants were removed and the RNA pellets were washed with 1 ml 75% Ethanol. The samples were centrifuged again for 5 min (7500 g, 4 °C) and the supernatants removed. The RNA pellets were dried at room temperature and finally resuspended in 20 μL dH₂O. PolyA⁺-RNA was isolated from total RNA using the Dynabeads mRNA purification kit (Thermo Fisher Scientific) following the protocol of the supplier and eluted in dH₂O. For first strand cDNA synthesis 150 ng of polyA⁺-RNA, 1 μL 50 μM oligo(dT)20 primer (Thermo Fisher Scientific), 1 μL 10 mM 2-deoxynucleoside 5-triphosphate (dNTP) solution mix (New England Biolabs, Ipswich, MA, USA) and dH₂O were mixed in a total volume of 13 μL. After incubation for 5 min at 65 °C, 4 μL 5x SSIV Buffer (Thermo Fisher Scientific), 1 μL 100 mM 1,4-dithiothreitol (Thermo Fisher Scientific), 1 μL RNaseOut (Thermo Fisher Scientific), and 1 μL Superscript IV reverse transcriptase (Thermo Fisher Scientific) were added. Synthesis of cDNA was carried out at 52 °C for 10 min followed by 10 min at 80 °C. For PCR amplification of sequences coding for HvirSNMP2, the following primers were used: HvirSNMP2 5'-ATCAAA-GAGGACGATGTCCCGA-3' and 5'- CAGCTGTGGAATGTTGTTGATC-3'. PCR products were visualized using agarose gel electrophoresis and ethidium bromide staining.

2.4. SDS-PAGE and western blot

Cells were grown to a confluency of 80–90% in T75 flasks and induced by adding tetracycline to a final concentration of 5 μg/ml for 24h. Tetracycline addition was repeated 3h before collecting the cells for

protein analysis. Cells were washed off from the flask surface and transferred to a 2 ml reaction tube using 1.5 ml lysis buffer (50 mM Tris-HCl, 150 mM NaCl, 1 mM EDTA, pH 7.4) supplemented with 1% Triton X-100, 5% Glycerol and SigmaFAST protease inhibitor cocktail (Merck, Darmstadt, Germany; one tablet diluted in 100 ml of stock lysis buffer). After incubation for 3 min on an orbital shaker at room temperature, the samples were transferred to a fresh reaction tube, rotated for 30 min on an overhead shaker at 4 °C and subsequently centrifuged at 2000 g for 5 min at 4 °C. The supernatant was used for SDS-PAGE and Western Blot analysis. 20 µg of total protein of the supernatant were utilized per lane on a 12% SDS-gel. Two identically loaded gels were prepared in parallel and either stained with Coomassie blue, or electro blotted with a semi-dry apparatus onto a methanol-activated PVDF membrane (Carl Roth, Karlsruhe, Germany) soaked in transfer buffer (25 mM Tris, 192 mM glycine, 20% methanol) for 1 h at 200 mA. After protein transfer, the membrane was incubated for 1 h in TBST (100 mM Tris, 150 mM NaCl, pH 7.5 supplemented with 0.05% Tween 20) with 7% milk powder followed by treatment with the rabbit-anti-HvirSNMP2-ab (Blankenburg et al., 2019) diluted 1:500 in TBST with 3.5% milk powder overnight at 4 °C. Subsequently, the membrane was washed 3 times for 10 min with TBST, incubated in goat-anti-rabbit alkaline phosphatase (Thermo Fisher Scientific) diluted 1:10,000 in TBST with 3.5% milk powder for 1 h at room temperature. After washing 3 times for 10 min in TBST and 2 times for 10 min in substrate buffer (100 mM Tris-HCl, 100 mM NaCl, 5 mM MgCl₂, pH 9.5) the membranes were incubated in 25 µg/ml nitro blue tetrazolium and 50 µg/ml 5-brom-4-chlor-3-indolyl phosphate in substrate buffer for 2 h. The color reaction was stopped by incubating the membranes for 5 min in dH₂O.

2.5. Live cell imaging of fatty acid uptake

Cells (~30000 per well) were seeded onto 10-well CELLview™ Slides (Greiner Bio-One) 48h prior to the experiments and grown in 200 µl DMEM to a confluency of around 70–80%. Cells of different lines (TREx/S2, TREx) were seeded on the upper and the lower row of wells of the slides, respectively. 24h after seeding and at 5–6h before the experiments the cells were induced by adding 1 µl tetracycline solution (1 mg/ml). For live cell imaging, the cell-prepared slides were inserted into the microscope stage of a widefield fluorescence microscope DMI8 (Leica Microsystems, Wetzlar, Germany). Unless specified otherwise a 40× dry objective was used. The fatty acid uptake assay was conducted with one well at a time and started by carefully removing the growth medium and immediately adding 200 µl of working solution. The working solution consisted of a specific concentration of either a BODIPY™ FL C16- fluorescent fatty acid analog (BODIPY FL C16, Thermo Fisher Scientific, Stock solution: 10 mM in DMSO) or BODIPY™ 500/510 C₄, C₉- fluorescent fatty acid analog (BODIPY C4C9, Thermo Fisher Scientific, Stock solution: 10 mM in DMSO), diluted in cell culture grade sterile filtered PBS pH 7.4 (Merck) and supplemented with 0.05% Trypan blue (Thermo Fisher Scientific) to quench extracellular BODIPY signals. For the SNMP2 inhibition experiments, cells were pretreated with 50 µM sulfo-N-succinimidyl oleate (SSO; Cayman Chemical, Ann Arbor, MI, USA) with 0.1% DMSO or only 0.1% DMSO in cell culture grade PBS for 60s prior to adding the working solution.

For monitoring the fluorescent fatty acid analog uptake into cells over time, images of the cells were captured in the transmitted light as well as the FITC fluorescence channels of the DMI8 microscope every 7s starting immediately after adding the working solution to the wells. 24 time points were recorded giving a total imaging time of 168 s. This protocol and duration turned out to be best to ensure full cell viability and exclude phototoxic effects in the experiments. For the recording the acquisition mode of the software Leica Application Suite X (LAS X, Leica Microsystems GmbH) was applied. The uptake of the fatty acid fluorescent analogs into single cells was evaluated by arbitrarily choosing cells as regions of interest (ROI) and tracing their outlines in the transmitted light channel using the Analysis function of LAS X. After selecting

25 cells per replicate in the transmitted light channel, the mean intensities of the labelled ROIs in the fluorescent FITC channel were extracted to calculate for each cell the relative change in fluorescent intensity over time by $(F_t - F_0)/F_0$. The mean (\pm SD) relative changes in fluorescent intensity ($\Delta F/F_0$) of TREx or TREx/S2 cells over time were calculated from all selected cells of at least four independent replicates using the LASx software.

2.6. Fluorescence immunohistochemistry (FIHC)

FIHC experiments were performed as described previously (Blankenburg et al., 2019). Antennae of adult *H. virescens* were fixed for 2 h at 4 °C in 4 % paraformaldehyde and 0.5 % glutaraldehyde in phosphate buffer (1.4 mM KH₂PO₄, 8 mM Na₂HPO₄, pH 7.4) followed by three washing steps for 10 min in phosphate buffered saline (PBS, 145 mM NaCl, 1.4 mM KH₂PO₄, 8 mM Na₂HPO₄, pH 7.1). Antennae were transferred into 10 % sucrose solution (in phosphate buffer) for 1 h at room temperature followed by 25 % sucrose solution (in phosphate buffer) over night at 8 °C. After embedding the antennae in O.C.T Tissue Tek freezing medium (Sakura Finetek Europe, Alphen aan den Rijn, The Netherlands) at –20 °C, 12 µm cryosections were prepared and subsequently thaw mounted onto Eprelia SuperFrost Plus Adhesion microscope slides (Thermo Fisher Scientific). The sections were encircled with Liquid Blocker (Plano, Wetzlar, Germany) and then treated with PBS supplemented with 0.01 % Tween 20 for 5 min. Next, the sections were treated with 50 mM NH₄Cl (in PBS pH 7.1) for 5 min, PBS for 5 min and FIHC blocking solution (10 % normal goat serum, 0.5 % Triton X-100 in PBS pH 7.1), for 30 min at room temperature. Subsequently, the sections were incubated with rabbit-anti-HvirSNMP2 ab (1:200 in blocking solution) over night at 8 °C in a humid box, followed by washing the slides three times for 5 min with PBS and the incubation with goat-anti-rabbit AF488-conjugated secondary antibodies (1:1000) (Jackson ImmunoResearch, Ely, Great Britain), goat-anti-HRP Cy3 (1:400) (Jackson ImmunoResearch) and DAPI (1:1000, Thermo Fisher Scientific) diluted in PBS, for 1 h at room temperature. After washing the slides three times for 5 min with PBS, the sections were mounted in Mowiol (Merck; 20 g Mowiol 4–88, 2.4 g n-propyl-gallate, 40 ml glycerine, 80 ml PBS pH 7.1) and covered with a coverslip.

2.7. Whole mount in situ hybridization combined with immunohistochemistry

Whole mount fluorescent in situ hybridization (WM-FISH) was conducted as described earlier (Krieger et al., 2005) with a few modifications. For the experiments, 0.2 ml reaction tubes were used and all steps were incubated under constant rotation on an overhead shaker and at room temperature unless specified otherwise. Antennae of *B. mori* were prepared from cold anesthetized animals. The side branches were dissected from the main antennal stem and immediately transferred into 4% paraformaldehyde (in 100 mM NaHCO₃, pH 9.5). After incubation for 20–24h at 4 °C, the samples were washed for 1 min in PBS (pH 7.1), 10 min in 200 mM HCl and 2 min in PBS with 1% Triton X-100. The samples were then prehybridized at 55 °C in a hybridization oven (Jena Analytik, Jena, Germany) for at least 6h in whole mount hybridization solution [50% formamide, 5 × SSC (750 mM NaCl, 75 mM sodium citrate, pH 7.0), 1 × Denhardt's reagent (50 µg/ml yeast RNA, 1% Tween 20, 0.1% CHAPS, 5 mM EDTA) pH 8.0] followed by hybridization at 55 °C for 48–72 h in the same solution containing a digoxigenin labelled antisense RNA probe of the coding region of *B. mori* SNMP2 (Acc. No. XP_037870755). The DIG-labelled antisense riboprobe was generated from a BmorSNMP2 cDNA containing plasmid using an RNA transcription system (Merck).

Afterwards, the antennal samples were washed four times for 15 min in preheated 0.1 X SSC with 0.03% Triton X-100 at 60 °C in the hybridization oven and subsequently incubated in 1% blocking reagent (Akoya Biosciences, Marlborough, MA, USA) in TBS (100 mM Tris, 150

mM NaCl, pH 7.5) with 1% Triton X-100 over night at 4 °C. Samples were then treated with an anti-dig AP-conjugated antibody (Merck) diluted 1:500 in 1% blocking reagent in TBS for 48h at 4 °C. After washing five times for 10 min in TBS with 0.05% Tween 20 and one time for 5 min in 150 mM Tris-HCl pH 8.3, dig-labelled riboprobes were visualized by using the VECTOR RED alkaline phosphatase substrate kit (Vector Laboratories, Burlingame, CA, USA) as recommended by the manufacturer with components diluted in Tris-HCl (150 mM, pH 8.3) and substrate incubation for 5–7h at 4 °C. The samples were then washed with TBST three times for 10 min and treated with anti-HRP AF633 (Jackson ImmunoResearch) diluted 1:200 in TBST overnight at 4 °C for immuno-counterstaining of neurons. After washing the samples three times for 10 min with TBST and once for 5 min with H₂O, the antennal fragments were mounted in mowiol filled into the center of three layers of self-adhesive hole reinforcement rings (Herma GmbH, Filderstadt, Germany) placed on microscope slides and sealed with a coverslip.

2.8. Fatty acid uptake assay with antenna

The antennae of *H. virescens* and *B. mori* were carefully removed from the heads and placed into working solution (50 mM BODIPY FL C16 in PBS) for 1 h without submerging the base of the antenna. For *H. virescens*, the antennae were then briefly rinsed in PBS before being transferred into fixative solution (4% PFA in PBS) for 2h at 4 °C. The antennae were then washed three times for 10 min with PBS, embedded into O.C.T Tissue embedding medium, sectioned (12 µm) with a cryomicrotome and thaw mounted onto SuperFrost Adhesion microscope slides. After sectioning, the antennal sections were rinsed three times for 5 min with PBS, incubated in FIHC blocking solution for 30 min and then treated with anti-HRP Cy3 and DAPI for 1h. Sections were washed three times for 5 min in PBS, once for 5 min with H₂O and then mounted with mowiol and a cover slip. For *B. mori* antennae, the side branches were first dissected off of the main antennal branch and then transferred into the fixative solution overnight at 4 °C. Then the antennal fragments were rinsed twice with PBS for 10 min, briefly washed with water and transferring onto microscope slides with mowiol as described for the samples in WM-FISH. To test the effect of the SSO inhibitor on the antenna, the antenna were treated with an SSO solution (100 µM SSO, 0.4% DMSO in PBS pH 7.4) for 1 h at room temperature prior to the uptake assay with BODIPY FL C16. Afterwards, antenna were carefully removed at their bases and treated with the BODIPY FL C16 working solution as mentioned for *H. virescens*. Control experiments were performed with antenna treated in the same solution omitting SSO (0.4% DMSO in PBS pH 7.4).

2.9. Analysis of antennal samples by confocal microscopy

Sections from the FIHC experiments and whole mount preparations of the WM-FISH experiments, as well as the fatty acid uptake assays on moth antenna were analyzed on a LSM 880 confocal laser scanning microscope (Carl Zeiss Microscopy, Jena, Germany). Confocal image stacks of the fluorescence and transmitted-light channels were taken and used to make projections of optical planes applying the ZEN Black software (Carl Zeiss Microscopy). Pictures were not altered except for adjusting the brightness or contrast for a uniform tone within a single figure.

2.10. Behavioral experiments on *Bombyx mori* males

When exposed to females releasing sex pheromones, male silk moths respond by rapidly flapping their wings for some time, a behavior named the wing-fluttering response. To compare the response of untreated and SSO-Inhibitor-treated male *B. mori* to female released sex pheromones the duration of the flutter dance of the males was used as a measure. For this, 0–2 day old males were separately kept in plastic containers (11 cm

× 7.5 cm x 4 cm). In the experiment, an adult female (0–3 day old) was held 10 cm above an individual male for 30 s eliciting an immediate male wing fluttering response. The total male response time was measured until the male stopped wing beating and remained stationary for more than 2 min. Afterwards, the male was placed head first until its thorax into a 2 ml reaction tube filled with 500 µL inhibitor solution (100 µM SSO with 0.4% DMSO in PBS pH 7.4), thus just its antenna and head were fully submerged in inhibitor solution. Control experiments were conducted with males treated in the same way with 0.4% DMSO in PBS. After treatment for 1h at room temperature, the males were placed back into their individual containers and left to dry for 15 min. Subsequently, the males were exposed again to females for 30 s and their wing flutter response was measured. The response durations of the males before and after their respective treatments were compared and analyzed for statistical differences using a paired T-test.

3. Results

3.1. SNMP2 mediates an increased cellular uptake of a fluorescent fatty acid analog

For functional investigations towards a possible involvement of the SNMP2 protein in the transport of lipophilic fatty acid compounds, we generated a stable cell line, termed TReX/S2 cells, carrying the HvirSNMP2 coding sequence. The transcription of the HvirSNMP2 gene in TReX/S2 cells after tetracycline induction was verified using reverse transcriptase PCR and HvirSNMP2 specific primers. Amplification of PCR products of the anticipated size were obtained with cDNA generated from TReX/S2 cells but not with cDNA from parental TReX cells (Fig. 1A). In order to test if gene expression also leads to the production of the SNMP2 protein, we performed Western blot analysis with total protein extracts of induced TReX and the TReX/S2 cells using an anti-HvirSNMP2 antibody (Fig. 1B). A clear band slightly above the predicted molecular weight of about 59 kDa was obtained only in the TReX/S2 cells. Since SNMP proteins display a number of glycosylation sites (Gomez-Diaz et al., 2016), we presume that post-translational modifications likely cause the HvirSNMP2 protein to run higher than the predicted molecular weight. Together, the results demonstrate successful expression of SNMP2 in the TReX/S2 line on both the mRNA and the protein level.

To determine if HvirSNMP2 can mediate an increased cellular uptake of lipophilic fatty acids, we incubated parental TReX cells and SNMP2-expressing TReX/S2 cells with a fluorophore-conjugated long-chain fatty acid analog, termed BODIPY FL C16. We first compared the fluorescent signals in both lines directly after the application of 10 µM BODIPY FL C16 (0 s) and at the end of the uptake assay (168 s later) (Fig. 1C). No intrinsic fluorescence was observed in cells of either line directly after the addition of the fatty acid analog (0 s). In contrast, imaging of the same cells after 168 s, revealed only weak fluorescence signals in TReX cells whereas SNMP2-expressing TReX/S2 cells showed intense fluorescent labeling. This result shows that the amount of fluorescent fatty acid analog taken up by the TReX/S2 cells vastly differs from that of the TReX cells (Fig. 1C).

In order to monitor the uptake of 10 µM BODIPY FL C16 over time, we performed live cell imaging experiments by measuring the fluorescence of individual cells in 7s increments over a period of 168 s after treatment (24 time points). From this we calculated for each time point the relative change of fluorescent intensity in relation to the initial fluorescence ($\Delta F/F_0$). The mean relative fluorescence changes (\pm SD) of cells determined from 5 independent experiments with 25 arbitrarily selected each are shown in Fig. 1D. It is getting clear that the parental TReX cells show a steady but rather low increase in fluorescence intensity, i. e. an uptake of BODIPY FL C16. In comparison, the results for the SNMP2-expressing cells show a much higher and rapid uptake of the fluorescent fatty acid analog over the whole 168 s duration of the experiments (Fig. 1D).

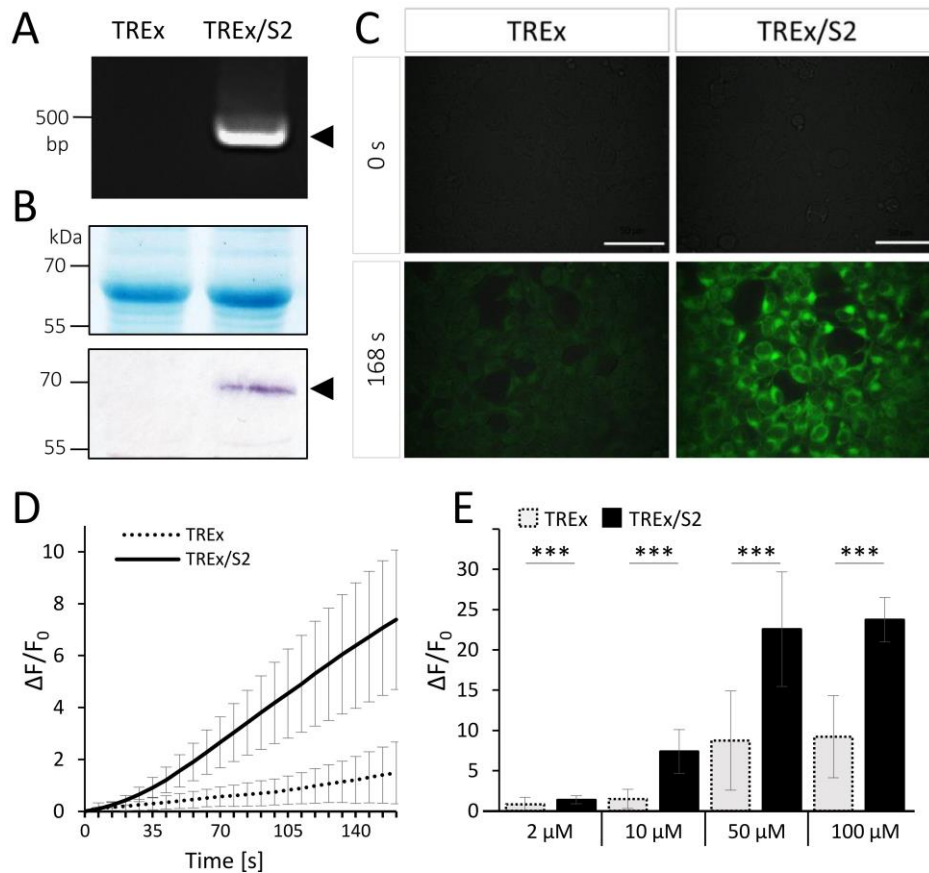


Fig. 1. SNMP2 mediates an increased cellular uptake of long-chain fatty acids. **A** SNMP2 gene expression in TREx/S2 as verified by RT-PCR with HvirSNMP2 specific primers. A band of the expected size (arrowhead) was only obtained with cDNA from TREx/S2 cells but not from the parental TREx cells. **B** SDS-PAGE and Western Blot analysis of total protein extracts from TREx and TREx/S2 cells. The upper panel shows all proteins of an SDS-PAGE stained with Coomassie blue. The lower panel shows the immunoblot using the anti-HvirSNMP2-ab that visualized a clear protein band in the TREx/S2 lane (arrowhead). **C** Uptake of BODIPY FL C16 (10 μM) into TREx and TREx/S2 cells at 0s and at 168s after application of the fatty acid analog. Images were taken with a 63× immersion objective and processed with the Leica LASx software (scale bars = 50 μm). **D** live cell imaging measurements of the fatty acid uptake in TREx and TREx/S2 cells. Images were taken in 7s increments after the application of 10 μM BODIPY FL C16 using a 40× dry objective. The mean (\pm SD) relative changes in fluorescent intensity ($\Delta F/F_0$) in cells over time were calculated from five independent replicates with 25 randomly selected cells each using the LASx software. **E** relative changes of fluorescent intensity in TREx and TREx/S2 cells after 168s using different concentrations of BODIPY FL C16 (mean \pm SD). Data were determined from five independent replicates with 20–25 cells each. Asterisks denote significant differences using an unpaired T-test (***) $p < 0.001$.

We also tested parental TREx cells and the TREx/S2 cells with different concentrations of BODIPY FL C16 and compared the change in fluorescence intensity after 168 s (Fig. 1 E). We found a concentration dependent increase in fluorescence intensity in both cell lines. However, at all concentrations tested, a significantly higher fatty acid analog uptake was measured in the TREx/S2 cells compared to TREx cells. Overall, the results demonstrate that the presence of SNMP2 causes a rapid and increased cellular uptake of the long-chain fatty acid analog BODIPY FL C16 into TREx cells.

To approach the specificity of the BODIPY FL C16 uptake, further live cell imaging experiments were performed with another BODIPY fatty acid analog, BODIPY C4C9, where the position of the BODIPY fluorophore is shifted towards the middle of the molecule, closer to the fatty acid carboxyl group (Fig. S2). In these experiments, no differences in the uptake were observed between the TREx and the TREx/S2 cells (Fig. S3).

These results denote some selectivity of SNMP2 in mediating the cellular uptake of lipophilic fatty acids.

3.2. The CD36 inhibitor SSO impairs the SNMP2-mediated fatty acid uptake

We next attempted to suppress the SNMP2-mediated uptake of long-chain fatty acids into TREx cells by applying a known CD36 protein inhibitor, sulfo-N-succinimidyl oleate (SSO). Therefore, we pretreated the TREx and TREx/S2 cells with 50 μM SSO for 1 min before testing the uptake of 10 μM BODIPY FL C16 by live cell imaging measurements. For TREx cells we found no difference in the time course and extent of the fatty acid analog uptake between the SSO pretreated cells (Fig. 2 A) and untreated cells (Fig. 1 D), indicating that SSO does not impair regular TREx cell functions. However, when analyzing TREx/S2 cells, we

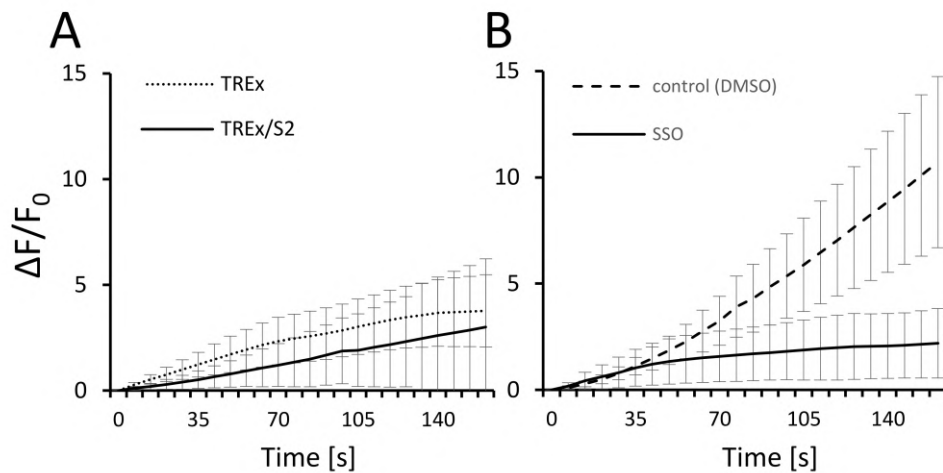


Fig. 2. SSO inhibits the SNMP2-mediated uptake of the long-chain fatty acid analog BODIPY FL C16. **A** Uptake of 10 μM BODIPY FL C16 in TREx and TREx/S2 cells after SSO pretreatment (50 μM SSO/0.1% DMSO). Live cell imaging measurements were performed in 7s increments over 168 s. The relative changes in fluorescent intensity ($\Delta F/F_0$) of the mean (\pm SD) cellular values calculated from four independent replicates with 25 randomly selected cells each. **B** TREx/S2 cells were either pretreated with 50 μM SSO/0.1% DMSO or only 0.1% DMSO (control) prior to live cell imaging of the BODIPY FL C16 uptake. $\Delta F/F_0$ changes represent the mean values (\pm SD) of cells calculated from six (SSO) and eight (control) independent replicates with 25 randomly selected cells each.

observed a clear reduction in fluorescence signal intensity in SSO-pretreated cells (Fig. 2A) compared to non-treated cells (Fig. 1 D), with the extent of the BODIPY FL C16 uptake in the SSO pretreated TREx/S2 cells now resembling the uptake in the parental TREx cells (Fig. 2 A). To ensure that the solvent (DMSO) used to solubilize SSO does not impact SNMP2 function, we performed additional control experiments with TREx/S2 cells preincubated with either the SSO working solution or the same solution without SSO (Fig. 2 B). This revealed no reduced uptake in TREx/S2 cells when SSO was omitted, demonstrating no effect of the DMSO solvent on SNMP2 function. Altogether, the experiments suggest that SSO inhibits SNMP2's function and in consequence attenuates the uptake of the lipophilic fatty acid analog BODIPY FL C16 into TREx/S2 cells.

3.3. Support cells of the *H. virescens* antenna express SNMP2 and can take up fatty acids from the sensillum lymph

We next tried to approach, whether an uptake of lipophilic fatty acids from the sensillum lymph may also exist in the antenna and whether SNMP2-expressing support cells are involved. To investigate the ability of support cells to take up lipophilic fatty acids from the sensillum lymph, we incubated entire intact male *H. virescens* antennae in BODIPY FL C16 solution, allowing the compound to enter the sensillum lymph via pores in the sensillum's cuticle. After treatment, antennal sections were prepared and additionally treated with anti-HRP and DAPI to visualize neurons and nuclei, respectively.

The results of the antennal fatty acid uptake assays revealed intensive BODIPY FL C16 labeling of cells throughout the antennal segments as demonstrated by the horizontal section shown in Fig. 3 A. The BODIPY FL C16 labeling pattern was complementary to the neuronal staining that visualized OSNs (Fig. 3A–C), demonstrating that non-neuronal cells have specifically taken up the fatty acid analog. This is further evidenced by closer inspections of a longitudinal section, revealing that the BODIPY FL C16 signals are attributed to non-neuronal support cells, which directly border the bases of olfactory sensilla and are associated with OSNs that show no labeling by the fatty acid analog

(Fig. 3 B and C, C'). Within the cells, the BODIPY FL C16 signals partly accumulated in a dot-like pattern (arrowheads in Fig. 3, C'). Control experiments with antenna incubated in a solution omitting the fluorescent fatty acid analog showed only the neuronal staining pattern and some cuticle's autofluorescence but no labelling in the green BODIPY fluorescence channel (Fig. S4).

In order to evaluate if the same cells that take up the fatty acid analog also express SNMP2, we set out to compare the support cell labeling pattern obtained in the BODIPY FL C16 uptake assay with the topography of the SNMP2-expressing support cells in the *H. virescens* antenna. Therefore, we performed FIHC with an anti-HvirSNMP2 specific antibody on antennal sections together with anti-HRP and DAPI counterstaining (Fig. 3 D - F'). Similar to the BODIPY FL C16 support cell labeling, the FIHC experiments exhibited the presence of SNMP2 in multiple, non-neuronal cells (Fig. 3 D and E). Moreover, exploring longitudinal sections shows that SNMP2 is localized in the support cells closely associated with OSNs at the bases of olfactory sensilla (Fig. 3 E and F). These results are in accordance with our previous FIHC and FISH experiments demonstrating broad SNMP2 expression in most if not all antennal support cells of *H. virescens* olfactory sensilla (Blankenburg et al., 2019; Forstner et al., 2008). Unfortunately, attempts to use the anti-SNMP2 antibody in BODIPY FL C16 uptake/SNMP2 co-labeling experiments were not successful. This was probably due to the extended protocol required for FIHC with anti-SNMP2-ab, leading to a loss of the BODIPY FL C16 signal from sections.

Overall, the support cell labelling pattern evoked by the anti-SNMP2 antibody clearly coincides with the pattern of BODIPY FL C16-positive cells revealed in the antennal fatty acid uptake assays. This strongly suggests that the SNMP2-expressing cells are the same support cells that are able to take up the fatty acid analog.

3.4. Fatty acid uptake and SNMP2-expression in support cells of the *Bombyx mori* antenna

To address the question if SNMP2-expressing support cells in other moths are also capable of taking up fatty acids from the sensillum lymph,

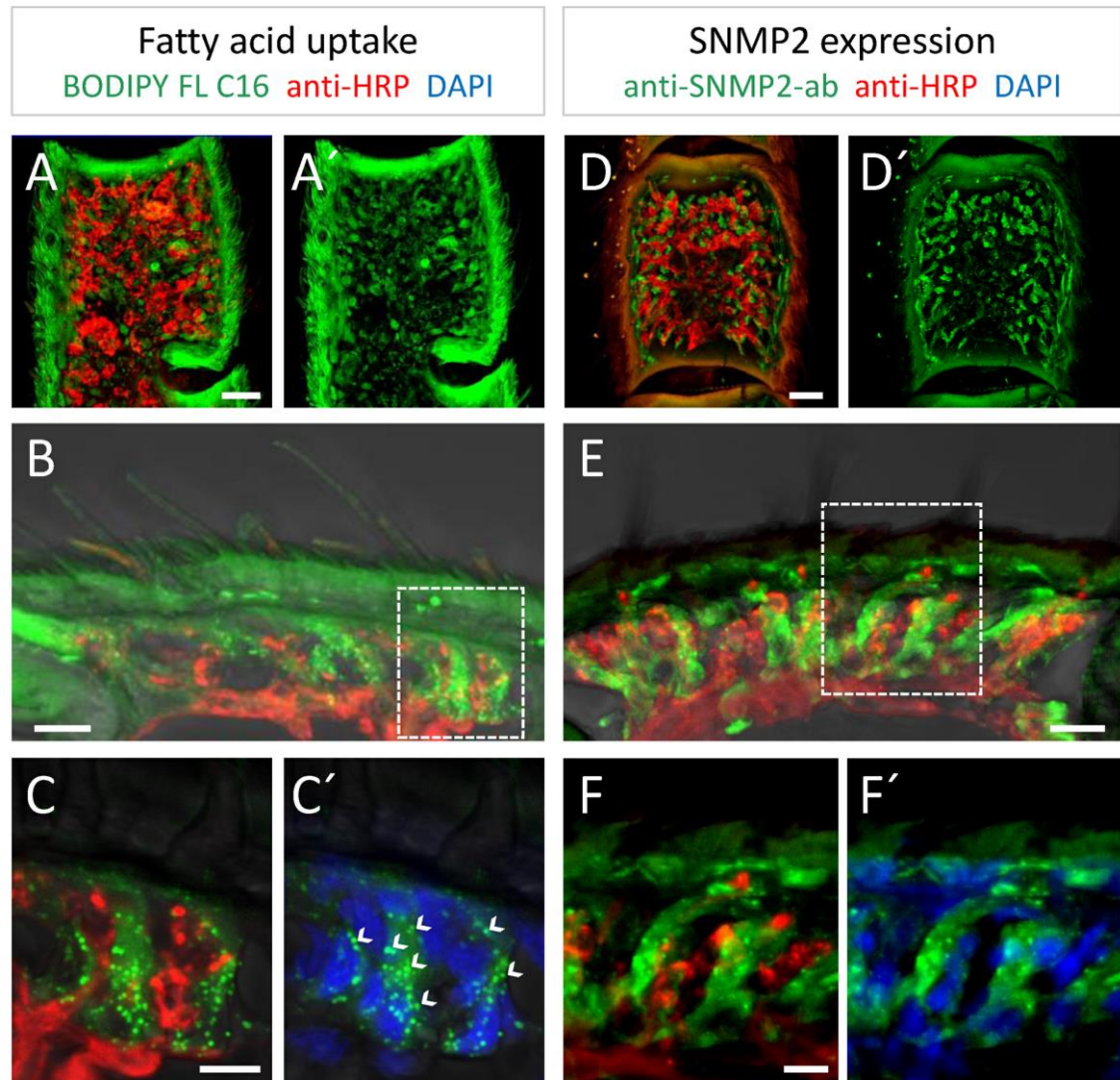


Fig. 3. Support cells of the antenna of *H. virescens* express SNMP2 and take up fatty acids from the sensillum lymph. Antennal sections were treated with anti-HRP to visualize OSNs (red) and DAPI to visualize nuclei (blue). **A-C'** Sections of antenna that were incubated with the fatty acid analog BODIPY FL C16 (green). **A** and **A'** Visualization of BODIPY FL C16-positive cells and neurons in a horizontal section. **B** Longitudinal section showing support cells that display BODIPY FL C16 signals and are associated with non-labelled OSNs underneath olfactory sensilla. **C** and **C'** show a higher magnification of cells in the region boxed in **B**. Arrowheads indicate dot-like signals in support cells. **D-F'** SNMP2-positive cells were visualized by FIHC using anti-HvirSNMP2-ab (green). **D** and **D'** distribution of multiple non-neuronal SNMP2-positive cells and OSNs on a horizontal antennal section. **E** SNMP2 expression in support cells that are associated with OSNs underneath olfactory sensilla. **F** and **F'** higher magnification of the boxed region shown in **E**. Images **A**, **B**, **C**, **D**, **E**, **F**: overlay of the red and green channels. **A'** and **D'** green channel. **C'** and **F'**: overlay of the green and blue channels. Scale bars: **A** and **D** = 20 μ m; **B** and **E** = 10 μ m; **C** and **F** = 5 μ m.

we analyzed the antenna of the silk moth *Bombyx mori*. Therefore, we first characterized the SNMP2-expressing cells in this species. In lack of a *B. mori* SNMP2-specific antibody we alternatively used fluorescence in situ hybridization (FISH) with a dig-labelled SNMP2 riboprobe combined with FIHC using the anti-HRP antibody to visualize the SNMP2-expressing cells and neurons, respectively.

Due to the distinctive morphology of the *B. mori* antenna, which has long sensilla on side branches that protrude out of a main trunk,

sectioning of the antenna proved difficult. Therefore, we applied combined FISH/FIHC on whole mount samples of the antennal side branches. Using this method, we produced samples with well-preserved antennal tissue and sensilla structures, though we noted that in confocal LSM analysis the antennal cuticle emits strong autofluorescence depending on the optical plane being imaged (Fig. 4 A, asterisk).

In *B. mori*, all the trichoid and basiconic sensilla are located on one side of the antenna. Accordingly, we found anti-HRP labelled OSNs

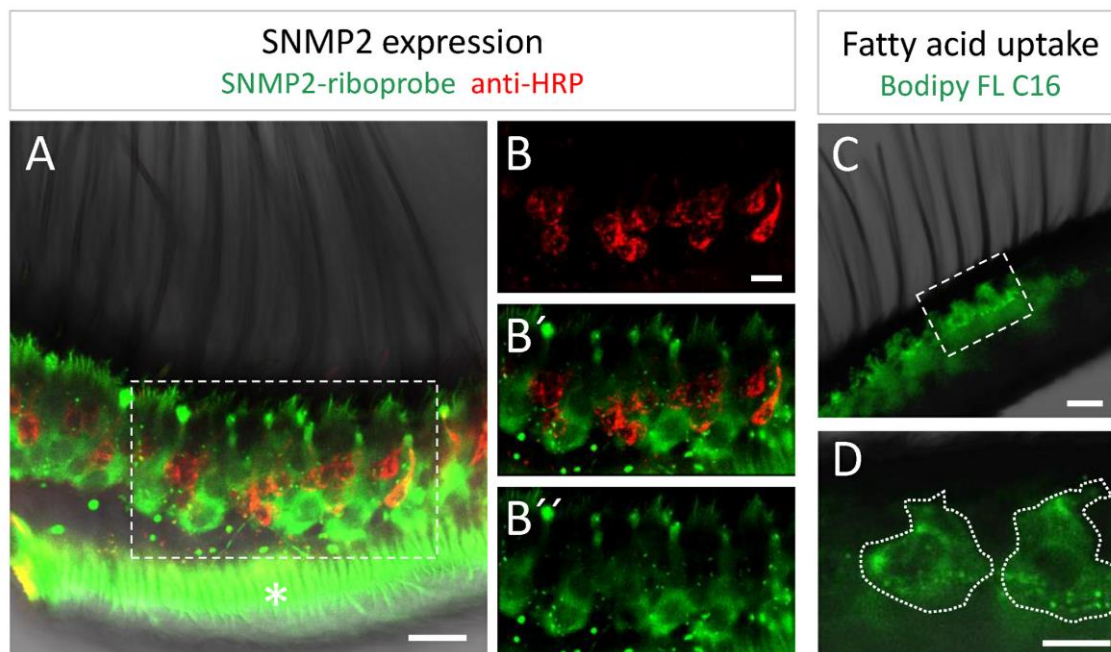


Fig. 4. Antennal support cells of *B. mori* express SNMP2 and can take up fatty acids from the sensillum lymph. A-B'' Combined whole mount FISH and FIHC conducted on an antennal side branch utilizing an SNMP2-riboprobe (green) to visualize SNMP2 expression and anti-HRP (red) to visualize OSNs. A SNMP2-positive cells are situated beneath the olfactory sensilla. B-B'' Show a higher magnification in different channels of the region boxed in A. C-D Antenna of *B. mori* treated with BODIPY FL C16 (green). C BODIPY FL C16-positive cells were detected underneath the olfactory sensilla. D higher magnification of the area boxed in C showing uptake of BODIPY FL C16 in support cells (encircled). The Asterisk (*) in A denotes autofluorescence of the cuticle. A and B': overlay of red and green channels. B: red channel. B'', C and D: green channel. Scale bars: A and C = 20 μ m; B and D = 10 μ m.

arranged below the antennal surface carrying the olfactory sensilla (Fig. 4 A and B). In addition, the SNMP2 riboprobe visualized numerous, strikingly large SNMP2-positive cells in the antenna that were closely associated with the OSNs (Fig. 4 A and B'). Typical for support cells, these cells show extension towards the base of the sensilla. In addition, the co-staining of OSNs and SNMP2-positive cells exemplifies the typical differences in the size and morphology of these cell types (Fig. 4 B'). Overall, the WM-FISH results elucidated a broad expression of SNMP2 in the morphologically distinct support cells in the antenna of *B. mori*.

We next tested if support cells of *B. mori* are also able to take up a fatty acid analog that enters a sensillum by incubating the antennae of males in a solution with BODIPY FL C16. In these experiments we found numerous cells displaying BODIPY FL C16 signals underneath the side of the antennal side branches harboring the majority of the olfactory sensilla (Fig. 4 C, supplementary). When analyzed at a higher magnification, it becomes apparent that BODIPY FL C16 signals, some of which appear as dot-like accumulations, are located in distinct and large cells, with a morphology typical for support cells and resembling the shape of the SNMP2-expressing cells. Together, our experiments with *B. mori* antenna revealed results similar to *H. virescens*, indicating the ability of support cells to take up fatty acids from the sensillum lymph, which, in terms of morphology and topography, correspond to SNMP2-expressing support cells.

3.5. SSO treatment of the antenna inhibits uptake of fatty acids from the lymph

To possibly link the observed BODIPY FL C16 uptake into antennal support cells to a role of SNMP2 in this process, we investigated if

treatment of the antenna with the inhibitor SSO may impair the cellular uptake of the long-chain fatty acid analog from the sensillum lymph. Towards this goal we used the antenna of *B. mori* because it permits the analysis of whole mount preparations, which were regarded best suited for determining potential SSO inhibitor-induced changes of the BODIPY FL C16 uptake within antennal structures.

In control experiments antennal samples were pretreated for 1 h with 0.4% DMSO in PBS, which was used to dissolve SSO, before applying the fatty acid analog for 1 h. Analysis of the control samples visualized BODIPY FL C16-positive support cells, indicating that they retain their ability to take up fatty acids from the sensillum lumen upon solvent treatment (Fig. 5 A). In contrast, antenna subjected to SSO pretreatment (100 μ M SSO, 0.4% DMSO in PBS) under otherwise identical conditions, showed diminished BODIPY FL C16 signals in the support cells (Fig. 5 B). Moreover, when analyzing the sensillum lumen, we noticed obvious differences in the luminal fluorescence signals between SSO-treated and control antenna (Fig. 5 C and D). Along the sensillum lumen of control antenna we rarely observed fluorescent signals, with occasional signals restricted to the base of the sensilla (Fig. 5 C). In contrast, in the SSO treated antenna, BODIPY FL C16 signals were regularly found localized along the entire length of the sensillum shafts (Fig. 5 D). Together our results demonstrate that SSO treatment of the antenna blocks the uptake of BODIPY FL C16 from the sensillum lymph into the support cells. Moreover, they indicate that this leads to an accumulation of the fatty acid analog in the sensillum lumen.

3.6. Effect of SSO treatment on pheromone-elicited behavior

In *B. mori*, the female-released sex pheromones, i. e. the unsaturated

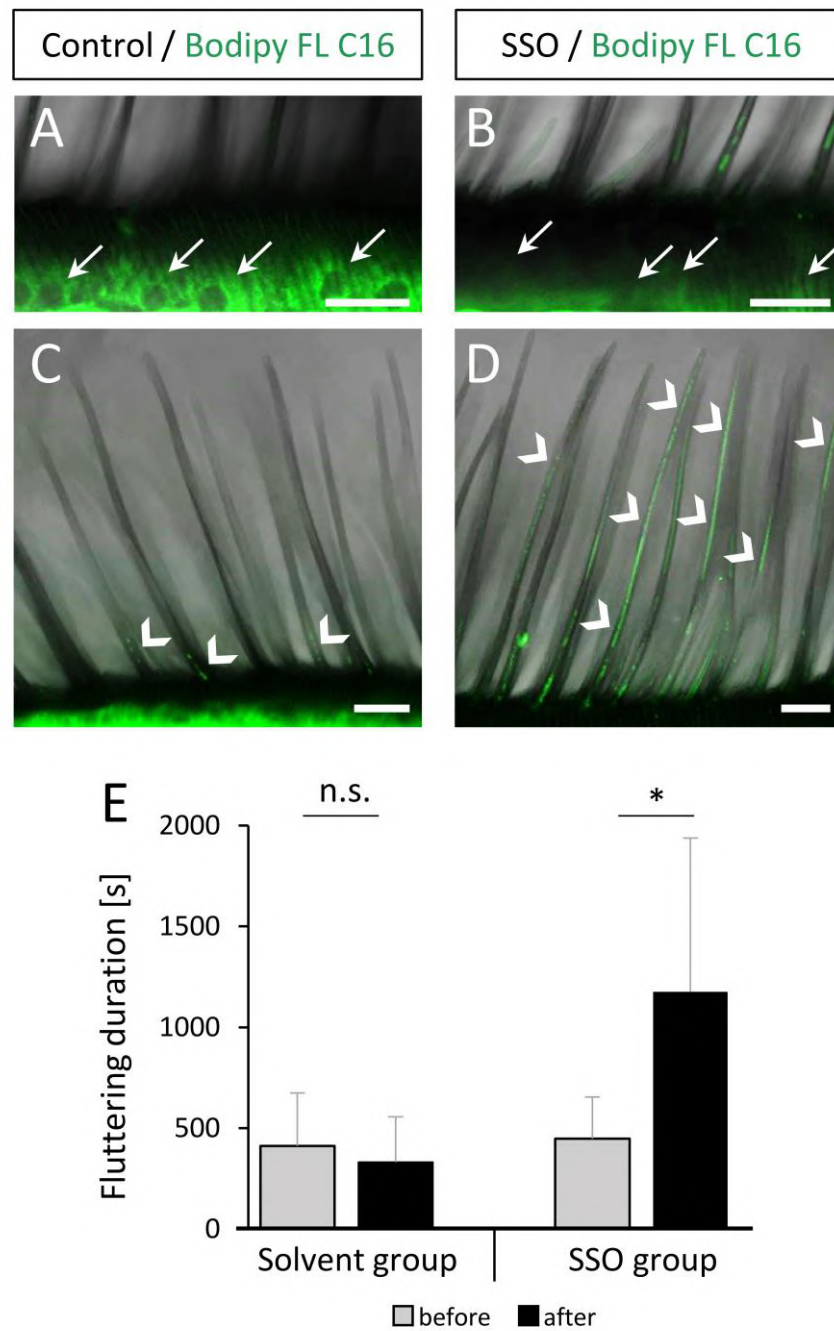


Fig. 5. SSO treatment of the *B. mori* antenna affects the uptake of fatty acids from the sensillum lymph and alters the behavioral response in males. Antenna were treated with either control (0.4% DMSO in PBPs) or inhibitor solutions (100 μ M SSO, 0.4% DMSO in PBPs). **A-D** Antenna were incubated with the fatty acid analog BODIPY FL C16 (green) after treatment. Scale bars = 20 μ m. **A** Support cells (arrows) take up BODIPY FL C16 in control treatments. **B** Reduced uptake of BODIPY FL C16 into support cells after SSO treatment. **C** few BODIPY FL C16 signals (arrowheads) in the sensillum lumen in control treated antenna. **D** BODIPY FL C16 signals along the entire length of sensillum shafts in SSO treated antenna. **E** Wing fluttering duration of males (mean \pm SD) after exposure to female pheromones before and after treatment with either solvent (n = 12) or SSO in solvent (n = 12). n.s. = not significant, **p = 0.0067 in a paired T-test.

long-chain alcohol and aldehyde Bombykol and Bombykal, respectively are inactivated to the corresponding long-chain fatty acids, which have to be rapidly removed from the sensillum lymph to prevent product inhibition of the inactivation process and, in consequence, accumulation of active sex pheromone in the lymph. Because we found SSO to impair the uptake of fatty acids from the lymph into support cells of *B. mori* we asked if SSO treatment of the antenna may possibly also alter the effective removal of sex pheromone inactivation products in males of *B. mori* and thus may lead to an altered behavioral response. We used the duration of the wing fluttering response as a measure to evaluate the impact of SSO on male pheromone-elicited behavior. First, we determined the duration of the wing-fluttering response of untreated individual males to female sex pheromone exposure. Subsequently, the intact antennae of individual males were incubated for 1 h in either PBS, 0.4 % DMSO (solvent-group) or 100 μ M SSO in solvent (SSO-group). After allowing the antenna to dry for 15 min the exposure to females was repeated and the duration of the wing-fluttering response was determined again.

Prior to their respective treatments, the males of the SSO group ($n = 12$) and solvent group ($n = 12$) showed similar mean wing-fluttering response durations of 412 s ($SD \pm 263$ s) and 448 s ($SD \pm 224$ s), respectively. In males that were then treated with solvent, no significant differences in their wing-fluttering duration was found compared to before their treatment (Fig. 5 E), indicating that the solvent itself does not affect the duration of the male wing fluttering response. In contrast, in the SSO-group, we measured a significant difference between the duration of the wing-fluttering response before and after SSO treatment (Fig. 5 E). SSO treated males exhibited a prolonged wing-fluttering when presented to female releasing pheromones, with a mean duration of 1175 s ($SD \pm 764$ s), which is more than twice the mean duration of the initial response. Overall, the experiments with *B. mori* show that SSO treatment of male antenna lead to altered behavioral responses to female sex pheromones, possibly due to disturbance of the proper removal of their fatty acid inactivation products.

4. Discussion

In this study we assessed a possible role of SNMP2 and support cells of insect olfactory sensilla in the elimination of lipophilic “waste products” from the sensillum lymph. In many moth species, such products result from the inactivation of female sex pheromones, representing long-chain unsaturated aliphatic alcohols or aldehydes, which are converted by ODEs in the sensillum lymph into the corresponding long-chain fatty acids following OSN activation (Tasayco and Prestwich, 1990; Pelletier et al., 2007; Rybczynski et al., 1990; Kasang and Weiss, 1974). The rapid pheromone inactivation and removal of their inactivation products from the sensillum lymph is considered to be essential for maintaining the functionality of the sensilla and thus the proper repetitive detection of pheromones (Vogt and Riddiford, 1981; Pelletier et al., 2023; Durand et al., 2011).

Our live cell imaging experiments with HvirSNMP2-expressing cells showed that the presence of SNMP2 mediates an increased and rapid cellular uptake of the fatty acid analog BODIPY FL C16 with increasing extracellular concentrations of the analog leading to an increased uptake into the cells. No increase in uptake was observed when testing the BODIPY C4C9 analog, indicating some ligand specificity of HvirSNMP2. Our findings for SNMP2 are reminiscent to functions of mammalian CD36 proteins, which facilitate the internalization of certain long-chain fatty acids into cells and accelerate the rate of fatty acid uptake (Koonen et al., 2005; Glatz and Luiken, 2018; Drover et al., 2008; Abumrad et al., 1993; Pepino et al., 2014; Glatz et al., 2022). Similarly, other insect-specific members of the CD36 family outside of the SNMP clade, namely NinaD and Santa Maria act in the uptake of lipids (carotenoids) (Wang et al., 2007; Kiefer et al., 2002; Giovannucci and Stephenson, 1999). Thus, a role of SNMP2s in the transport of lipophilic compounds across cell membranes is in line with the function attributed to various

CD36 family members. In further support of functional similarities to the mammalian CD36 protein and of an SNMP2-mediated transport mechanism, we found that the CD36 inhibitor SSO abolished the BODIPY FL C16 uptake into SNMP2-expressing cells. In the mammalian CD36 protein, SSO binds to a distinct lysine in the apical part of the large protein ectodomain, which supposedly interacts with the carboxyl group of long-chain fatty acids, resulting in a reduction of the CD36-mediated fatty acid internalization (Pepino et al., 2014; Harmon and Abumrad, 1993; Kuda et al., 2013). Although it remains unknown how SSO impairs SNMP2's function, our data demonstrate that SSO is not just a potent inhibitor of mammalian CD36 proteins, but also of the insect-specific SNMP2 proteins.

In the antenna of *H. virescens* and *B. mori*, SNMP2 is exclusively expressed in the non-neuronal support cells found at the base of the sensilla. While in this study we focused on its possible role in the clearance of sex pheromone inactivation products, we are aware of SNMP2's broad expression in support cells of not only pheromone-sensitive sensilla but also of sensilla tuned to the reception of other behaviorally relevant odorants (Blankenburg et al., 2019; Gu et al., 2013; Sun et al., 2019). Therefore, it is conceivable that SNMP2 may also be involved in cleaning the sensillum lymph from inactivation products resulting from lipophilic general odorants or from lipophilic compounds that have entered a sensillum accidentally. In experiments with *H. virescens* and *B. mori* we found that in SNMP2-expressing cells the same fatty acid analog, BODIPY FL C16 can be taken up, suggesting some overlapping ligand spectra of SNMP2 in different moth species. However, to clarify the selectivity and specificity of SNMP2 further investigations with a spectrum of various lipophilic ligand are necessary. Noteworthy, a previous study conducted on the moth *Lymantria dispar* has reported the presence high levels of long-chain fatty acids in the sensillum lymph (Nardella et al., 2015). This was suggested to facilitate pheromone partition in the lymph and pheromone binding to pheromone binding proteins. Therefore, in addition to pheromone clearance, the SNMP2 may also be involved in further processes i.e. homeostasis of the fatty acids that comprise the emulsion in the lymph.

Generally, members of the CD36 protein receptor/transporter family are multifunctional and have a broad ligand spectrum for various lipophilic molecules, including different long-chain fatty acids as well as other lipids derived from fatty acids (Silverstein and Febbraio, 2009; Martin et al., 2011; Abumrad and Goldberg, 2016; Zhao et al., 2021; Jimenez-Dalmaroni et al., 2009; Chen et al., 2022; Gomez-Diaz et al., 2016).

Based on our data, we suggest that SNMP2 proteins in support cells of insect antenna significantly contribute to the maintenance of the sensillum function by quickly removing undesired long-chain fatty acids from the sensillum lymph into support cells. In accordance with such a function, our previous detailed FIHC study on the antenna of *H. virescens* localized SNMP2 at the apical side of the support cells (Blankenburg et al., 2019), where microvilli structures largely increase the cellular surface of support cells and directly border the sensillum lymph (Keil, 1989; Gnatzy et al., 1984). Moreover, recent immunogold labelling experiments with locust antenna localized the SNMP2 protein in the microvilli-membranes of support cells (Cassau et al., 2022).

Microvilli structures are generally sites of high extensive exchange across membranes (Sharkova et al., 2023; Houdusse and Titus, 2021). Such an extensive exchange appears to also exist over the microvilli membranes of olfactory support cells. When treating intact antenna with the fluorescent fatty acid analog, we found that support cells of both *H. virescens* and *B. mori* were able to efficiently take up the compound from the sensillum lymph. This indicates that support cells of olfactory sensilla not only control sensillum lymph homeostasis by secreting proteins and ions (Thurm and Küppers, 1980), but also by absorbing molecules which could otherwise alter the composition of the sensillum lymph and impact the function of the olfactory unit. Interestingly, evidence for a clearance function of support cells was also provided by studying gustatory sensilla of the cockroach's maxillary palps infiltrated

with the fluorescent dye Lucifer yellow, where it was found that the support cells of these sensilla were able to take up and clear the substance from the sensillum lymph (Seidl, 1992). This may hint on a crucial role of support cells for sensillum lymph maintenance in olfactory and gustatory sensilla of insects.

In our antennal uptake assays with BODIPY FL C16, we regularly found fluorescent signals accumulating in a dot-like pattern within support cells of *H. virescens* and, albeit less pronounced, in support cells of *B. mori*. This may suggest that in olfactory support cells the absorbed lipophilic compounds end up in vesicles and subsequently in lipid droplets as described for the CD36-dependent uptake of free fatty acids in adipocytes, which appears to involve dynamic endocytosis processes leading to the formation of vesicles and lipid droplets (Hao et al., 2020).

We found that pretreatment of antenna with SSO led to a reduced uptake of BODIPY FL C16 from the sensillum lymph into support cells, resembling the reduced uptake observed upon SSO treatment of the SNMP2-expressing cell line. Notably, compared to sensilla of untreated antenna, the lumen of sensilla from SSO-incubated antenna showed strong fluorescent signals indicating that the lymph was still filled with significant amounts of the fatty acid analog. This finding further corroborates that SSO can interfere with the support cell's clearance of extracellular fatty acids from the sensillum lymph causing an accumulation of lipids in the perireceptor space. Whether this is a result of direct SSO binding to the SNMP2 expressed in the support cells needs to be investigated.

Since we observed that SSO impacts the proper function of sensilla with regard to the clearance of fatty acids, which are metabolites in the inactivation of female-released moth pheromones, we analyzed the possible consequences of an SSO inhibition on the pheromone-induced behavior of male *B. mori* moths. Males of this species react sensitively to the female's emitting pheromones with a typical fluttering of their wings, which we found considerably prolonged after SSO treatment. This suggests that SSO treatment has a substantial impact on the pheromone responsiveness of male moths by probably inhibiting the clearance of extracellular fatty acids derived from the inactivation of pheromones by ODEs. Worth mentioning, disrupting any part of the ODE activity also leads to prolonged olfactory responses (Cherteremps et al., 2012; Fraichard et al., 2020), indicating that in general, the improper clearance of odorants can impact olfactory driven behavior.

Overall, our data suggest an important role of support cells in regulating the removal of lipophilic waste compounds from the sensillum lymph, thereby maintaining the proper function of the olfactory unit as a whole. In these processes SNMP2 may play an essential role in mediating the elimination of lipophilic fatty acids from the sensillum lymph such as the inactivation products of moth pheromones. In this way support cells and SNMP2 would ensure a rapid reset of the perireceptor environment in preparation to subsequent stimuli and might be of particularly relevance in moths to maintain the overall high temporal resolution of the pheromone detection system.

Author contributions

Sina Cassau: Conceptualization, Investigation, Methodology, Analysis and Interpretation of data, Visualization, Writing – original draft; Jürgen Krieger: Conceptualization, analysis and interpretation of data, Writing – review & editing.

Declaration of competing interest

The authors declare no conflict of interest.

Data availability

Data will be made available on request.

Acknowledgments

Doreen Sander is acknowledged for excellent technical assistance.

Appendix A. Supplementary data

Supplementary data to this article can be found online at <https://doi.org/10.1016/j.ibmb.2023.104046>.

References

- Abumrad, N.A., El-Maghrabi, M.R., Amri, E.Z., Lopez, E., Grimaldi, P.A., 1993. Cloning of a rat adipocyte membrane protein implicated in binding or transport of long-chain fatty acids that is induced during preadipocyte differentiation. Homology with human CD36. *J. Biol. Chem.* 268, 17665–17668. [https://doi.org/10.1016/S0021-9258\(17\)46753-6](https://doi.org/10.1016/S0021-9258(17)46753-6).
- Abumrad, N.A., Goldberg, I.J., 2016. CD36 actions in the heart: lipids, calcium, inflammation, repair and more? *Biochim. Biophys. Acta* 1861, 1442–1449. <https://doi.org/10.1016/j.bbali.2016.03.015>.
- Benton, R., 2022. Drosophila olfaction: past, present and future. *Proc. Biol. Sci.* 289, 20222054. <https://doi.org/10.1098/rspb.2022.2054>.
- Benton, R., Vannice, K.S., Vosshall, L.B., 2007. An essential role for a CD36-related receptor in pheromone detection in *Drosophila*. *Nature* 450, 289–293. <https://doi.org/10.1038/nature06328>.
- Blankenburg, S., Cassau, S., Krieger, J., 2019. The expression patterns of SNMP1 and SNMP2 underline distinct functions of two CD36-related proteins in the olfactory system of the tobacco budworm *Heliothis virescens*. *Cell Tissue Res.* 378, 485–497. <https://doi.org/10.1007/s00441-019-03066-y>.
- Carde, R.T., Willis, M.A., 2008. Navigational strategies used by insects to find distant, wind-borne sources of odor. *J. Chem. Ecol.* 34, 854–866. <https://doi.org/10.1007/s10886-008-9484-5>.
- Cassau, S., Krieger, J., 2021. The role of SNMPs in insect olfaction. *Cell Tissue Res.* 383, 21–33. <https://doi.org/10.1007/s00441-020-03336-0>.
- Cassau, S., Sander, D., Karcher, T., Laue, M., Hause, G., Breer, H., Krieger, J., 2022. The sensilla-specific expression and subcellular localization of SNMP1 and SNMP2 reveal novel insights into their roles in the antenna of the Desert Locust *Schistocerca gregaria*. *Insects* 13. <https://doi.org/10.3390/insects13070579>.
- Chen, Y., Zhang, J., Cui, W., Silverstein, R.L., 2022. CD36, a signaling receptor and fatty acid transporter that regulates immune cell metabolism and fate. *J. Exp. Med.* 219. <https://doi.org/10.1084/jem.20211314>.
- Cherteremps, T., Francois, A., Durand, N., Rosell, G., Dekker, T., Lucas, P., Maibeche-Coisne, M., 2012. A carboxylesterase, Esterase-6, modulates sensory physiological and behavioral response dynamics to pheromone in *Drosophila*. *BMC Biol.* 10, 56. <https://doi.org/10.1186/1741-7007-10-56>.
- Drover, V.A., Nguyen, D.V., Bastie, C.C., Darlington, Y.F., Abumrad, N.A., Pessin, J.E., London, E., Sahoo, D., Phillips, M.C., 2008. CD36 mediates both cellular uptake of very long chain fatty acids and their intestinal absorption in mice. *J. Biol. Chem.* 283, 13108–13115. <https://doi.org/10.1074/jbc.M708086200>.
- Durand, N., Carot-Sans, G., Bozzolan, F., Rosell, G., Siauxat, D., Debernard, S., Cherteremps, T., Maibeche-Coisne, M., 2011. Degradation of pheromone and plant volatile components by a same odorant-degrading enzyme in the cotton leafworm, *Spodoptera litoralis*. *PLoS One* 6, e29147. <https://doi.org/10.1371/journal.pone.0029147>.
- Fleischer, J., Krieger, J., 2018. Insect pheromone receptors - key elements in sensing intraspecific chemical signals. *Front. Cell. Neurosci.* 12, 425. <https://doi.org/10.3389/fncel.2018.00425>.
- Forstner, M., Gohl, T., Gondesens, I., Raming, K., Breer, H., Krieger, J., 2008. Differential expression of SNMP-1 and SNMP-2 proteins in pheromone-sensitive hairs of moths. *Chem. Senses* 33, 291–299. <https://doi.org/10.1093/chemse/bjm087>.
- Fraichard, S., Legendre, A., Lucas, P., Chauvel, I., Faure, P., Neiers, F., Artur, Y., Briand, L., Ferveur, J.F., Heydel, J.M., 2020. Modulation of sex pheromone discrimination by a UDP-glycosyltransferase in *Drosophila melanogaster*. *Genes* 11. <https://doi.org/10.3390/genes11030237>.
- Giovannucci, D.R., Stephenson, R.S., 1999. Identification and distribution of dietary precursors of the *Drosophila* visual pigment chromophore: analysis of carotenoids in wild type and ninaD mutants by HPLC. *Vis. Res.* 39, 219–229. [https://doi.org/10.1016/S0042-6989\(98\)00184-9](https://doi.org/10.1016/S0042-6989(98)00184-9).
- Glatz, J.F.C., Luiken, J., 2018. Dynamic role of the transmembrane glycoprotein CD36 (SR-B2) in cellular fatty acid uptake and utilization. *J. Lipid Res.* 59, 1084–1093. <https://doi.org/10.1194/jlr.R082933>.
- Glatz, J.F.C., Nabben, M., Luiken, J., 2022. CD36 (SR-B2) as master regulator of cellular fatty acid homeostasis. *Curr. Opin. Lipidol.* 33, 103–111. <https://doi.org/10.1097/MOL.0000000000000819>.
- Gnatzy, W., Mohren, W., Steinbrecht, R.A., 1984. Pheromone receptors in *Bombyx mori* and *Antheraea pernyi*. II. Morphometric analysis. *Cell Tissue Res.* 235, 35–42. <https://doi.org/10.1007/BF00213720>.
- Gomez-Diaz, C., Bargeton, B., Abuin, L., Bukar, N., Reina, J.H., Bartoi, T., Graf, M., Ong, H., Ulbrich, M.H., Masson, J.F., Benton, R., 2016. A CD36 ectodomain mediates insect pheromone detection via a putative tunnelling mechanism. *Nat. Commun.* 7, 11866. <https://doi.org/10.1038/ncomms11866>.
- Grosse-Wilde, E., Svatos, A., Krieger, J., 2006. A pheromone-binding protein mediates the bombykol-induced activation of a pheromone receptor *in vitro*. *Chem. Senses* 31, 547–555. <https://doi.org/10.1093/chemse/bjj059>.

- Gu, S.H., Yang, R.N., Guo, M.B., Wang, G.R., Wu, K.M., Guo, Y.Y., Zhou, J.J., Zhang, Y.J., 2013. Molecular identification and differential expression of sensory neuron membrane proteins in the antennae of the black cutworm moth *Agrotis ipsilon*. *J. Insect Physiol.* 59, 430–443. <https://doi.org/10.1016/j.jinsphys.2013.02.003>.
- Hao, J.W., Wang, J., Guo, H., Zhao, Y.Y., Sun, H.H., Li, Y.F., Lai, X.Y., Zhao, N., Wang, X., Xie, C., Hong, L., Huang, X., Wang, H.R., Li, C.B., Liang, B., Chen, S., Zhao, T.J., 2020. CD36 facilitates fatty acid uptake by dynamic palmitoylation-regulated endocytosis. *Nat. Commun.* 11, 4765. <https://doi.org/10.1038/s41467-020-18565-8>.
- Harmon, C.M., Abumrad, N.A., 1993. Binding of sulfo-succinimidyl fatty acids to adipocyte membrane proteins: isolation and amino-terminal sequence of an 88-kD protein implicated in transport of long-chain fatty acids. *J. Membr. Biol.* 133, 43–49. <https://doi.org/10.1007/BF00231876>.
- Houdusse, A., Titus, M.A., 2021. The many roles of myosins in filopodia, microvilli and stereocilia. *Curr. Biol.* 31, R586–R602. <https://doi.org/10.1016/j.cub.2021.04.005>.
- Ishida, Y., Leal, W.S., 2005. Rapid inactivation of a moth pheromone. *Proc. Natl. Acad. Sci. U. S. A.* 102, 14075–14079.
- Jimenez-Dalmaroni, M.J., Xiao, N., Corper, A.L., Verdino, P., Ainge, G.D., Larsen, D.S., Painter, G.F., Rudd, P.M., Dwek, R.A., Hoebe, K., Beutler, B., Wilson, I.A., 2009. Soluble CD36 ectodomain binds negatively charged diacylglycerol ligands and acts as a co-receptor for TLR2. *PLoS One* 4, e7411. <https://doi.org/10.1371/journal.pone.0007411>.
- Jin, X., Ha, T.S., Smith, D.P., 2008. SNMP is a signaling component required for pheromone sensitivity in *Drosophila*. *Proc. Natl. Acad. Sci. U. S. A.* 105, 10996–11001. <https://doi.org/10.1073/pnas.0803309105>.
- Kasang, G., Weiss, N., 1974. Thin-layer chromatographic analysis of radioactively labeled insect pheromones - metabolites of [bombykol-H-3]. *Journal of Chromatography* 92, 401–417. [https://doi.org/10.1016/S0021-9673\(00\)85751-9](https://doi.org/10.1016/S0021-9673(00)85751-9).
- Keil, T.A., 1982. Contacts of pore tubules and sensory dendrites in antennal chemosensilla of a silkworm: demonstration of a possible pathway for olfactory molecules. *Tissue Cell* 14, 451–462. [https://doi.org/10.1016/0040-8166\(82\)90039-8](https://doi.org/10.1016/0040-8166(82)90039-8).
- Keil, T.A., 1989. Fine structure of the pheromone-sensitive sensilla on the antenna of the hawkmoth, *Manduca sexta*. *Tissue Cell* 21, 139–151. [https://doi.org/10.1016/0040-8166\(89\)90028-1](https://doi.org/10.1016/0040-8166(89)90028-1).
- Kiefer, C., Sumser, E., Wernet, M.F., Von Lintig, J., 2002. A class B scavenger receptor mediates the cellular uptake of carotenoids in *Drosophila*. *Proc Natl Acad Sci U S A* 99, 10581–10586. <https://doi.org/10.1073/pnas.162182899>.
- Koonen, D.P., Glatz, J.F., Bonen, A., Luiken, J.J., 2005. Long-chain fatty acid uptake and FAT/CD36 translocation in heart and skeletal muscle. *Biochim. Biophys. Acta* 1736, 163–180.
- Krieger, J., Grosse-Wilde, E., Gohl, T., Breer, H., 2005. Candidate pheromone receptors of the silkworm *Bombyx mori*. *Eur. J. Neurosci.* 21, 2167–2176. <https://doi.org/10.1111/j.1460-9568.2005.04058.x>.
- Kuda, O., Pietka, T.A., Demianova, Z., Kudova, E., Cvacka, J., Kopecky, J., Abumrad, N. A., 2013. Sulfo-N-succinimidyl oleate (SSO) inhibits fatty acid uptake and signaling for intracellular calcium via binding CD36 lysine 164: SSO also inhibits oxidized low density lipoprotein uptake by macrophages. *J. Biol. Chem.* 288, 15547–15555. <https://doi.org/10.1074/jbc.M113.473298>.
- Leal, W.S., 2013. Odorant reception in insects: roles of receptors, binding proteins, and degrading enzymes. *Annu. Rev. Entomol.* 58, 373–391. <https://doi.org/10.1146/annurev-ento-120811-153635>.
- Martin, C., Chevrot, M., Poirier, H., Passilly-Degrace, P., Niot, I., Besnard, P., 2011. CD36 as a lipid sensor. *Physiol. Behav.* 105, 33–42. <https://doi.org/10.1016/j.physbeh.2011.02.029>.
- Nardella, J., Terrado, M., Honson, N.S., Plettner, E., 2015. Endogenous fatty acids in olfactory hairs influence pheromone binding protein structure and function in *Lymantria dispar*. *Arch. Biochem. Biophys.* 579, 73–84. <https://doi.org/10.1016/j.abb.2015.05.007>.
- Nichols, Z., Vogt, R.G., 2008. The SNMP/CD36 gene family in Diptera, Hymenoptera and Coleoptera: *Drosophila melanogaster*, *D. pseudoobscura*, *Anopheles gambiae*, *Aedes aegypti*, *Apis mellifera*, and *Tribolium castaneum*. *Insect Biochem. Mol. Biol.* 38, 398–415. <https://doi.org/10.1016/j.ibmb.2007.11.003>.
- Pelletier, J., Bozzolan, F., Solvar, M., Francois, M.C., Jacquin-Joly, E., Maibeche-Coisne, M., 2007. Identification of candidate aldehyde oxidases from the silkworm *Bombyx mori* potentially involved in antennal pheromone degradation. *Gene* 404, 31–40. <https://doi.org/10.1016/j.gene.2007.08.022>.
- Pelletier, J., Dawit, M., Ghaninia, M., Marois, E., Ignell, R., 2023. A mosquito-specific antennal protein is critical for the attraction to human odor in the malaria vector *Anopheles gambiae*. *Insect Biochem. Mol. Biol.* 159, 103988 <https://doi.org/10.1016/j.ibmb.2023.103988>.
- Pepino, M.Y., Kuda, O., Samovski, D., Abumrad, N.A., 2014. Structure-function of CD36 and importance of fatty acid signal transduction in fat metabolism. *Annu. Rev. Nutr.* 34, 281–303. <https://doi.org/10.1146/annurev-nutr-071812-161220>.
- Pregitzer, P., Greschista, M., Breer, H., Krieger, J., 2014. The sensory neurone membrane protein SNMP1 contributes to the sensitivity of a pheromone detection system. *Insect Mol. Biol.* 23, 733–742. <https://doi.org/10.1111/imb.12119>.
- Renou, M., 2014. Pheromones and general odor perception in insects. In: Mucignat-Caretta, C. (Ed.), *Neurobiology of Chemical Communication*. CRC Press/Taylor & Francis, Boca Raton (FL).
- Robertson, H.M., Martos, R., Sears, C.R., Todres, E.Z., Walden, K.K., Nardi, J.B., 1999. Diversity of odourant binding proteins revealed by an expressed sequence tag project on male *Manduca sexta* moth antennae. *Insect Mol. Biol.* 8, 501–518. <https://doi.org/10.1046/j.1365-2583.1999.00146.x>.
- Rybczynski, R., Vogt, R.G., Lerner, M.R., 1990. Antennal-specific pheromone-degrading aldehyde oxidases from the moths *Antheraea polyphemus* and *Bombyx mori*. *J. Biol. Chem.* 265, 19712–19715. [https://doi.org/10.1016/S0021-9258\(17\)45430-5](https://doi.org/10.1016/S0021-9258(17)45430-5).
- Sanes, J.R., Hildebrand, J.G., 1976. Structure and development of antennae in a moth, *Manduca sexta*. *Dev. Biol.* 51, 280–299. [https://doi.org/10.1016/0012-1606\(76\)90144-5](https://doi.org/10.1016/0012-1606(76)90144-5).
- Schmidt, H.R., Benton, R., 2020. Molecular mechanisms of olfactory detection in insects: beyond receptors. *Open Biol* 10, 200252. <https://doi.org/10.1098/rsob.200252>.
- Seidl, S., 1992. Structure and function of the theogen cell in contact chemosensitive sensilla of periplaneta-Americana L (Blattodea, Blattellidae). *Int. J. Insect Morphol. Embryol.* 21, 235–250. [https://doi.org/10.1016/0020-7322\(92\)90019-J](https://doi.org/10.1016/0020-7322(92)90019-J).
- Sharkova, M., Chow, E., Erickson, T., Hocking, J.C., 2023. The morphological and functional diversity of apical microvilli. *J. Anat.* 242, 327–353. <https://doi.org/10.1111/joa.13781>.
- Silverstein, R.L., Febbraio, M., 2009. CD36, a scavenger receptor involved in immunity, metabolism, angiogenesis, and behavior. *Sci. Signal.* 2, 1–8. <https://doi.org/10.1126/scisignal.272re3>.
- Steinbrecht, R.A., 1997. Pore structures in insect olfactory sensilla: a review of data and concepts. *Int. J. Insect Morphol. Embryol.* 26, 229–245. [https://doi.org/10.1016/S0020-7322\(97\)00024-X](https://doi.org/10.1016/S0020-7322(97)00024-X).
- Steinbrecht, R.A., Gnatzy, W., 1984. Pheromone receptors in *Bombyx mori* and *Antheraea pernyi*. I. Reconstruction of the cellular organization of the sensilla trichodea. *Cell Tissue Res.* 235, 25–34. <https://doi.org/10.1007/bf00213719>.
- Stengl, M., 2010. Pheromone transduction in moths. *Front. Cell. Neurosci.* 4, 133. <https://doi.org/10.3389/fncel.2010.00133>.
- Sun, L., Wang, Q., Zhang, Y., Yan, Y., Guo, H., Xiao, Q., Zhang, Y., 2019. Expression patterns and colocalization of two sensory neurone membrane proteins in *Ectophasia obliqua* Prout, a geometrid moth pest that uses Type-II sex pheromones. *Insect Mol. Biol.* 28, 342–354. <https://doi.org/10.1111/imb.12555>.
- Tasayco, M.L., Prestwich, G.D., 1990. Aldehyde-oxidizing enzymes in an adult moth: in vitro study of aldehyde metabolism in *Heliothis virescens*. *Arch. Biochem. Biophys.* 278, 444–451. [https://doi.org/10.1016/0003-9861\(90\)90283-5](https://doi.org/10.1016/0003-9861(90)90283-5).
- Thurm, U., Küppers, J., 1980. Epithelial physiology of insect sensilla. In: Locke, M., Smiths, D.S. (Eds.), *Insect Biology in the Future*. Academic Press, New York, pp. 735–763.
- Van Der Goes Van Naters, W., 2014. *Drosophila* pheromones: from reception to perception. In: Mucignat-Caretta, C. (Ed.), *Neurobiology of Chemical Communication*. CRC Press/Taylor & Francis, Boca Raton (FL).
- Vogt, R.G., Miller, N.E., Litvack, R., Fandino, R.A., Sparks, J., Staples, J., Friedman, R., Dickens, J.C., 2009. The insect SNMP gene family. *Insect Biochem. Mol. Biol.* 39, 448–456. <https://doi.org/10.1016/j.ibmb.2009.03.007>.
- Vogt, R.G., Riddiford, L.M., 1981. Pheromone binding and inactivation by moth antennae. *Nature* 293, 161–163. <https://doi.org/10.1038/293161a0>.
- Vogt, R.G., Sparks, J.T., Fandino, R.A., Ashourian, K.T., 2020. Reflections on antennal proteins: the evolution of pheromone binding proteins. In: Blomquist, G., Vogts, R.G. (Eds.), *Diversity of Pheromone Degrading Enzymes; and the Distribution and Behavioral Roles of SNMPS*. Insect Pheromone Biochemistry and Molecular Biology. Elsevier Academic Press, London.
- Wang, T., Jiao, Y., Montell, C., 2007. Dissection of the pathway required for generation of vitamin A and for *Drosophila* phototransduction. *J. Cell Biol.* 177, 305–316. <https://doi.org/10.1083/jcb.200610081>.
- Yew, J.Y., Chung, H., 2017. *Drosophila* as a holistic model for insect pheromone signaling and processing. *Curr Opin Insect Sci* 24, 15–20. <https://doi.org/10.1016/j.cois.2017.09.003>.
- Zacharuk, 1985. In: Kerkutt, G.A., Gilberts, L.S. (Eds.), *Antenna and Sensilla*. *Comprehensive Insect Physiology, Biochemistry and Pharmacology*. Pergamon, Oxford, pp. 1–69.
- Zhang, J., Walker, W.B., Wang, G., 2015. Pheromone reception in moths: from molecules to behaviors. *Prog. Mol. Biol. Transl. Sci.* 130, 109–128. <https://doi.org/10.1016/bs.pmbts.2014.11.005>.
- Zhao, L., Li, Y., Ding, Q., Li, Y., Chen, Y., Ruan, X.Z., 2021. CD36 senses dietary lipids and regulates lipids homeostasis in the intestine. *Front. Physiol.* 12, 669279 <https://doi.org/10.3389/fphys.2021.669279>.

Supplementary Data for Manuscript 3

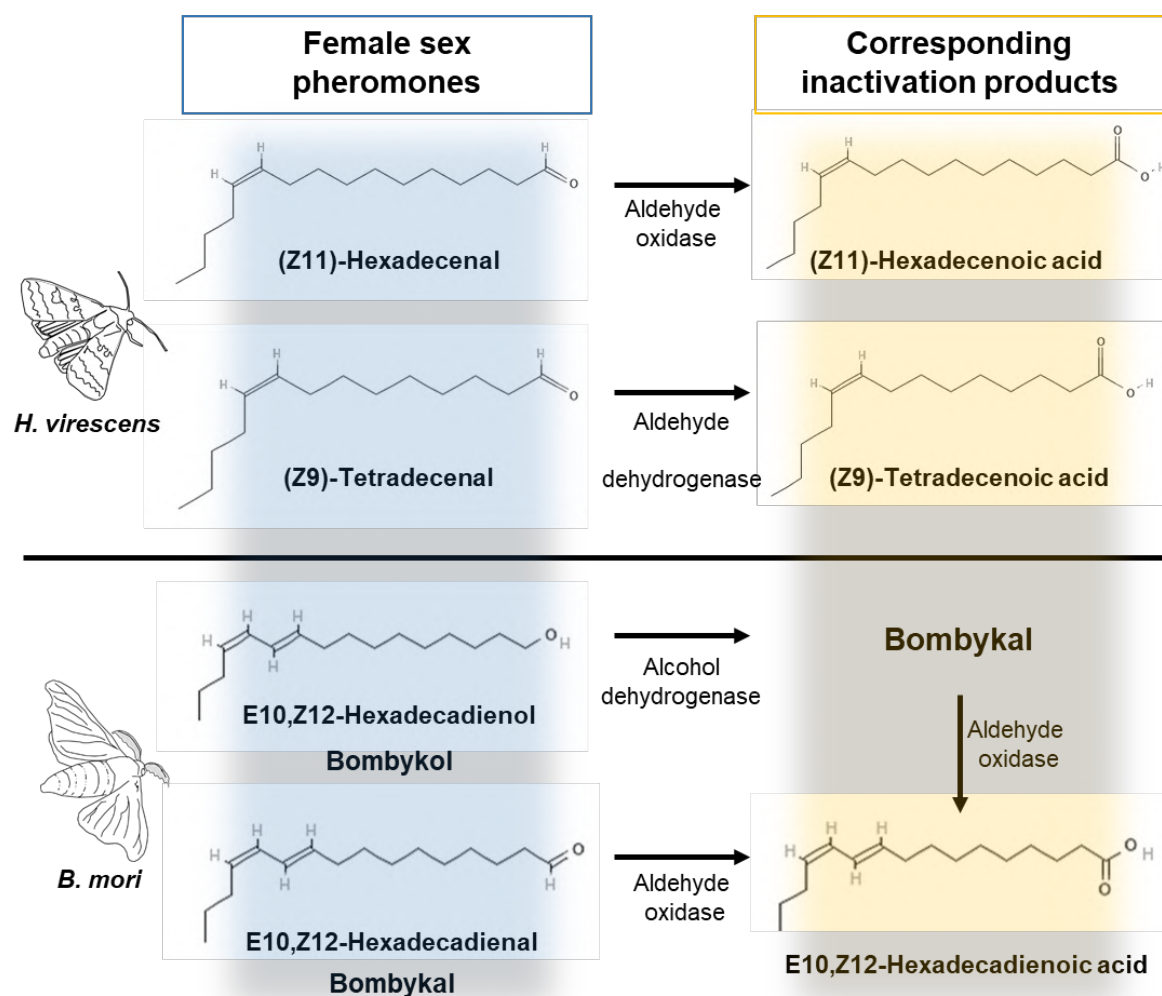


Fig. S1 Sex pheromone components of the moths *Heliothis virescens* and *Bombyx mori* and their respective inactivation products. The left side (blue) depicts the chemical structures of the main pheromone molecules. The right side (yellow) depicts the chemical structures of the long-chain fatty acid pheromone inactivation products resulting from conversion by the indicated odorant degrading enzymes.

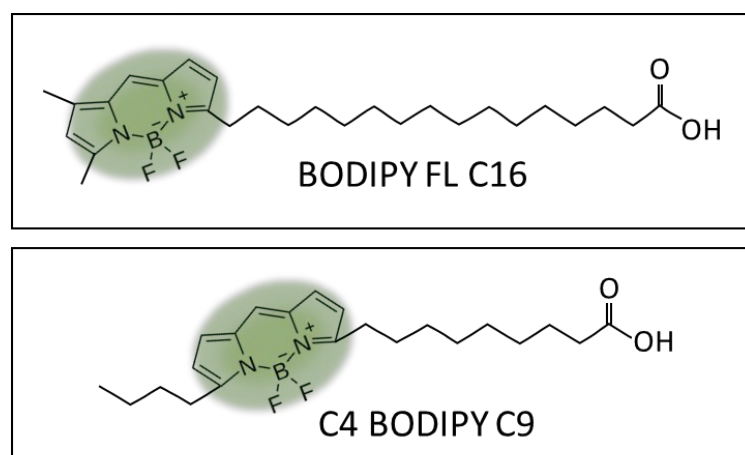


Fig. S2 Chemical structures of the fatty acid analogs used in the experiments. Green area indicates the position of the fluorophore BODIPY within the chain structures of BODIPY FL C16 (upper panel) and of C4-BODIPY-C9 (lower panel).

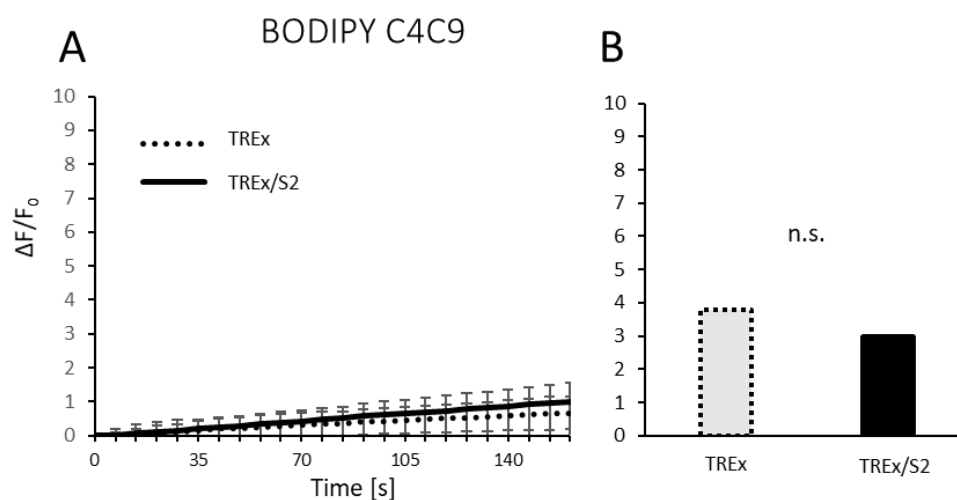


Fig. S3 SNMP2-expressing cells do show an increased cellular uptake of the fluorescent fatty acid analog BODIPY C4C9. **A** live cell imaging measurements of the fatty acid analog uptake in TReX and TReX/S2 cells. Images were taken in 7s increments after the application of 10 μ M BODIPY FL C16 using a 40x dry objective. The mean (\pm SD) relative changes in fluorescent intensity ($\Delta F/F_0$) in cells over time were calculated from five independent replicates with 25 randomly selected cells each using the LASx software. **B** relative change in fluorescent intensity of the TReX and TReX/S2 cells after 168s seconds. No significant differences (n.s.) were determined between the cell lines using an unpaired T-test

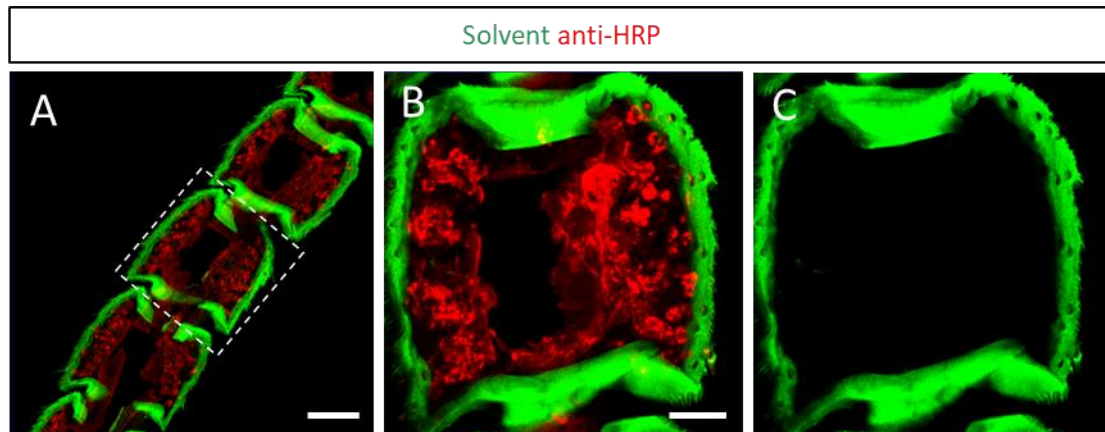


Fig. S4 Assessment of background fluorescence (green) in antenna of *H. virescens* incubated in the solvent DMSO used for solubilization of BODIPY FL C16 prior to sectioning and counterstaining with anti-HRP (red) to visualize neurons. **A** different antennal segments showed only neuronal staining. Overlay of the red and green channels. **B-C** higher magnification of the boxed region in A. **B** overlay of the red and green channels. **C** only green channel showing no intrinsic fluorescence of antennal cells. Scale bars: A = 50 μm , B = 20 μm .

Chapter 5. Discussion

In the scope of this thesis, the roles of SNMPs in insect olfaction were assessed with different approaches and under various aspects. The investigations revealed a sensillum-type and cell-type specific expression of the SNMP1 and SNMP2 proteins as well as their subcellular localization in the antenna of adult *Schistocerca gregaria* and during locust development suggesting specific functions of the two SNMP-types in OSNs and support cells of locust sensilla (**Manuscript 1** and **Manuscript 2**). Uncovering the localization of SNMP types serves as an important prerequisite for targeted functional investigations. Such investigations were conducted for the support cell-expressed SNMP2 of the moths *Heliothis virescens* and *Bombyx mori* in **Manuscript 3** and provided first evidence that support cells and SNMP2 proteins may be involved in sensillum lymph homeostasis through the removal of lipophilic "waste products" such as fatty acids resulting from the inactivation of sex pheromones.

5.1 Expression topography of SNMPs in locusts

Despite there being comprehensive data regarding the antennal distribution and cell-specific expression of the SNMPs in holometabolous insects such as in moths and flies, little is known about the localization of the proteins in hemimetabolous insects, such as locusts. Therefore, in Manuscript 1, the antennal expression topography and subcellular localization of SNMP1- and SNMP2-proteins of adult *S. gregaria* were comprehensively examined using newly generated SNMP type-specific antibodies targeting the ectodomains of the respective proteins. In addition, the developmental expression and distribution of the SNMP proteins was addressed by investigating the 1st, 3rd and 5th instar nymphs (Manuscript 2).

5.1.1 SNMP1 expression and function in olfactory sensory neurons

The SNMP1 expression was first assessed by performing fluorescence immunohistochemistry (FIHC) on antennal sections of adult *S. gregaria* (Manuscript 1). This revealed that the protein is found in a considerable number of OSNs and their dendrites of trichoid and basiconic sensilla along the antenna. The dendritic labelling of SNMP1 was corroborated through immunogold labelling experiments, where the protein was detected in a subset of dendritic structures within the basiconic sensillum lumen. Furthermore, in the adult antenna, anti-SNMP1 immune reactivity coincided with the labelling of ORco-positive OSNs including their dendrites. These findings are in line with previous results visualizing SNMP1 transcripts by fluorescence *in situ* hybridization (FISH) in subsets of OR-expressing OSNs in these sensillum types (Jiang et al., 2016). The SNMP1 protein was not detected in OSNs innervating coeloconic sensilla, which in *S. gregaria* have been noted to

express IRs (Guo et al., 2013). Correspondingly, SNMP1 in other insects, such as *D. melanogaster* (Benton et al., 2007) and *M. mediator* (Shan et al., 2020), was found co-expressed with ORs and not with IRs. Thus, the generated results from the locust further validate that the SNMP1 subtype in insects is confined to OSNs expressing olfactory receptors of the OR family.

When further exploring the sensillum-specific distribution using the anti-SNMP1 antibody on antennal sections of adult *S. gregaria*, it was revealed that all OSNs innervating trichoid sensilla were positive for SNMP1. Similar results were obtained for *Locusta migratoria*, suggesting that all OSNs in locust trichoid sensilla rely on SNMP1 for the appropriate detection of odorants. Expression of the SNMP1 subtype in all OSNs of trichoid sensilla was also reported in some other insects, for instance in *D. melanogaster* (Benton et al., 2007) and in female *H. virescens* moths (Zielonka et al., 2018; Blankenburg et al., 2019). Noteworthy, in males of *H. virescens*, only a single OSN of the generally two to three OSNs innervating the trichoid sensillum is positive for SNMP1 (Blankenburg et al., 2019), demonstrating that SNMP1 expression is not generally associated with all OSNs of trichoid sensilla. In the fly and in moth species, various studies demonstrated that SNMP1-positive OSNs of trichoid sensilla sensitively detect pheromones and that SNMP1 is required for proper odor sensing (Pregitzer et al., 2014; Liu et al., 2020; Gomez-Diaz et al., 2016; Li et al., 2014). In this regard, it is possible that at least some SNMP1-expressing OSNs of locust trichoid sensilla are responsive to pheromones. Indeed, early single sensillum recoding (SSR) conducted on *S. gregaria* trichoid sensilla have demonstrated their responsiveness to a putative sex pheromone component (Ochieng and Hansson, 1999).

In contrast to the trichoid sensilla, only subsets of OSNs were labelled by the anti-SNMP1 antibody in basiconic sensilla. The same sensillum-specific pattern was also observed in the antenna of the migratory locust, *L. migratoria*, indicating that the SNMP1 expression topography in OSNs is conserved across various locust species. These findings also highlight that in locusts, only a fraction of the basiconic OSNs appears to rely on SNMP1 for the proper detection of odorants. In support of this concept, previous *in situ* hybridization studies on the *S. gregaria* antenna have uncovered that out of 83 ORs localized to basiconic OSNs, only 30 ORs were co-expressed with SNMP1 in the same OSN (Pregitzer et al., 2017; Pregitzer et al., 2019). In addition, SSR recordings of basiconic sensilla in *L. migratoria* revealed responses to a variety of odorants, including plant-derived volatiles, nymphal body odors and pheromones, such as the pheromones 4-vinylanisole (4VA) and phenylacetoneitrile (PAN) (Ochieng and Hansson, 1999; Chen et al., 2022a; Chang et al., 2023). Altogether, this demonstrates that in locusts a combination of SNMP1-dependent and SNMP1-independent OSNs exists in basiconic sensilla both of which are necessary to accommodate for the detection of a large spectrum of behaviorally relevant odorants.

Considering the expansive expression topography of SNMP1 in populations of trichoid and basiconic OSNs and the co-expression with a large number of different ORs, it is conceivable that in locusts, SNMP1-positive OSNs may serve a dual purpose. They may contribute to the sensitive detection of pheromones and, in addition, to behaviorally relevant general odorants, indicating for example food sources or appropriate oviposition sites. In line with this notion, SNMP1 is expressed in all trichoid OSNs in *S. gregaria* (Manuscript 1) with some OSNs indicated to respond to pheromone components (Ochieng and Hansson, 1999). While in *L. migratoria*, where SNMP1 is also expressed in all OSNs innervating the trichoid sensillum (Manuscript 1), distinct trichoid OSNs express the receptor type OR3, which recognizes various non-pheromone ligands (You et al., 2016). Moreover, electrophysiological recordings from trichoid sensilla of *L. migratoria* demonstrated OSN responsiveness to fecal volatiles as opposed to tested putative sex pheromones (Cui et al., 2011). A role beyond pheromone detection is also supported from studies on *D. melanogaster* SNMP1, which was shown to be necessary for the detection of the pheromone cVA (Benton et al., 2007; Gomez-Diaz et al., 2016) as well as the plant volatile Farnesol (Ronderos et al., 2014) by different trichoid OSN populations. However, in locusts, the overall extent of how SNMP1 contributes to the detection of pheromonal and non-pheromonal compounds remains largely unknown.

Since locusts are hemimetabolous insects, their antennae undergo a successive development, with little morphological differences observed in the general structure. However, it is unclear if the cell- and sensillum-specific SNMP1 expression pattern observed in adult *S. gregaria* is similar in larval stages and remains conserved throughout its development. Therefore, a characterization of the SNMP1 expression pattern in the antenna of juvenile stages of *S. gregaria* was addressed (Manuscript 2).

Firstly, the outer morphology of the antennal sensilla structures of adults, fifth instar nymphs and first instar nymphs were assessed, to determine if there are any distinctions between the olfactory sensilla of the different stages. The trichoid, basiconic and coeloconic sensilla showed no obvious morphological differences throughout their development, indicating that from the first instar stage onwards, the defining morphology of the olfactory units does not undergo any major restructuring. No development changes in the morphology of the olfactory sensilla were also observed for the locust species, *Schistocerca americana* (Chapman, 2002) and *L. migratoria* (Chapman and Greenwood, 1986), which altogether supports the notion that in locusts, the sensillum shape and repertoire is already established in freshly hatched nymphs and remains the same until the adult stage. The only notable difference between the developmental stages in locusts is reflected in the total number of olfactory sensilla, as the quantity of each olfactory sensillum type increases with each molt (Ochieng et al., 1998).

Analysis of the antennal distribution of SNMP1 in the 1st, 3rd and 5th instar nymphs in FIHC experiments revealed numerous anti-SNMP1 positive OSNs. When assessing the sensillum-specific distribution of SNMP1, it became evident that like in the adult antenna, all OSNs innervating the trichoid sensilla are SNMP1-positive while no SNMP1-expressing OSNs are housed in the coeloconic sensilla. In addition, SNMP1 is expressed in only a subset of basiconic OSNs, corroborating SNMP1-dependent and SNMP1-independent olfactory detection mechanisms in the developing antenna for this sensillum type.

Given the proposed co-receptor function of SNMP1 and its requirement for sensitive pheromone detection in OSNs of adult insects, it is conceivable that younger locust developmental stages also rely on OSN-expressed SNMP1 for the proper detection of behaviorally relevant odors. In this regard, analysis of the larval antenna of the moth *H. virescens* revealed sensilla with OSNs responsive to the minor sex pheromone component Z9:14Ald, and found co-expression of SNMP1 with the receptor HR6 tuned to Z9:14Ald (Zielonka et al., 2016). Moreover, electrophysiological recordings of basiconic sensilla on the antenna of *L. migratoria* nymphs revealed OSN responsiveness to PAN mediated by the receptor OR70 (Chang et al., 2023). Another study showed that basiconic sensilla of all *L. migratoria* developmental stages respond to the 4VA detected by OR35 (Chen et al., 2022a). However, co-expression of these locust pheromone receptors with SNMP1 has not been analyzed. In addition, given SNMP1's broad expression in numerous OSNs along the nymph antenna, it is possible that similar to adults, not all SNMP1-positive OSNs in the nymph stages are dedicated to the detection of pheromones.

5.1.2 SNMP1 and SNMP2 expression in non-neuronal support cells

A new revelation that emerged in both adult and larval stages (Manuscripts 1 and 2) was that in locusts, expression of the SNMP1 subtype was not restricted to OSNs as anti-SNMP1 immune reactivity was also detected in support cells. These findings seem to be in contradiction to a previous *in situ* hybridization study, which detected SNMP1 only in OSNs of the *S. gregaria* antenna (Jiang et al., 2016). However, this discrepancy could possibly be explained due to a lack of a neuronal counter stain in the *in situ* hybridization study, making it difficult to accurately characterize the expression in OSNs and non-neuronal support cells. To test if the visualization of SNMP1 in support cells was not due to unspecific labelling by the primary antibody, additional control experiments were conducted by applying an antisense SgreSNMP1 riboprobe and a neuronal marker in a combined *in situ* hybridization/FIHC experiment (Manuscript 1). The results clearly confirmed the expression of SNMP1 in non-neuronal support cells.

Similar to its neuronal expression, the SNMP1 expression in support cells showed a sensillum specific pattern in *S. gregaria* adults and nymphs as well as in adult *L. migratoria*. SNMP1 expression in support cells strictly correlated with the presence of SNMP1-positive OSNs in the trichoid and basiconic sensilla. In other words, if there were SNMP1 positive OSNs in a sensillum, there were also SNMP1 positive support cells. A similar situation was observed in *D. melanogaster* where SNMP1-positive support cells were associated with SNMP1-positive OSNs in trichoid sensilla (Benton et al., 2007). Remarkably, in SNMP1-deficient fruit flies, rescue of SNMP1 in OSNs was sufficient to reestablish sensitive responsiveness to the pheromone cVA, whereas the rescue of SNMP1 in only the support cells did not result in the reinstated sensitive phenotype (Benton et al., 2007). Altogether, this implies that in flies and locusts, the SNMP1 subtype can play different roles in olfaction, depending on its cell-specific expression. This greatly differs to moths, where SNMP1-expression was shown to be restricted to OSNs of trichoid sensilla, indicating that moth SNMP1 has adapted a more specialized role in the olfactory system i. e. in the detection of odorants such as sex pheromones (Zhang et al., 2015a; Jiang et al., 2016; Blankenburg et al., 2019; Sun et al., 2019).

Compared to SNMP1, *S. gregaria* SNMP2 expression in the antenna of adults was only detected in the non-neuronal support cells (Manuscript 1). Additionally, the SNMP2 type expression pattern is established early i. e. the first nymphal stage and is retained throughout development (Manuscript 2). Immunohistochemistry experiments localized the SNMP2 protein in support cells of the two most abundant sensillum types: the basiconic and coeloconic sensilla (Manuscripts 1 and 2). Although no double labelling experiments were conducted to assess a possible co-expression of both SNMP subtypes in the same cells of the basiconic sensillum, a previous study in *S. gregaria* demonstrated a differential expression pattern of SNMP1 and SNMP2 through double *in situ* hybridization experiments, indicating that they are expressed in different cells (Jiang et al., 2016).

In the immunohistochemistry experiments of this thesis with the SNMP2 specific antibody (Manuscripts 1 and 2), no SNMP2 protein was detected in cells housed in trichoid sensilla. However, whether this is in fact due to the absence of SNMP2 in support cells of locust trichoid sensilla or possibly due to SNMP2 protein levels below the antibody detection limit remains uncertain. In this context, it is worth mentioning that the SNMP1 protein appears strikingly abundant in the trichoid support cells. It is therefore possible that in the trichoid sensilla, the support cells have replaced SNMP2 with SNMP1, where it may fulfil a function similar to SNMP2 of the basiconic and coeloconic support cells.

In accordance with the notion that in support cells SNMP1 and SNMP2 may perform analogous functions, both proteins were localized in the microvilli membranes of the support cells in

immunogold labelling experiments (Manuscript 1). These microvilli membranes are found on the apical most side of the support cells at the direct interface to the sensillum lymph, which are considered regions of high transmembrane transport (Steinbrecht and Gnatzy, 1984). A previous study conducted on the moth *A. ipsilon* localized SNMP1 and SNMP2 within the sensillum's structure through immunogold labelling experiments, however, the specific subcellular localization of the non-neuronal SNMP2 could not be clarified (Gu et al., 2013). In prior FHC experiments conducted on the antenna of the moth *H. virescens*, SNMP2 expression was also located on the apical pole of support cells facing the sensillum lymph (Blankenburg et al., 2019), indicating a conserved function of support cell SNMPs across different insect taxa. Thus, based on the subcellular localization of support cell-expressed SNMPs in the microvilli as well as their categorization into the CD36 family of lipid receptors and transporters, it has been suggested that the proteins might play an important role in the sensillum lymph maintenance processes (Forstner et al., 2008). This will be discussed more thoroughly in the upcoming chapter.

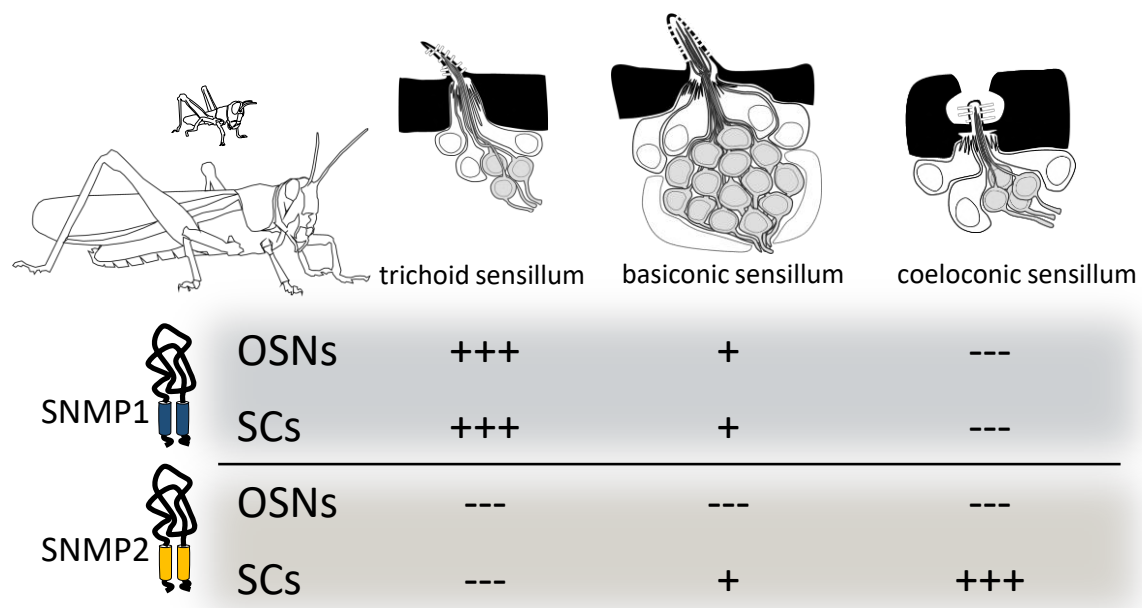


Figure 8. Depiction of the cell- and sensillum type-specific expression of SNMP1 and SNMP2 in the locust *S. gregaria*. The expression topography of the two SNMP subtypes remains consistent throughout the locust's development, from the first nymph stage until the adult stage. The organization of the three different olfactory sensilla (trichoid, basiconic and coeloconic) is shown at the top. The upper panel (blue) denotes the expression pattern for SNMP1. The lower panel (yellow) denotes the expression for SNMP2. + indicates the presence of the protein in a subset of cells. +++ indicates the presence of the protein in all cells. --- indicates no protein detected.

Overall, the findings of Manuscript 1 and Manuscript 2 establish that the distribution of both SNMP1 and SNMP2 is comparable across all developmental stages and indicates that the

hemimetabolous locusts strongly rely on both SNMP types beginning from the first nymphal stage onwards. Although SNMP1 in larval antennae of holometabolous *H. virescens* has been documented, the larvae possess a drastically different olfactory system and SNMP expression topography compared to adults, as in larvae SNMP1 is expressed in OSNs of the B1, B2 and B3 sensilla (Zielonka et al., 2016), while in adults, it is expressed in OSNs of the trichoid sensilla (Zielonka et al., 2018; Blankenburg et al., 2019). In contrast, the expression patterns of both SNMP types in the 1st, 3rd, and 5th instar nymphs of the hemimetabolous *S. gregaria* matched that of the adults very closely (Manuscript 1, Manuscript 2). Whether or not the nymphal stages rely on SNMPs in the exact same contexts as the adult locusts is unclear. Perhaps the similarities in the locust SNMP expression topography could implicate a certain degree of overlap in the odors to which nymph and adult locusts are exposed to, as different developmental stages appear at the same time in the same environment (Peng et al., 2020).

In summary, a unique cell- and sensillum-specific expression pattern attributed to each SNMP subtype has emerged in locusts. SNMP1 was found in OSNs and support cells of the trichoid and basiconic sensilla, while SNMP2 was found only in the support cells of the basiconic and coeloconic sensilla. This is in contrast to the differential tissue expression observed in moths, where SNMP1 expression is restricted to OSNs of the pheromone sensitive trichoid sensilla, while SNMP2 was found in countless support cells of various olfactory sensilla (Forstner et al., 2008; Blankenburg et al., 2019). Furthermore, the detailed immunogold labelling of both SgreSNMP1 and SgreSNMP2 in the microvilli of the basiconic support cells represent the first clear localization of SNMPs in these subcellular structures.

5.2 The roles of SNMP2 and support cells in sensillum lymph clearance

Most of what is known about the functions of insect SNMPs is based on studies that addressed the OSN-expressed SNMP1 type. Investigations, mainly carried out on SNMP1 of *D. melanogaster* and a few lepidopteran species, including *H. virescens* and *Helicoverpa armigera*, uncovered SNMP1 as a crucial olfactory protein contributing to the rapid and sensitive detection to sex pheromones (Pregitzer et al., 2014; Li et al., 2014; Gomez-Diaz et al., 2016; Benton et al., 2007). The current data suggest a model where SNMP1 in the dendrites of OSNs acts as a co-receptor that takes over lipophilic odorants from OBPs and transfers the signal molecules via its large tunnel-like ectodomain towards an adjacent OR_x/ORco complex (Gomez-Diaz et al., 2016; Benton et al., 2007; German et al., 2013). Yet in comparison to the neuronal SNMP1, relatively little is known about the

non-neuronal support cell-expressed SNMP2 type, with no functional investigations having been conducted to date. Therefore, using moths as a model, since their antenna show a clear differential expression of SNMP1 and SNMP2 in OSNs and support cells, respectively, a possible role of SNMP2 in previously proposed clearance processes, i. e. the elimination of lipophilic “waste products” from the sensillum lymph of olfactory sensilla (Forstner et al., 2008), was assessed (Manuscript 3).

In many moth species, including *H. virescens* and *B. mori*, such “waste products” stem from the inactivation of aliphatic unsaturated long-chain alcohol or aldehyde sex pheromone components into the corresponding long-chain fatty acids, a process that is catalyzed by ODEs in the sensillum lymph (Kasang and Weiss, 1974; Rybczynski et al., 1990; Tasayco and Prestwich, 1990; Pelletier et al., 2007). The swift inactivation of the pheromone molecules and fast removal of their inactivation products out of the sensillum lymph maintains perireceptor events in the olfactory sensilla and assures the efficient temporal resolution of OSNs to upcoming stimuli (Vogt and Riddiford, 1981; Durand et al., 2011; Pelletier et al., 2023). Although earlier studies have attempted to track odorants once they enter the sensillum lymph by using radioactive labelled pheromones, the appearance of radioactivity in the distinct cells of a sensillum was not examined and thus, the fate of the odorants and their inactivation products remained uncertain (Kasang, 1974; Kanaujia and Kaissling, 1985).

Manuscript 3 approaches the role of moth SNMP2 and support cells in the removal of such “waste products” due to its localization in support cell microvilli (Manuscript 1) as well as its membership to the CD36 family of lipid transporters (Rogers et al., 1997; Blankenburg et al., 2019). The live cell imaging experiments conducted with the HvirSNMP2-expressing cell line demonstrated that SNMP2 mediates a rapid and increased uptake of the long-chain fatty acid analog BODIPY FL C16 into cells in a concentration dependent manner (Manuscript 3). No increase in uptake was observed when testing another long-chain fatty acid analog, BODIPY C4C9, indicating a degree of ligand specificity for HvirSNMP2. These results indicate that moth SNMP2 resembles the functions of mammalian CD36 proteins, which have been noted to drive the cellular uptake of certain long-chain fatty acids as well as rapidly facilitate the internalization of lipids (Abumrad et al., 1993; Koonen et al., 2005; Drover et al., 2008; Pepino et al., 2014; Glatz and Luiken, 2018; Glatz et al., 2022). Correspondingly, NinaD and Santa Maria that represent non-SNMP members of the insect-specific CD36 family facilitate the cellular uptake of carotenoids (Giovannucci and Stephenson, 1999; Kiefer et al., 2002; Wang et al., 2007). Therefore, the cellular uptake of lipid compounds enabled by SNMP2 corresponds to the distinctive function of CD36 family members in the transmembrane transport of lipids.

In support of a functional similarity, the known CD36 inhibitor SSO led to an abolished uptake of BODIPY FL C16 in the HvirSNMP2-expressing cell line (Manuscript 3). In experiments conducted with mammalian CD36, the inhibitor SSO was shown to bind to a distinct lysine in the apical part of the large ectodomains, which interacts with the carboxyl group of long-chain fatty acids, leading to the attenuated CD36-mediated fatty acid uptake (Harmon and Abumrad, 1993; Pepino et al., 2014; Kuda et al., 2013). Interestingly, a recent phylogenetic and protein structure analysis revealed that the apex of CD36 proteins determines its ligand specificity and interaction, and suggested that altering the apical region of the protein can result in the failed binding and transport of lipid ligands (Boohar et al., 2023). Although it remains uncertain how SSO affects the function of SNMP2, the inhibition experiments have clearly demonstrated that SSO is not only an inhibitor to mammalian CD36 but also to the insect-specific SNMP2 proteins.

How long-chain fatty acids are internalized into cells via SNMP2 is unclear. Members of the CD36 protein family have been described to take up extracellular fatty acids in different mechanisms. One model proposes that mammalian CD36 proteins integrate long-chain fatty acids directly into the cell membrane, to facilitate the rapid transport of the fatty acids into the cell via diffusion (Jay et al., 2020). Another study suggested that upon binding of a fatty acid ligand onto the CD36 ectodomain, conformational changes are initiated, allowing the direct entrance of the fatty acids into the cell somata via the tunnel in the protein's ectodomain (Pepino et al., 2014). More recently, a study determined fatty acids remain bound to CD36, which are both internalized in vesicles via endocytosis (Hao et al., 2020). Thus, multiple pathways have been described for the CD36-mediated uptake of lipids.

Assessing the distribution of SNMP2 in the antennae of the moths *H. virescens* and *B. mori* exposed its broad expression in the non-neuronal support cells found at the base of the olfactory sensilla. Although the primary focus of Manuscript 3 was on assessing the role of SNMP2 in the potential clearance of female sex pheromone inactivation products in moths, it is possible that SNMP2's function may extend further, including the clearance of general odorant inactivation products or lipophilic compounds that have entered a sensillum accidentally. Moreover, as SNMP2 is expressed in support cells of both sexes (Blankenburg et al., 2019; Gu et al., 2013; Sun et al., 2019), it is possible that the protein might drive the removal of lipophilic molecules of not just pheromone-sensitive sensilla but also of sensilla tuned to general odorants in both male and female moths.

When treating the intact antennae of male *H. virescens* and *B. mori* with the long-chain BODIPY FL C16-fatty acid analog, it was found that in both species, the support cells previously shown to express SNMP2, absorbed the analog. This suggests that the SNMP2 proteins in different moth species possess an overlapping, possibly broad ligand spectrum. However, to elucidate the

selectivity of SNMP2s from different species, additional uptake assays with multiple lipophilic ligands should be performed. With respect to selectivity, in many cases, individual CD36 family members are involved in multifunctional processes and have been noted to possess a broad ligand spectrum, ranging from diverse long-chain fatty acids to other lipids of different moieties, which are often derived from fatty acids (Silverstein and Febbraio, 2009; Martin et al., 2011; Abumrad and Goldberg, 2016; Zhao et al., 2021; Jimenez-Dalmaroni et al., 2009; Chen et al., 2022b).

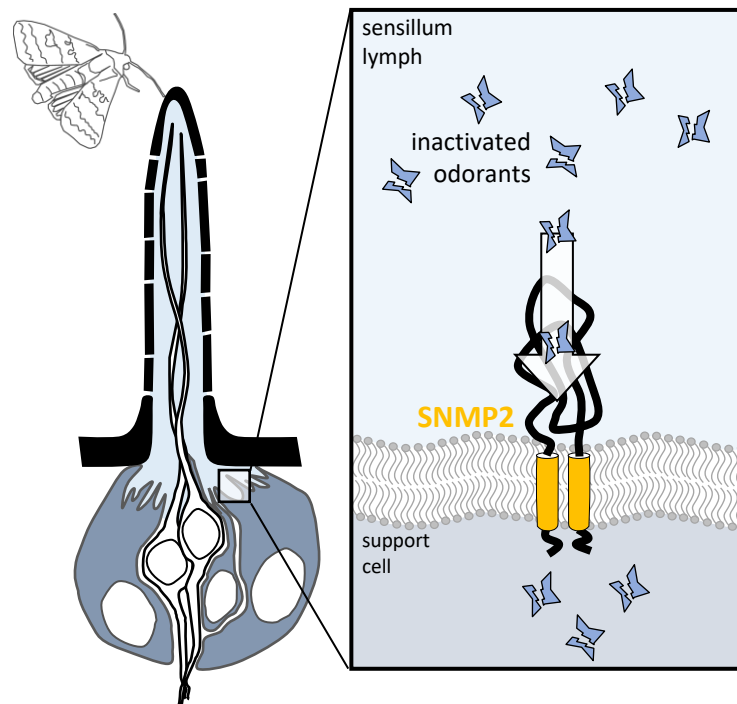


Figure 9. Proposed model for SNMP2's role in mediating the uptake of lipophilic inactivated odorants from the sensillum lymph into support cells in moths. The SNMP2 protein, located at the apical side of the support cells facing the sensillum lymph, translocates extracellular long-chain fatty acids, stemming from pheromone inactivation by ODEs, via its ectodomain into the support cell somata. The efficient and rapid clearance of such “waste products” from the sensillum lymph aids in the maintenance of the sensillum for proper odor detection.

Overall, the *in vivo* data presented in Manuscript 3 speak for a function of antennal SNMP2 proteins in support cells in the maintenance of the sensillum by removing excess long-chain fatty acids from the sensillum lymph into support cells (Figure 9). This likely takes place at the microvilli structures at the apical side at the direct border to the sensillum lymph (Keil, 1989; Gnatzy et al., 1984), which are commonly noted as sites of high exchange across cell membranes (Houdusse and Titus, 2021; Sharkova et al., 2023). Therefore, in addition to secreting proteins and ions (Thurm and Küppers, 1980), support cells of olfactory sensilla may control the sensillum lymph homeostasis by also clearing molecules which could potentially modify the sensillum lymph composition and could impair the overall function of the olfactory unit. Such a clearance function might be a general property of support cells in chemosensory sensilla as support cells of dye-infiltrated gustatory

sensilla on the maxillary palps of the cockroach, absorbed the substance and cleared the sensillum lymph (Seidl, 1992).

In the antennal BODIPY FL C16-fatty acid analog uptake assays, the fluorescent signals often accumulated in dotted patterns within the support cells of *H. virescens* and *B. mori* (Manuscript 3). This suggests that in support cells of the olfactory sensilla, lipophilic compounds, which enter the cells, could end up in vesicles and subsequently in lipid droplets. Similarly, in mammalian adipocytes, CD36-dependent uptake of fatty acids appeared to involve dynamic endocytosis activity, leading to the formation of vesicles and lipid droplets (Hao et al., 2020).

The pretreatment of the antenna with the CD36-inhibitor SSO prior to the fatty acid uptake assay resulted in the reduced absorption of BODIPY FL C16 into support cells, comparable to the reduced uptake observed in the SSO pretreated HvirSNMP2 cell culture line (Manuscript 3). Remarkably, the lumen of the SSO-pretreated sensilla showed strong fluorescent signals compared to the lumen of untreated sensilla indicating that the sensillum lymph of SSO-treated sensilla was not cleared of the fatty acid analog. These results indicate that an SSO-evoked interference of support cell performance can lead to an accumulation of fatty acids in the perireceptor space. However, it remains to be investigated whether this is a direct result of SSO binding to the SNMP2 proteins of the support cells.

Given that SSO affected the clearance of the long-chain fatty acid analog, it was conceivable that SSO might also affect the clearance of moth sex pheromone inactivation products resulting from ODE activity. Consequently, this would lead to their accumulation in the sensillum lymph thus affecting the proper function of the olfactory unit and ultimately, the response of sex pheromone-driven behavior. Therefore, the effect of antennal SSO treatment on pheromone-induced behavior in male *B. mori* was tested (Manuscript 3). *B. mori* males respond sensitively to female sex pheromones by fluttering their wings. This behavior was considerably prolonged by SSO treatment of the antenna compared to mock-treated males. The result showed that SSO treatment has a profound impact on the sex pheromone response of male *B. mori* possibly by inhibiting the SNMP2-mediated clearance of fatty acid sex pheromone inactivation products that could inhibit ODE activity. Notably, previous studies showed that hindering any part of ODE activity leads to prolonged olfactory responses (Chertemps et al., 2012; Fraichard et al., 2020) and indeed, rapid pheromone inactivation plays an important role in the temporal resolution of the sensillum (Vogt et al., 1985; Ishida and Leal, 2005), suggesting that overall, the inadequate removal of odorants can influence odor-guided behavior.

The full extent of SNMP2's functional mechanism in the antenna is unclear as it might be possible that SNMP2 expressed in the moth antenna drives the cellular uptake of fatty acids in tandem with other support cell-expressed proteins. While in cell culture experiments, HvirSNMP2 was shown capable of transporting fatty acids without any other antennal proteins, it is possible that in support cells SNMP2 acts in concert with other proteins. In fact, mammalian members of the CD36 family involved in long-chain fatty acid uptake processes interact with so-called fatty acid transport proteins and fatty acid binding proteins to facilitate the proper transport of fatty acids across the cell membrane (Bonen et al., 1999; Chabowski et al., 2007). However, studies have also shown that mammalian CD36 proteins alone are sufficient in mediating the uptake of fatty acids and cellular lipid homeostasis (Glatz et al., 2022; Silverstein and Febbraio, 2009). Indeed, the detailed mechanisms of CD36-facilitated long-chain fatty acid uptake is still debated (Glatz and Luiken, 2018). In this regard future investigations on the SNMP2-interactome, by means of co-immunoprecipitation, co-expression studies or structure-based prediction approaches (Rao et al., 2014), can give more insights into how sensillum lymph "waste products" are removed.

The functional studies on moths have provided first functional data regarding SNMP2's role in olfaction and demonstrated that support cells are not only able to secrete substances, but also absorb them from the sensillum lymph. It is conceivable that antennal support cells and SNMP2 orthologs found in different insect orders may also be involved in sensillum lymph clearance processes. In support of this notion, the immunogold labelling experiments on the locust antenna found SgreSNMP2 localized in the microvilli structures that have extensive contact to the basiconic sensillum lumen (Manuscript 1). In addition, SgreSNMP2 was detected in support cells of coeloconic sensilla, which, unlike basiconic sensilla, are typically innervated by IR-expressing instead of OR-expressing OSNs (Guo et al., 2013). This indicates that SNMP2 in the microvilli membrane of support cells may be integral for translocating a very broad spectrum of general lipophilic odorants, pheromones or their inactivation products out of the sensillum lymph, regardless of the sensillum's molecular equipment.

Interestingly, in locusts, the SNMP1 subtype was also localized in the microvilli of the support cells. Therefore, it is plausible that locust SNMP1 in support cells may serve a similar function to SNMP2 i.e. in the removal of "waste products" such as extracellular lipophilic molecules. Though no such role has yet been described for SNMP1 in the olfactory system of insects, in *D. melanogaster* prothoracic gland cells, SNMP1 was identified to drive the uptake of lipids, necessary for the synthesis of ecdysone. In fact, knocking down SNMP1 in the prothoracic gland led to a reduced lipid droplet content in the cells with lipid storage being rescued when SNMP1 is overexpressed (Talamillo et al., 2013).

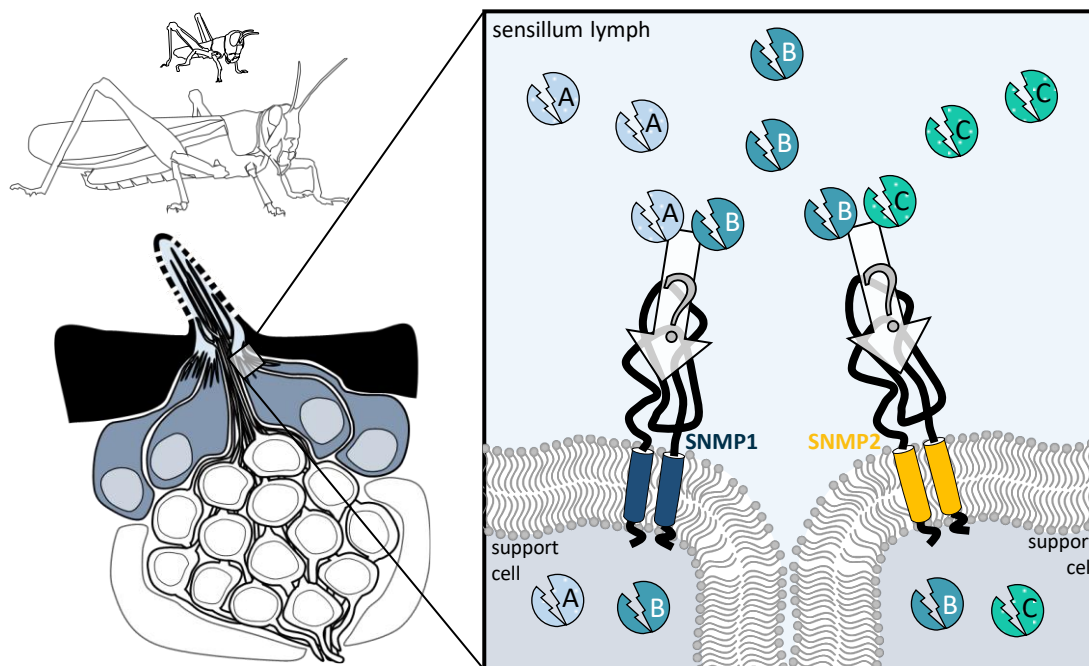


Figure 10. Proposed model of the contribution of the non-neuronal SNMPs in sensillum lymph clearance processes in basiconic sensilla of nymph and adult locusts. SgreSNMP1 and SgreSNMP2 are localized in the apical microvilli membranes of different support cells bordering the basiconic sensillum lumen. The different support cells might possess specific ligand spectra according to the SNMP type they express. SNMP1 in support cells could mediate the uptake of given inactive odorants (A) detected by SNMP1-positive OSNs. SNMP2 in support cells could mediate the uptake of other inactive odorants (C) detected by SNMP1-independent OSNs. Some of the inactive “waste products” (B) could be translocated by both SNMP1 and SNMP2 into support cells.

Considering that SgreSNMP1 and SgreSNMP2 are found in different populations of support cells in the locust antenna (Manuscript 1, Jiang et al., 2016), their ligand spectra might also differ and they could remove different substances from the sensillum lymph. In this context, only SNMP1-expressing support cells were found in trichoid sensilla where all OSNs express SNMP1. Thus, it is possible that the non-neuronal SNMP1 in support cells is specifically adapted to the removal of inactivated odorants previously detected by ORs in SNMP1 co-expressing OSNs. Similarly, in basiconic sensilla, comprising SNMP1-positive and -negative OSN-populations, the SNMP1 and SNMP2 in support cells may be adapted to the respective inactivation products of odorants detected by SNMP1-coexpressed ORs and non-SNMP1-coexpressed ORs. However, this does not exclude the possibility that certain inactivation products might be transported by both SNMP1 and SNMP2 in the locust basiconic sensillum. Either way, the presence of both SNMP subtypes in the support cells might aid in the efficient and rapid removal of specific substances from the sensillum lumen of the basiconic sensilla, as depicted in Figure 10. However, such a model explaining the

existence of two different SNMP subtypes in locust support cells must be proven by future functional investigations.

In conclusion, the data presented in this thesis suggest that in insects, non-neuronal SNMPs may play an essential role in the uptake of extracellular long-chain fatty acids from the sensillum lymph into support cells. The proper function of the SNMP2 proteins in the antenna could be necessary to avoid the overstimulation of OSNs by the same odorants. By mediating the removal of long-chain fatty acids stemming from inactivation products, SNMP2-positive support cells could facilitate the rapid reset of the perireceptor space in preparation for incoming odorants, thus maintaining an overall high temporal resolution of the olfactory system.

References

- Abumrad, N.A., El-Maghrabi, M.R., Amri, E.Z., Lopez, E. and Grimaldi, P.A., 1993. Cloning of a rat adipocyte membrane protein implicated in binding or transport of long-chain fatty acids that is induced during preadipocyte differentiation. Homology with human CD36. *J Biol Chem.* 268, 17665-8. 10.1016/S0021-9258(17)46753-6.
- Abumrad, N.A. and Goldberg, I.J., 2016. CD36 actions in the heart: Lipids, calcium, inflammation, repair and more? *Biochim Biophys Acta.* 1861, 1442-9. 10.1016/j.bbalip.2016.03.015.
- Ai, H. and Kanzaki, R., 2004. Modular organization of the silkworm antennal lobe macroglomerular complex revealed by voltage-sensitive dye imaging. *J. Exp. Biol.* 207, 633-644. 10.1242/jeb.00784.
- Almaas, T.J. and Mustaparta, H., 1990. Pheromone reception in tobacco budworm moth, *Heliothis virescens*. *J. Chem. Ecol.* 16, 1331-1347. 10.1007/BF01021030.
- Almaas, T.J. and Mustaparta, H., 1991. *Heliothis virescens*: Response characteristics of receptor neurons in sensilla trichodea type 1 and type 2. *J. Chem. Ecol.* 17, 953-972. 10.1007/BF01395602.
- Ando, T., Sekine, S., Inagaki, S., Misaki, K., Badel, L., Moriya, H., Sami, M.M., Itakura, Y., Chihara, T., Kazama, H., Yonemura, S. and Hayashi, S., 2019. Nanopore formation in the cuticle of an insect olfactory sensillum. *Curr. Biol.* 29, 1512-+. 10.1016/j.cub.2019.03.043.
- Anton, S. and Hansson, B.S., 1996. Antennal lobe interneurons in the desert locust *Schistocerca gregaria* (Forsk.) (Forsk.): processing of aggregation pheromones in adult males and females. *J. Comp Neurol.* 370, 85-96. 10.1002/(SICI)1096-9861(19960617)370:1<85::AID-CNE8>3.0.CO;2-H. .
- Baker, T.C., Ochieng, S.A., Cosse, A.A., Lee, S.G., Todd, J.L., Quero, C. and Vickers, N.J., 2004. A comparison of responses from olfactory receptor neurons of *Heliothis subflexa* and *Heliothis virescens* to components of their sex pheromone. *J. Comp. Physiol. A.* 190, 155-165. 10.1007/s00359-003-0483-2.
- Baker, T.C., Zhou, Q., Linn, C.E., Baker, J.Y. and Tighe, T.B., 2022. Surface properties and architectures of male moth trichoid sensilla investigated using atomic force microscopy. *Insects.* 13, 10.3390/insects13050423.
- Barolo, S., Walker, R.G., Polyanovsky, A.D., Freschi, G., Keil, T. and Posakony, J.W., 2000. A notch-independent activity of suppressor of hairless is required for normal mechanoreceptor physiology. *Cell.* 103, 957-69. 10.1016/S0092-8674(00)00198-7.
- Benton, R., 2022. *Drosophila* olfaction: past, present and future. *Proc. Biol. Sci.* 289, 20222054. 10.1098/rspb.2022.2054.
- Benton, R., Sachse, S., Michnick, S.W. and Vosshall, L.B., 2006. Atypical membrane topology and heteromeric function of *Drosophila* odorant receptors in vivo. *PLoS Biol.* 4, e20. 10.1371/journal.pbio.0040020.
- Benton, R., Vannice, K.S., Gomez-Diaz, C. and Vosshall, L.B., 2009. Variant ionotropic glutamate receptors as chemosensory receptors in *Drosophila*. *Cell.* 136, 149-162. 10.1016/j.cell.2008.12.001.
- Benton, R., Vannice, K.S. and Vosshall, L.B., 2007. An essential role for a CD36-related receptor in pheromone detection in *Drosophila*. *Nature.* 450, 289-293. 10.1038/nature06328.
- Berg, B.G., Almaas, T.J., Bjaalie, J.G. and Mustaparta, H., 1998. The macroglomerular complex of the antennal lobe in the tobacco budworm moth *Heliothis virescens*: specified subdivision in four compartments according to information about biologically significant compounds. *J. Comp. Physiol. A.* 183, 669-682. 10.1007/s003590050290.
- Berg, B.G., Zhao, X.C. and Wang, G., 2014. Processing of pheromone information in related species of heliothine moths. *Insects.* 5, 742-61. 10.3390/insects5040742.
- Bicker, G. and Stern, M., 2020. Structural and functional plasticity in the regenerating olfactory system of the migratory locust. *Front. Physiol.* 11, 10.3389/fphys.2020.608661.
- Blankenburg, S., Cassau, S. and Krieger, J., 2019. The expression patterns of SNMP1 and SNMP2 underline distinct functions of two CD36-related proteins in the olfactory system of the tobacco budworm *Heliothis virescens*. *Cell Tissue Res.* 378, 485-497. 10.1007/s00441-019-03066-y.

- Boeckh, J. and Boeckh, V., 1979. Threshold and odor specificity of pheromone-sensitive neurons in the deutocerebrum of *Antheraea pernyi* and *Antheraea polyphemus* (Saturnidae). *J Comp Physiol.* 132, 235-242. 10.1007/BF00614495.
- Boeckh, J., Kaissling, K.E. and Schneider, D., 1965. Insect olfactory receptors. *Cold Spring Harb. Symp. Quant. Biol.* 30, 263-280. 10.1101/sqb.1965.030.01.028
- Bonen, A., Miskovic, D. and Kiens, B., 1999. Fatty acid transporters (FABPpm, FAT, FATP) in human muscle. *Can. J. Appl. Physiol.* 24, 515-523. 10.1139/h99-033.
- Boohar, R.T., Vandepas, L.E., Traylor-Knowles, N. and Browne, W.E., 2023. Phylogenetic and protein structure analyses provide insight into the evolution and diversification of the CD36 domain "Apex" among Scavenger Receptor Class B proteins across Eukarya. *Genome Biol Evol.* 15, 10.1093/gbe/evad218.
- Brand, P., Robertson, H.M., Lin, W., Pothula, R., Klingeman, W.E., Jurat-Fuentes, J.L. and Johnson, B.R., 2018. The origin of the odorant receptor gene family in insects. *Elife.* 7, 10.7554/eLife.38340.
- Brieger, G. and Butterworth, F.M., 1970. *Drosophila melanogaster*: identity of male lipid in reproductive system. *Science.* 167, 1262. 10.1126/science.167.3922.1262.
- Brito, N.F., Moreira, M.F. and Melo, A.C., 2016. A look inside odorant-binding proteins in insect chemoreception. *J. Insect Physiol.* 95, 51-65. 10.1016/j.jinsphys.2016.09.008.
- Butenandt, A., Beckmann, R., Stamm, D. and Hecker, E., 1959. Über den Sexuallockstoff des Seidenspinners *Bombyx mori*, Reindarstellung und Konstitution. *Zeitschr. Naturfor.* 14, 283-284.
- Butterwick, J.A., Del Marmol, J., Kim, K.H., Kahlson, M.A., Rogow, J.A., Walz, T. and Ruta, V., 2018. Cryo-EM structure of the insect olfactory receptor Orco. *Nature.* 560, 447-452. 10.1038/s41586-018-0420-8.
- Cassau, S. and Krieger, J., 2021. The role of SNMPs in insect olfaction. *Cell Tissue Res.* 383, 21-33. 10.1007/s00441-020-03336-0.
- Chabowski, A., Gorski, J., Luiken, J.J., Glatz, J.F. and Bonen, A., 2007. Evidence for concerted action of FAT/CD36 and FABPpm to increase fatty acid transport across the plasma membrane. *Prostaglandins Leukot Essent Fatty Acids.* 77, 345-53. 10.1016/j.plefa.2007.10.017.
- Chang, H., Cassau, S., Krieger, J., Guo, X., Knaden, M., Kang, L. and Hansson, B.S., 2023. A chemical defense deters cannibalism in migratory locusts. *Science.* 380, 537-543. 10.1126/science.ade6155.
- Chapman, R.F., 2002. Development of phenotypic differences in sensillum populations on the antennae of a grasshopper, *Schistocerca americana*. *J. Morphol.* 254, 186-94. 10.1002/jmor.10026.
- Chapman, R.F. and Greenwood, M., 1986. Changes in distribution and abundance of antennal sensilla during growth of *Locusta migratoria* L. (Orthoptera: Acrididae). *Int. J. Morphol. and Embryol.* 15, 83-96. 10.1016/0020-7322(86)90009-7.
- Chen, D., Hou, L., Wei, J., Guo, S., Cui, W., Yang, P., Kang, L. and Wang, X., 2022a. Aggregation pheromone 4-vinylanisole promotes the synchrony of sexual maturation in female locusts. *Elife.* 11, 10.7554/eLife.74581.
- Chen, Y., Zhang, J., Cui, W. and Silverstein, R.L., 2022b. CD36, a signaling receptor and fatty acid transporter that regulates immune cell metabolism and fate. *J. Exp. Med.* 219, 10.1084/jem.20211314.
- Chertemps, T., Francois, A., Durand, N., Rosell, G., Dekker, T., Lucas, P. and Maibeche-Coisne, M., 2012. A carboxylesterase, Esterase-6, modulates sensory physiological and behavioral response dynamics to pheromone in *Drosophila*. *BMC. Biol.* 10, 56. 10.1186/1741-7007-10-56.
- Chung, Y.D., Zhu, J.C., Han, Y.G. and Kernan, M.J., 2001. *nompA* encodes a PNS-specific, ZP domain protein required to connect mechanosensory dendrites to sensory structures. *Neuron.* 29, 415-428. Doi 10.1016/S0896-6273(01)00215-X.
- Clyne, P.J., Certel, S.J., De Bruyne, M., Zaslavsky, L., Johnson, W.A. and Carlson, J.R., 1999. The odor specificities of a subset of olfactory receptor neurons are governed by Acj6, a POU-domain transcription factor. *Neuron.* 22, 339-347. 10.1016/s0896-6273(00)81094-6.
- Couto, A., Alenius, M. and Dickson, B.J., 2005. Molecular, anatomical, and functional organization of the *Drosophila* olfactory system. *Curr. Biol.* 15, 1535-1547. 10.1016/j.cub.2005.07.034.
- Cui, X., Wu, C. and Zhang, L., 2011. Electrophysiological response patterns of 16 olfactory neurons from the trichoid sensilla to odorant from fecal volatiles in the locust, *Locusta migratoria manilensis*. *Arch. Insect Biochem. Physiol.* 77, 45-57. 10.1002/arch.20420

- Dahanukar, A., Hallem, E.A. and Carlson, J.R., 2005. Insect chemoreception. *Curr. Opin. Neurobiol.* 15, 423-430. 10.1016/j.conb.2005.06.001.
- De Bruyne, M. and Baker, T.C., 2008. Odor detection in insects: volatile codes. *J. Chem. Ecol.* 34, 882-897. 10.1007/s10886-008-9485-4.
- De Fouchier, A., Walker, W.B., 3rd, Montagne, N., Steiner, C., Binyameen, M., Schlyter, F., Chertemps, T., Maria, A., Francois, M.C., Monsempe, C., Anderson, P., Hansson, B.S., Larsson, M.C. and Jacquin-Joly, E., 2017. Functional evolution of Lepidoptera olfactory receptors revealed by deorphanization of a moth repertoire. *Nat Commun.* 8, 15709. 10.1038/ncomms15709.
- Del Marmol, J., Yedlin, M.A. and Ruta, V., 2021. The structural basis of odorant recognition in insect olfactory receptors. *Nature.* 597, 126-131. 10.1038/s41586-021-03794-8.
- Drover, V.A., Nguyen, D.V., Bastie, C.C., Darlington, Y.F., Abumrad, N.A., Pessin, J.E., London, E., Sahoo, D. and Phillips, M.C., 2008. CD36 mediates both cellular uptake of very long chain fatty acids and their intestinal absorption in mice. *J Biol Chem.* 283, 13108-15. 10.1074/jbc.M708086200.
- Durand, N., Carot-Sans, G., Bozzolan, F., Rosell, G., Siauxsat, D., Debernard, S., Chertemps, T. and Maibeche-Coisne, M., 2011. Degradation of pheromone and plant volatile components by a same odorant-degrading enzyme in the cotton leafworm, *Spodoptera littoralis*. *PLoS ONE.* 6, e29147. 10.1371/journal.pone.0029147.
- Elgar, M.A., Zhang, D., Wang, Q., Wittwer, B., Thi Pham, H., Johnson, T.L., Freelance, C.B. and Coquilleau, M., 2018. Insect antennal morphology: the evolution of diverse solutions to odorant perception. *Yale J Biol Med.* 91, 457-469.
- Engsontia, P., Sangket, U., Chotigeat, W. and Satasook, C., 2014. Molecular evolution of the odorant and gustatory receptor genes in lepidopteran insects: implications for their adaptation and speciation. *J. Mol. Evol.* 79, 21-39. 10.1007/s00239-014-9633-0.
- Fleischer, J. and Krieger, J., 2018. Insect pheromone receptors - key elements in sensing intraspecific chemical signals. *Front. Cell. Neurosci.* 12, 425. 10.3389/fncel.2018.00425.
- Fleischer, J., Pregitzer, P., Breer, H. and Krieger, J., 2018. Access to the odor world: olfactory receptors and their role for signal transduction in insects. *Cell. Mol. Life Sci.* 75, 485-508. 10.1007/s00018-017-2627-5.
- Forstner, M., Breer, H. and Krieger, J., 2009. A receptor and binding protein interplay in the detection of a distinct pheromone component in the silkworm *Antheraea polyphemus*. *Int. J. Biol. Sci.* 5, 745-757. 10.7150/ijbs.5.745.
- Forstner, M., Gohl, T., Gondesén, I., Raming, K., Breer, H. and Krieger, J., 2008. Differential expression of SNMP-1 and SNMP-2 proteins in pheromone-sensitive hairs of moths. *Chem. Senses.* 33, 291-299. 10.1093/chemse/bjm087.
- Fraichard, S., Legendre, A., Lucas, P., Chauvel, I., Faure, P., Neiers, F., Artur, Y., Briand, L., Ferveur, J.F. and Heydel, J.M., 2020. Modulation of sex pheromone discrimination by a UDP-glycosyltransferase in *Drosophila melanogaster*. *Genes (Basel).* 11, 10.3390/genes11030237.
- Galindo, K. and Smith, D.P., 2001. A large family of divergent *Drosophila* odorant-binding proteins expressed in gustatory and olfactory sensilla. *Genetics.* 159, 1059-1072. 10.1093/genetics/159.3.1059
- Gao, Q. and Chess, A., 1999. Identification of candidate *Drosophila* olfactory receptors from genomic DNA sequence. *Genomics.* 60, 31-39. 10.1006/geno.1999.5894.
- German, P.F., Van Der Poel, S., Carraher, C., Kralicek, A.V. and Newcomb, R.D., 2013. Insights into subunit interactions within the insect olfactory receptor complex using FRET. *Insect Biochem. Mol. Biol.* 43, 138-145. 10.1016/j.ibmb.2012.11.002.
- Giovannucci, D.R. and Stephenson, R.S., 1999. Identification and distribution of dietary precursors of the *Drosophila* visual pigment chromophore: analysis of carotenoids in wild type and ninaD mutants by HPLC. *Vision Research.* 39, 219-229. 10.1016/S0042-6989(98)00184-9.
- Glatz, J.F.C. and Luiken, J., 2018. Dynamic role of the transmembrane glycoprotein CD36 (SR-B2) in cellular fatty acid uptake and utilization. *J Lipid Res.* 59, 1084-1093. 10.1194/jlr.R082933.
- Glatz, J.F.C., Nabben, M. and Luiken, J., 2022. CD36 (SR-B2) as master regulator of cellular fatty acid homeostasis. *Curr Opin Lipidol.* 33, 103-111. 10.1097/MOL.0000000000000819.
- Gnatzy, W., Mohren, W. and Steinbrecht, R.A., 1984. Pheromone receptors in *Bombyx mori* and *Antheraea pernyi*. II. Morphometric analysis. *Cell Tissue Res.* 235, 35-42. 10.1007/BF00213720.

- Gohl, T. and Krieger, J., 2006. Immunolocalization of a candidate pheromone receptor in the antenna of the male moth, *Heliothis virescens*. *Invert. Neurosci.* 6, 13-21. 10.1007/s10158-005-0012-9.
- Gomez-Diaz, C., Bargeton, B., Abuin, L., Bukar, N., Reina, J.H., Bartoi, T., Graf, M., Ong, H., Ulbrich, M.H., Masson, J.F. and Benton, R., 2016. A CD36 ectodomain mediates insect pheromone detection via a putative tunnelling mechanism. *Nat. Commun.* 7, 11866. 10.1038/ncomms11866.
- Gomez-Diaz, C. and Benton, R., 2013. The joy of sex pheromones. *EMBO Rep.* 14, 874-883. 10.1038/embor.2013.140.
- Grabe, V. and Sachse, S., 2018. Fundamental principles of the olfactory code. *Biosystems.* 164, 94-101. 10.1016/j.biosystems.2017.10.010.
- Grabe, V., Strutz, A., Baschwitz, A., Hansson, B.S. and Sachse, S., 2015. Digital in vivo 3D atlas of the antennal lobe of *Drosophila melanogaster*. *J. Comp. Neurol.* 523, 530-44. 10.1002/cne.23697.
- Grosse-Wilde, E., Gohl, T., Bouche, E., Breer, H. and Krieger, J., 2007. Candidate pheromone receptors provide the basis for the response of distinct antennal neurons to pheromonal compounds. *Eur. J. Neurosci.* 25, 2364-2373. 10.1111/j.1460-9568.2007.05512.x.
- Grosse-Wilde, E., Svatos, A. and Krieger, J., 2006. A pheromone-binding protein mediates the bombykol-induced activation of a pheromone receptor *in vitro*. *Chem. Senses.* 31, 547-555. 10.1093/chemse/bjj059.
- Gu, S.H., Yang, R.N., Guo, M.B., Wang, G.R., Wu, K.M., Guo, Y.Y., Zhou, J.J. and Zhang, Y.J., 2013. Molecular identification and differential expression of sensory neuron membrane proteins in the antennae of the black cutworm moth *Agrotis ipsilon*. *J. Insect Physiol.* 59, 430-443. 10.1016/j.jinsphys.2013.02.003.
- Guo, M., Krieger, J., Grosse-Wilde, E., Missbach, C., Zhang, L. and Breer, H., 2013. Variant ionotropic receptors are expressed in olfactory sensory neurons of coeloconic sensilla on the antenna of the desert locust (*Schistocerca gregaria*). *Int J Biol Sci.* 10, 1-14. 10.7150/ijbs.7624.
- Guo, X., Yu, Q., Chen, D., Wei, J., Yang, P., Yu, J., Wang, X. and Kang, L., 2020. 4-Vinylanisole is an aggregation pheromone in locusts. *Nature.* 584, 584-588. 10.1038/s41586-020-2610-4.
- Ha, T.S. and Smith, D.P., 2006. A pheromone receptor mediates 11-cis-vaccenyl acetate-induced responses in *Drosophila*. *J. Neurosci.* 26, 8727-8733. 10.1523/JNEUROSCI.0876-06.2006.
- Ha, T.S. and Smith, D.P., 2009. Odorant and pheromone receptors in insects. *Front. Cell. Neurosci.* 3, 10. 10.3389/neuro.03.010.2009.
- Hansson, B.S. and Stensmyr, M.C., 2011. Evolution of insect olfaction. *Neuron.* 72, 698-711. 10.1016/j.neuron.2011.11.003.
- Hao, J.W., Wang, J., Guo, H., Zhao, Y.Y., Sun, H.H., Li, Y.F., Lai, X.Y., Zhao, N., Wang, X., Xie, C., Hong, L., Huang, X., Wang, H.R., Li, C.B., Liang, B., Chen, S. and Zhao, T.J., 2020. CD36 facilitates fatty acid uptake by dynamic palmitoylation-regulated endocytosis. *Nat Commun.* 11, 4765. 10.1038/s41467-020-18565-8.
- Harmon, C.M. and Abumrad, N.A., 1993. Binding of sulfosuccinimidyl fatty acids to adipocyte membrane proteins: isolation and amino-terminal sequence of an 88-kD protein implicated in transport of long-chain fatty acids. *J Membr Biol.* 133, 43-9. 10.1007/BF00231876.
- Hassanali, A., Njagi, P.G. and Bashir, M.O., 2005. Chemical ecology of locusts and related acridids. *Annu. Rev. Entomol.* 50, 223-45. 10.1146/annurev.ento.50.071803.130345.
- Heinbockel, T. and Kaissling, K.-E., 1996. Variability of olfactory receptor neuron responses of female silkmoths (*Bombyx mori* L.) to benzoic acid and (+)-linalool. *J. Insect Physiol.* 42, 565-578. 10.1016/0022-1910(95)00133-6.
- Hildebrand, J.G. and Shepherd, G.M., 1997. Mechanisms of olfactory discrimination: converging evidence for common principles across phyla. *Annu. Rev. Neurosci.* 20, 595-631. 10.1146/annurev.neuro.20.1.595.
- Houdusse, A. and Titus, M.A., 2021. The many roles of myosins in filopodia, microvilli and stereocilia. *Curr Biol.* 31, R586-R602. 10.1016/j.cub.2021.04.005.
- Ishida, Y. and Leal, W.S., 2005. Rapid inactivation of a moth pheromone. *Proc. Natl. Acad. Sci. U. S. A.* 102, 14075-14079. 10.1073/pnas.0505340102.
- Jaffar-Bandjee, M., Steinmann, T., Krijnen, G. and Casas, J., 2020. Insect pectinate antennae maximize odor capture efficiency at intermediate flight speeds. *Proc. Natl. Acad. Sci. U. S. A.* 117, 28126-28133. 10.1073/pnas.2007871117.

- Jana, S.C., Dutta, P., Jain, A., Singh, A., Adusumilli, L., Girotra, M., Kumari, D., Shirolkar, S. and Ray, K., 2021. Kinesin-2 transports Orco into the olfactory cilium of *Drosophila melanogaster* at specific developmental stages. *PLoS Genet.* 17, e1009752. 10.1371/journal.pgen.1009752.
- Jarriault, D. and Mercer, A., 2012. Queen mandibular pheromone: questions that remain to be resolved. *Apidologie.* 43, 292-307. 10.1007/s13592-011-0117-6.
- Jay, A.G., Simard, J.R., Huang, N. and Hamilton, J.A., 2020. SSO and other putative inhibitors of FA transport across membranes by CD36 disrupt intracellular metabolism, but do not affect FA translocation. *J Lipid Res.* 61, 790-807. 10.1194/jlr.RA120000648.
- Jiang, X., Pregitzer, P., Grosse-Wilde, E., Breer, H. and Krieger, J., 2016. Identification and characterization of two "Sensory Neuron Membrane Proteins" (SNMPs) of the desert locust, *Schistocerca gregaria* (Orthoptera: Acrididae). *J. Insect Sci.* 16, 33. 10.1093/jisesa/iew015.
- Jiang, X.C., Ryl, M., Krieger, J., Breer, H. and Pregitzer, P., 2018. Odorant binding proteins of the desert locust *Schistocerca gregaria* (Orthoptera, Acrididae): topographic expression patterns in the antennae. *Front. Physiol.* 9, 10.3389/fphys.2018.00417.
- Jimenez-Dalmaroni, M.J., Xiao, N., Corper, A.L., Verdino, P., Ainge, G.D., Larsen, D.S., Painter, G.F., Rudd, P.M., Dwek, R.A., Hoebe, K., Beutler, B. and Wilson, I.A., 2009. Soluble CD36 ectodomain binds negatively charged diacylglycerol ligands and acts as a co-receptor for TLR2. *PLoS ONE.* 4, e7411. 10.1371/journal.pone.0007411.
- Jin, X., Ha, T.S. and Smith, D.P., 2008. SNMP is a signaling component required for pheromone sensitivity in *Drosophila*. *Proc. Natl. Acad. Sci. U. S. A.* 105, 10996-11001. 10.1073/pnas.0803309105.
- Jorgensen, K., Almaas, T.J., Marion-Poll, F. and Mustaparta, H., 2007. Electrophysiological characterization of responses from gustatory receptor neurons of sensilla chaetica in the moth *Heliothis virescens*. *Chem. Senses.* 32, 863-879. 10.1093/chemse/bjm057.
- Joseph, R.M. and Carlson, J.R., 2015. *Drosophila* chemoreceptors: A molecular interface between the chemical world and the brain. *Trends Genet.* 31, 683-95. 10.1016/j.tig.2015.09.005.
- Kaissling, K.-E., Kasang, G., Bestmann, H.J., Stransky, W. and Vostrowsky, O., 1978. A new pheromone of the silkworm moth *Bombyx mori*. *Naturwissenschaften.* 65, 382-384. 10.1007/BF00439702.
- Kaissling, K.E., 1996. Peripheral mechanisms of pheromone reception in moths. *Chem. Senses.* 21, 257-268. 10.1093/chemse/21.2.257.
- Kaissling, K.E., 2009. Olfactory perireceptor and receptor events in moths: a kinetic model revised. *J. Comp Physiol A Neuroethol. Sens. Neural Behav. Physiol.* 195, 895-922. 10.1007/s00359-009-0461-4.
- Kaissling, K.E., 2014. Pheromone reception in insects: the example of silk moths. *Neurobiology of Chemical Communication.* ed. C. Mucignat-Carettas, Boca Raton (FL).
- Kanaujia, S. and Kaissling, K.E., 1985. Interactions of pheromone with moth antennae - adsorption, desorption and transport. *Journal of Insect Physiology.* 31, 71-81. 10.1016/0022-1910(85)90044-7.
- Karlson, P. and Lüscher, M., 1959. Pheromones - new term for a class of biologically active substances. *Nature.* 183, 55-56. 10.1038/183055a0.
- Kasang, G., 1974. Uptake of sex-pheromone H-3 bombykol and related compounds by male and female *Bombyx* antennae. *Journal of Insect Physiology.* 20, 2407-2422. 10.1016/0022-1910(74)90027-4.
- Kasang, G., Schneider, D. and Schäfer, W., 1978. The silkworm moth *Bombyx mori*. *Naturwissenschaften.* 65, 337-338. 10.1007/BF00368376.
- Kasang, G. and Weiss, N., 1974. Thin-Layer Chromatographic Analysis of Radioactively Labeled Insect Pheromones - Metabolites of [Bombykol-H-3]. *Journal of Chromatography.* 92, 401-417. 10.1016/S0021-9673(00)85751-9.
- Keil, T.A., 1984. Reconstruction and morphometry of silkworm olfactory hairs: a comparative study of sensilla trichodea on the antennae of male *Antheraea polyphemus* and *Antheraea pernyi* (Insecta, Lepidoptera). *Zoomorphology.* 104, 147-156. 10.1007/BF00312133.
- Keil, T.A., 1987. Structure of isolated sensilla and sensory neurons in vitro: Observations on developing silkworm antennae. *Cell Tiss. Res.* 520, 543-549. 10.1007/BF00218945.
- Keil, T.A., 1989. Fine structure of the pheromone-sensitive sensilla on the antenna of the hawkmoth, *Manduca sexta*. *Tissue Cell.* 21, 139-51. 10.1016/0040-8166(89)90028-1.

- Keil, T.A., 1992. Fine-structure of a developing insect olfactory organ - morphogenesis of the silkmoth antenna. *Microscopy Research and Technique*. 22, 351-371. 10.1002/jemt.1070220405.
- Keil, T.A., 1993. Dynamics of immotile olfactory cilia in the silkmoth *Antheraea*. *Tissue & Cell*. 25, 573-587. 10.1016/0040-8166(93)90010-I.
- Keil, T.A., 1997. Comparative Morphogenesis of sensilla: A Review. *Int. J. Insect Morphol & Embryol*. 26, 151-160. 10.1016/S0020-7322(97)00017-2.
- Keil, T.A., 2012. Sensory cilia in arthropods. *Arthropod. Struct. Dev.* 41, 515-534. 10.1016/j.asd.2012.07.001.
- Keil, T.A. and Steinbrecht, R.A., 1983. Beziehungen zwischen Sinnes-, Hüll- und Gliazellen in epidermalen Mechano- und Chemorezeptoren von Insekten. *Verh. Dtsch. Zool. Ges.*
- Keil, T.A. and Steiner, C., 1990. Morphogenesis of the Antenna of the Male Silkmoth, *Antheraea polyphemus*: 1. The Leaf-Shaped Antenna of the Pupa from Diapause to Apolysis. *Tissue & Cell*. 22, 319-336. 10.1016/0040-8166(90)90007-V.
- Kiefer, C., Sumser, E., Wernet, M.F. and Von Lintig, J., 2002. A class B scavenger receptor mediates the cellular uptake of carotenoids in *Drosophila*. *Proc. Natl. Acad. Sci. U. S. A.* 99, 10581-6. 10.1073/pnas.162182899.
- Kim, M.S., Repp, A. and Smith, D.P., 1998. LUSH odorant-binding protein mediates chemosensory responses to alcohols in *Drosophila melanogaster*. *Genetics*. 150, 711-721. 10.1093/genetics/150.2.711.
- Kim, S.H., Lee, Y., Akitake, B., Woodward, O.M., Guggino, W.B. and Montell, C., 2010. *Drosophila* TRPA1 channel mediates chemical avoidance in gustatory receptor neurons. *Proc. Natl. Acad. Sci U. S. A.* 107, 8440-8445. 10.1073/pnas.1001425107.
- Kirkness, E.F., Haas, B.J., Sun, W., Braig, H.R., Perotti, M.A., Clark, J.M., Lee, S.H., Robertson, H.M., Kennedy, R.C., Elhaik, E., Gerlach, D., Kriventseva, E.V., Elsik, C.G., Graur, D., Hill, C.A., Veenstra, J.A., Walenz, B., Tubio, J.M., Ribeiro, J.M., Rozas, J., Johnston, J.S., Reese, J.T., Popadic, A., Tojo, M., Raoult, D., Reed, D.L., Tomoyasu, Y., Kraus, E., Mittapalli, O., Margam, V.M., Li, H.M., Meyer, J.M., Johnson, R.M., Romero-Severson, J., Vanzeer, J.P., Alvarez-Ponce, D., Vieira, F.G., Aguade, M., Guirao-Rico, S., Anzola, J.M., Yoon, K.S., Strycharz, J.P., Unger, M.F., Christley, S., Lobo, N.F., Seufferheld, M.J., Wang, N., Dasch, G.A., Struchiner, C.J., Madey, G., Hannick, L.I., Bidwell, S., Joardar, V., Caler, E., Shao, R., Barker, S.C., Cameron, S., Bruggner, R.V., Regier, A., Johnson, J., Viswanathan, L., Utterback, T.R., Sutton, G.G., Lawson, D., Waterhouse, R.M., Venter, J.C., Strausberg, R.L., Berenbaum, M.R., Collins, F.H., Zdobnov, E.M. and Pittendrigh, B.R., 2010. Genome sequences of the human body louse and its primary endosymbiont provide insights into the permanent parasitic lifestyle. *Proc. Natl. Acad. Sci U. S. A.* 107, 12168-12173. 10.1073/pnas.1003379107.
- Klein, U., 1987. Sensillum-lymph proteins from antennal olfactory hairs of the moth *Antheraea polyphemus* (Saturniidae). *Insect Biochem.* 17, 1193-1204. 10.1016/0020-1790(87)90093-X.
- Klun, J.A., Plimmer, J.R., Bierl-Leonhardt, B.A., Sparks, A.N. and Chapman, O.L., 1979. Trace chemicals: The essence of sexual communication systems in *Heliothis* species. *Science*. 204, 1328-1329. 10.1126/science.204.4399.1328.
- Koenig, C., Hirsh, A., Bucks, S., Klinner, C., Vogel, H., Shukla, A., Mansfield, J.H., Morton, B., Hansson, B.S. and Grosse-Wilde, E., 2015. A reference gene set for chemosensory receptor genes of *Manduca sexta*. *Insect Biochem. Mol. Biol.* 66, 51-63. 10.1016/j.ibmb.2015.09.007.
- Koonen, D.P., Glatz, J.F., Bonen, A. and Luiken, J.J., 2005. Long-chain fatty acid uptake and FAT/CD36 translocation in heart and skeletal muscle. *Biochim. Biophys. Acta*. 1736, 163-180. 10.1016/j.bbali.2005.08.018. .
- Koutroumpa, F.A. and Jacquin-Joly, E., 2014. Sex in the night: fatty acid-derived sex pheromones and corresponding membrane pheromone receptors in insects. *Biochimie*. 107 Pt A, 15-21. 10.1016/j.biochi.2014.07.018.
- Krieger, J., Grosse-Wilde, E., Gohl, T. and Breer, H., 2005. Candidate pheromone receptors of the silkmoth *Bombyx mori*. *Eur. J. Neurosci*. 21, 2167-2176. 10.1111/j.1460-9568.2005.04058.x.
- Krieger, J., Grosse-Wilde, E., Gohl, T., Dewer, Y.M.E., Raming, K. and Breer, H., 2004. Genes encoding candidate pheromone receptors in a moth (*Heliothis virescens*). *Proc. Natl. Acad. Sci. U. S. A.* 101, 11845-11850. 10.1073/pnas.0403052101.

- Krieger, J., Raming, K., Dewer, Y.M.E., Bette, S., Conzelmann, S. and Breer, H., 2002. A divergent gene family encoding candidate olfactory receptors of the moth *Heliothis virescens*. *Eur. J. Neurosci.* 16, 619-628. 10.1046/j.1460-9568.2002.02109.x.
- Kuda, O., Pietka, T.A., Demianova, Z., Kudova, E., Cvacka, J., Kopecky, J. and Abumrad, N.A., 2013. Sulfo-N-succinimidyl oleate (SSO) inhibits fatty acid uptake and signaling for intracellular calcium via binding CD36 lysine 164: SSO also inhibits oxidized low density lipoprotein uptake by macrophages. *J Biol Chem.* 288, 15547-55. 10.1074/jbc.M113.473298.
- Kurtovic, A., Widmer, A. and Dickson, B.J., 2007. A single class of olfactory neurons mediates behavioural responses to a *Drosophila* sex pheromone. *Nature.* 446, 542-546. 10.1038/nature05672.
- Kvello, P., Lofaldli, B.B., Rybak, J., Menzel, R. and Mustaparta, H., 2009. Digital, three-dimensional average shaped atlas of the *Heliothis virescens* brain with integrated gustatory and olfactory neurons. *Front Syst. Neurosci.* 3, 14. 10.3389/neuro.06.014.2009.
- Kwon, J.Y., Dahanukar, A., Weiss, L.A. and Carlson, J.R., 2007. The molecular basis of CO₂ reception in *Drosophila*. *Proc. Natl. Acad. Sci. U. S. A.* 104, 3574-8. 10.1073/pnas.0700079104.
- Larsson, M.C., Domingos, A.I., Jones, W.D., Chiappe, M.E., Amrein, H. and Vosshall, L.B., 2004. Or83b encodes a broadly expressed odorant receptor essential for *Drosophila* olfaction. *Neuron.* 43, 703-714. 10.1016/j.neuron.2004.08.019.
- Larter, N.K., Sun, J.S. and Carlson, J.R., 2016. Organization and function of *Drosophila* odorant binding proteins. *Elife.* 5, 10.7554/eLife.20242.
- Laughlin, J.D., Ha, T.S., Jones, D.N. and Smith, D.P., 2008. Activation of pheromone-sensitive neurons is mediated by conformational activation of pheromone-binding protein. *Cell.* 133, 1255-1265. 10.1016/j.cell.2008.04.046.
- Leal, W.S., 2013. Odorant reception in insects: roles of receptors, binding proteins, and degrading enzymes. *Annu. Rev. Entomol.* 58, 373-391. 10.1146/annurev-ento-120811-153635.
- Leal, W.S., Ishida, Y., Pelletier, J., Xu, W., Rayo, J., Xu, X. and Ames, J.B., 2009. Olfactory proteins mediating chemical communication in the navel orangeworm moth, *Amyelois transitella*. *PLoS ONE.* 4, e7235. 10.1371/journal.pone.0007235.
- Lemke, R.S., Pregitzer, P., Eichhorn, A.S., Breer, H., Krieger, J. and Fleischer, J., 2020. SNMP1 and odorant receptors are co-expressed in olfactory neurons of the labial and maxillary palps from the desert locust *Schistocerca gregaria* (Orthoptera: Acrididae). *Cell Tissue Res.* 379, 275-289. 10.1007/s00441-019-03083-x.
- Li, Y., Zhang, J., Chen, D., Yang, P., Jiang, F., Wang, X. and Kang, L., 2016. CRISPR/Cas9 in locusts: Successful establishment of an olfactory deficiency line by targeting the mutagenesis of an odorant receptor co-receptor (Orco). *Insect Biochem. Mol. Biol.* 79, 27-35. 10.1016/j.ibmb.2016.10.003.
- Li, Z., Ni, J.D., Huang, J. and Montell, C., 2014. Requirement for *Drosophila* SNMP1 for rapid activation and termination of pheromone-induced activity. *PLoS Genet.* 10, e1004600. 10.1371/journal.pgen.1004600.
- Liu, C., Zhang, J., Liu, Y., Wang, G. and Dong, S., 2014. Expression of SNMP1 and SNMP2 genes in antennal sensilla of *Spodoptera exigua* (Hubner). *Arch. Insect Biochem. Physiol.* 85, 114-126. 10.1002/arch.21150.
- Liu, S., Chang, H., Liu, W., Cui, W., Liu, Y., Wang, Y., Ren, B. and Wang, G., 2020. Essential role for SNMP1 in detection of sex pheromones in *Helicoverpa armigera*. *Insect Biochem. Mol. Biol.* 127, 103485. 10.1016/j.ibmb.2020.103485.
- Liu, S., Qiao, F., Liang, Q.M., Huang, Y.J., Zhou, W.W., Gong, Z.J., Cheng, J. and Zhu, Z.R., 2013. Molecular characterization of two Sensory Neuron Membrane Proteins from *Chilo suppressalis* (Lepidoptera: Pyralidae). *Ann. Entomol. Soc. Am.* 106, 378-384. 10.1603/AN12099.
- Lundin, C., Kall, L., Kreher, S.A., Kapp, K., Sonnhammer, E.L., Carlson, J.R., Heijne, G. and Nilsson, I., 2007. Membrane topology of the *Drosophila* OR83b odorant receptor. *FEBS Lett.* 581, 5601-5604. 10.1016/j.febslet.2007.11.007.
- Maida, R., Mameli, M., Muller, B., Krieger, J. and Steinbrecht, R.A., 2005. The expression pattern of four odorant-binding proteins in male and female silk moths, *Bombyx mori*. *J. Neurocytol.* 34, 149-163. 10.1007/s11068-005-5054-8.
- Martin, C., Chevrot, M., Poirier, H., Passilly-Degrace, P., Niot, I. and Besnard, P., 2011. CD36 as a lipid sensor. *Physiol. Behav.* 105, 33-42. 10.1016/j.physbeh.2011.02.029.

- Menuz, K., Larter, N.K., Park, J. and Carlson, J.R., 2014. An RNA-Seq Screen of the Antenna Identifies a Transporter Necessary for Ammonia Detection. *Plos Genetics*. 10, 10.1371/journal.pgen.1004810.
- Nakagawa, T., Sakurai, T., Nishioka, T. and Touhara, K., 2005. Insect sex-pheromone signals mediated by specific combinations of olfactory receptors. *Science*. 307, 1638-1642. 10.1126/science.1106267.
- Nakano, M., Morgan-Richards, M., Trewick, S.A. and Clavijo-McCormick, A., 2022. Chemical Ecology and Olfaction in Short-Horned Grasshoppers (Orthoptera: Acrididae). *J. Chem. Ecol.* 48, 121-140. 10.1007/s10886-021-01333-3.
- Nichols, Z. and Vogt, R.G., 2008. The SNMP/CD36 gene family in Diptera, Hymenoptera and Coleoptera: *Drosophila melanogaster*, *D. pseudoobscura*, *Anopheles gambiae*, *Aedes aegypti*, *Apis mellifera*, and *Tribolium castaneum*. *Insect Biochem. Mol. Biol.* 38, 398-415. 10.1016/j.ibmb.2007.11.003.
- Nolte, A., Funk, N.W., Mukunda, L., Gawalek, P., Werckenthin, A., Hansson, B.S., Wicher, D. and Stengl, M., 2013. In situ tip-recordings found no evidence for an Orco-based ionotropic mechanism of pheromone-transduction in *Manduca sexta*. *PLoS ONE*. 8, e62648. 10.1371/journal.pone.0062648.
- Nolte, A., Gawalek, P., Koerte, S., Wei, H., Schumann, R., Werckenthin, A., Krieger, J. and Stengl, M., 2016. No evidence for ionotropic pheromone transduction in the hawkmoth *Manduca sexta*. *PLoS ONE*. 11, e0166060. 10.1371/journal.pone.0166060.
- Ochieng, S.A., Hallberg, E. and Hansson, B.S., 1998. Fine structure and distribution of antennal sensilla of the desert locust, *Schistocerca gregaria* (Orthoptera: Acrididae). *Cell Tissue Res.* 291, 525-536. 10.1007/s004410051022.
- Ochieng, S.A. and Hansson, B.S., 1999. Responses of olfactory receptor neurones to behaviourally important odours in gregarious and solitary desert locust, *Schistocerca gregaria*. *Physiol. Entomol.* 24, 28-36. 10.1046/j.1365-3032.1999.00107.x.
- Patel, M. and Rangan, A., 2021. Olfactory encoding within the insect antennal lobe: The emergence and role of higher order temporal correlations in the dynamics of antennal lobe spiking activity. *Journal of Theoretical Biology*. 522, 10.1016/j.jtbi.2021.110700.
- Pelletier, J., Bozzolan, F., Solvar, M., Francois, M.C., Jacquin-Joly, E. and Maibeche-Coisne, M., 2007. Identification of candidate aldehyde oxidases from the silkworm *Bombyx mori* potentially involved in antennal pheromone degradation. *Gene*. 404, 31-40. 10.1016/j.gene.2007.08.022.
- Pelletier, J., Dawit, M., Ghaninia, M., Marois, E. and Ignell, R., 2023. A mosquito-specific antennal protein is critical for the attraction to human odor in the malaria vector *Anopheles gambiae*. *Insect Biochem Mol Biol*. 159, 103988. 10.1016/j.ibmb.2023.103988.
- Peng, W., Ma, N.L., Zhang, D., Zhou, Q., Yue, X., Khoo, S.C., Yang, H., Guan, R., Chen, H., Zhang, X., Wang, Y., Wei, Z., Suo, C., Peng, Y., Yang, Y., Lam, S.S. and Sonne, C., 2020. A review of historical and recent locust outbreaks: Links to global warming, food security and mitigation strategies. *Environ Res.* 191, 110046. 10.1016/j.envres.2020.110046.
- Pepino, M.Y., Kuda, O., Samovski, D. and Abumrad, N.A., 2014. Structure-function of CD36 and importance of fatty acid signal transduction in fat metabolism. *Annu. Rev. Nutr.* 34, 281-303. 10.1146/annurev-nutr-071812-161220.
- Pogue, M.G., 2013. Revised status of *Chloridea* Duncan and (Westwood), 1841, for the *Heliothis virescens* species group (Lepidoptera: Noctuidae: Heliothinae) based on morphology and three genes. *Syst. Entomol.* 38, 523-542. 10.1111/syen.12010.
- Poivet, E., Gallot, A., Montagne, N., Glaser, N., Legeai, F. and Jacquin-Joly, E., 2013. A comparison of the olfactory gene repertoires of adults and larvae in the noctuid moth *Spodoptera littoralis*. *PLoS ONE*. 8, 10.1371/journal.pone.0060263.
- Pophof, B., 1997. Olfactory responses recorded from sensilla coeloconica of the silkworm *Bombyx mori*. *Physiol. Entomol.* 22, 239-248. 10.1111/j.1365-3032.1997.tb01164.x.
- Pregitzer, P., Greschista, M., Breer, H. and Krieger, J., 2014. The sensory neurone membrane protein SNMP1 contributes to the sensitivity of a pheromone detection system. *Insect Mol. Biol.* 23, 733-742. 10.1111/imb.12119.
- Pregitzer, P., Jiang, X., Grosse-Wilde, E., Breer, H., Krieger, J. and Fleischer, J., 2017. In search for pheromone receptors: certain members of the odorant receptor family in the desert locust

- Schistocerca gregaria* (Orthoptera: Acrididae) are co-expressed with SNMP1. *Int. J. Biol. Sci.* 13, 911-922. 10.7150/ijbs.18402.
- Pregitzer, P., Jiang, X., Lemke, R.S., Krieger, J., Fleischer, J. and Breer, H., 2019. A subset of odorant receptors from the desert locust *Schistocerca gregaria* is co-expressed with the Sensory Neuron Membrane Protein 1. *Insects*. 10, 350. 10.3390/insects10100350.
- Prelic, S., Mahadevan, V.P., Venkateswaran, V., Lavista-Llanos, S., Hansson, B.S. and Wicher, D., 2022. Functional Interaction Between Olfactory Sensory Neurons and Their Support Cells. *Front. Cell. Neuro.* 15, 10.3389/fncel.2021.789086.
- Qiu, C.Z., Zhou, Q.Z., Liu, T.T., Fang, S.M., Wang, Y.W., Fang, X., Huang, C.L., Yu, Q.Y., Chen, C.H. and Zhang, Z., 2018. Evidence of peripheral olfactory impairment in the domestic silkworms: insight from the comparative transcriptome and population genetics. *BMC Genomics*. 19, 10.1186/s12864-018-5172-1.
- Ramaswamy, S. and Roush, R.T., 1986. Sex pheromone titers in females of *Heliothis virescens* from three geographical locations (Lepidoptera, Noctuidae). *Entomol. Gen.* 12, 19-23. 10.1127/entom.gen/12/1986/19.
- Rao, V.S., Srinivas, K., Sujini, G.N. and Kumar, G.N., 2014. Protein-protein interaction detection: methods and analysis. *Int J Proteomics*. 2014, 147648. 10.1155/2014/147648.
- Regnier, F.E. and Law, J.H., 1968. Insect pheromones. *J. Lipid Res.* 9, 541-551. 10.1016/S0022-2275(20)42699-9.
- Renou, M. and Anton, S., 2020. Insect olfactory communication in a complex and changing world. *Curr Opin Insect Sci.* 42, 1-7. 10.1016/j.cois.2020.04.004.
- Rihani, K., Ferveur, J.F. and Briand, L., 2021. The 40-Year Mystery of Insect Odorant-Binding Proteins. *Biomolecules*. 11, 10.3390/biom11040509.
- Robertson, H.M., Martos, R., Sears, C.R., Todres, E.Z., Walden, K.K. and Nardi, J.B., 1999. Diversity of odourant binding proteins revealed by an expressed sequence tag project on male *Manduca sexta* moth antennae. *Insect Mol. Biol.* 8, 501-518. 10.1046/j.1365-2583.1999.00146.x.
- Robertson, H.M., Warr, C.G. and Carlson, J.R., 2003. Molecular evolution of the insect chemoreceptor gene superfamily in *Drosophila melanogaster*. *Proc. Natl. Acad. Sci. U. S. A.* 100, 14537-14542. 10.1073/pnas.2335847100.
- Roelofs, W.L., Hill, A.S., Carde, R.T. and Baker, T.C., 1974. Two sex pheromone components of the tobacco budworm moth, *Heliothis virescens*. *Life Sci.* 14, 1555-62. 10.1016/0024-3205(74)90166-0.
- Rogers, M.E., Krieger, J. and Vogt, R.G., 2001a. Antennal SNMPs (sensory neuron membrane proteins) of Lepidoptera define a unique family of invertebrate CD36-like proteins. *J. Neurobiol.* 49, 47-61. 10.1002/neu.1065.
- Rogers, M.E., Steinbrecht, R.A. and Vogt, R.G., 2001b. Expression of SNMP-1 in olfactory neurons and sensilla of male and female antennae of the silkmoth *Antheraea polyphemus*. *Cell Tissue Res.* 303, 433-446. 10.1007/s004410000305.
- Rogers, M.E., Sun, M., Lerner, M.R. and Vogt, R.G., 1997. Snmp-1, a novel membrane protein of olfactory neurons of the silk moth *Antheraea polyphemus* with homology to the CD36 family of membrane proteins. *J. Biol. Chem.* 272, 14792-14799. 10.1074/jbc.272.23.14792
- Ronderos, D.S., Lin, C.C., Potter, C.J. and Smith, D.P., 2014. Farnesol-detecting olfactory neurons in *Drosophila*. *J. Neurosci.* 34, 3959-68. 10.1523/JNEUROSCI.4582-13.2014.
- Rybczynski, R., Vogt, R.G. and Lerner, M.R., 1990. Antennal-specific pheromone-degrading aldehyde oxidases from the moths *Antheraea polyphemus* and *Bombyx mori*. *J Biol Chem.* 265, 19712-5. 10.1016/S0021-9258(17)45430-5.
- Sakurai, T., Nakagawa, T., Mitsuno, H., Mori, H., Endo, Y., Tanoue, S., Yasukochi, Y., Touhara, K. and Nishioka, T., 2004. Identification and functional characterization of a sex pheromone receptor in the silkmoth *Bombyx mori*. *Proc. Natl. Acad. Sci. U. S. A.* 101, 16653-16658. 10.1073/pnas.0407596101.
- Sakurai, T., Namiki, S. and Kanzaki, R., 2014. Molecular and neural mechanisms of sex pheromone reception and processing in the silkmoth *Bombyx mori*. *Front. Physiol.* 5, 125. 10.3389/fphys.2014.00125.
- Sanes, J.R. and Hildebrand, J.G., 1976a. Origin and morphogenesis of sensory neurons in an insect antenna. *Dev. Biol.* 51, 300-319. 10.1016/0012-1606(76)90145-7.

- Sanes, J.R. and Hildebrand, J.G., 1976b. Structure and development of antennae in a moth, *Manduca sexta*. *Dev. Biol.* 51, 280-299. 10.1016/0012-1606(76)90144-5.
- Sato, K., Pellegrino, M., Nakagawa, T., Nakagawa, T., Vosshall, L.B. and Touhara, K., 2008. Insect olfactory receptors are heteromeric ligand-gated ion channels. *Nature.* 452, 1002-1006. 10.1038/nature06850.
- Schachtner, J., Schmidt, M. and Homberg, U., 2005. Organization and evolutionary trends of primary olfactory brain centers in Tetraconata (Crustacea plus Hexapoda). *Arthropod Struct Dev.* 34, 257-299. 10.1016/j.asd.2005.04.003.
- Schmidt, H.R. and Benton, R., 2020. Molecular mechanisms of olfactory detection in insects: beyond receptors. *Open Biol.* 10, 200252. 10.1098/rsob.200252.
- Schneider, D., 1964. Insect Antennae. *Annu. Rev. Entomol.* 9, 103-+. 10.1146/annurev.en.09.010164.000535.
- Schneider, D., 1992. 100 Years of Pheromone Research - an Essay on Lepidoptera. *Naturwissenschaften.* 79, 241-250. 10.1007/Bf01175388.
- Seidelmann, K. and Ferenz, H.J., 2002. Courtship inhibition pheromone in desert locusts, *Schistocerca gregaria*. *J. Insect Physiol.* 48, 991-996. 10.1016/S0022-1910(02)00178-6.
- Seidelmann, K., Luber, K. and Ferenz, H.J., 2000. Analysis of release and role of benzyl cyanide in male desert locusts, *Schistocerca gregaria*. *J. Chem. Ecol.* 26, 1897-1910. 10.1023/A:1005500908499.
- Seidl, S., 1992. Structure and function of the thecogen cell in contact chemosensitive sensilla of *Periplaneta americana* L. (Blattodea, Blattidae). *Int J of Insect Morphol Embryol.* 21, 235-250. 10.1016/0020-7322(92)90019-J.
- Shan, S., Wang, S.N., Song, X., Khashaveh, A., Lu, Z.Y., Dhilloo, K.H., Li, R.J., Gao, X.W. and Zhang, Y.J., 2020. Molecular characterization and expression of sensory neuron membrane proteins in the parasitoid *Microplitis mediator* (Hymenoptera: Braconidae). *Insect Sci.* 27, 425-439. 10.1111/1744-7917.12667.
- Shanbhag, S.R., Müller, B. and Steinbrecht, R.A., 2000. Atlas of olfactory organs of *Drosophila melanogaster*. 2. Internal organization and cellular architecture of olfactory sensilla. *Arthropod Struct Dev.* 29, 211-229. 10.1016/S1467-8039(00)00028-1.
- Sharkova, M., Chow, E., Erickson, T. and Hocking, J.C., 2023. The morphological and functional diversity of apical microvilli. *J Anat.* 242, 327-353. 10.1111/joa.13781.
- Shields, V.D.C. and Hildebrand, J.G., 2001. Recent advances in insect olfaction, specifically regarding the morphology and sensory physiology of antennal sensilla of the female sphinx moth *Manduca sexta*. *Microsc. Res. Tech.* 55, 307-329. 10.1002/jemt.1180.
- Silbering, A.F., Rytz, R., Grosjean, Y., Abuin, L., Ramdya, P., Jefferis, G.S. and Benton, R., 2011. Complementary function and integrated wiring of the evolutionarily distinct *Drosophila* olfactory subsystems. *J. Neurosci.* 31, 13357-13375. 10.1523/JNEUROSCI.2360-11.2011.
- Silverstein, R.L. and Febbraio, M., 2009. CD36, a scavenger receptor involved in immunity, metabolism, angiogenesis, and behavior. *Sci. Signal.* 2, 1-8. 10.1126/scisignal.272re3.
- Skiri, H.T., Galizia, C.G. and Mustaparta, H., 2004. Representation of primary plant odorants in the antennal lobe of the moth *Heliothis virescens* using calcium imaging. *Chem. Senses.* 29, 253-267. 10.1093/chemse/bjh026.
- Slessor, K.N., Kaminski, L.A., King, G.G.S., Borden, J.H. and Winston, M.L., 1988. Semiochemical Basis of the Retinue Response to Queen Honey Bees. *Nature.* 332, 354-356. 10.1038/332354a0.
- Slessor, K.N., Winston, M.L. and Le Conte, Y., 2005. Pheromone Communication in the Honeybee (*Apis mellifera* L.). *J. Chem Ecol.* 31, 2731-2745. 10.1007/s10886-005-7623-9.
- Smart, R., Kiely, A., Beale, M., Vargas, E., Carraher, C., Kralicek, A.V., Christie, D.L., Chen, C., Newcomb, R.D. and Warr, C.G., 2008. *Drosophila* odorant receptors are novel seven transmembrane domain proteins that can signal independently of heterotrimeric G proteins. *Insect Biochem. Mol. Biol.* 38, 770-780. 10.1016/j.ibmb.2008.05.002.
- Steele, T.J., Lanz, A.J. and Nagel, K.I., 2023. Olfactory navigation in arthropods. *J. Comp Physiol A Neuroethol Sens Neural Behav Physiol.* 209, 467-488. 10.1007/s00359-022-01611-9.
- Steinbrecht, R.A., 1970. Zur Morphometrie der Antenne des Seidenspinners, *Bombyx mori* L.: Zahl und Verteilung der Rietsensillen (Insecta, Lepidoptera). *Z. Morph. Tiere.* 68, 93-126. 10.1007/BF00277500.

- Steinbrecht, R.A., 1996. Structure and function of insect olfactory sensilla. *Ciba Found. Symp.* 200, 158-174. 10.1002/9780470514948.ch13.
- Steinbrecht, R.A., 1997. Pore structures in insect olfactory sensilla: A review of data and concepts. *Int. J. Insect Morphol. Embryol.* 26, 229-245. 10.1016/S0020-7322(97)00024-X.
- Steinbrecht, R.A. and Gnatzy, W., 1984. Pheromone receptors in *Bombyx mori* and *Antheraea pernyi*. I. Reconstruction of the cellular organization of the sensilla trichodea. *Cell Tissue Res.* 235, 25-34. 10.1007/bf00213719.
- Steinbrecht, R.A., Lee, J.K., Altner, H. and Zimmermann, B., 1989. Volume and Surface of Receptor and Auxiliary Cells in Hygroreceptive Thermoreceptive Sensilla of Moths (*Bombyx mori*, *Antheraea pernyi*, and *Antheraea polyphemus*). *Cell Tissue Res.* 255, 59-67. 10.1007/BF00229066.
- Steinbrecht, R.A., Ozaki, M. and Ziegelberger, G., 1992. Immunocytochemical localization of pheromone-binding protein in moth antennae. *Cell Tissue Res.* 270, 287-302. 10.1007/BF00328015.
- Steinwender, B., Thrimawithana, A.H., Crowhurst, R.N. and Newcomb, R.D., 2015. Pheromone receptor evolution in the cryptic leafroller species, *Ctenopseustis obliquana* and *C. herana*. *J. Mol. Evol.* 80, 42-56. 10.1007/s00239-014-9650-z.
- Stengl, M., 2010. Pheromone transduction in moths. *Front. Cell. Neurosci.* 4, 133. 10.3389/fncel.2010.00133.
- Stowers, L. and Logan, D.W., 2008. LUSH shapes up for a starring role in olfaction. *Cell.* 133, 1137-1139. 10.1016/j.cell.2008.06.010.
- Su, J., Zhao, B.G., Zhang, A.J., Bu, X.L., Chen, J., Yan, Z.D. and Wang, S.F., 2019. Pore-ridge nanostructures on the surface of trichoid sensilla of the male silkworm: Aerodynamic trapping and transporting of the pheromone molecules. *Arthropod Struct Dev.* 52, 10.1016/j.asd.2019.06.004.
- Sun, H., Bu, L.A., Su, S.C., Guo, D., Gao, C.F. and Wu, S.F., 2023. Knockout of the odorant receptor co-receptor, *orco*, impairs feeding, mating and egg-laying behavior in the fall armyworm *Spodoptera frugiperda*. *Insect Biochem Mol Biol.* 152, 10.1016/j.ibmb.2022.103889.
- Sun, L., Wang, Q., Zhang, Y., Yan, Y., Guo, H., Xiao, Q. and Zhang, Y., 2019. Expression patterns and colocalization of two sensory neurone membrane proteins in *Ectropis obliqua* Prout, a geometrid moth pest that uses Type-II sex pheromones. *Insect Mol. Biol.* 28, 342-354. 10.1111/imb.12555.
- Symonds, M.R. and Elgar, M.A., 2008. The evolution of pheromone diversity. *Trends Ecol. Evol.* 23, 220-228. 10.1016/j.tree.2007.11.009.
- Talamillo, A., Herboso, L., Pirone, L., Perez, C., Gonzalez, M., Sanchez, J., Mayor, U., Lopitz-Otsoa, F., Rodriguez, M.S., Sutherland, J.D. and Barrio, R., 2013. Scavenger receptors mediate the role of SUMO and Ftz-f1 in *Drosophila* steroidogenesis. *PLoS Genet.* 9, e1003473. 10.1371/journal.pgen.1003473.
- Tanaka, K., Uda, Y., Ono, Y., Nakagawa, T., Suwa, M., Yamaoka, R. and Touhara, K., 2009. Highly selective tuning of a silkworm olfactory receptor to a key mulberry leaf volatile. *Curr. Biol.* 19, 881-890. 10.1016/j.cub.2009.04.035.
- Tasayco, M.L. and Prestwich, G.D., 1990. Aldehyde-oxidizing enzymes in an adult moth: in vitro study of aldehyde metabolism in *Heliothis virescens*. *Arch. Biochem. Biophys.* 278, 444-451. 10.1016/0003-9861(90)90283-5.
- Thurm, U. and Küppers, J., 1980. Epithelial physiology of insect sensilla. Insect biology in the future. eds. M. Locke & D.S. Smiths, pp. 735-763. Academic Press, New York.
- Tittiger, C. and Blomquist, G.J., 2017. Pheromone biosynthesis in bark beetles. *Curr. Opin. Insect Sci.* 24, 68-74. 10.1016/j.cois.2017.09.005.
- Torto, B., Njagi, P.G.N., Hassanali, A. and Amiani, H., 1996. Aggregation pheromone system of nymphal gregarious desert locust, *Schistocerca gregaria* (Forsk.). *J. Chem. Ecol.* 22, 2273-2281. 10.1007/Bf02029546.
- Torto, B., Obeng-Ofori, D., Njagi, P.G., Hassanali, A. and Amiani, H., 1994. Aggregation pheromone system of adult gregarious desert locust *Schistocerca gregaria* (Forsk.). *J. Chem. Ecol.* 20, 1749-1762. 10.1007/BF02059896.
- Uvarov, B.P., 1966. Grasshoppers and Locusts: A Handbook of General Acridology, Cambridge University Press.
- Vickers, N.J., Christensen, T.A., Mustaparta, H. and Baker, T.C., 1991. Chemical communication in heliothine moths. III. Flight behavior of male *Helicoverpa zea* and *Heliothis virescens* in response

- to varying ratios of intra- and interspecific pheromone compounds. *J. Comp. Physiol. A.* 169, 275-280. 10.1007/BF00206991.
- Vogt, R.G., 2003. Biochemical diversity of odor detection: OBPs, ODEs and SNMPs. Insect pheromone biochemistry and molecular biology. The biosynthesis and detection of pheromones and plant volatiles. eds. G. Blomquist & R.G. Vogts, pp. 391-445. Elsevier Academic Press, London.
- Vogt, R.G., Prestwich, G.D. and Riddiford, L.M., 1987. Visualization of a Putative Pheromone Receptor-Protein Using a Tritium-Labeled Photoaffinity Analog. *Chem. Senses.* 12, 705-705.
- Vogt, R.G., Prestwich, G.D. and Riddiford, L.M., 1988. Sex pheromone receptor proteins. Visualization using a radiolabeled photoaffinity analog. *J. Biol. Chem.* 263, 3952-3959. 10.1016/S0021-9258(18)69018-0.
- Vogt, R.G. and Riddiford, L.M., 1981. Pheromone binding and inactivation by moth antennae. *Nature.* 293, 161-163. 10.1038/293161a0.
- Vogt, R.G., Riddiford, L.M. and Prestwich, G.D., 1985. Kinetic properties of a sex pheromone-degrading enzyme: the sensillar esterase of *Antheraea polyphemus*. *Proc. Natl. Acad. Sci. U. S. A.* 82, 8827-8831. 10.1073/pnas.82.24.8827.
- Vogt, R.G., Sparks, J.T., Fandino, R.A. and Ashourian, K.T., 2020. Reflections on antennal proteins: the evolution of pheromone binding proteins; diversity of pheromone degrading enzymes; and the distribution and behavioral roles of SNMPs. Insect pheromone biochemistry and molecular biology. eds. G. Blomquist & R.G. Vogts, Elsevier Academic Press, London.
- Vosshall, L.B., Amrein, H., Morozov, P.S., Rzhetsky, A. and Axel, R., 1999. A spatial map of olfactory receptor expression in the *Drosophila* antenna. *Cell.* 96, 725-736. 10.1016/S0092-8674(00)80582-6.
- Vosshall, L.B. and Hansson, B.S., 2011. A unified nomenclature system for the insect olfactory coreceptor. *Chem. Senses.* 36, 497-498. 10.1093/chemse/bjr022.
- Vosshall, L.B., Wong, A.M. and Axel, R., 2000. An olfactory sensory map in the fly brain. *Cell.* 102, 147-159. 10.1016/S0092-8674(00)00021-0.
- Vulpe, A., Kim, H.S., Ballou, S., Wu, S.T., Grabe, V., Gonzales, C.N., Liang, T., Sachse, S., Jeanne, J.M., Su, C.Y. and Menuz, K., 2021. An ammonium transporter is a non-canonical olfactory receptor for ammonia. *Curr. Biology.* 31, 3382-+. 10.1016/j.cub.2021.05.025.
- Wang, T., Jiao, Y. and Montell, C., 2007. Dissection of the pathway required for generation of vitamin A and for *Drosophila* phototransduction. *J. Cell Biol.* 177, 305-316. 10.1083/jcb.200610081.
- Wang, W.W., He, P.Y., Liu, T.X., Jing, X.F. and Zhang, S.Z., 2023. Morphology and Distribution of Antennal Sensilla on *Spodoptera frugiperda* (Lepidoptera: Noctuidae) Larvae and Adults. *Diversity-Basel.* 15, 10.3390/d15090992.
- Wang, Z., Yang, P., Chen, D., Jiang, F., Li, Y., Wang, X. and Kang, L., 2015. Identification and functional analysis of olfactory receptor family reveal unusual characteristics of the olfactory system in the migratory locust. *Cell. Mol. Life Sci.* 72, 4429-43. 10.1007/s00018-015-2009-9.
- Wicher, D. and Miazzi, F., 2021. Functional properties of insect olfactory receptors: ionotropic receptors and odorant receptors. *Cell Tissue Res.* 383, 7-19. 10.1007/s00441-020-03363-x.
- Wicher, D., Schafer, R., Bauernfeind, R., Stensmyr, M.C., Heller, R., Heinemann, S.H. and Hansson, B.S., 2008. *Drosophila* odorant receptors are both ligand-gated and cyclic-nucleotide-activated cation channels. *Nature.* 452, 1007-1011. 10.1038/nature06861.
- Williams, J.L.D., 1988. Nodes on the Large Pheromone-Sensitive Dendrites of Olfactory Hairs of the Male Silkworm, *Antheraea polyphemus* (Cramer) (Lepidoptera, Saturniidae). *Int. J. Insect Morphol. Embryol.* 17, 145-151. 10.1016/0020-7322(88)90008-6.
- Xiao, S., Sun, J.S. and Carlson, J.R., 2019. Robust olfactory responses in the absence of odorant binding proteins. *Elife.* 8, e51040. 10.7554/eLife.51040.
- Xu, M., Guo, H., Hou, C., Wu, H., Huang, L.Q. and Wang, C.Z., 2016. Olfactory perception and behavioral effects of sex pheromone gland components in *Helicoverpa armigera* and *Helicoverpa assulta*. *Sci. Rep.* 6, 22998. 10.1038/srep22998.
- Xu, P.X., Atkinson, R., Jones, D.N.M. and Smith, D.P., 2005. *Drosophila* OBP LUSH is required for activity of pheromone-sensitive neurons. *Neuron.* 45, 193-200. 10.1016/j.neuron.2004.12.031.
- Xu, W., Zhang, H., Liao, Y. and Papanicolaou, A., 2020. Characterization of sensory neuron membrane proteins (SNMPs) in cotton bollworm *Helicoverpa armigera* (Lepidoptera: Noctuidae). *Insect Sci.* 00, 1-11. 10.1111/1744-7917.12816.

- Yang, Y., Krieger, J., Zhang, L. and Breer, H., 2012. The olfactory co-receptor Orco from the migratory locust (*Locusta migratoria*) and the desert locust (*Schistocerca gregaria*): identification and expression pattern. *Int. J. Biol. Sci.* 8, 159-170. 10.7150/ijbs.8.159.
- Yao, C.A., Ignell, R. and Carlson, J.R., 2005. Chemosensory coding by neurons in the coeloconic sensilla of the *Drosophila* antenna. *J. Neurosci.* 25, 8359-8367. 10.1523/JNEUROSCI.2432-05.2005.
- You, Y., Smith, D.P., Lv, M. and Zhang, L., 2016. A broadly tuned odorant receptor in neurons of trichoid sensilla in locust, *Locusta migratoria*. *Insect Biochem. Mol. Biol.* 79, 66-72. 10.1016/j.ibmb.2016.10.008.
- Younus, F., Chertemps, T., Pearce, S.L., Pandey, G., Bozzolan, F., Coppin, C.W., Russell, R.J., Maïbèche-Coisne, M. and Oakeshott, J.G., 2014. Identification of candidate odorant degrading gene/enzyme systems in the antennal transcriptome of *Drosophila melanogaster*. *Insect Biochem. Mol. Biology.* 53, 30-43. 10.1016/j.ibmb.2014.07.003.
- Zacharuk, R.Y., 1980. Ultrastructure and Function of Insect Chemosensilla. *Annu Rev Entomol.* 25, 27-47. 10.1146/annurev.en.25.010180.000331.
- Zhang, H.J., Xu, W., Chen, Q.M., Sun, L.N., Anderson, A., Xia, Q.Y. and Papanicolaou, A., 2020. A phylogenomics approach to characterizing sensory neuron membrane proteins (SNMPs) in Lepidoptera. *Insect Biochem. Mol. Biol.* 118, 103313. 10.1016/j.ibmb.2020.103313.
- Zhang, J., Liu, Y., Walker, W.B., Dong, S.L. and Wang, G.R., 2015a. Identification and localization of two sensory neuron membrane proteins from *Spodoptera litura* (Lepidoptera: Noctuidae). *Insect Sci.* 22, 399-408. 10.1111/1744-7917.12131.
- Zhang, J., Yan, S., Liu, Y., Jacquin-Joly, E., Dong, S. and Wang, G., 2015b. Identification and functional characterization of sex pheromone receptors in the common cutworm (*Spodoptera litura*). *Chem. Senses.* 40, 7-16. 10.1093/chemse/bju052.
- Zhao, L., Li, Y., Ding, Q., Li, Y., Chen, Y. and Ruan, X.Z., 2021. CD36 Senses Dietary Lipids and Regulates Lipids Homeostasis in the Intestine. *Front Physiol.* 12, 669279. 10.3389/fphys.2021.669279.
- Zhou, X., Slone, J.D., Rokas, A., Berger, S.L., Liebig, J., Ray, A., Reinberg, D. and Zwiebel, L.J., 2012. Phylogenetic and transcriptomic analysis of chemosensory receptors in a pair of divergent ant species reveals sex-specific signatures of odor coding. *PLoS Genet.* 8, e1002930. 10.1371/journal.pgen.1002930.
- Zielonka, M., Breer, H. and Krieger, J., 2018. Molecular elements of pheromone detection in the female moth, *Heliothis virescens*. *Insect Sci.* 25, 389-400. 10.1111/1744-7917.12434.
- Zielonka, M., Gehrke, P., Badeke, E., Sachse, S., Breer, H. and Krieger, J., 2016. Larval sensilla of the moth *Heliothis virescens* respond to sex pheromone components. *Insect Mol. Biol.* 25, 666-78. 10.1111/imb.12253.
- Zufall, F. and Domingos, A.I., 2018. The structure of Orco and its impact on our understanding of olfaction. *J. Gen. Physiology.* 150, 1602-1605. 10.1085/jgp.201812226.

Acknowledgments

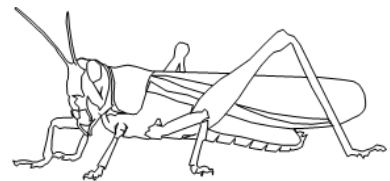
First of all, I want to express my deepest gratitude to my “Doktorvater”, **Prof. Jürgen Krieger**. There are so many things I want to thank you for, like hiring me as a PhD student, giving me such an interesting topic to work on, allowing me freedom to include my own ideas into the projects while helping me focus on the right direction, and so much more. You were always extremely patient when I had questions (and I know that I can ask a lot) and I really enjoyed the various discussions we had, ranging from the earliest studies on insect olfaction, up and coming methods and papers, anecdotes from past experiments, and how to structure manuscripts. I have learned so much over the last years that I will take with me to my next projects. Thank you!!!

I also want to thank **Prof. Dr. Monika Stengl** and **PD Dr. Dieter Wicher** for taking the time to read and review this thesis.

To the Animal Physiology group: thank you for being my lab family and being very supportive. I am especially grateful to **Doreen Sander**, for all the great and fun work together. Thank you for maintaining the lab and keeping a steady supply of standard buffers and solutions ready. I also want to thank you for the support I received when teaching, especially during the blood physiology course. Most of all, thank you so much for the countless times of kind, motivational words. Vielen Dank für alles, liebe Doreen.

I also want to thank **Dr. Jörg Fleischer**, for the many discussions, where I learned about mammalian olfaction, lab methods, papers, and even more light-hearted topics, such as chocolate and Lake Garda. You were always so willing to help when I had any questions or needed anything. A big thank you also goes to **Kathrin Dietze**, for teaching me a lot of important methods in the lab, most notably *in situ* hybridization. I always enjoyed working with you and eating lunch together. To **Nicole Mann** I want to say thank you for always being so kind, helpful and patient, no matter how often I asked the same questions. I really appreciate your help.

I want to thank all current and former PhD, Masters and Bachelor students for creating such a fun environment to work in. Thanks to all the Hiwi students who kept the locust cultures alive. I am also so, so thankful to the students I was able to mentor. **Tim, Jessie, Jule, Angi, and Maria**, I learned so much during our time together. Everyone was so different and it was fun adapting to everyone and their projects, I am so glad to have worked with each of you.





Thank you to all the great people that I was able to cooperate with. Big thank you goes to **Dr. Dr. Gerd Hause** and **Simone Fraas**, for all the help with transmission electron microscopy. I really enjoyed my time in your group and had a lot of fun in your labs. I also want to thank **Dr. Michael Laue** for offering his help with the cryofixation of our antennal samples. Thank you to **Dr. Stephanie Krüger** for our work together with the scanning electron microscope and for always being so helpful when I had questions, even when they went beyond our work together. I want to thank the different cooperation partners for publications that were not included in this thesis because I got a great perspective into works which were outside of my own SNMP-world. Also, thank you to all the lab equipment, pipettes, the LSM, for all the results!

I am so thankful for having such great friends, who were with me during a lot of ups and downs during these last few years. Thank you so much to **Solli, Kira, Patrick, Sarah, Maxi, Jann, Max, Lara, Ron, Filip** and **Alex**! You are amazing friends.

Thank you to my family, especially my sister **Deb**, and my in-laws, **Freia** and **Manfred**. Thank you for all your support, motivation and kindness. I am grateful to our cat, **Ori**. I know that if cats could read you probably wouldn't be reading this, but I am so happy to have you in my life! To the most handsome, hardworking and lovely person I know, my husband **Leander**, thank you. If I thanked you for everything you do for me, it would end up being longer than this thesis. You are such a reliable partner and I know that as long as I have you, everything will be great. I am excited for our future!

Curriculum vitae

Personal Information

Name: Sina Cassau

Birth date and place: [REDACTED]

Nationality: [REDACTED]

Experience and education

02/2019 – 01/2024 Research Associate/PhD Student

Martin Luther University Halle-Wittenberg (Halle, Germany)

Institute of Biology / Department of Zoology / Animal Physiology

10/2015 – 01/2019 Master of Science degree (Biology)

Martin Luther University Halle-Wittenberg (Halle, Germany)

Thesis: Investigation of the expression patterns and function of sensory neuron membrane proteins (SNMPs) in the antennae of different Insects

10/2012 – 01/2016 Bachelor of Science degree (Biology)

Martin Luther University Halle-Wittenberg (Halle, Germany)

Thesis: Development of the internal morphology in insect larvae of the order Thysanoptera

08/2009 – 08/2011 International Baccalaureate Diploma

Cebu International School (Cebu, Philippines)

Additional training

04/2019 **“High-accuracy CLEM: Applications at room temperature and in cryo”**

EMBO Practical course, EMBL Heidelberg (Germany)

06/2017 **„Tierschutz, Versuchstierkunde und Tierexperimentelles Arbeiten“**

Martin Luther University Halle-Wittenberg (Halle, Germany)

Conferences

03/2023 **Meeting of the German Neuroscience Society (NWG), Göttingen**

Poster contribution: The role of SNMP2 in the olfactory processes of moths

Poster contribution: The sensilla specific expression and subcellular localization of SNMP1 and SNMP2 reveal novel insights into their roles in the antenna of the desert locust *Schistocerca gregaria*

07/2022 **International Congress of Entomology (ICE), Helsinki**

Poster contribution: "Sensory neuron membrane proteins (SNMPs)" indicate distinct roles in olfactory signal detection in insects

09/2019 **NeuroDoWo, Würzburg**

Poster contribution: Two "Sensory neuron membrane proteins (SNMPs)" indicate distinct roles in chemosensory signal detection of the noctuid moth *Heliothis virescens*

03/2019 **Meeting of the German Neuroscience Society (NWG), Göttingen**

Poster contribution: The expression pattern of two “Sensory Neuron Membrane Proteins” emphasizes different roles of the CD36-related proteins in the olfactory system of moths

03/2019 **DGaaE – Entomology Conference, Halle**

Poster Contribution: The expression pattern of two “Sensory neuron membrane proteins” emphasizes different roles in the olfactory signal detection system of the noctuid moth *Heliothis virescens*

Travel Grant

07/2022 **Promotion of women of MLU Halle-Wittenberg (Frauenförderung) for ICE 2022**

Teaching

- 2023** Practical Course BSc: Animal Physiology – “Blood Physiology”
 Project Module MSc: Western Blot, Immunohistochemistry, microscopy (one week)
- 2022** Project Module BSc: WB, IHC, microscopy (two weeks)
 Practical Course BSc: Animal Physiology – “Blood Physiology”
 Project Module MSc: WB, IHC, microscopy (one week)
- 2021** Project Module BSc: WB, IHC, microscopy (two week)
 Practical Course BSc: Animal Physiology – “Blood Physiology”
 Project Module MSc: WB, IHC, microscopy (one week)
- 2020** Project Module BSc: WB, IHC, microscopy (two weeks)
 Practical Course BSc: Animal Physiology – “Blood Physiology”
 Project Module MSc: cell culture, WB, IHC, microscopy (one week)
- 2019** Project Module BSc: WB, IHC, microscopy (two weeks)
 Practical Course BSc: Animal Physiology – “Blood Physiology”
 Project Module MSc: cell culture, IHC, microscopy (one week)

Co-supervision of BSc. Theses

- 2023** „Untersuchungen zur Funktion der SNMP-exprimierenden Stützzellen olfaktorischer Sensillen auf der Antenne der Wüstenheuschrecke *Schistocerca gregaria*“. Martin Luther University, Halle-Wittenberg
- 2022** „Untersuchung der SNMP-Expression in verschiedenen Entwicklungsstadien der Wüstenheuschrecke *Schistocerca gregaria* und der Wanderheuschrecke *Locusta migratoria*“. Martin Luther University, Halle-Wittenberg
- 2022** “Untersuchungen zu Expression von Fatty Acid Transport Proteins in chemosensorischen System der Wüstenheuschrecke *Schistocerca gregaria*“. Martin Luther University, Halle-Wittenberg

- 2021** „Heterologe Expression und Aufreinigung der Ektodomäne von SNMP1 und SNMP2 des Nachtfalters *Heliothis virescens* und der Heuschrecke *Schistocerca gregaria*“.
Martin Luther University, Halle-Wittenberg
- 2019** “Characterization of the expression of SNMPs in chemosensory organs of the tobacco budworm *Heliothis virescens* (Lepidoptera: Noctuidae)”.
Martin Luther University, Halle-Wittenberg

Sina Cassau, Halle (Saale)

List of Publications

- Schuh, E., **Cassau, S.**, Ismaieel, A.R., Stieber, R., Krieger, J., Hansson, B.S., Sachse, S. and Bisch-Knaden, S., 2024. Females smell differently: characteristics and significance of the most common olfactory sensilla of female silkmoths. *Proceedings of the Royal Society Biological Sciences*. 291, 20232578. 10.1098/rspb.2023.2578.
- Cassau, S.** and Krieger, J., 2023. Evidence for a role of SNMP2 and antennal support cells in sensillum lymph clearance processes of moth pheromone-responsive sensilla. *Insect Biochemistry and Molecular Biology*. 164, 104046. 10.1016/j.ibmb.2023.104046.
- Chang, H.T., **Cassau, S.**, Krieger, J., Guo, X.J., Knaden, M., Kang, L. and Hansson, B.S., 2023. A chemical defense deters cannibalism in migratory locusts. *Science*. 380, 537-543. 10.1126/science.ade6155.
- Cassau, S.**, Degen, A., Kruger, S. and Krieger, J., 2023. The specific expression patterns of sensory neuron membrane proteins are retained throughout the development of the desert locust *Schistocerca gregaria*. *Current Research in Insect Science*. 3, 100053. 10.1016/j.cris.2023.100053.
- Cassau, S.**, Sander, D., Karcher, T., Laue, M., Hause, G., Breer, H. and Krieger, J., 2022. The sensilla-specific expression and subcellular localization of SNMP1 and SNMP2 reveal novel insights into their roles in the antenna of the Desert Locust *Schistocerca gregaria*. *Insects*. 13, 10.3390/insects13070579.
- Fleischer, J., Rausch, A., Dietze, K., Erler, S., **Cassau, S.** and Krieger, J., 2022. A small number of male-biased candidate pheromone receptors are expressed in large subsets of the olfactory sensory neurons in the antennae of drones from the European honey bee *Apis mellifera*. *Insect Science*. 29, 749-766. 10.1111/1744-7917.12960.
- Zhang, J., Komail Raza, S.A., Wei, Z., Keeseey, I.W., Parker, A.L., Feistel, F., Chen, J., **Cassau, S.**, Fandino, R.A., Grosse-Wilde, E., Dong, S., Kingsolver, J., Gershenson, J., Knaden, M. and Hansson, B.S., 2022. Competing beetles attract egg laying in a hawkmoth. *Current Biology*. 32, 861-869 e8. 10.1016/j.cub.2021.12.021.
- Cassau, S.** and Krieger, J., 2021. The role of SNMPs in insect olfaction. *Cell and Tissue Research*. 383, 21-33. 10.1007/s00441-020-03336-0.
- Blankenburg, S., **Cassau, S.** and Krieger, J., 2019. The expression patterns of SNMP1 and SNMP2 underline distinct functions of two CD36-related proteins in the olfactory system of the tobacco budworm *Heliothis virescens*. *Cell and Tissue Research*. 378, 485-497. 10.1007/s00441-019-03066-y.

Appendix

Eidesstattliche Erklärung

Hiermit erkläre ich an Eides statt, dass ich mich mit der vorliegenden Arbeit erstmals um die Erlangung des Doktorgrades bewerbe, die vorliegende Arbeit selbstständig und ohne fremde Hilfe verfasst, andere als die von mir angegebenen Quellen und Hilfsmittel nicht benutzt und die den verwendeten Werken wörtlich oder inhaltlich entnommen Stellen als solche kenntlich gemacht habe.

Sina Cassau

Halle (Saale),

Bestätigung des Betreuers der Dissertation von Frau Cassau, Sina

Hiermit bestätige ich als Betreuer/in der o. g. Dissertation, dass die gemeinsame Arbeit mehrerer Personen an der Arbeit durch den Forschungsgegenstand gerechtfertigt ist.

Mit freundlichen Grüßen,

Datum:

Prof. Dr. Jürgen Krieger

Beiträge aller Autoren (Author contributions)

Chapter 2: Manuscript 1

[Sina Cassau, Doreen Sander, Thomas Karcher, Michael Laue, Gerd Hause, Heinz Breer, Jürgen Krieger (2022), “The Sensilla-Specific Expression and Subcellular Localization of SNMP1 and SNMP2 Reveal Novel Insights into Their Roles in the Antenna of the Desert Locust *Schistocerca gregaria*”, *Insects*, **Volume 13**, 579. DOI 10.3390/insects13070579]

	Author01 S. Cassau [%]	Author02 D. Sander [%]	Author03 T. Karcher [%]	Author04 M. Laue [%]	Author05 G. Hause [%]	Author06 H. Breer [%]	Author07 J. Krieger [%]
Entwurf (Design)	50%	-	-	-	-	-	50%
Umsetzung (Implementation)	80%	5%	5%	5%	5%	-	-
Auswertung (Analysis)	90%	-	-	-	-	-	10%
Schreiben (Writing)	67%	-	-	-	-	3%	30%

Chapter 3: Manuscript 2

[Sina Cassau, Angelina Degen, Stephanie Krüger, Jürgen Krieger (2023), “The specific expression patterns of sensory neuron membrane proteins are retained throughout the development of the desert locust *Schistocerca gregaria*”, *Current Research in Insect Science*, **Volume 3**, 100053. DOI 10.1016/j.cris.2023.100053]

	Author01 S. Cassau [%]	Author02 A. Degen [%]	Author03 S. Krüger [%]	Author04 J. Krieger [%]
Entwurf (Design)	80%	-	-	20%
Umsetzung (Implementation)	30%	60%	10%	-
Auswertung (Analysis)	60%	30%	5%	5%
Schreiben (Writing)	60%	-	-	40%

Chapter 4: Manuscript 3

[Sina Cassau, Jürgen Krieger (2023), "Evidence for a role of SNMP2 and antennal support cells in sensillum lymph clearance processes of moth pheromone-responsive sensilla", *Insect Biochemistry and Molecular Biology*, Volume 164, 104046. DOI 10.1016/j.ibmb.2023.104046]

	Author01 S. Cassau [%]	Author02 J. Krieger [%]
Entwurf (Design)	85%	15%
Umsetzung (Implementation)	100%	-
Auswertung (Analysis)	95%	5%
Schreiben (Writing)	70%	30%

Datum:

Cassau, Sina

Prof. Dr. Jürgen Krieger